

**IN VITRO BASED MECHANISTIC STUDY ON THE ROLE OF FRUCTOSE
AND PALMITATE IN THE GENESIS OF STEATOSIS IN HEPG2 CELL LINE**

by

SWAPNA SASI U S
10BB16A39016

A thesis submitted to the
Academy of Scientific & Innovative Research
for the award of the degree of

DOCTOR OF PHILOSOPHY

in
SCIENCE

Under the supervision of
Prof. (Dr) K G RAGHU



Council of Scientific and Industrial Research - National Institute for Interdisciplinary
Science and Technology (CSIR - NIIST), Thiruvananthapuram, Kerala - 695019, India



Academy of Scientific and Innovative Research
AcSIR Headquarters, CSIR-HRDC campus
Sector 19, Kamla Nehru Nagar,
Ghaziabad, U.P. - 201 002, India

September - 2021



राष्ट्रीय अंतर्विषयी विज्ञान तथा प्रौद्योगिकी संस्थान
NATIONAL INSTITUTE FOR INTERDISCIPLINARY SCIENCE AND TECHNOLOGY


वैज्ञानिक तथा औद्योगिक अनुसंधान परिषद्
इंडस्ट्रियल इस्टेट पी. ओ. पाप्पनकोड, तिरुवनंतपुरम, भारत - 695 019

Council of Scientific and Industrial Research
Industrial Estate P.O., Pappanamcode, Thiruvananthapuram, India-695 019

Certificate

This is to certify that the work incorporated in this Ph.D. thesis entitled, "*In vitro based mechanistic study on the role of fructose and palmitate in the genesis of steatosis in HepG2 cell line*", submitted by *Swapna Sasi U S* to the Academy of Scientific and Innovative Research (AcSIR), in partial fulfillment of the requirements for the award of the Degree of *Doctor of Philosophy in Biological Sciences*, embodies original research work carried-out by the student. We, further certify that this work has not been submitted to any other University or Institution in part or full for the award of any degree or diploma. Research material(s) obtained from other source(s) and used in this research work has/have been duly acknowledged in the thesis. Image(s), illustration(s), figure(s), table(s) etc., used in the thesis from other source(s), have also been duly cited and acknowledged.


Swapna Sasi U S
16-09-2021


Dr. K G Raghu
16-09-2021

Statements of Academic Integrity

I Swapna Sasi U S, a Ph.D. student of the Academy of Scientific and Innovative Research (AcSIR) with Registration No. 10BB16A39016 hereby undertake that, the thesis entitled "*In vitro* based mechanistic study on the role of fructose and palmitate in the genesis of steatosis in HepG2 cell line" has been prepared by me and that the document reports original work carried out by me and is free of any plagiarism in compliance with the UGC Regulations on "*Promotion of Academic Integrity and Prevention of Plagiarism in Higher Educational Institutions (2018)*" and the CSIR Guidelines for "*Ethics in Research and in Governance (2020)*".



16-09-2021

Thiruvananthapuram

It is hereby certified that the work done by the student, under my/our supervision, is plagiarism-free in accordance with the UGC Regulations on "*Promotion of Academic Integrity and Prevention of Plagiarism in Higher Educational Institutions (2018)*" and the CSIR Guidelines for "*Ethics in Research and in Governance (2020)*".



Dr. K G Raghu

16-09-2021

Thiruvananthapuram

ACKNOWLEDGEMENT

With great pleasure, I express my sincere gratitude to my research supervisor Prof. (Dr) K G Raghu, for furnishing an opportunity to explore the exciting field of science. His valuable guidance, encouragement, timely advice, continuous support and patience made my research more comfortable. Without his assistance and dedicated involvement in each and every step, this thesis would have never been accomplished. I would like to thank you very much for your understanding over these past five years. I am genuinely indebted to his kindness during the challenging time and extremely satisfied to be connected with a kind-hearted person like Dr K G Raghu.

I also extend my deep gratitude to Dr. A. Ajayaghosh, Director and Dr. Suresh Das, former Director, CSIR – NIIST, Trivandrum for granting me to be with this prestigious institution and also for providing necessary facilities and atmosphere for carrying out the research work. I am also thankful to Mr. V.V Venugopal, Dr, Dileep Kumar B.S, Mr.M.M Sreekumar and Dr. A. Sundaresan, present and former heads of Agro Processing and Technology Division for their experienced advice and encouragement.

I would like to offer my special thanks to Doctoral Advisory Committee members: Dr. Madhavan Nampoothiri K, Dr. Dileep Kumar B.S, and Dr. Nisha P for their insightful advice and assistance during the course of my research work. I would also like to show my obligations to the present and former AcSIR co-ordinators, Dr. Karunakaran V, Dr. Suresh C.H and Dr. Luxmi Varma for their constant monitoring and timely advice for completing AcSIR requirements.

My sincere thank also goes to the scientists, Dr. Jayamurthy P, Dr. Priya S, Dr. Reshma M V, Dr. Beena Joy, Mr. Soban Kumar D.R, Dr. Anjineyulu Kothakota, Ms. Divya Mohan, Dr. Venkatesh R and Mr. Venkatesh T of Agro Processing and Technology Division for their valuable remarks during the divisional meeting.

Getting through my dissertation required more than academic support and I have many people to thank. I am pleased to say thank you to Dr. Sindhu G, Dr. Shyni G L, Dr. Soumya R.S, Dr. Genu George, Dr. Salin Raj, Dr. Anupama Nair, and Dr. Preetha Rani M R for their inspiring discussions, precious help and support during each and every stages of my research activities. Their immense support actually guided me to rectify numerous things. A heartfelt thank you for all that you have done.

Some special words of gratitude go to my friends Ms. Sreelekshmi Mohan, Ms. Sruthi C R, Ms. Poornima M S, and Ms. Roopasree O J, who have always been a major source of support and happiness, with whom I shared many memorable evenings in and out of the lab. Thanks for a great time and great memories! Special thanks to Ms. Jesmina A S for her immense support to carry out the AcSIR societal project.

It is my pleasure to thank Ms. Eveline M Anto, Ms. Lekshmi S, Ms. Lekshmi Krishnan, Ms. Taniya M S, Ms. Anagha Nair, Ms. Anusha, Mr. Billu Abraham, Ms. Sannya, Ms. Shini, Ms. Nidhina, Ms. Reshmitha, Dr. Varsha K, Dr. Sini S, Mr. Pratheesh and Mr. Sreejith and all other friends of Agro Processing and Technology Division for all the fun we had in the past few years. I'm humbled and appreciative of all you've done for me.

I also place on record my sense of gratitude to one and all the members of the library, administrative, academic programme committee and technical staff of NIIST, who directly or indirectly, have lent their hand in this venture. I am also indebted to University Grants Commission, New Delhi, for financial assistance in the form of research fellowships.

Most importantly, none of this could have happened without my family. No more words to express all the unconditional love and support given to me by my beloved parents, Mr. Sasi Kumar and Mrs. Usha Kumari, have been selfless in giving me the best of everything. I am forever indebted to my parents for giving me the opportunities and experiences that have made me who I am. The unconditional love and support from my husband Mr. Renjithlal helped me to move ahead to accomplish my ambition. No more words to express appreciation for him.

I also express my sincere thanks to my father -in- law, Mr. Muraleedharan, mother -in- law, Mrs. Sujamani for their constant support and affection. Thanks to my sister -in-law, Ms. Reshma and brother -in-law, Mr. Abhilash for always being there for me as a friend.

Above all, I humbly praise and thank the Almighty for His constant blessings.

Swapna Sasi U S

TABLE OF CONTENTS

Sl.No	Contents	Page
1.	Certificate	i
2.	Statements of Academic Integrity	ii
3.	Acknowledgement	iii - iv
4.	Table of contents	v
5.	Chapter contents	vi - xi
6.	List of figures	xii - xiii
7.	List of abbreviations	xiv - xvi
8.	Chapter text	1 - 147
9.	Abstract	148
10.	List of publications	149
11.	List of scientific meetings	150 - 151

CHAPTER CONTENTS

CHAPTER 1: INTRODUCTION

1.1	Modern diet and health	1
1.2	Non alcoholic steatohepatitis (NASH)	2
1.2.1	Prevalence and incidence of NASH	2
1.2.2	Pathogenesis of NASH	4
1.2.3	Mechanism of steatosis development	6
1.3	Dietary fructose: Principal source of hepatic de novo lipogenesis	7
1.4	Lipotoxicity	9
1.5	Oxidative stress and NASH	10
1.6	Mitochondrial dysfunction and NASH	11
1.7	ER stress and NASH	13
1.8	Inflammation and NASH	17
1.9	Role of micronutrients in NASH	18
1.9.1	Role of iron in NASH	18
1.9.1.1	Effect of iron deficiency on hepatic lipids	19
1.9.1.2	Effects of iron overload on hepatic lipids	20
1.9.2	Role of antioxidant vitamins in NASH	21
1.9.2.1	Vitamin K (VK)	22
1.10	Diagnosis and treatment strategies of NASH	24
1.10.1	Weight loss	25
1.10.2	Dietary fat	25
1.10.3	Intake of low carbohydrate	25
1.11	Aims and objectives	26
	References	27 - 42

CHAPTER 2: DEVELOPMENT OF STEATOSIS IN HEPG2 CELL LINE WITH FRUCTOSE AND PALMITATE

2.1	Introduction	43
2.2	Materials and methods	44
2.2.1	Chemicals and reagents	44
2.2.2	Cell culture	44
2.2.3	Fructose and palmitate treatments of HepG2 cells	45
2.2.4	Cell viability	45
2.2.5	Oil-red-O staining	46
2.2.6	Triglyceride assay	46
2.2.7	Glycerol assay	46
2.2.8	Intracellular cholesterol accumulation	47
2.2.9	Western blot	47
2.2.10	Statistical analysis	48
2.3	Results	48
2.3.1	Effect of fructose and palmitate on cell viability	48
2.3.2	Effect of fructose and palmitate on lipid accumulation	48
2.3.3	Effect of fructose and palmitate on intracellular TG content	49
2.3.4	Effect of fructose and palmitate on lipolysis	50
2.3.5	Effect of fructose and palmitate on cholesterol accumulation	51
2.3.6	Effect of fructose and palmitate on lipid metabolism	52
2.4	Discussion	52
2.5	Summary and conclusion	56
	References	56 - 60

CHAPTER 3: EFFECT OF HIGH FRUCTOSE AND PALMITATE ON MITOCHONDRIAL BIOENERGETICS

3.1	Introduction	61
3.1.1	NASH and hepatic mitochondria	62
3.2	Materials and methods	64

3.2.1	Chemicals and reagents	64
3.2.2	Cell culture and treatment	64
3.2.3	Fructose and palmitate treatments of HepG2 cells	65
3.2.4	Mitochondrial superoxide production	65
3.2.5	Mitochondrial membrane potential ($\Delta\Psi_m$)	65
3.2.6	Mitochondria isolation	66
3.2.7	Mitochondrial respiratory complexes	66
3.2.8	Oxygen consumption assay	67
3.2.9	Aconitase activity	67
3.2.10	Intracellular calcium content	67
3.2.11	Caspase - 3 fluorometric assay	67
3.2.12	Flow cytometric analysis with annexin V/PI	68
3.2.13	Western blot	68
3.2.14	Statistical analysis	68
3.3	Results	69
3.3.1	Effect of HFP on mitochondrial superoxide	69
3.3.2	Effect of HFP on $\Delta\Psi_m$	70
3.3.3	Effect of HFP on mitochondrial bioenergetics	71
3.3.4	Effect of HFP on oxygen consumption rate and aconitase activity	72
3.3.5	Effect of HFP on mitochondrial dynamics	72
3.3.6	Effect of HFP on mitochondrial biogenesis	73
3.3.7	Effect of HFP on calcium homeostasis	74
3.3.8	Effect of HFP on apoptosis	75
3.4	Discussion	76
3.5	Summary and conclusion	80
	References	81 - 87

CHAPTER 4: UPR^{ER} AND UPR^{mt}: MOLECULAR TARGETS OF FRUCTOSE AND PALMITATE INDUCED STEATOSIS IN HEPG2 CELLS

4.1	Introduction	88
4.1.1	Unfolded protein response in endoplasmic reticulum (UPR ^{ER}) and NASH	89
4.1.2	Unfolded protein response in mitochondria (UPR ^{mt}) and NASH	90
4.1.3	Mitochondria associated ER membrane (MAM) and NASH	90
4.2	Materials and methods	92
4.2.1	Chemicals and reagents	92
4.2.2	Cell culture and treatment	92
4.2.3	Fructose and palmitate treatments of HepG2 cells	92
4.2.4	Enzyme - linked immunosorbent assay (ELISA)	93
4.2.5	Immunofluorescence analysis	93
4.2.6	Western blot	93
4.2.7	Statistical analysis	94
4.3	Results	94
4.3.1	Effect of HFP on lipogenesis <i>via</i> IRE1 α / XBP1 arm of UPR ^{ER}	94
4.3.2	Effect of HFP on ATF6 pathway of UPR ^{ER}	95
4.3.3	Effect of HFP on PERK pathway of UPR ^{ER}	96
4.3.4	Effect of HFP on UPR ^{mt} pathway	97
4.3.5	Effect of HFP on mutual interaction between ER and mitochondria	97
4.4	Discussion	98
4.5	Summary and conclusion	102
	References	103 - 106

CHAPTER 5: ROLE OF IRON AND VITAMIN K ON FRUCTOSE AND PALMITATE INDUCED STEATOSIS IN HEPG2 CELLS

5.1	Introduction	107
5.2	Materials and methods	108
5.2.1	Chemicals and reagents	108

5.2.2	Cell culture and treatment	109
5.2.3	Induction of steatosis and treatment	109
5.2.4	Cell viability assay	109
5.2.5	Prussian blue staining	110
5.2.6	Oil-red-O staining	110
5.2.7	Lipid peroxidation	110
5.2.8	Preparation of cell lysate for antioxidant enzyme activities	111
5.2.8.1	Activity of superoxide dismutase	111
5.2.8.2	Determination of catalase activity	111
5.2.8.3	Activity of glutathione	111
5.2.9	Acridine orange / ethidium bromide staining (AO / EtBr)	112
5.2.10	Detection of ROS	112
5.2.11	Detection of secretory cytokines by ELISA	112
5.2.12	Immunofluorescence Analysis	112
5.2.13	Western blot	113
5.2.14	Statistical Analysis	113
5.3	Results	113
5.3.1	Effect of iron on cell viability	113
5.3.2	Effect of iron on HFP induced cell death	113
5.3.3	Iron uptake in HepG2 cells	114
5.3.4	Effect of iron on HFP induced lipid accumulation	115
5.3.5	Expression of transferrin receptor and ferritin during steatosis	117
5.3.6	Effect of iron on HFP induced oxidative stress	118
5.3.7	Effect of iron on HO-1 during steatosis	119
5.3.8	Effect of iron on HFP mediated inflammation through NF- κ B translocation	120
5.3.9	Effect of iron on HFP induced cytokine secretion	121
5.3.10	Effect of iron on HFP induced apoptotic and necrotic effects	122
5.3.11	Effect of iron on intrinsic pathway of apoptosis	123
5.4	Discussion	124
5.5	Role of vitamin k on fructose and palmitate induced steatosis	127

	Introduction	
5.6	Cell culture and treatment	128
5.7	Induction of steatosis and treatment	128
5.8	Results	128
5.8.1	Effect of VK ₁ on cell viability	128
5.8.2	Effect of VK ₁ on HFP induced cell death	128
5.8.3	Effect of VK ₁ on lipid accumulation	129
5.8.4	Effect of VK ₁ on intracellular ROS generation and Nrf2 expression	130
5.8.5	Effect of VK ₁ on antioxidant enzyme activity	131
5.8.6	Effect of VK ₁ on NF- κ B translocation during cellular steatosis	132
5.8.7	Effect of VK ₁ on proinflammatory cytokine formation <i>via</i> oxidative stress	133
5.8.8	Effect of VK ₁ on MAPKs pathway in HepG2 cells during steatosis	134
5.9	Discussion	136
5.10	Summary and conclusion	139
	References	140 - 144

CHAPTER 6: SUMMARY AND CONCLUSION

145-147

LIST OF FIGURES

Figure No.	Title	Page No.
Figure 1.1	The spectrum of NAFLD	2
Figure 1.2	Prevalence of NASH worldwide	3
Figure 1.3	Prevalence of fatty liver in children	4
Figure 1.4	Pathogenesis of NASH	5
Figure 1.5	Overview of fructose metabolism within hepatocytes	8
Figure 1.6	Overview of mammalian unfolded protein response system	15
Figure 1.7	The iron cycle	19
Figure 2.1	Schematic experimental setup of cell culture	45
Figure 2.2	Fructose and palmitate affect the cell viability of HepG2 cells	48
Figure 2.3	Fructose and palmitate induced intracellular lipid accumulation	49
Figure 2.4	Fructose and palmitate induced TG accumulation	50
Figure 2.5	Fructose and palmitate mediated lipolysis	50
Figure 2.6	Fructose and palmitate induced intracellular cholesterol accumulation	51
Figure 2.7	Fructose and palmitate induced steatogenesis in HepG2 cells	52
Figure 2.8	Standardized <i>in vitro</i> cell based model of steatosis	56
Figure 3.1	HFP induces mitochondrial superoxide generation in HepG2 cells	69
Figure 3.2	HFP causes dissipation of $\Delta\Psi_m$	70
Figure 3.3	HFP adversely affects mitochondrial bioenergetics during steatosis	71
Figure 3.4	HFP adversely affects oxygen consumption and aconitase activity	72
Figure 3.5	HFP induces imbalance in mitochondrial dynamics	73
Figure 3.6	HFP reduces mitobiogenesis during steatosis	74
Figure 3.7	HFP affects intracellular calcium homeostasis	75
Figure 3.8	HFP initiates apoptosis <i>via</i> caspase 3 activation	76
Figure 3.9	Schematic representation of mitochondrial dysfunction during steatosis	81
Figure 4.1	HFP stimulates lipogenesis <i>via</i> activation of IRE1 / XBP1 arm of UPR ^{ER} in HepG2 cells	94

Figure 4.2	HFP induces ER stress in HepG2 cells <i>via</i> upregulation of ATF6 pathway of UPR ^{ER}	95
Figure 4.3	HFP stimulates the activation of PERK pathway of ER stress	96
Figure 4.4	Conserved stress response pathway UPR ^{mt} was adversely affected during steatosis	97
Figure 4.5	HFP induced steatosis impaired the mutual interaction between ER and mitochondria	98
Figure 4.6	Schematic representation of altered UPR system during high calorie induced steatosis	102
Figure 5.1	Effect of iron on cell viability	114
Figure 5.2	Prussian blue staining of treated HepG2 cells	115
Figure 5.3	Effect of iron on lipid accumulation during HFP induced steatosis	116
Figure 5.4	Detection of iron proteins during HFP induced steatosis	117
Figure 5.5	Effect of iron on oxidative stress during HFP induced steatosis	118
Figure 5.6	Effect of iron on the expression of HO-1 during steatosis	119
Figure 5.7	Effect of iron on NF- κ B translocation during HFP induced steatosis	120
Figure 5.8	Effect of iron on proinflammatory cytokines during HFP induced steatosis	121
Figure 5.9	Effect of iron on apoptotic and necrotic cells during HFP induced steatosis	122
Figure 5.10	Effect of iron on apoptosis during HFP induced steatosis	123
Figure 5.11	Effect of VK ₁ on cell viability	129
Figure 5.12	Effect of VK ₁ on intracellular lipid accumulation during HFP induced steatosis	130
Figure 5.13	Effect of VK ₁ on oxidative stress during HFP induced steatosis	131
Figure 5.14	Effect of VK ₁ on endogenous antioxidant status during HFP induced steatosis	132
Figure 5.15	Effect of VK ₁ on NF- κ B translocation during HFP induced steatosis	133
Figure 5.16	Effect of VK ₁ on proinflammatory cytokines during HFP induced steatosis	134
Figure 5.17	Effect of VK ₁ on signaling factors involved in MAPKs pathway during HFP induced steatosis	135
Figure 5.18	Schematic representations on the role of iron and vitamin K during steatosis	139

ABBREVIATIONS

ACC	:	Acetyl-CoA carboxylase
ALD	:	Alcoholic liver disease
AMPK	:	Adenosine monophosphate activated protein kinase
AO / EtBr	:	Acridine orange / ethidium bromide staining
ATF4	:	Activating transcription factor 4
ATF6	:	Activating transcription factor 6
ATP	:	Adenosine triphosphate
Bcl-X1	:	B-cell lymphoma - extra large
BHT	:	2,6-di-tert-butyl-4-methylphenol butylated hydroxytoluene
Bip	:	Binding immunoglobulin protein
BMI	:	Body mass index
BSA	:	Bovine serum albumin
CHOP	:	C/EBP homologous protein
ChREBP	:	Carbohydrate - responsive element - binding protein
CRP	:	C - reactive protein
DCFH-DA	:	Dichloro-dihydro-fluorescein diacetate
DMSO	:	Dimethyl sulfoxide
DNL	:	De novo lipogenesis
DRP1	:	Dynamin-related protein 1
EDTA	:	Ethylene diamine tetracetic acid
eIF2 α	:	Eukaryotic translation initiation factor - 2 α
ELISA	:	Enzyme-linked immunosorbent assay
ER	:	Endoplasmic reticulum
ERAD	:	ER associated degradation
ERK1/2	:	Extracellular signal-regulated protein kinase
ETC	:	Electron transport chain
FAS	:	Fatty acid synthase
FBPase	:	Fructose 1, 6 - bisphosphatase
FBS	:	Fetal bovine serum

FDA	:	Food and Drug Administration
FFA	:	Free fatty acids
FIS1	:	Fission 1 protein
GAPDH	:	Glyceraldehyde 3 - phosphate dehydrogenase
GRP78	:	Glucose - regulated protein 78
GSH	:	Glutathione
HBSS	:	Hank's balanced salt solution
HCC	:	Hepatocellular carcinoma
HFCS	:	High fructose corn syrup
HO-1	:	Haem oxygenase 1
Hsp	:	Heat shock protein
IP3R	:	Inositol 1,4,5-trisphosphate receptors
IR	:	Insulin resistance
IRE1	:	Inositol - requiring enzyme 1
I κ B- β	:	Inhibitor of NF- κ B kinase subunit β
JNK	:	c - jun N - terminal kinase
LDL	:	Low - density lipoprotein
MAM	:	Mitochondria associated ER membrane
MAPK	:	Mitogen activated protein kinases
MCP-1	:	Monocyte chemoattractant protein - 1
MDA	:	Malondialdehyde
MEM	:	Minimum essential medium
MFN2	:	Mitofusin-2
MtDNA	:	Mitochondrial DNA
MTT	:	3-(4,5-dimethylthiazol-2-yl)-2,5-diphenyl tetrazolium bromide
MUFA	:	Mono unsaturated fatty acids
NAFLD	:	Non alcoholic fatty liver disease
NASH	:	Non alcoholic steatohepatitis
NF- κ B	:	Nuclear factor kappa B
NLRP3	:	NOD - like receptor family pyrin domain containing 3
Nrf2	:	Nuclear factor erythroid 2 - related factor 2

NTBI	:	Non-transferrin bound iron
OPA1	:	Optic atrophy 1
OXPPOS	:	Oxidative phosphorylation
PBS	:	Phosphate buffered saline
PDI	:	Protein disulphide isomerase
PERK	:	Protein kinase RNA-like endoplasmic reticulum kinase
PGC-1 α	:	Peroxisome proliferator - activated receptor gamma coactivator 1 α
PPAR – α	:	Peroxisome proliferator - activated receptor α
PUFA	:	Polyunsaturated fatty acids
PVDF	:	Polyvinylidene difluoride
RIPA	:	Radioimmunoprecipitation assay buffer
ROS	:	Reactive oxygen species
SCD-1	:	Stearoyl - CoA - desaturase - 1
SDS-PAGE	:	Sodium dodecyl sulfate polyacrylamide gel electrophoresis
SOD	:	Superoxide dismutase
SREBP-1c	:	Sterol regulatory element - binding protein 1c
STZ	:	Streptozotocin
T2DM	:	Type 2 diabetes mellitus
TBA	:	Thiobarbituric acid assay
TG	:	Triglyceride
TNF- α	:	Tumor necrosis factor alpha
UPR	:	Unfolded protein response
UPR ^{ER}	:	Unfolded protein response in endoplasmic reticulum
UPR ^{mt}	:	Unfolded protein response in mitochondria
VDAC	:	Voltage-dependent anion channels
VK	:	Vitamin K
XBP-1	:	X-box binding protein 1
$\Delta\Psi_m$:	Mitochondrial membrane potential

CHAPTER 1

INTRODUCTION & REVIEW OF LITERATURE

1.1 Modern diet and health

A balanced diet plays an essential role in the maintenance of health and prevention of diseases. It provides protection from many chronic non - communicable diseases such as heart diseases, diabetes and cancer. Eventhough nutrition prevents the onset of nutritional deficiencies, both under and overnutrition lead to disease development. Over nutrition not only affects the health but also promotes the development of different kinds of diseases that in turn adversely affect the quality of life, survival and reproduction in human beings. Majority of the people are unaware of the food they eat, its nutritional value and effects of these foods especially junk foods on health. Available evidence reveals the fact that over the past few decades, the quality of diet has declined drastically due to increased energy intake from junk foods. ‘Junk food’ simply means calorie rich food with little or no nutritional value. Since these foods have no dietetic significance and macronutrients such as proteins, healthy fats, micronutrients like vitamins, minerals, amino acids, and fibre contents are negligible, hence considered as unhealthy (Shridhar et al., 2015). The amount of refined sugars mainly in the form of high fructose corn syrup, trans fat, white flour, polyunsaturated fat and food additives are also higher. All these agents help to improve flavor, texture and shelf life and are found to be hazardous to our health and threaten life expectancy. In the last few decades, the consumption of junk foods has increased worldwide and the major driving force behind its consumption includes changes in lifestyle, ready availability, taste, easy to consume and marketing strategies. It has been reported that there is a strong positive correlation between junk food consumption and obesity among individuals (Mohammadbeigi et al., 2018). Globally Indians are amongst the top ten lists of most frequent junk food consumers and they are at the greater risk of developing obesity, type 2 diabetes mellitus (T2DM), cardiovascular diseases, hypertension, hyperlipidemia and liver diseases.

1.2 Non alcoholic steatohepatitis (NASH)

Fatty liver diseases are categorized into non alcoholic fatty liver disease (NAFLD) and NASH. NAFLD depicts a range of liver disorders recognized in individuals that do not consume a significant amount of alcohol (< 10 g / day for women and < 20 g / day for men) (Browning et al., 2004). The spectrum of NAFLD ranges from simple hepatic steatosis to hepatocellular carcinoma (HCC). Hepatic steatosis can be defined as the most common liver disease caused mainly due to triglyceride accumulation (TG) exceeding 5% of hepatocytes or 5% of the liver weight (Hoyumpa et al., 1975; Yeh & Brunt, 2007). Hepatic steatosis is followed by NASH characterized by inflammation deriving from the reactive oxygen species (ROS) products of mitochondrial dysfunction. Persistent inflammation leads to the development of scar tissues around the liver and blood vessels surrounding the liver, a stage called fibrosis. As disease severity increases, scar tissues replace the normal tissues, a condition referred to as cirrhosis. Cirrhosis ultimately leads to HCC, the sixth most common cancer in the world (Figure 1.1)

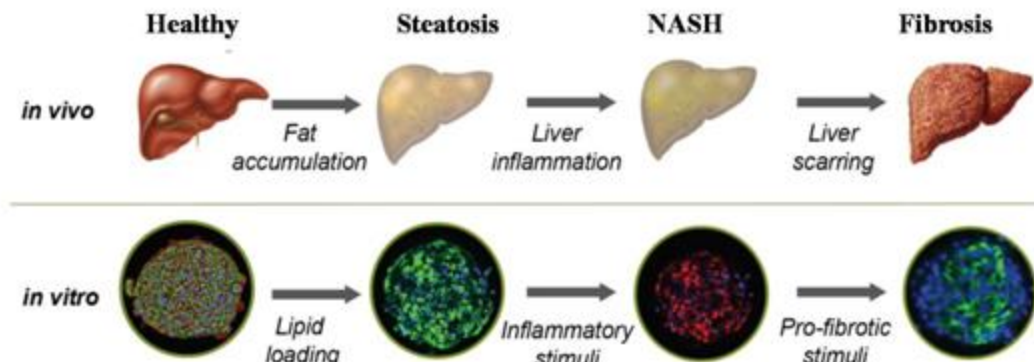


Figure 1.1 The spectrum of NAFLD

(<https://insphero.com/products/liver/disease-models/nash/>)

1.2.1 Prevalence and incidence of NASH

There has been expanding evidence promoting a very huge prevalence of NAFLD and NASH in the general population. Globally, the prevalence is around 25.2% and a high prevalence rate has been reported in the Middle East (31.8%) and South American countries (30.4%). Also the reported prevalence of NAFLD in Europe, Asia and North America are 23.7%, 27.4% and 24.1% respectively (Younossi et al., 2016) (Figure 1.2). It has been estimated that the prevalence of NASH in the general population lies between 1.5% and 6.45%. These tremendous

rates for NASH are mainly being driven by the universal epidemic of diabetes and obesity (Younossi et al., 2018; Chalasani et al., 2018). Studies have reported that the future concern of NAFLD in the United States is predicted to rise considerably due to the continuing increase in diabetes and obesity. By 2030, the prevalence of NASH will increase by 63% in the US, leading to an increasing incidence of NASH related cirrhosis by 168%, HCC by 137% and liver related deaths by 178% (Estes et al., 2018).

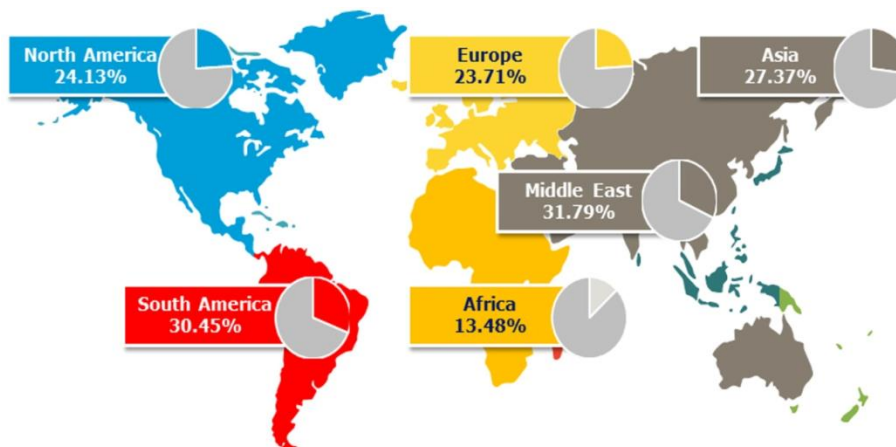


Figure 1.2 Prevalence of NASH worldwide (Younossi et al., 2018)

An additional facet of NASH in Asia is called “lean NASH” or “non obese NASH” where the individual possess normal body mass index but handles the energy metabolism defectively. Lean NASH has also been reported in the pediatric population where the prevalence is around 26 - 60%. It is expected that both obese and lean NASH share a frequent altered metabolic profile with an excess of abdominal adipose tissue and increased prevalence of metabolic diseases. The incidence of NASH is also related to personal variables or medical conditions and miscellaneous random factors. This comprises treatment with certain classes of drugs, bariatric surgery, and vulnerability to various environmental toxins (Adams & Angulo, 2006). The prevalence of NASH is still higher in distinct cohorts such as those having T2DM and morbidly obese. Globally the prevalence of NASH among T2DM patients was 61.1%. The development of NASH is directly related to obesity and prevalence shown to increase with increasing body mass index. Other risk factors linked with NASH include presence of metabolic syndrome, hyperlipidemia, and hypercholesterolemia. In addition to these, factors like age, sex and ethnicity can also have a considerable influence on the risk of NASH. Moreover, the prevalence is higher in older patients and increases with age, male sex, and Hispanic ethnicity

(Lonardo et al., 2015). Moreover, the prevalence of NASH is higher in men and post menopausal women suggesting the multiple effects of sex hormones on steatosis. It has been reported that estrogen has a profound effect on genes involved in lipid biosynthesis. There is a notable interaction between central obesity, NASH and insulin resistance also (Farrell & Larter, 2006).

Epidemiological studies suggested that the prevalence of NASH in India is around 9 - 32% of the general population. The most striking aspect is that the prevalence has also been reported in school children (Das et al., 2017) and is more common in obese children (8 - 80%) than normal weight children (3 - 10%). Higher body mass index (BMI) was also observed to be a risk factor for both sexes. The prevalence also shows a direct correlation with age. In addition, family history of hypertension, diabetes, and liver disease were present in 12.8%, 6.4% and 3.5% of children respectively and was not linked with severity of liver disease. However, with concern of under nutrition, the prevalence of fatty liver due to overweight and metabolic syndrome among children may vary from published records.

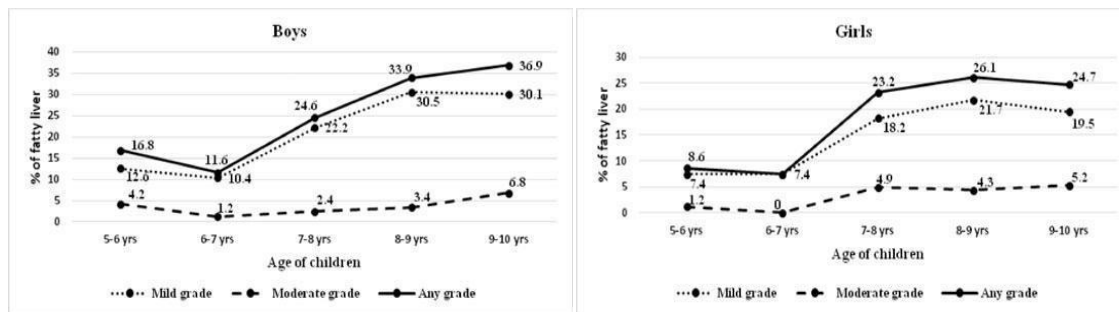


Figure 1.3 Prevalence of fatty liver in children (Das et al., 2017)

1.2.2 Pathogenesis of NASH

The pathophysiology behind NASH is a complex process with multiplex complications. Liver steatosis appears as an after effect of imbalance between hepatic lipid accumulation (due to increased influx of free fatty acids (FFAs) and hepatic lipid clearance (by FFA oxidation and very low density lipoprotein excretion) (Conlon et al., 2013). To explain the pathogenesis, a “two hit” hypothesis was proposed over decades ago (Day & James, 1998) to make an access to unravel the progression from NAFLD to NASH. The “first hit” is peripheral insulin resistance (IR) as a leading cause concomitant with obesity and metabolic syndrome.

During IR, there will be an increased lipolysis in adipose tissue, results in the delivery of FFA to the liver and ends up in intracellular TG accumulation. Moreover de novo lipogenesis

(DNL) also possesses a pivotal role in FFA synthesis where excess carbohydrates are converted into fatty acids and esterified into TG (Paglialunga & Dehn, 2016). Certainly, it has been proposed that hepatic TG accumulation is also a consequence of saturation of FFA oxidation (Gaggini et al., 2013). On the contrary, several studies suggested the protective effect of TG (Koliwad et al., 2010) as increased level of intrahepatic TG may be a biomarker instead of a causative factor of IR (Amaro et al., 2010).

The “second hit” that promotes the disease progression is mainly oxidative stress, which in terms may explain the progression to liver fibrosis. Oxidative stress induces hepatocellular injury by inactivating membrane sodium channels and inhibiting enzymes of the mitochondrial respiratory chain. Besides this, oxidative stress induces lipid peroxidation and cytokine secretion and thus endorses the advancement from simple steatosis to NASH (Leamy et al., 2013). But later the “two hit” hypothesis can no longer completely explain the pathogenesis of NASH, so Tilg & Moschen (2010) proposed the “multiple parallel hits” model since many hits may act in parallel favoring the progression from NAFLD to NASH. Along with this, multiple interactions among environmental, hormonal, nutritional and predisposing genetic variants were portrayed in terms of the “multiple hit” hypothesis.

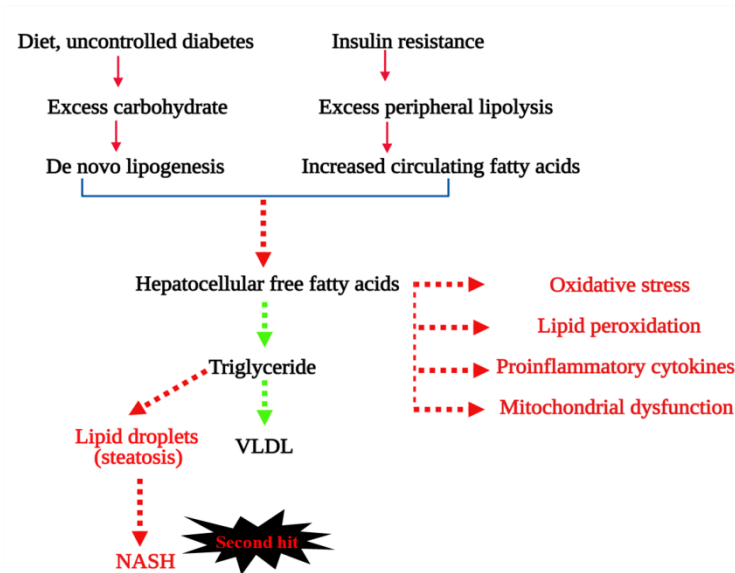


Figure 1.4 Pathogenesis of NASH

The initial events arise due to the development of obesity and IR in liver and adipose tissue. IR is the pivotal mechanism that leads to lipotoxicity, ER stress, disturbed autophagy, and finally hepatocyte injury and inflammation (Arab et al., 2018). Moreover, dysregulation of peripheral lipolysis, excess carbohydrate, dietary fat and DNL cause increased hepatocellular FFA results in lipotoxic condition. These lipotoxic FFAs are separated into TG *via* acyl-CoA synthetic activity for storage and mitochondrial β oxidation. The accumulation of TG in hepatocytes cytoplasm is called steatosis, the widely accepted hallmark of NAFLD (Leoni et al., 2018). Irresistible lipotoxicity promotes ROS formation, ER stress and hepatocellular dysfunction followed by fibrosis development over time.

1.2.3 Mechanism of steatosis development

Hepatic lipid homeostasis is firmly coordinated by a complex system of signaling pathways driven by hormones, transcription factors, and nuclear receptors with insulin signaling playing a fundamental role (Hardy et al., 2016). Alteration in insulin signaling in liver and adipose tissue seems to be the pioneer event. Development of IR in adipose tissue leads to lipolysis results in excess influx of non esterified fatty acids to the liver where they are absorbed by hepatocytes in a facilitated manner. The initial step of TG accumulation is mainly due to the imbalance between its synthesis and utilization. Dietary fat and DNL are the two other potent sources that favor hepatic lipid accumulation. The synthesis of fatty acid is catalyzed mainly by two enzymes, acetyl-CoA carboxylase (ACC) and fatty acid synthase (FAS). At the transcriptional level, these two enzymes are controlled *via* the activation of sterol regulatory element - binding protein 1c (SREBP-1c) by insulin and activation of carbohydrate - responsive element - binding protein (ChREBP) by glucose. During NASH, DNL increases considerably due to hyperinsulinemia and excess intake of simple sugars like fructose stimulate SREBP - 1c and ChREBP respectively (Softic et al., 2016).

The development of hepatic steatosis is intensified by dietary caloric and intake of specific nutrients. Among dietary factors, fructose is the powerful inducer of hepatic DNL. Compared to cells of other tissues, hepatocytes are exposed to higher concentrations of fructose because after absorption fructose is directly transported to the liver *via* the portal vein (Softic et al., 2016). Fructose has been shown to induce lipogenic expression and stimulates DNL (Janevski et al., 2012). It has been proposed that fructose enhances the disease severity by reducing cellular energy and increasing metabolic byproduct, uric acid. Evidence also suggested

that fructose imposes greater risks compared to glucose. It also strongly promotes hyperlipidemia (Chong et al., 2007). The metabolism of fructose is not strictly regulated like glucose and it bypasses the rate limiting step catalyzed by phosphofructokinase of glycolysis. Therefore, fructose can directly provide dihydroxyacetone phosphate, glyceraldehydes and trioses that may enter the Krebs cycle and convert into glucose or lactate or enter into gluconeogenesis or lipogenesis. Researchers revealed that compared to high glucose (60%), high fructose (60%) fed rats have been shown to have increased expression of lipogenic genes including FAS (Koo et al., 2008). This group later proved the potential effect of fructose in elevating the level of ChREBP and SREBP-1 within the nucleus of rat livers. Fructose fed groups also increase the conversion of glucose to glycogen. On the other hand, sustained fructose feeding reduces the conversion of glucose to glycogen. Sometimes, fructose to glucose conversion may cause lipogenic effects. To avoid that possibility, fructose 1, 6 - bisphosphatase (FBPase) inhibitor was used in an *in vitro* model cultured in low and high glucose or fructose. Fructose also reinforces the expression of fructokinase and aldolase B expression (Koo et al., 2008) for efficient fructolysis.

1.3 Dietary fructose: Principal source of hepatic de novo lipogenesis

Fructose is a monosaccharide found naturally in fruits and some vegetables. Before industrialization, fructose was strictly limited in the human diet. A fructose content of 5 -10% by weight is found in grapes, raw apples, persimmons and blueberries. However in the last few decades, there was a rapid rise of fructose consumption chiefly in the form of high fructose corn syrup (HFCS). A study revealed that fructose content in several soft drinks and beverages is approximately 65%. A large number of meta analyses suggested that the risk of metabolic syndrome; increased TG levels, visceral fat and DNL is directly proportional to the consumption of sugar sweetened beverages (Ferder et al., 2010). Fructose is also a potential source of NASH due to its ability to act as a substrate for DNL and also bypassing the major rate limiting step catalyzed by phosphofructokinase. While glucose metabolism occurs in each cell of the body, fructose metabolism is entirely restricted in the liver. Hence continuous fructose consumption imposes a metabolic burden on the liver by inducing fructokinase and FAS. Due to the increased phosphorylation of fructose to fructose -1- phosphate, there is an intense fall in hepatic adenosine triphosphate (ATP). Consequently the accumulated ADP serves as substrate for uric acid formation. Soluble uric acid possess several proinflammatory effects including nuclear factor

kappa B (NF-κB) activation, stimulation of monocyte chemoattractant protein - 1 (MCP-1) and NOD - like receptor family pyrin domain containing 3 (NLRP3) inflammasomes (Wan et al., 2016). All these events lead to hepatic oxidative damage and lipid peroxidation.

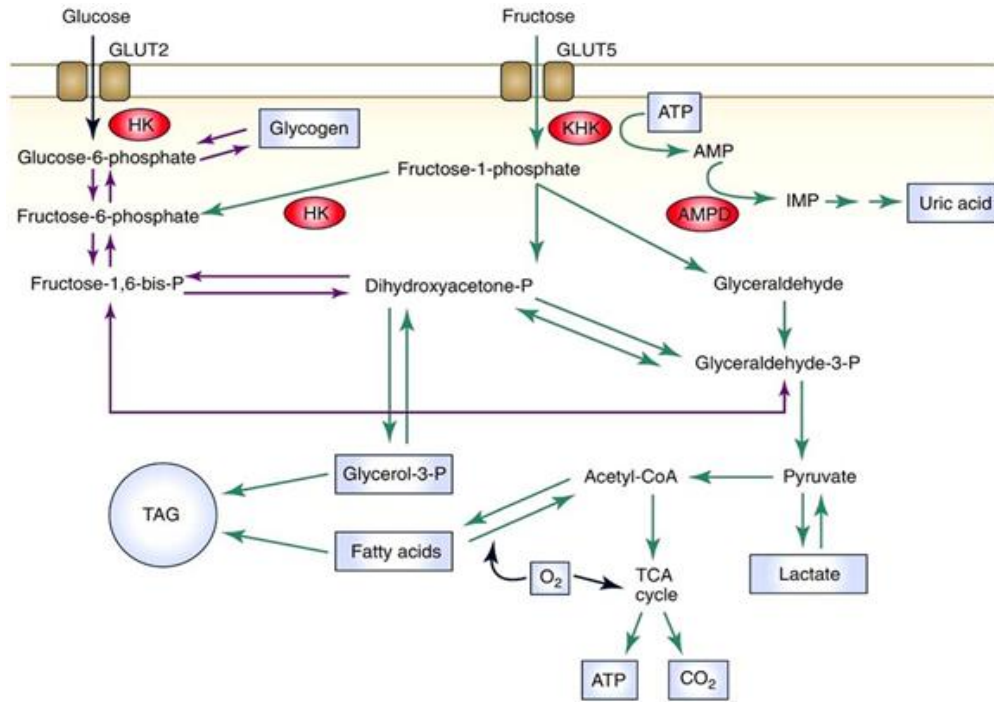


Figure 1.5 Overview of fructose metabolism within hepatocytes (Pinnick & Hodson, 2019)

A large number of observational and experimental studies have manifested the deleterious effects of dietary fructose consumption on insulin resistance, obesity, hepatic steatosis and NAFLD related fibrosis. Animal studies demonstrated that administration of HFCS for 16 weeks developed hepatic steatosis with necroinflammatory changes (Neuschwander et al., 2012). Fructose feeding also induces the activation of several lipogenic genes: FAS, ACC and stearoyl - CoA desaturase - 1 (SCD-1) (Rodriguez et al., 2009). Administration of fructose for seven years in cynomolgus monkeys revealed an increase in liver fat and hepatic fibrosis, where the degree of fibrosis is related with the duration of fructose exposure (Cydylo et al., 2017). Fructose induced metabolic syndrome was also observed in rhesus monkeys (Bremer et al., 2011). To evaluate the effects of decreasing fructose intake in NASH patients, dietary interventions have also been subjected to investigations. A six month dietary study in NASH patients resulted in decrease in fructose content by half with drastic reduction in hepatic lipid content, improved fasting plasma insulin levels and BMI (Volynets et al., 2013). Most of the

experimental and clinical studies recommend a positive correlation between NASH and fructose intake. However, one epidemiological study from Finland found an inverse relationship between NASH and fructose intake. Here the consumption of soft drinks is less than 10% of the population and fruit intake was more prevalent (Kanerva et al., 2014). The presence of fructose in fruits is feasible to induce metabolic syndrome; moreover they also possess ascorbate, flavonols, and other antioxidants that may conflict with the effects of fructose.

It has been reported that consumption of glucose or fructose sweetened beverages in obese and overweight individuals results in hepatic DNL and hypertriglyceridemia. Although both glucose and fructose consuming groups attained similar amounts of weight, only the fructose consuming groups exhibited significant increase in visceral adipose volume (Stanhope et al., 2009). The concentration of plasma lipid, lipoproteins and markers of lipid metabolism and lipoprotein remodeling were increased during fructose consumption but remained consistent for glucose concentration. Another randomized cross over study (Hochuli et al., 2014) reported that a limited amount of fructose supplementation (40 g / day) upregulates fatty acid synthesis, but not high sucrose or glucose (80 g / day).

1.4 Lipotoxicity

Saturated fatty acids play a key role in the “second hits” that stimulate disease progression. Hepatocyte cell death in NASH because of lipotoxicity is called lipoapoptosis. The extent of lipoapoptosis is positively correlated to NASH severity. The presence of excess FFAs in hepatocytes that are converted into TG is associated with increased lipoapoptosis. During NASH, the accumulation of saturated fatty acids is higher compared to monounsaturated fatty acids (MUFA) and polyunsaturated fatty acids (PUFA). The 16 - carbon palmitate and 18 - carbon stearate are the major saturated fatty acids associated with disease progression (Malhi & Gores, 2008). In cultured hepatocytes, the molecular pathways that mediate palmitate toxicity have been attractively exemplified (Malhi & Gores, 2008; Musso et al., 2018). It has the potential to activate both intrinsic and extrinsic mediated apoptosis in hepatocytes. To date, it is well defined that ER and oxidative stress induced by FFA activate numerous signaling pathways including the activation of intracellular stress activated kinase c - jun N - terminal kinase (JNK) (Malhi et al., 2006), up regulation of proapoptotic proteins Bim, degradation of antiapoptotic proteins B-cell lymphoma - extra large (Bcl-xL) and inhibitor of apoptosis proteins. Diacylglycerols, ceramides, lysophosphatidyl choline and free cholesterol are the other lipotoxic

species that promote steatosis (Musso et al., 2018). During lipotoxicity, damaged hepatocytes release cytokines, chemokines, extracellular vesicles and other intracellular molecules that can activate Kupffer cells, hepatic stellate cells and also recruit other immune cells. Thus lipotoxicity favors inflammation and disease progression.

1.5 Oxidative stress and NASH

Oxidative stress can be defined as the status under which the generation of ROS exceeds the detoxification capacity of antioxidants. Liver is the central organ where several oxidative processes occur and is the crucial target of oxidative stress induced damage. In the liver, the imbalance of antioxidant status contributes to the pathogenesis and progression of persistent liver diseases including NAFLD (Li et al., 2015). The accumulation of fat in the liver provides cue for excessive ROS generation in mitochondria, endoplasmic reticulum (ER) stress, inflammation, cellular injury and cell death. The major sources of oxidative stress during NASH include oxidative phosphorylation (OXPHOS) in mitochondria that generates ATP along with superoxide anions. In addition, β oxidation in mitochondria and peroxisomes are other potential sources for oxidative stress. ER is another vital organelle responsible for reactive oxygen species (ROS) production mainly due to cytochrome P450 activity or due to increased C/EBP homologous protein (CHOP) expression. Inflammatory responses are another definite source that furnishes oxidative stress.

In hepatocytes, oxidative stress stimulates signals for inflammatory responses and activation of cell death pathways (Al-Asmari et al., 2016). The translocation of redox sensitive transcription factor, nuclear factor erythroid 2 - related factor 2 (Nrf2) to the nucleus is initiated by high levels of ROS, where it promotes the transcription of antioxidant genes which are modulated by antioxidant response elements. Interestingly, Nrf2 also brings the expression of several detoxifying enzymes that eliminate radicals from cytosol, mitochondria and ER. Nrf2 possesses an elaborative role in lipid metabolism hence affording protection against liver damage during the development of steatosis and steatohepatitis (Galicía et al., 2020). Nrf2 alleviates hepatic steatosis by repressing the expression of lipogenic enzymes. Certain *in vivo* studies showed a negative correlation between Nrf2 induced transcription and hepatic lipogenesis (Zhang et al., 2012). There are also controversial studies that failed to detect an effect on lipid metabolism and even described the positive relation of Nrf2 with lipid accumulation.

It has been proposed that NF- κ B pathway due to its role in oxidative stress mediated responses can act as a therapeutic target in liver diseases. Moreover, NF- κ B signaling is closely associated with both prooxidant as well as antioxidant effects which are related to the activation of ER stress response (Lingappan, 2018). Since it is a redox sensitive transcription factor, its activation is regulated by ROS through proinflammatory cytokines like tumor necrosis factor alpha (TNF- α). In general, it has been proclaimed that NF- κ B negatively regulates the transcription of Nrf2 and its deficiency is associated with enhanced NF- κ B activation (Pan et al., 2012). Since hepatic oxidative stress and inflammation are associated with increased oxidative metabolism of saturated fatty acids, these are often incompletely oxidized in the mitochondria leading to ROS production and organelle dysfunction (Masarone et al., 2018).

Oxidative stress also causes deleterious effects on macromolecules ensuing in the formation of toxic products like malondialdehyde (MDA), 8-isoprostane, lipid peroxides etc. These radicals are formed due to hydroxyl radical attack to fatty acyl chains of triglycerides and phospholipids. Lipid peroxides may act as a causative factor for reactive molecule generation or impairment of cellular structures and architecture. By considering this, oxidative stress and impaired lipid metabolism can be an efficient target for NASH.

1.6 Mitochondrial dysfunction and NASH

Mitochondria are key organelles that play a pivotal role in energy generation from glucose and lipid metabolism. Much evidence pointed out that NASH was principally characterized by the presence of mitochondrial dysfunction (Caldwell, 1999). In hepatocytes, the balance between fat and energy is regulated by mitochondrial activities like β oxidation of FFAs, electron transfer, ATP and ROS production (Grattagliano et al., 2012). Mitochondrial dysfunction alters the balance between prooxidant and antioxidant mechanisms. The resulting ROS generation blocks the β oxidation of fatty acids so that influx of non metabolized fatty acids to the cytosol increases. The liver tissue from patients with NASH indicates high levels of ROS mediated mitochondrial DNA (mtDNA) damage (Pessayre, 2007). It has been reported that during IR associated NASH, mitochondrial dysfunction may be the stimulator of fatty acid accumulation in hepatocytes (Silva et al., 2008). It is also noted that during the early stage of fat infiltration in hepatocytes, a large number of adaptive metabolic mechanisms are intervened by mitochondria to prevent oxidative stress and ROS production.

Increased cholesterol accumulation is also a major factor associated with steatosis to NASH transition. The cholesterol content is negatively correlated with mitochondrial glutathione (mtGSH) in NASH patients (Gan et al., 2014). Decreased mtGSH may arise due to the damage to mtGSH transport system, which helps in the transportation of GSH from cytosol to mitochondria. High cholesterol level is also responsible for alteration in membrane permeability. Recently it has been reported that a combination of high cholesterol diet and high fat diet synergistically facilitate disease progression (Bellanti, 2018). Moreover, an increase in cholesterol is negatively affecting ATP synthesis mediated by ATP synthase and ATP / ADP exchange in the inner and outer mitochondrial membranes (Campbell et al., 2007).

Excess FFAs and increased insulin resistance condition leads to an increase in the permeability of the inner mitochondrial membrane. As a result there will be a dissipation of mitochondrial membrane potential ($\Delta\Psi_m$) culminating in impaired mitochondrial functions and enhanced ROS generation. Alteration in $\Delta\Psi_m$ may also generate “electron leakage” due to the decreased activity of various complexes in the electron transport chain (ETC). This established the direct relation between electron and oxygen leading to ROS formation. The hepatic tissues from obese (*ob / ob*) mice have been shown to have high levels of lipogenesis from glucose (Begriche et al., 2010), increased mitochondrial superoxide and lipid peroxidation, reduced levels of ETC components and decreased ATP levels. Studies explained that prolonged mitochondrial dysfunction activates adenosine monophosphate activated protein kinase (AMPK) and JNK which is known to be mitogen activated protein kinases (MAPKs) (Herzig & Shaw, 2018). Activation of these signaling pathways plays an essential role in the development of liver diseases and injuries: steatosis, NASH, fibrosis and HCC (Quinlan et al., 2003).

It is well known that mitochondrial complex I and complex II are the major sites for superoxide production (Kotiadis et al., 2014). An enzyme named superoxide dismutase converts superoxide into hydrogen peroxide (H_2O_2) which can cause mitochondrial damage or initiate stress signaling response. Even with exposure to oxidative stress and ROS, there is a continuous mitochondrial remodeling which comprises mitochondria fission and fusion, dynamics of energy expenditure and gene expression (Sunny et al., 2017). Mitochondria undergo morphological changes with the help of different molecules like dynamin - related protein 1 (DRP1), mitochondrial fission 1 protein (FIS1), mitofusin-2 (MFN2) and optic atrophy 1 (OPA1). Along with morphological control, selective degradation of damaged mitochondria is also monitored

via a process called mitophagy. AMPK can induce mitophagy and also activate glucose and fatty acid oxidation pathways by stimulating the activation of peroxisome proliferator - activated receptor gamma coactivator 1 α (PGC-1 α) (Herzig & Shaw, 2018). Activated PGC-1 α interacts with peroxisome proliferator - activated receptor α (PPAR- α) and induces the expression of enzymes involved in fatty acid metabolism later on stimulating mitochondrial fatty acid oxidation. They are also fundamental for coordinating the transcriptional activity of several nuclear and mitochondrial genes that encode components of ETC *via* transcription factors like Nrf1 and 2 (Clementi & Nisoli, 2005). Several Nrf2 activators possess protective functions by regulating the biosynthesis and regeneration of glutathione and favorable NAD⁺/NADPH ratio to control ROS generation (Holmstrom et al., 2016).

During NASH, there will be impairment in mitochondrial protein synthesis (Mansouri et al., 2018). Since the mitochondrial genome is highly susceptible for oxidative damage, it can result in overall mtDNA depletion. Downregulation of mtDNA encoded polypeptides and lower activity of complex I, III, IV and V have also been found in steatohepatitis (Santamaria et al., 2003). Sirtuins are a class of NAD⁺ dependent deacetylase sophisticated in oxidative damage of both alcoholic liver disease (ALD) and NAFLD. By activating long-chain acyl-CoA dehydrogenase, sirtuin 3 (SIRT3) can increase β oxidation of FFAs. Its activity was also decreased in animal models with fatty liver. This indicates down regulation of SIRT3 during a high fat diet can take up pathological processes. Sirtuins can bring out various metabolic improvements by using NAD⁺ as the co-substrate (Gariani et al., 2016). In this way, depletion in NAD⁺ can achieve mitochondrial dysfunction obstructing the adaptive response resolved by sirtuins to high hepatic FFA levels.

1.7 ER stress and NASH

Generally, ER is the central organelle that provides a highly specialized environment for the production and post translational modification of proteins, lipid synthesis and maintenance of calcium homeostasis. The hepatocytes are rich in ER and it possesses miraculous space to adapt various intracellular and extracellular changes to preserve hepatic metabolic functions. Due to its high capacity for protein synthesis, the development of ER stress response plays a significant role in the prevention and pathological changes in liver diseases (Malhi & Kaufman, 2011). Yet in humans, numerous disruptions like hyperlipidemia, inflammation, drugs etc. can affect ER homeostasis in hepatocytes thereby pave the way for alteration in lipid metabolism and liver

disease. In order to restore the ER homeostasis, eukaryotic cells possess an evolutionarily conserved pathway termed unfolded protein response (UPR) system. ER stress and UPR are implicated in the development of steatosis and progression to NASH; hence it has become a subject of substantial interest in recent years.

The UPR system in ER consists of three transmembrane ER resident stress sensor proteins: inositol - requiring enzyme 1 (IRE1), Protein kinase RNA-like endoplasmic reticulum kinase (PERK), and activating transcription factor (ATF6). During normal stages, these proteins are maintained in the inactive stage by glucose - regulated protein 78 (GRP78). When misfolded proteins accumulate above the threshold level, GRP78 dissociates from the sensor proteins priming all branches of UPR for activation. Protein disulphide isomerase (PDI) may also control the sensor proteins (Eletto et al., 2014).

IRE1 is the most conserved ER stress transducer. During ER stress, it dissociates from the binding immunoglobulin protein (Bip) and autophosphorylation promotes the splicing of X-box binding protein 1 (XBP1) mRNA and producing transcriptionally active form of XBP1. It acts as a transcriptional factor that enters the nucleus and regulates gene expressions that are involved in ER protein folding and secretion, ER membrane biogenesis, lipid synthesis and ER associated degradation (ERAD) (Hassler et al., 2015). It has been proved that genetic ablation of either IRE1 or XBP1 results in embryonic lethality with major liver defects (Reimold et al., 2000; Zhang et al., 2005). Under sustained ER stress conditions, activated IRE1 stimulates the JNK pathway for triggering apoptosis. In the last few years, researchers are mainly focussing on arrays of novel regulators and post translational modifications to tune the UPR stress sensor activity (Hetz & Papa, 2018).

ATF6 is a basic leucine – zipper transcription factor function in cell-tissue specific manner. Once activated, it translocates to the Golgi apparatus where it is processed by proteases, S1P and S2P. The cleaved cytosolic fragment enters the nucleus and regulates transcription of genes including XBP1. ATF6 also forms a complex with SREBP2 to suppress the transcription and prevent its lipogenic effect.

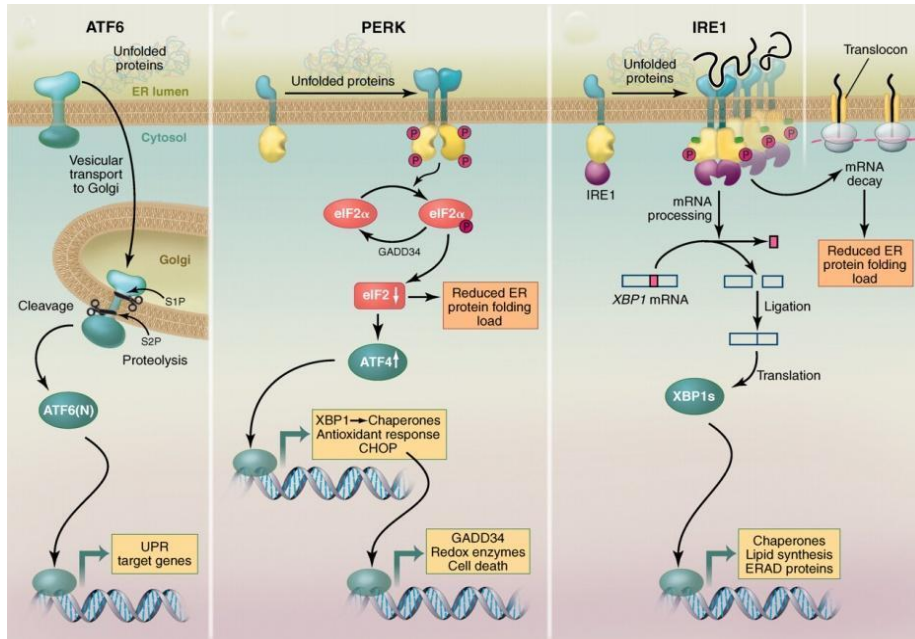


Figure 1.6 Overview of mammalian unfolded protein response system (Walter & Ron, 2011)

PERK is a serine / threonine transmembrane protein kinase. The dissociation of Bip from the luminal side of PERK leads to its oligomerization and autophosphorylation. Activated PERK regulates protein synthesis *via* eukaryotic translation initiation factor - 2 α (eIF2 α). eIF2 α in its phosphorylated form halts mRNA translation and thus prevents protein overload to ER. This inhibition also favors the translation of UPR mRNAs like activating transcription factor 4 (ATF4), which performs a vital role in protein folding, redox homeostasis, aminoacid metabolism, autophagy and apoptosis (Ameri & Harris, 2008). The prolonged ER stress insists on the PERK - eIF2 α - ATF4 complex to convert the survival signal into an apoptotic signal. Although PERK and ATF6 are not essential for liver development, studies conducted on global knockouts have demonstrated that both are necessary to facilitate recovery from dietary or pharmacological challenges (Yamamoto et al., 2010).

The ER stress induction was first reported in the livers of genetic and diet induced NASH models (Ozcan et al., 2004). This finding have also been confirmed in mice fed with methionine - choline deficient diet exhibiting hepatic steatosis without obesity (Rahman et al., 2007) and other obese animal models (Wang et al., 2006; Sreejayan et al., 2008). More recently, the activation of UPR factors was also disclosed in the livers of patients with NAFLD or NASH (Puri et al., 2008). In this context, specific nutrients have been found to activate the UPR. It has

been reported that saturated fatty acids induce ER stress (Boden et al., 2011) and high glucose also stimulate protein glycosylation and hexosamine biosynthetic pathway beyond that which normally happens in ER (Sage et al., 2010).

It has been well known that ER stress favors alteration in lipid metabolism and hepatic steatosis. In recent times, several studies exploited the role of unique arms of UPR and their downstream signaling molecules in cell culture and animal models to elucidate their functions in lipid metabolism. Firstly it has been reported that the PERK - eIF2 α - ATF4 pathway regulates lipogenesis and hepatic steatosis. Deletion of PERK inhibits the continuous expression of lipogenic enzymes (Bobrovnikova et al., 2008). Moreover, eIF2 α mediated signaling results in declined hepatic steatosis in high fat diet animals (Oyadomari et al., 2008). Protein kinase mediated p-eIF2 α increases the ATF4 translocation. Studies showed that ATF4 knockout mice are protected from diet induced obesity, hypertriglyceridemia and steatosis. In addition, depletion of ATF4 reduces the expression of lipogenic genes such as PPAR γ , SREBP-1c, ACC, and FAS in liver and white adipose tissue (Wang et al., 2010, Xiao et al., 2013).

Secondly, it has been reported that the hepatic lipid homeostasis during ER stress was maintained by the IRE1 - XBP1 pathway. Mice with specific deletion of IRE1 when treated with ER stress inducers develop severe hepatic steatosis due to the down regulation of major transcriptional regulators and enzymes involved in TG biosynthesis (Zhang et al., 2011). The assembly and secretion of hepatic VLDL is also under the control of the IRE1 - XBP1 pathway. In hepatocytes, XBP1 regulates lipogenesis by binding to the promoters of a subset of lipogenic genes including SCD1 and ACC2. Therefore liver of mice with XBP1 deletion showed a decline in de novo lipid biosynthesis.

Third, ATF6 also plays an intensive role in ER stress induced lipid accumulation. In cultured liver and kidney cells, it has been revealed that nuclear ATF6 interacts with the nuclear form of SREBP2; thereby antagonizing SREBP2 regulated transcription of lipogenic genes and lipid accumulation (Zeng et al., 2004). ATF6 deficient mice showed a greater degree of hepatic steatosis and glucose intolerance in association with increased expression of SREBP-1c during high fat diet conditions (Usui et al., 2012). While considering the role of ER in lipid metabolism, DNL takes place in ER where excess free saturated fatty acids are incorporated into phospholipids of ER membrane. This results in alteration in mitochondrial membrane permeability, release of calcium from intracellular stores and activation of proinflammatory and

cell death pathways. Excess saturated fatty acids also induce the expression of chaperone GRP78, resulting in the activation of IRE1, ATF6 and PERK pathway of UPR.

1.8 Inflammation and NASH

The central role of oxidative stress and inflammation in the development of hepatic steatosis have been deciphered and highlighted for decades. Hepatic oxidative stress and inflammation are primarily engaged during the pathological progressive process creating an atrocious cycle to aggravate hepatic steatosis. Recent studies suggested that various components like oxidative stress associated with lipid peroxidation, cytokine activation, and endogenous toxins of fructose metabolites are crucial for the development of inflammation (Nomura & Yamanouchi, 2012).

The non esterified hepatic lipid induces mitochondrial dysfunction and ER stress leads to the activation of two major regulators of inflammatory pathways: JNK and NF- κ B. Activation of these messengers aggravates hepatic IR and intra hepatic cytokine production. Thus both ER stress and inflammation are short term adaptive systems, critical for the survival of the organism, but become detrimental when chronically engaged. Experiments proved that specific inflammatory triggers may signal through different branches of UPR, like the ATF6 branch of UPR activates the inhibitor of NF- κ B kinase subunit β (I κ K- β) / NF- κ B signaling pathway. *In vitro* studies revealed that induction of UPR culminates in increased expression of proinflammatory molecules such as TNF- α , interleukin 6 (IL-6), interleukin 8 (IL-8) and MCP-1 (Li et al., 2015).

Activation of the I κ K- β / NF- κ B signaling pathway is the key event during NASH, since the development of steatosis is strongly related with hepatic inflammation. High fat diet induced steatosis in murine models displayed elevated hepatic expression of inflammatory cytokines such as TNF- α , IL-6, and IL-1 β along with increased NF- κ B activity (Cai et al., 2005). It has also been disclosed that high fat diet induced inflammatory gene expression can be prevented *via* liver specific inhibition of NF- κ B. In hepatocytes, free fatty acids are able to upregulate the I κ K- β / NF- κ B pathway providing further evidence that hepatic free fatty acids contribute inflammation. In patients with NASH, the serum and hepatic levels of TNF- α were elevated and are directly correlated with disease severity (Crespo et al., 2001). Likewise, serum IL-6 was also elevated in both animal and human models of NAFLD (Tarantino et al., 2009). Additionally, data has been suggested that NF- κ B activation and inflammation can promote carcinogenesis.

The development of chronic inflammation is associated with hepatic steatosis that also plays a pivotal role in HCC development (Day, 2006).

1.9 Role of micronutrients in NASH

Micronutrients are defined as nutrients that are needed in only microgram or milligram quantities for physiological functions. It includes minerals, vitamins, electrolytes and carotenoids. These are mainly required for enzymatic activity, intermediary metabolism, and metabolic response to illness. Since liver plays a central role in the transport and storage of many micronutrients, derangement in energy and nutrient homeostasis will lead to the progression of liver diseases including NASH.

1.9.1 Role of iron in NASH

Liver is the centre for iron and lipid metabolism and also the primary site for the interaction between these two metabolic pathways. Iron is an essential micronutrient required for all cellular functions. The concentration of iron in the total human body is between 3.5 and 5 g (Coates, 2014) and is unevenly distributed throughout the body with roughly 1 g being stored in the liver. Almost 75% of the iron is functional. Erythrocytes account for about 2.5 g of iron whereas other tissues like muscles account for about 0.3 g of iron. Under normal physiological condition, the level of free iron in the circulatory system is very low referred as non-transferrin bound iron (NTBI) (Porter et al., 2016; Carreau et al., 2016) and this systemic iron is regulated *via* a liver secreted iron hormone called hepcidin. High level of free iron occurs only during situations of iron overload and is mainly due to the ingestion of excess iron in the form of diet supplements or in patients with defective iron metabolism. The lack or resistance to hepcidin due to mutations also results in excessive iron deposition in various organs. The human body has an innate tendency to store iron, which results in iron overload to toxicity. Even though the liver is highly resistant to iron toxicity, additional factors are enforced for iron damage. Excess hepatic iron is common to a number of diseases, both hereditary (e.g., hemochromatosis) or acquired (e.g., chronic liver disease). In the former, iron accumulation leads to direct liver damage and the gradual development of micronodular cirrhosis and HCC. In chronic liver disease, low to moderate grade excess iron is ample to cause cardinal liver disease to accelerate and worsen (Pietrangelo, 2015).

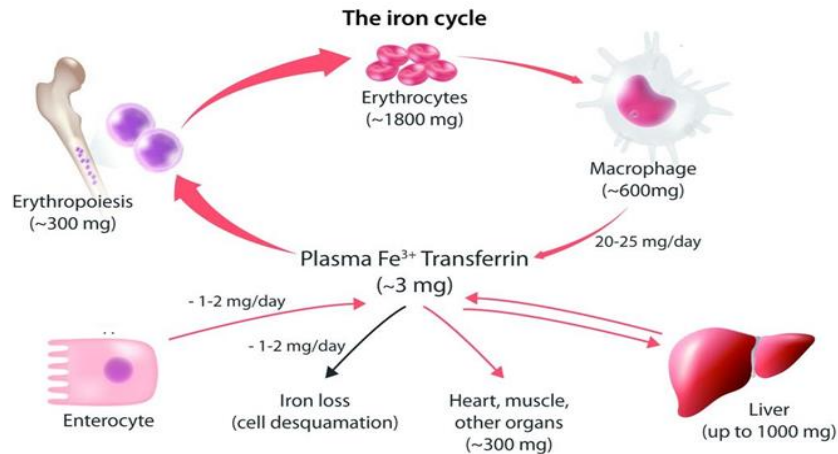


Figure 1.7 The iron cycle (Camaschella et al., 2020)

Over the past few decades, the role of iron in the genesis of NASH has been of substantial interest. Even if conflicting results have been accessed, most studies support the fact that iron plays a fundamental role in hepatic lipogenesis. The role of iron in liver injury, fibrogenesis, and cancer development is also now well recognized. In liver, excess free iron, as a catalyst of Fenton reaction can contribute to redox activation and free radical formation ensuing in lipid peroxidation and impose direct oxidative stress and inflammation to hepatocytes, the current topic of much research in the field of NAFLD / NASH. It has been established that 30% - 70% of patients with NAFLD / NASH possess iron overload conditions. Recently studies have shown that iron has direct effects on lipid metabolism. Alteration in hepatic iron stores results in inappropriate lipid storage and secretion.

1.9.1.1 Effect of iron deficiency on hepatic lipids

Anaemia / hypoxia are characterized by decreased fat uptake due to impaired peripheral lipolysis, but increased fat accumulation in the liver. Rat model of anaemia / hypoxia with iron deficiency reveals a decrease in the activity of lipoprotein lipase and hepatic lipase (Muratsubaki et al., 2003). On the contrary, iron deficiency in rats has been exhibited an increase in hepatic lipogenesis, ensuing in cellular TG accumulation and steatosis (Sherman, 1978; Bartholmey & Sherman, 1985). Moreover, the reduced rate of β oxidation of fatty acids promotes the conversion of fatty acids to TG synthesis. The expression of hepatic carnitine, the transporter for long chain fatty acids, was also found to be downregulated during the iron deficient condition. This result was supported by genomic studies that reveal a circumstantial increase in gene

expression related to lipogenesis and decrease in gene expression related to hepatic β oxidation (Davis et al., 2012). Along with increased lipogenesis, iron deficiency can also impaired the function of hepatic enzymes involved in cholesterol metabolism. It has been postulated that nutritional depletion in rats results in variations in fatty acid composition of hepatic phospholipids, arguing impaired desaturation of essential and saturated fatty acids (Cunnane, 1987). SCD-1 is required for the conversion of saturated fatty acids to unsaturated form and the activity of this enzyme is mainly catalyzed by iron. A reduction in the activity of SCD-1 during iron deficiency may interpret the increased saturated composition of fatty acids in the liver (Stangl & Kirchgessner, 1998). It is expected that some of the conflicted results due to iron deficiency can be explained in part by the specifics of the model system, or by the means of inducing iron deficiency.

1.9.1.2 Effects of iron overload on hepatic lipids

Oxidative stress and lipid peroxidation are the two major events that occur during iron overload. This can alter the fatty acid content of cellular membranes leading to their disruption and damage to organelles and ruination of mitochondrial oxidative metabolism. The free radical generation can alter the ratio between saturated and unsaturated membrane phospholipids and thereby disrupt membrane fluidity. It has been reported that PUFA may exert an inhibitory effect on lipogenic genes *via* peroxidative cytotoxic effects (Foretz et al., 1999). Several studies reported conflicting results on the effect of iron overload on hepatic lipid metabolism according to different experimental models. Enzymes involved in hepatic cholesterol metabolism also showed variable responses during iron overload. An increase in the activity of acyl-CoA cholesterol acyltransferase and decrease in HMG - CoA reductase activity has been observed in rats with dietary iron overload (Brunet et al., 1999). However, a recent study reported an upregulation in HMG - CoA reductase activity and cholesterol synthesis during hepatic iron overload condition (Graham et al., 2010).

Evidence from *in vitro* studies in HepG2 cells indicates an increase in intracellular lipid droplets during iron overload (Cabrita et al., 2005). These transitions are also associated with certain characteristics of apoptosis and cell death like increased expression of phosphatidylserine in the outer leaflet of plasma membrane (Elmore, 2007). Cell death of mature hepatocytes disproportionate to their competence to regenerate has been assigned as “third hit” in the pathogenesis of NAFLD / NASH well known for its advancement of fibrosis (Dowman et al.,

2010). The significance of iron overload in NAFLD is a widely accepted hypothesis. Nonetheless, it is also desirable that oxidative stress, steatosis and cytokines that are intrinsic to NASH pathophysiology secondarily lead to iron overload. It will then work in a feed forward manner to provoke more oxidative stress and inflammation thereby creating the environment more supportive for the third hit (Dowman et al., 2010; Diehl, 2005). Supporting this interpretation, hepatic iron deposition was also noted in non-biliary causes of cirrhosis such as ALD, chronic viral hepatitis as well as NASH. It has been explained that after liver injury, regenerating hepatocytes exhibited an increased expression of transferrin receptor, which could play a crucial role in hepatic iron overloading (Lee et al., 2003). Another aspect of increased liver iron accumulation is mainly due to alterations in the level of ferroportin and iron regulatory peptide hepcidin (Fujita & Takei, 2011). In addition, choline deficient mice developing steatosis implicates a negative correlation of hepcidin and ferroportin mRNA with hepatic lipid concentration, arguing that increased dietary intake and lowered hepatic iron efflux may lead to increased hepatic iron content (Tsuchiya et al., 2010).

1.9.2 Role of antioxidant vitamins in NASH

The liver plays a vital role in micronutrient metabolism. Hence any deregulation of this micronutrient metabolism may contribute to the pathogenesis of NAFLD. Vitamins regulate several enzymatic processes in the liver, and disorder in vitamin metabolism is believed to play a crucial role in the progression of NAFLD (Raza et al., 2020). Clinical evidence demonstrates that dietary supplementation with various kinds of polyphenols significantly improves NASH (Della et al., 2017) and has beneficial effects on hepatic fat accumulation, liver inflammation and fibrosis. Certain *in vitro* experimental models proved that antioxidant vitamins can prevent lipid accumulation *via* AMPK phosphorylation (Xia et al., 2019). There is evidence that shows protective effects of antioxidants against NAFLD / NASH since oxidative stress is linked to NAFLD (Yang et al., 2018). Vitamin C and vitamin E are classical antioxidants that scavenge free radicals and provide protection against oxidative stress. There is evidence that shows the beneficial effect of these vitamins against NAFLD/ NASH (Yang et al., 2018). It has also been reported that vitamin C and vitamin E supplementation improves the status of NAFLD, but significant alterations in serum lipid markers were not reported (Ivancovsky et al., 2019). Vitamin C or ascorbic acid is an essential water soluble vitamin obtained from the diet. The protective effect of vitamin C such as reduced hepatic steatosis and hepatocellular ballooning

was obtained in an experimental model of NAFLD. However, it is not able to reverse liver inflammation and histological features of NASH in a choline deficient diet. In the high fat diet model of NAFLD, ascorbic acid supplementation improves visceral obesity, inflammation and apoptosis *via* the upregulation of PPAR α and genes encoding β oxidation enzymes (Ipsen et al., 2014). Vitamin E is a lipid soluble, normally stored in liver and fat tissue. The most common isoform of this vitamin is tocopherol, the direct scavengers of ROS and RNS. They regulate the expression of detoxifying enzymes such as superoxide dismutase (SOD), glutathione and catalase (Hadzi et al., 2018). In clinical trials, vitamin E reduces NAFLD associated inflammation and impedes disease severity (Vilar et al., 2020). Furthermore, it contributes cellular protection owing to its antiinflammatory and antiapoptotic effects (Perumpail et al., 2018). However, vitamin E treatment alone is insufficient to improve the histological outcome in diabetic NASH patients (Bril et al., 2019) hence is not recommended to current guidelines (Chalasani et al., 2018). Recently it has been validated that vitamin E reduces hepatic DNL by preventing the maturation and translocation of SREBP-1 to the nucleus (Podszun et al., 2020). Besides this, in mice models of NAFLD, hepatic steatosis induced by fructose feeding is ameliorated by vitamin E, which was also observed in *in vitro* experiments (He et al., 2019).

Vitamin A or retinoic acid is an essential fat-soluble vitamin. It also causes reduction in liver triacylglycerol content and moderately increases ketogenesis (Amengual et al., 2010). Another fat soluble vitamin, vitamin D has benefited increasing attention in various research fields. Recently, it has been described that vitamin D possesses a crucial role in the regulation of cytokines production, hepatocytes apoptosis and even liver fibrosis (Roth et al., 2012). A meta analysis revealed that vitamin D supplementation is beneficial for T2DM combined with NAFLD (Wang et al., 2020). However literature on the role of vitamin K in NAFLD is very limited and its role in lipid metabolism is also not much subject for investigation.

1.9.2.1 Vitamin K (VK)

VK is a group of fat soluble vitamins. Human body requires VK mainly for blood clotting, bone metabolism and blood calcium regulation. It is an indispensable cofactor required for the post translational modification of hepatic blood coagulation proteins like prothrombin, factor II, VII, IX and X (Furie & Furie, 1990). It also aids in converting their glutamic acid residues into γ -carboxyglutamic acid residues. Recently, other vital functions performed by VK in addition to coagulation such as its role in cell growth and apoptosis, vascular calcification and

in bone metabolism have widely fascinated the attention of researchers (Furie & Furie, 1990; Cranenburg et al., 2007; Kaneki et al., 2006; Berkner & Runge, 2004; Sweatt et al., 2003, Yokoyama et al., 2008). It has also been reported that VK in combination with vitamin C presented anticancer activity. VK is a group of structurally related molecules that exists in two forms naturally; vitamin K₁ (VK₁ / phylloquinone) and vitamin K₂ (VK₂ / menaquinone). VK₁ is found mainly in green leafy vegetables: lettuce, broccoli, spinach, cabbage, fermented soy etc. whereas VK₂ are chiefly produced by the bacteria of the human intestine where it is utilized them as redox reagents in electron transport and oxidative phosphorylation. VK₁ is metabolized and more than half the amount is excreted by the organisms, whereas VK₂ is carried from low density lipoprotein to extra liver tissues.

A large number of investigations have delineated the effect of VK on cytotoxicity of cancer cells (Dasari et al., 2017). Various mechanisms responsible for cell growth arrest and control of proliferation have also been described. Yet most of them deal with the regulation of redox balance and induction of oxidative stress in cancer cells due to the quinone structure of VK. It has been suggested that VK induces apoptosis *via* modifying intracellular calcium homeostasis and also through the activation of various pro-apoptotic factors: JNK and NF- κ B. The modes of action of VK on different cell types have been portrayed, but still the mechanisms remain unclear. Several human studies reported the valuable role of VK in improving glucose tolerance, IR and also for ameliorating the risk of T2DM (Rasekhi et al., 2015, Yoshida et al., 2008). However, limited animal studies examined the significance of VK on glucose metabolism. The beneficial role of VK₁ has been demonstrated (Varsha et al., 2015) by decreasing radical formation, and restoring antioxidant enzyme activities in pancreatic tissues of the streptozotocin (STZ) treated rats. Immunohistochemical studies also unveiled the implications of VK₁ in reducing NF- κ B activation and expression of inducible nitric oxide synthase in the islets of STZ treated rats. This recommends the beneficial role of VK₁ in suppressing the activation of proinflammatory genes and oxidative stress in islet cells thereby monitoring glucose homeostasis in STZ induced diabetic rats.

The critical role of VK₁ in inflammation has also been subjected for investigation and has proved that VK₁ supplementation decreased the expression of IL-6 mRNA (Ohsaki et al., 2010). Results also pointed out that deficiency of VK was associated with high concentration of cytokines, IL-6 and C-reactive protein (CRP). However the detailed molecular mechanism

behind the regulation of proinflammatory cytokines remains ambiguous. Interestingly, recent studies described the potential role of VK in regulating dyslipidemia (Sogabe et al., 2011) by reducing the plasma levels of total cholesterol in hypercholesterolemic rabbits. Another study reported that both VK₁ and VK₂ significantly reduced the fat accumulation and serum triacylglycerol compared to control diet fed rats (Sogabe et al., 2011). On the contrary, it has also been stated that VK₁ has no effect on lipid profile in women with rheumatoid arthritis (Kolahi et al., 2015).

1.10 Diagnosis and treatment strategies of NASH

The development of NAFLD is clinically silent and is usually detected when tests for other diseases are done. The diagnosis is incidental due to abnormal liver enzymes or imaging and mainly results from steatosis. Once liver disease is suspected, confirmation has been done after the exclusion of other potential causes of steatosis. Since alcoholic hepatitis is clinically indistinguishable from NASH, it is essential to rule out significant alcohol consumption (consumption > 20 g daily) (Angulo et al., 1999). Moreover it is necessary to investigate dietary history, medications used, clinical and family history of liver diseases. For the diagnosis of hepatic steatosis, transabdominal ultrasonography is the approved first line imaging investigation owed to its inexpensive, non-invasive and widely accessible properties. This method is highly efficient if the hepatic steatosis is not less than 31% (Saadeh et al., 2002). For the detection of liver fibrosis in children and adults, fibroScan is widely used which is a non-invasive ultrasound based elastography and it takes less than 5 minutes to complete the procedure. However, liver biopsy is considered as the most accepted examination since it can be used to distinguish steatohepatitis from simple steatosis by providing an estimate of extent of necroinflammatory activity and also to visualize fibrotic and architectural variations. In the absence of likelihood diagnosis, NAFLD usually presents asymptotically. The most frequent initial symptoms include fatigue and malaise which cannot be correlated with disease severity. About 50% of patients suffered from hepatosplenomegaly. As the disease severity increases, the spleen enlarges and the liver shrinks in size. The presence of hypotension is also observed due to reduced total systemic vascular resistance.

Till now there is no treatment and therapies approved by the US Food and Drug Administration (FDA) for NAFLD and NASH. The only accepted treatment strategy for NASH management involves lifestyle modifications, weight loss along with exercise and a diet that

possesses low cholesterol, fructose and saturated fats like the Mediterranean diet. It has been recommended that 7% weight reduction may be sufficient in dealing steatosis and inflammation. A study comprising 154 NAFLD patients proved that lifestyle modification over one year period resulted in 64% remissions in the lifestyle modification group where only 20% remissions in the control group (Wong et al., 2013).

1.10.1 Weight loss

NASH can be ameliorated by weight loss. NASH patients have been shown to have a high energy intake compared with healthy controls. Studies have been reported that combination of both dietary intervention and physical activity results in weight loss of 9.3% body weight compared to the control group. They also showed significant histological improvements: reduced steatosis, lobular formation and hepatocytes ballooning (Promrat et al., 2010).

1.10.2 Dietary fat

It has been suggested that a high fat diet (> 37% of energy) is a major independent risk factor for the development and progression of NASH. Epidemiological studies unveil the fact that Mediterranean diets exert beneficial effects on cardiovascular diseases and metabolic syndromes (Gillingham et al., 2011). In the liver of patients with IR, olive oil plays a central role in TG reduction and postprandial glucose production (Assy et al., 2009). The presence of MUFA in olive oil results in the activation of NF- κ B, TNF- α and interleukin secretion. Evidence from animal (Gonzalez et al., 2009) and human research (Parker et al., 2012) describes the fact that dietary supplementation with omega-3 PUFA may impede NAFLD or reduce liver fat independent of weight loss. Fish oils exert protective effects on NAFLD due to the abundant source of PUFAs, eicosapentaenoic acid and docosahexaenoic acid. Another study reported that PUFA treated groups exhibited complete regression of fatty liver in 33% of patients with 50% reduction of liver fat. However, only 27% patients show reduction in liver fat while receiving the standard diet (Spadaro *et al.*, 2008).

1.10.3 Intake of low carbohydrate

A diet having low fat and high carbohydrate is well known to promote DNL. Those patients with liver disease following a low carbohydrate diet accomplished an obvious reduction in hepatic TG level (55%) compared with patients following an energy restricted diet. Compared to a high carbohydrate low energy diet, a low carbohydrate low energy diet exerts a differential effect on hepatic steatosis. Research on rodents and humans have demonstrated that fatty liver

can be reversed by reducing the intake of carbohydrate sources like high glycemic grains, added sugars, and fructose (Jensen et al., 2012). This will significantly reduce IR, inflammation and mainly DNL. Based on the current research, varying the relation between total fat and carbohydrate with or without energy intake is advisable. A meta-analysis of randomized clinical trials found that a low carbohydrate diet exerts a long term effect on weight loss compared to a low fat diet (Haghighatdoost et al., 2016). A key factor for a low carbohydrate diet is that it potentially decreases body weight, HbA1c, serum lipids and blood pressure in patients with T2DM (Unwin et al., 2020).

1.11 Aims and objectives

The Indian economy is undoubtedly in its growth phase. The quality of life has improved, lifestyles are undergoing drastic changes, but paradoxically economic evolution has gifted a few lifestyle illnesses with far reaching consequences and increasing health care burden. Rising affluence, changes in lifestyle, junk food habits and obesity have all contributed in varying degrees to the lifestyle health crisis. NAFLD is the most prevalent liver disease in human history. It is closely associated with diabetes; hypertension and high cholesterol evolves out of unbalanced, faulty lifestyle. Heart disease is also quite prevalent among patients with fatty liver. Since there is no FDA approved drugs for the treatment of NAFLD, elucidation of molecular events associated with liver disease will enable us to understand basic biology of the disease. This will definitely help us to design various strategies for therapeutic intervention.

The major objectives of the study include

- Standardization of *in vitro* model of steatosis in HepG2 cell line by incubating cell with fructose and palmitate
- Elucidation on the role of mitochondria in the genesis of fructose and palmitate induced steatosis in HepG2 cells
- Investigation on the role of unfolded protein response system during fructose and palmitate induced steatosis in HepG2 cells
- Role of iron and vitamin K on fructose and palmitate induced steatosis in HepG2 cells

References

- Adams, L.A. & Angulo, P. 2006, "Treatment of non-alcoholic fatty liver disease".
- Al-Asmari, A.K., Khan, A.Q. and Al-Masri, N., 2016. Mitigation of 5-fluorouracil-induced liver damage in rats by vitamin C via targeting redox-sensitive transcription factors. *Human & experimental toxicology*, 35(11), pp.1203-1213.
- Amaro, A., Fabbrini, E., Kars, M., Yue, P., Schechtman, K., Schonfeld, G. and Klein, S., 2010. Dissociation between intrahepatic triglyceride content and insulin resistance in familial hypobetalipoproteinemia. *Gastroenterology*, 139(1), pp.149-153.
- Amengual, J., Ribot, J., Bonet, M.L. and Palou, A., 2010. Retinoic acid treatment enhances lipid oxidation and inhibits lipid biosynthesis capacities in the liver of mice. *Cellular Physiology and Biochemistry*, 25(6), pp.657-666.
- Ameri, K. and Harris, A.L., 2008. Activating transcription factor 4. *The international journal of biochemistry & cell biology*, 40(1), pp.14-21.
- Angulo, P., Keach, J.C., Batts, K.P. and Lindor, K.D., 1999. Independent predictors of liver fibrosis in patients with nonalcoholic steatohepatitis. *Hepatology*, 30(6), pp.1356-1362.
- Arab, J.P., Arrese, M. and Trauner, M., 2018. Recent insights into the pathogenesis of nonalcoholic fatty liver disease. *Annual Review of Pathology: Mechanisms of Disease*, 13, pp.321-350.
- Assy, N., Nassar, F., Nasser, G. and Grosovski, M., 2009. Olive oil consumption and non-alcoholic fatty liver disease. *World journal of gastroenterology: WJG*, 15(15), p.1809.
- Bartholmey, S.J. and Sherman, A.R., 1985. Carnitine levels in iron-deficient rat pups. *The Journal of nutrition*, 115(1), pp.138-145.
- Begriche, K., Massart, J. and Fromenty, B., 2010. Effects of β -aminoisobutyric acid on leptin production and lipid homeostasis: mechanisms and possible relevance for the prevention of obesity. *Fundamental & clinical pharmacology*, 24(3), pp.269-282.
- Bellanti, F., Villani, R., Tamborra, R., Blonda, M., Iannelli, G., di Bello, G., Facciorusso, A., Poli, G., Iuliano, L., Avolio, C. and Vendemiale, G., 2018. Synergistic interaction of fatty acids and oxysterols impairs mitochondrial function and limits liver adaptation during nafld progression. *Redox biology*, 15, pp.86-96.

- Berkner, K.L. and Runge, K.W., 2004. The physiology of vitamin K nutriture and vitamin K-dependent protein function in atherosclerosis. *Journal of Thrombosis and Haemostasis*, 2(12), pp.2118-2132.
- Bobrovnikova-Marjon, E., Hatzivassiliou, G., Grigoriadou, C., Romero, M., Cavener, D.R., Thompson, C.B. and Diehl, J.A., 2008. PERK-dependent regulation of lipogenesis during mouse mammary gland development and adipocyte differentiation. *Proceedings of the National Academy of Sciences*, 105(42), pp.16314-16319.
- Boden, G., Song, W., Duan, X., Cheung, P., Kresge, K., Barrero, C. and Merali, S., 2011. Infusion of glucose and lipids at physiological rates causes acute endoplasmic reticulum stress in rat liver. *Obesity*, 19(7), pp.1366-1373.
- Bremer, A.A., Stanhope, K.L., Graham, J.L., Cummings, B.P., Wang, W., Saville, B.R. and Havel, P.J., 2011. Fructose-fed rhesus monkeys: a nonhuman primate model of insulin resistance, metabolic syndrome, and type 2 diabetes. *Clinical and translational science*, 4(4), pp.243-252.
- Bril, F., Biernacki, D.M., Kalavalapalli, S., Lomonaco, R., Subbarayan, S.K., Lai, J., Tio, F., Suman, A., Orsak, B.K., Hecht, J. and Cusi, K., 2019. Role of vitamin E for nonalcoholic steatohepatitis in patients with type 2 diabetes: a randomized controlled trial. *Diabetes Care*, 42(8), pp.1481-1488.
- Browning, J.D., Szczepaniak, L.S., Dobbins, R., Nuremberg, P., Horton, J.D., Cohen, J.C., Grundy, S.M. and Hobbs, H.H., 2004. Prevalence of hepatic steatosis in an urban population in the United States: impact of ethnicity. *Hepatology*, 40(6), pp.1387-1395.
- Brunet, S., Thibault, L., Delvin, E., Yotov, W., Bendayan, M. and Levy, E., 1999. Dietary iron overload and induced lipid peroxidation are associated with impaired plasma lipid transport and hepatic sterol metabolism in rats. *Hepatology*, 29(6), pp.1809-1817.
- Cabrita, M., Pereira, C.F., Rodrigues, P., Cardoso, E.M. and Arosa, F.A., 2005. Altered expression of CD1d molecules and lipid accumulation in the human hepatoma cell line HepG2 after iron loading. *The FEBS journal*, 272(1), pp.152-165.
- Cai, D., Yuan, M., Frantz, D.F., Melendez, P.A., Hansen, L., Lee, J. and Shoelson, S.E., 2005. Local and systemic insulin resistance resulting from hepatic activation of IKK- β and NF- κ B. *Nature medicine*, 11(2), pp.183-190.

- Caldwell, S.H., 1999. Swerdlow RH, Khan EM, Iezzoni JC, Hespenheide EE, Parks JK, Parker WD Jr. *Mitochondrial abnormalities in non-alcoholic steatohepatitis. J Hepatol*, 31, pp.430-434.
- Camaschella, C., Nai, A. and Silvestri, L., 2020. Iron metabolism and iron disorders revisited in the hepcidin era. *Haematologica*, 105(2), p.260.
- Campbell, A.M. and Chan, S.H., 2007. The voltage dependent anion channel affects mitochondrial cholesterol distribution and function. *Archives of biochemistry and biophysics*, 466(2), pp.203-210.
- Carreau, N., Tremblay, D., Savona, M., Kremyanskaya, M. and Mascarenhas, J., 2016. Ironing out the details of iron overload in myelofibrosis: Lessons from myelodysplastic syndromes. *Blood reviews*, 30(5), pp.349-356.
- Chalasani, N., Younossi, Z., Lavine, J.E., Charlton, M., Cusi, K., Rinella, M., Harrison, S.A., Brunt, E.M. and Sanyal, A.J., 2018. The diagnosis and management of nonalcoholic fatty liver disease: practice guidance from the American Association for the Study of Liver Diseases. *Hepatology*, 67(1), pp.328-357.
- Chong, M.F., Fielding, B.A. and Frayn, K.N., 2007. Metabolic interaction of dietary sugars and plasma lipids with a focus on mechanisms and de novo lipogenesis. *Proceedings of the Nutrition Society*, 66(1), pp.52-59.
- Clementi, E. and Nisoli, E., 2005. Nitric oxide and mitochondrial biogenesis: a key to long-term regulation of cellular metabolism. *Comparative Biochemistry and Physiology Part A: Molecular & Integrative Physiology*, 142(2), pp.102-110.
- Coates, T.D., 2014. Physiology and pathophysiology of iron in hemoglobin-associated diseases. *Free Radical Biology and Medicine*, 72, pp.23-40.
- Conlon, B.A., Beasley, J.M., Aebbersold, K., Jhangiani, S.S. and Wylie-Rosett, J., 2013. Nutritional management of insulin resistance in nonalcoholic fatty liver disease (NAFLD). *Nutrients*, 5(10), pp.4093-4114.
- Cranenburg, E.C., Schurgers, L.J. and Vermeer, C., 2007. Vitamin K: the coagulation vitamin that became omnipotent. *Thrombosis and haemostasis*, 98(07), pp.120-125.
- Crespo, J., Fern, P., Hern, M., Mayorga, M. and Pons-Romero, F., 2001. Gene expression of tumor necrosis factor [alpha] and TNF-receptors, p55 and p75, in nonalcoholic steatohepatitis patients. *Hepatology*, 34(6), pp.1158-1163.

- Cunnane, S.C. and McAdoo, K.R., 1987. Iron intake influences essential fatty acid and lipid composition of rat plasma and erythrocytes. *The Journal of nutrition*, 117(9), pp.1514-1519.
- Cydylo, M.A., Davis, A.T. and Kavanagh, K., 2017. Fatty liver promotes fibrosis in monkeys consuming high fructose. *Obesity*, 25(2), pp.290-293.
- Das, M.K., Bhatia, V., Sibal, A., Gupta, A., Gopalan, S., Sardana, R., Sahni, R., Roy, A. and Arora, N.K., 2017. Prevalence of nonalcoholic fatty liver disease in normal-weight and overweight preadolescent children in Haryana, India. *Indian pediatrics*, 54(12), pp.1012-1016.
- Dasari, S., Ali, S.M., Zheng, G., Chen, A., Dontaraju, V.S., Bosland, M.C., Kajdacsy-Balla, A. and Munirathinam, G., 2017. Vitamin K and its analogs: Potential avenues for prostate cancer management. *Oncotarget*, 8(34), p.57782.
- Davis, M.R., Rendina, E., Peterson, S.K., Lucas, E.A., Smith, B.J. and Clarke, S.L., 2012. Enhanced expression of lipogenic genes may contribute to hyperglycemia and alterations in plasma lipids in response to dietary iron deficiency. *Genes & nutrition*, 7(3), pp.415-425.
- Day, C.P. and James, O.F., 1998. Steatohepatitis: a tale of two “hits”?
- Day, C.P., 2006. From fat to inflammation. *Gastroenterology*, 130(1), pp.207-210
- Della Pepa, G., Vetrani, C., Lombardi, G., Bozzetto, L., Annuzzi, G. and Rivellese, A.A., 2017. Isocaloric dietary changes and non-alcoholic fatty liver disease in high cardiometabolic risk individuals. *Nutrients*, 9(10), p.1065.
- Diehl, A.M., 2005. Lessons from animal models of NASH. *Hepatology Research*, 33(2), pp.138-144.
- Dowman, J.K., Tomlinson, J.W. and Newsome, P.N., 2010. Pathogenesis of non-alcoholic fatty liver disease. *QJM: An International Journal of Medicine*, 103(2), pp.71-83.
- Eletto, D., Eletto, D., Dersh, D., Gidalevitz, T. and Argon, Y., 2014. Protein disulfide isomerase A6 controls the decay of IRE1 α signaling via disulfide-dependent association. *Molecular cell*, 53(4), pp.562-576.
- Elmore, S., 2007. Apoptosis: a review of programmed cell death. *Toxicologic pathology*, 35(4), pp.495-516.

- Estes, C., Razavi, H., Loomba, R., Younossi, Z. and Sanyal, A.J., 2018. Modeling the epidemic of nonalcoholic fatty liver disease demonstrates an exponential increase in burden of disease. *Hepatology*, 67(1), pp.123-133.
- Farrell, G.C. and Larter, C.Z., 2006. Nonalcoholic fatty liver disease: from steatosis to cirrhosis. *Hepatology*, 43(S1), pp.S99-S112.
- Ferder, L., Ferder, M.D. and Inserra, F., 2010. The role of high-fructose corn syrup in metabolic syndrome and hypertension. *Current hypertension reports*, 12(2), pp.105-112.
- Foretz, M., Foufelle, F and Ferre, P., 1999. Polyunsaturated fatty acids inhibit fatty acid synthase and spot-14-protein gene expression in cultured rat hepatocytes by a peroxidative mechanism. *Biochemical Journal*, 341(2), pp.371-376.
- Fujita, N. and Takei, Y., 2011. Iron overload in nonalcoholic steatohepatitis. *Advances in clinical chemistry*, 55, p.106.
- Furie, B. and Furie, B.C., 1990. Molecular basis of vitamin K-dependent gamma-carboxylation. G., Sofi, F., Milani, S., Abbate, R., Surrenti, C. & Casini, A. 2006, "Prolonged n-3 95 polyunsaturated fatty acid supplementation ameliorates hepatic steatosis in patients with non-alcoholic fatty liver disease: a pilot study". *Alimentary Pharmacology & Therapeutics*, vol. 23, no. 8, pp. 1143-1151.
- Gaggini, M., Morelli, M., Buzzigoli, E., DeFronzo, R.A., Bugianesi, E. and Gastaldelli, A., 2013. Non-alcoholic fatty liver disease (NAFLD) and its connection with insulin resistance, dyslipidemia, atherosclerosis and coronary heart disease. *Nutrients*, 5(5), pp.1544-1560.
- Galicia-Moreno, M., Lucano-Landeros, S., Monroy-Ramirez, H.C., Silva-Gomez, J., Gutierrez-Cuevas, J., Santos, A. and Armendariz-Borunda, J., 2020. Roles of Nrf2 in Liver Diseases: Molecular, Pharmacological, and Epigenetic Aspects. *Antioxidants*, 9(10), p.980.
- Gan, L.T., Van Rooyen, D.M., Koina, M.E., McCuskey, R.S., Teoh, N.C. and Farrell, G.C., 2014. Hepatocyte free cholesterol lipotoxicity results from JNK1-mediated mitochondrial injury and is HMGB1 and TLR4-dependent. *Journal of hepatology*, 61(6), pp.1376-1384.

- Gariani K., Menzies K. J., Ryu D., et al. Eliciting the mitochondrial unfolded protein response by nicotinamide adenine dinucleotide repletion reverses fatty liver disease in mice. *Hepatology*. 2016;63(4):1190–1204. doi: 10.1002/hep.28245.
- Gillingham, L.G., Harris-Janz, S. and Jones, P.J., 2011. Dietary monounsaturated fatty acids are protective against metabolic syndrome and cardiovascular disease risk factors. *Lipids*, 46(3), pp.209-228.
- González-Pérez, A., Horrillo, R., Ferre, N., Gronert, K., Dong, B., Morán-Salvador, E., Titos, E., Martínez-Clemente, M., López-Parra, M., Arroyo, V. and Claria, J., 2009. Obesity-induced insulin resistance and hepatic steatosis are alleviated by ω -3 fatty acids: a role for resolvins and protectins. *The FASEB journal*, 23(6), pp.1946-1957.
- Graham, R.M., Chua, A.C., Carter, K.W., Delima, R.D., Johnstone, D., Herbison, C.E., Firth, M.J., O'Leary, R., Milward, E.A., Olynyk, J.K. and Trinder, D., 2010. Hepatic iron loading in mice increases cholesterol biosynthesis. *Hepatology*, 52(2), pp.462-471.
- Grattagliano, I., de Bari, O., Bernardo, T.C., Oliveira, P.J., Wang, D.Q.H. and Portincasa, P., 2012. Role of mitochondria in nonalcoholic fatty liver disease-from origin to propagation. *Clinical biochemistry*, 45(9), pp.610-618.
- Hadzi-Petrushev, N., Dimovska, K., Jankulovski, N., Mitrov, D. and Mladenov, M., 2018. Supplementation with Alpha-Tocopherol and Ascorbic Acid to Nonalcoholic Fatty Liver Disease's Statin Therapy in Men. *Advances in pharmacological sciences*, 2018.
- Haghghatdoost, F., Salehi-Abargouei, A., Surkan, P.J. and Azadbakht, L., 2016. The effects of low carbohydrate diets on liver function tests in nonalcoholic fatty liver disease: A systematic review and meta-analysis of clinical trials. *Journal of research in medical sciences: The official journal of Isfahan University of Medical Sciences*, 21.
- Hardy, T., Oakley, F., Anstee, Q.M. and Day, C.P., 2016. Nonalcoholic fatty liver disease: pathogenesis and disease spectrum. *Annual Review of Pathology: Mechanisms of Disease*, 11, pp.451-496.
- Hassler, J.R., Scheuner, D.L., Wang, S., Han, J., Kodali, V.K., Li, P., Nguyen, J., George, J.S., Davis, C., Wu, S.P. and Bai, Y., 2015. The IRE1 α /XBP1s pathway is essential for the glucose response and protection of β cells. *PLoS Biol*, 13(10), p.e1002277.

- He, W., Xu, Y., Ren, X., Xiang, D., Lei, K., Zhang, C. and Liu, D., 2019. Vitamin E ameliorates lipid metabolism in mice with nonalcoholic fatty liver disease via Nrf2/CES1 signaling pathway. *Digestive diseases and sciences*, 64(11), pp.3182-3191.
- Herzig, S. and Shaw, R.J., 2018. AMPK: guardian of metabolism and mitochondrial homeostasis. *Nature reviews Molecular cell biology*, 19(2), p.121.
- Hetz, C. and Papa, F.R., 2018. The unfolded protein response and cell fate control. *Molecular cell*, 69(2), pp.169-181.
- Hochuli, M., Aeberli, I., Weiss, A., Hersberger, M., Troxler, H., Gerber, P.A., Spinass, G.A. and Berneis, K., 2014. Sugar-sweetened beverages with moderate amounts of fructose, but not sucrose, induce fatty acid synthesis in healthy young men: a randomized crossover study. *The Journal of Clinical Endocrinology & Metabolism*, 99(6), pp.2164-2172.
- Holmström, K.M., Kostov, R.V. and Dinkova-Kostova, A.T., 2016. The multifaceted role of Nrf2 in mitochondrial function. *Current opinion in toxicology*, 1, pp.80-91.
- Hoyumpa, A.M., Greene, H.L., Dunn, G.D. and Schenker, S., 1975. Fatty liver: biochemical and clinical considerations. *The American journal of digestive diseases*, 20(12), pp.1142-1170.
- Ipsen, D.H., Tveden-Nyborg, P. and Lykkesfeldt, J., 2014. Does vitamin C deficiency promote fatty liver disease development?. *Nutrients*, 6(12), pp.5473-5499.
- Ivancovsky-Wajcman, D., Fliss-Isakov, N., Salomone, F., Webb, M., Shibolet, O., Kariv, R. and Zelber-Sagi, S., 2019. Dietary vitamin E and C intake is inversely associated with the severity of nonalcoholic fatty liver disease. *Digestive and Liver Disease*, 51(12), pp.1698-1705.
- Janevski, M., Ratnayake, S., Siljanovski, S., McGlynn, M.A., Cameron-Smith, D. and Lewandowski, P., 2012. Fructose containing sugars modulate mRNA of lipogenic genes ACC and FAS and protein levels of transcription factors ChREBP and SREBP1c with no effect on body weight or liver fat. *Food & function*, 3(2), pp.141-149.
- Jensen-Urstad, A.P. and Semenkovich, C.F., 2012. Fatty acid synthase and liver triglyceride metabolism: housekeeper or messenger?. *Biochimica et Biophysica Acta (BBA)-Molecular and Cell Biology of Lipids*, 1821(5), pp.747-753.

- Kaneki, M., Hosoi, T., Ouchi, Y. and Orimo, H., 2006. Pleiotropic actions of vitamin K: protector of bone health and beyond?. *Nutrition*, 22(7-8), pp.845-852.
- Kanerva, N., Sandboge, S., Kaartinen, N.E., Männistö, S. and Eriksson, J.G., 2014. Higher fructose intake is inversely associated with risk of nonalcoholic fatty liver disease in older Finnish adults. *The American journal of clinical nutrition*, 100(4), pp.1133-1138.
- Kolahi, S., Gargari, B.P., Abbasi, M.M., Jafarabadi, M.A. and Shishavan, N.G., 2015. Effects of phylloquinone supplementation on lipid profile in women with rheumatoid arthritis: a double blind placebo controlled study. *Nutrition research and practice*, 9(2), p.186.
- Koliwad, S.K., Streeper, R.S., Monetti, M., Cornelissen, I., Chan, L., Terayama, K., Naylor, S., Rao, M., Hubbard, B. and Farese, R.V., 2010. DGAT1-dependent triacylglycerol storage by macrophages protects mice from diet-induced insulin resistance and inflammation. *The Journal of clinical investigation*, 120(3), pp.756-767.
- Koo, H.Y., Wallig, M.A., Chung, B.H., Nara, T.Y., Cho, B.S. and Nakamura, M.T., 2008. Dietary fructose induces a wide range of genes with distinct shift in carbohydrate and lipid metabolism in fed and fasted rat liver. *Biochimica et Biophysica Acta (BBA)-Molecular Basis of Disease*, 1782(5), pp.341-348.
- Kotiadis, V.N., Duchon, M.R. and Osellame, L.D., 2014. Mitochondrial quality control and communications with the nucleus are important in maintaining mitochondrial function and cell health. *Biochimica et Biophysica Acta (BBA)-General Subjects*, 1840(4), pp.1254-1265.
- Leamy, A.K., Egnatchik, R.A. and Young, J.D., 2013. Molecular mechanisms and the role of saturated fatty acids in the progression of non-alcoholic fatty liver disease. *Progress in lipid research*, 52(1), pp.165-174.
- Lee, A.W., Oates, P.S. and Trinder, D., 2003. Effects of cell proliferation on the uptake of transferrin-bound iron by human hepatoma cells. *Hepatology*, 38(4), pp.967-977.
- Leoni, S., Tovoli, F., Napoli, L., Serio, I., Ferri, S. and Bolondi, L., 2018. Current guidelines for the management of non-alcoholic fatty liver disease: A systematic review with comparative analysis. *World journal of gastroenterology*, 24(30), p.3361.

- Li, S., Tan, H.Y., Wang, N., Zhang, Z.J., Lao, L., Wong, C.W. and Feng, Y., 2015. The role of oxidative stress and antioxidants in liver diseases. *International journal of molecular sciences*, 16(11), pp.26087-26124.
- Lingappan, K., 2018. NF-κB in oxidative stress. *Current opinion in toxicology*, 7, pp.81-86.
- Lonardo, A., Bellentani, S., Argo, C.K., Ballestri, S., Byrne, C.D., Caldwell, S.H., Cortez-Pinto, H., Grieco, A., Machado, M.V., Miele, L. and Targher, G., 2015. Epidemiological modifiers of non-alcoholic fatty liver disease: Focus on high-risk groups. *Digestive and Liver Disease*, 47(12), pp.997-1006.
- Malhi, H. and Gores, G.J., 2008, November. Molecular mechanisms of lipotoxicity in nonalcoholic fatty liver disease. In *Seminars in liver disease* (Vol. 28, No. 4, p. 360). NIH Public Access.
- Malhi, H. and Kaufman, R.J., 2011. Endoplasmic reticulum stress in liver disease. *Journal of hepatology*, 54(4), pp.795-809.
- Malhi, H., Bronk, S.F., Werneburg, N.W. and Gores, G.J., 2006. Free fatty acids induce JNK-dependent hepatocyte lipoapoptosis. *Journal of Biological Chemistry*, 281(17), pp.12093-12101.
- Mansouri, A., Gattolliat, C.H. and Asselah, T., 2018. Mitochondrial dysfunction and signaling in chronic liver diseases. *Gastroenterology*, 155(3), pp.629-647.
- Masarone, M., Rosato, V., Dallio, M., Gravina, A.G., Aglitti, A., Loguercio, C., Federico, A. and Persico, M., 2018. Role of oxidative stress in pathophysiology of nonalcoholic fatty liver disease. *Oxidative medicine and cellular longevity*, 2018.
- Mohammadbeigi, A., Asgarian, A., Moshir, E., Heidari, H., Afrashteh, S., Khazaei, S. and Ansari, H., 2018. Fast food consumption and overweight/obesity prevalence in students and its association with general and abdominal obesity. *Journal of preventive medicine and hygiene*, 59(3), p.E236.
- Muratsubaki, H., Enomoto, K., Ichijoh, Y. and Yamamoto, Y., 2003. Hypertriglyceridemia associated with decreased post-heparin plasma hepatic triglyceride lipase activity in hypoxic rats. *Archives of physiology and biochemistry*, 111(5), pp.449-454.

- Musso, G., Cassader, M., Paschetta, E. and Gambino, R., 2018. Bioactive lipid species and metabolic pathways in progression and resolution of nonalcoholic steatohepatitis. *Gastroenterology*, 155(2), pp.282-302.
- Neuschwander-Tetri, B.A., Ford, D.A., Acharya, S., Gilkey, G., Basaranoglu, M., Tetri, L.H. and Brunt, E.M., 2012. Dietary trans-fatty acid induced NASH is normalized following loss of trans-fatty acids from hepatic lipid pools. *Lipids*, 47(10), pp.941-950.
- Nomura, K. and Yamanouchi, T., 2012. The role of fructose-enriched diets in mechanisms of nonalcoholic fatty liver disease. *The Journal of nutritional biochemistry*, 23(3), pp.203-208.
- Ohsaki, Y., Shirakawa, H., Miura, A., Giriwono, P.E., Sato, S., Ohashi, A., Iribe, M., Goto, T. and Komai, M., 2010. Vitamin K suppresses the lipopolysaccharide-induced expression of inflammatory cytokines in cultured macrophage-like cells via the inhibition of the activation of nuclear factor κ B through the repression of IKK α/β phosphorylation. *The Journal of nutritional biochemistry*, 21(11), pp.1120-1126.
- Oyadomari, S., Harding, H.P., Zhang, Y., Oyadomari, M. and Ron, D., 2008. Dephosphorylation of translation initiation factor 2 α enhances glucose tolerance and attenuates hepatosteatosis in mice. *Cell metabolism*, 7(6), pp.520-532.
- Özcan, U., Cao, Q., Yilmaz, E., Lee, A.H., Iwakoshi, N.N., Özdelen, E., Tuncman, G., Görgün, C., Glimcher, L.H. and Hotamisligil, G.S., 2004. Endoplasmic reticulum stress links obesity, insulin action, and type 2 diabetes. *Science*, 306(5695), pp.457-461.
- Paglialunga, S. and Dehn, C.A., 2016. Clinical assessment of hepatic de novo lipogenesis in non-alcoholic fatty liver disease. *Lipids in health and disease*, 15(1), pp.1-10.
- Pan, H., Wang, H., Wang, X., Zhu, L. and Mao, L., 2012. The absence of nrf2 enhances nf-b-dependent inflammation following scratch injury in mouse primary cultured astrocytes. *Mediators of inflammation*, 2012.
- Parker, H.M., Johnson, N.A., Burdon, C.A., Cohn, J.S., O'Connor, H.T. and George, J., 2012. Omega-3 supplementation and non-alcoholic fatty liver disease: a systematic review and meta-analysis. *Journal of hepatology*, 56(4), pp.944-951.
- Perumpail, B.J., Li, A.A., John, N., Sallam, S., Shah, N.D., Kwong, W., Cholankeril, G., Kim, D. and Ahmed, A., 2018. The Role of Vitamin E in the Treatment of NAFLD. *Diseases*, 6(4), p.86.

- Pessayre, D., 2007. Role of mitochondria in non-alcoholic fatty liver disease. *Journal of gastroenterology and hepatology*, 22, pp.S20-S27.
- Pietrangelo, A., 2015. Genetics, genetic testing, and management of hemochromatosis: 15 years since hepcidin. *Gastroenterology*, 149(5), pp.1240-1251.
- Pinnick, K.E. and Hodson, L., 2019. Challenging metabolic tissues with fructose: tissue-specific and sex-specific responses. *The Journal of physiology*, 597(14), pp.3527-3537.
- Podszun, M.C., Alawad, A.S., Lingala, S., Morris, N., Huang, W.C.A., Yang, S., Schoenfeld, M., Rolt, A., Ouwkerk, R., Valdez, K. and Umarova, R., 2020. Vitamin E treatment in NAFLD patients demonstrates that oxidative stress drives steatosis through upregulation of de-novo lipogenesis. *Redox biology*, 37, p.101710.
- Porter, J.B., de Witte, T., Cappellini, M.D. and Gattermann, N., 2016. New insights into transfusion-related iron toxicity: Implications for the oncologist. *Critical reviews in oncology/hematology*, 99, pp.261-271.
- Puri, P., Mirshahi, F., Cheung, O., Natarajan, R., Maher, J.W., Kellum, J.M. and Sanyal, A.J., 2008. Activation and dysregulation of the unfolded protein response in nonalcoholic fatty liver disease. *Gastroenterology*, 134(2), pp.568-576.
- Quinlan, C.L., Perevoshchikova, I.V., Hey-Mogensen, M., Orr, A.L. and Brand, M.D., 2013. Sites of reactive oxygen species generation by mitochondria oxidizing different substrates. *Redox biology*, 1(1), pp.304-312.
- Rahman, S.M., Schroeder-Gloeckler, J.M., Janssen, R.C., Jiang, H., Qadri, I., Maclean, K.N. and Friedman, J.E., 2007. CCAAT/enhancing binding protein β deletion in mice attenuates inflammation, endoplasmic reticulum stress, and lipid accumulation in diet-induced nonalcoholic steatohepatitis. *Hepatology*, 45(5), pp.1108-1117.
- Rasekhi, H., Karandish, M., Jalali, M.T., Mohammad-Shahi, M., Zarei, M., Saki, A. and Shahbazian, H., 2015. The effect of vitamin K1 supplementation on sensitivity and insulin resistance via osteocalcin in prediabetic women: a double-blind randomized controlled clinical trial. *European journal of clinical nutrition*, 69(8), pp.891-895.
- Raza, S., Tewari, A., Rajak, S. and Sinha, R.A., 2021. Vitamins and non-alcoholic fatty liver disease: A molecular insight☆. *Liver Research*.

- Reimold, A.M., Etkin, A., Clauss, I., Perkins, A., Friend, D.S., Zhang, J., Horton, H.F., Scott, A., Orkin, S.H., Byrne, M.C. and Grusby, M.J., 2000. An essential role in liver development for transcription factor XBP-1. *Genes & development*, 14(2), pp.152-157.
- Rodríguez-Calvo, R., Barroso, E., Serrano, L., Coll, T., Sánchez, R.M., Merlos, M., Palomer, X., Laguna, J.C. and Vázquez-Carrera, M., 2009. Atorvastatin prevents carbohydrate response element binding protein activation in the fructose-fed rat by activating protein kinase A. *Hepatology*, 49(1), pp.106-115.
- Roth, C.L., Elfers, C.T., Figlewicz, D.P., Melhorn, S.J., Morton, G.J., Hoofnagle, A., Yeh, M.M., Nelson, J.E. and Kowdley, K.V., 2012. Vitamin D deficiency in obese rats exacerbates nonalcoholic fatty liver disease and increases hepatic resistin and Toll-like receptor activation. *Hepatology*, 55(4), pp.1103-1111.
- Saadeh, S., Younossi, Z.M., Remer, E.M., Gramlich, T., Ong, J.P., Hurley, M., Mullen, K.D., Cooper, J.N. and Sheridan, M.J., 2002. The utility of radiological imaging in nonalcoholic fatty liver disease. *Gastroenterology*, 123(3), pp.745-750.
- Sage, A.T., Walter, L.A., Shi, Y., Khan, M.I., Kaneto, H., Capretta, A. and Werstuck, G.H., 2010. Hexosamine biosynthesis pathway flux promotes endoplasmic reticulum stress, lipid accumulation, and inflammatory gene expression in hepatic cells. *American Journal of Physiology-Endocrinology and Metabolism*, 298(3), pp.E499-E511.
- Santamaría, E., Avila, M.A., Latasa, M.U., Rubio, A., Martín-Duce, A., Lu, S.C., Mato, J.M. and Corrales, F.J., 2003. Functional proteomics of nonalcoholic steatohepatitis: mitochondrial proteins as targets of S-adenosylmethionine. *Proceedings of the National Academy of Sciences*, 100(6), pp.3065-3070.
- Sherman, A.R., 1978. Lipogenesis in iron-deficient adult rats. *Lipids*, 13(7), pp.473-478.
- Shridhar, G., Rajendra, N., Murigendra, H., Shridevi, P., Prasad, M., Mujeeb, M.A., Arun, S., Neeraj, D., Vikas, S., Suneel, D. and Vijay, K., 2015. Modern diet and its impact on human health. *Journal of Nutrition & Food Sciences*, 5(6), p.1.
- Silva, M.F., Aires, C.C., Luis, P.B. and Ruiten, J.P., 2008. IJ L, M. Duran, RJ Wanders and I. Tavares de Almeida. *J. Inherited Metab. Dis*, 31, pp.205-216.
- Softic, S., Cohen, D.E. and Kahn, C.R., 2016. Role of dietary fructose and hepatic de novo lipogenesis in fatty liver disease. *Digestive diseases and sciences*, 61(5), pp.1282-1293.

- Sogabe, N., Maruyama, R., Baba, O., Hosoi, T. and Goseki-Sone, M., 2011. Effects of long-term vitamin K1 (phylloquinone) or vitamin K2 (menaquinone-4) supplementation on body composition and serum parameters in rats. *Bone*, 48(5), pp.1036-1042.
- Spadaro, L., Magliocco, O., Spampinato, D., Piro, S., Oliveri, C., Alagona, C., Papa, G., Rabuazzo, A.M. and Purrello, F., 2008. Effects of n-3 polyunsaturated fatty acids in subjects with nonalcoholic fatty liver disease. *Digestive and Liver Disease*, 40(3), pp.194-199.
- Sreejayan, N., Dong, F., Kandadi, M.R., Yang, X. and Ren, J., 2008. Chromium alleviates glucose intolerance, insulin resistance, and hepatic ER stress in obese mice. *Obesity*, 16(6), pp.1331-1337.
- Stangl, G.I. and Kirchgessner, M., 1998. Different degrees of moderate iron deficiency modulate lipid metabolism of rats. *Lipids*, 33(9), pp.889-895.
- Stanhope, K.L., Schwarz, J.M., Keim, N.L., Griffen, S.C., Bremer, A.A., Graham, J.L., Hatcher, B., Cox, C.L., Dyachenko, A., Zhang, W. and McGahan, J.P., 2009. Consuming fructose-sweetened, not glucose-sweetened, beverages increases visceral adiposity and lipids and decreases insulin sensitivity in overweight/obese humans. *The Journal of clinical investigation*, 119(5), pp.1322-1334.
- Sunny, N.E., Bril, F. and Cusi, K., 2017. Mitochondrial adaptation in nonalcoholic fatty liver disease: novel mechanisms and treatment strategies. *Trends in Endocrinology & Metabolism*, 28(4), pp.250-260.
- Sweatt, A., Sane, D.C., Hutson, S.M. and Wallin, R., 2003. Matrix Gla protein (MGP) and bone morphogenetic protein-2 in aortic calcified lesions of aging rats. *Journal of Thrombosis and Haemostasis*, 1(1), pp.178-185.
- Tarantino, G., Conca, P., Pasanisi, F., Ariello, M., Mastrolia, M., Arena, A., Tarantino, M., Scopacasa, F. and Vecchione, R., 2009. Could inflammatory markers help diagnose nonalcoholic steatohepatitis?. *European journal of gastroenterology & hepatology*, 21(5), pp.504-511.
- Tilg, H. and Moschen, A.R., 2010. Evolution of inflammation in nonalcoholic fatty liver disease: the multiple parallel hits hypothesis. *Hepatology*, 52(5), pp.1836-1846.
- Tsuchiya, H., Sakabe, T., Akechi, Y., Ikeda, R., Nishio, R., Terabayashi, K., Matsumi, Y., Hoshikawa, Y., Kurimasa, A. and Shiota, G., 2010. A close association of abnormal

iron metabolism with steatosis in the mice fed a choline-deficient diet. *Biological and Pharmaceutical Bulletin*, 33(7), pp.1101-1104.

- Unwin, D., Khalid, A.A., Unwin, J., Crocombe, D., Delon, C., Martyn, K., Golubic, R. and Ray, S., 2020. Insights from a general practice service evaluation supporting a lower carbohydrate diet in patients with type 2 diabetes mellitus and prediabetes: a secondary analysis of routine clinic data including HbA1c, weight and prescribing over 6 years.
- Usui, M., Yamaguchi, S., Tanji, Y., Tominaga, R., Ishigaki, Y., Fukumoto, M., Katagiri, H., Mori, K., Oka, Y. and Ishihara, H., 2012. Atf6 α -null mice are glucose intolerant due to pancreatic β -cell failure on a high-fat diet but partially resistant to diet-induced insulin resistance. *Metabolism*, 61(8), pp.1118-1128.
- Varsha, M.S., Thiagarajan, R., Manikandan, R. and Dhanasekaran, G., 2015. Vitamin K1 alleviates streptozotocin-induced type 1 diabetes by mitigating free radical stress, as well as inhibiting NF- κ B activation and iNOS expression in rat pancreas. *Nutrition*, 31(1), pp.214-222.
- Vilar-Gomez, E., Vuppalanchi, R., Gawrieh, S., Ghabril, M., Saxena, R., Cummings, O.W. and Chalasani, N., 2020. Vitamin E improves transplant-free survival and hepatic decompensation among patients with nonalcoholic steatohepatitis and advanced fibrosis. *Hepatology*, 71(2), pp.495-509.
- Volynets, V., Machann, J., Küper, M.A., Maier, I.B., Spruss, A., Königsrainer, A., Bischoff, S.C. and Bergheim, I., 2013. A moderate weight reduction through dietary intervention decreases hepatic fat content in patients with non-alcoholic fatty liver disease (NAFLD): a pilot study. *European journal of nutrition*, 52(2), pp.527-535.
- Walter, P. and Ron, D., 2011. The unfolded protein response: from stress pathway to homeostatic regulation. *science*, 334(6059), pp.1081-1086.
- Wan, X., Xu, C., Yu, C. and Li, Y., 2016. Role of NLRP3 inflammasome in the progression of NAFLD to NASH. *Canadian Journal of Gastroenterology and Hepatology*, 2016.
- Wang, C., Huang, Z., Du, Y., Cheng, Y., Chen, S. and Guo, F., 2010. ATF4 regulates lipid metabolism and thermogenesis. *Cell research*, 20(2), pp.174-184.

- Wang, D., Wei, Y. and Pagliassotti, M.J., 2006. Saturated fatty acids promote endoplasmic reticulum stress and liver injury in rats with hepatic steatosis. *Endocrinology*, 147(2), pp.943-951.
- Wang, S., Cai, B., Han, X., Gao, Y., Zhang, X., Wang, R., Zhang, Y. and Chen, Q., 2020. Vitamin D supplementation for nonalcoholic fatty liver disease in type 2 diabetes mellitus: A protocol for a systematic review and meta-analysis. *Medicine*, 99(19).
- Wong, V.W.S., Chan, R.S.M., Wong, G.L.H., Cheung, B.H.K., Chu, W.C.W., Yeung, D.K.W., Chim, A.M.L., Lai, J.W.Y., Li, L.S., Sea, M.M.M. and Chan, F.K.L., 2013. Community-based lifestyle modification programme for non-alcoholic fatty liver disease: a randomized controlled trial. *Journal of hepatology*, 59(3), pp.536-542.
- Xia, H.M., Wang, J., Xie, X.J., Xu, L.J. and Tang, S.Q., 2019. Green tea polyphenols attenuate hepatic steatosis, and reduce insulin resistance and inflammation in high-fat diet-induced rats. *International journal of molecular medicine*, 44(4), pp.1523-1530.
- Xiao, G., Zhang, T., Yu, S., Lee, S., Calabuig-Navarro, V., Yamauchi, J., Ringquist, S. and Dong, H.H., 2013. ATF4 protein deficiency protects against high fructose-induced hypertriglyceridemia in mice. *Journal of biological chemistry*, 288(35), pp.25350-25361.
- Yamamoto, K., Takahara, K., Oyadomari, S., Okada, T., Sato, T., Harada, A. and Mori, K., 2010. Induction of liver steatosis and lipid droplet formation in ATF6 α -knockout mice burdened with pharmacological endoplasmic reticulum stress. *Molecular biology of the cell*, 21(17), pp.2975-2986.
- Yang, J.P., Shin, J.H., Seo, S.H., Kim, S.G., Lee, S.H. and Shin, E.H., 2018. Effects of antioxidants in reducing accumulation of fat in hepatocyte. *International journal of molecular sciences*, 19(9), p.2563.
- Yeh, M .M . & Brunt, E.M. 2007, "Pathology of nonalcoholic fatty liver disease", American
- Yokoyama, T., Miyazawa, K., Naito, M., Toyotake, J., Tauchi, T., Itoh, M., Yuo, A., Hayashi, Y., Georgescu, M.M., Kondo, Y. and Kondo, S., 2008. Vitamin K2 induces autophagy and apoptosis simultaneously in leukemia cells. *Autophagy*, 4(5), pp.629-640.
- Yoshida, M., Booth, S.L., Meigs, J.B., Saltzman, E. and Jacques, P.F., 2008. Phylloquinone intake, insulin sensitivity, and glycemic status in men and women. *The American journal of clinical nutrition*, 88(1), pp.210-215.

- Younossi, Z., Anstee, Q.M., Marietti, M., Hardy, T., Henry, L., Eslam, M., George, J. and Bugianesi, E., 2018. Global burden of NAFLD and NASH: trends, predictions, risk factors and prevention. *Nature reviews Gastroenterology & hepatology*, 15(1), pp.11-20.
- Younossi, Z.M., Koenig, A.B., Abdelatif, D., Fazel, Y., Henry, L. and Wymer, M., 2016. Global epidemiology of nonalcoholic fatty liver disease—meta-analytic assessment of prevalence, incidence, and outcomes. *Hepatology*, 64(1), pp.73-84.
- Zeng, L., Lu, M., Mori, K., Luo, S., Lee, A.S., Zhu, Y. and Shyy, J.Y.J., 2004. ATF6 modulates SREBP2-mediated lipogenesis. *The EMBO Journal*, 23(4), pp.950-958.
- Zhang, K., Wang, S., Malhotra, J., Hassler, J.R., Back, S.H., Wang, G., Chang, L., Xu, W., Miao, H., Leonardi, R. and Chen, Y.E., 2011. The unfolded protein response transducer IRE1 α prevents ER stress-induced hepatic steatosis. *The EMBO journal*, 30(7), pp.1357-1375.
- Zhang, K., Wong, H.N., Song, B., Miller, C.N., Scheuner, D. and Kaufman, R.J., 2005. The unfolded protein response sensor IRE1 α is required at 2 distinct steps in B cell lymphopoiesis. *The Journal of clinical investigation*, 115(2), pp.268-281.
- Zhang, Y.K.J., Wu, K.C., Liu, J. and Klaassen, C.D., 2012. Nrf2 deficiency improves glucose tolerance in mice fed a high-fat diet. *Toxicology and applied pharmacology*, 264(3), pp.305-314.

CHAPTER 2

DEVELOPMENT OF STEATOSIS IN HEPG2 CELL LINE WITH FRUCTOSE AND PALMITATE

2.1 Introduction

Liver diseases are rapidly turning up as global health preferences. The prevalence of NAFLD / NASH in India is around 9 - 32% of the general population (Dhamija et al., 2019) and an emerging global burden. It is primarily linked with diabetes, obesity and several other features of metabolic syndrome. Nonetheless, the basic molecular mechanisms involved in the development and progression of this disease are poorly inferred. Investigation of underlying molecular mechanisms and signaling pathways involved in it requires vigorous and well exemplified *in vitro* models.

More recently several *in vitro* models have been widely exploited for the study of development of liver disease. For the study of NAFLD / NASH, hepatocytes (common cell type in the liver, that accounts for about 80% of the cell population) treated with fatty acids have developed into a well established *in vitro* model (Ricchi et al., 2009; Chavez et al., 2012; Grasselli et al., 2017). Even though the metabolic activities of hepatoma cells are highly limited compared to primary hepatocytes, they provide several advantages for *in vitro* studies such as easy handling, high availability, unlimited life span and nearly stable phenotype. HepG2 is the one of the most trivial hepatocytes derived from the cell line, other being HuH7 cells. HepG2 cells are human hepatoma cell line that originated from a 15 year old Caucasian American male (Aden et al., 1979; Knowles et al., 1980) are non-tumorigenic in nature, possess high proliferation rate and commonly used in drug metabolism and hepatotoxicity studies (Donato et al., 2015). They also express several differentiated hepatic functions like synthesis and secretion of plasma proteins, metabolism of triglyceride and cholesterol, metabolism and transportation of lipoproteins, bile acid synthesis, glycogen synthesis and insulin signaling (Fearn & Hirst, 2006; Javitt, 1990, Dongiovanni et al., 2008).

An extensive number of researches were done on human hepatocytes models where the lipid accumulation in the cells was in direct proportion when cells were treated with different concentrations of lipids such as palmitate or oleic acid or both (Chavez et al., 2011; Hetherington et al., 2016; Dave et al., 2018). The differential effect of palmitic acid and oleic acid on lipid accumulation and apoptosis in cultured hepatocytes were also subjected for investigation (Ricchi et al., 2009). Furthermore, compared to saturated fatty acids like palmitate, MUFAs were less toxic to hepatocytes similar to other cell types. *In vitro* treatment of HepG2 cells with fructose also generates equivocal results. Fructose metabolism occurs in HepG2 cells (Hirahatake et al., 2011; Huang et al., 2011) and has been showed that HFCS treatment increases intracellular TG content in HepG2 cells (Collison et al., 2009) along with altered lipogenic gene expression and mitochondrial function in a dose dependent manner.

The aim of the experiments in this chapter was to develop an *in vitro* model of steatosis by incubating HepG2 cells with fructose (100 mM) and palmitate (100 μ M), for 24 hrs. This is followed by characterization of the model with various biochemical parameters relevant to steatosis.

2.2 Materials and methods

2.2.1 Chemicals and reagents

Fructose, sodium palmitate, 3-(4,5-dimethylthiazol-2-yl)-2,5-diphenyl tetrazolium bromide (MTT), dimethyl sulfoxide (DMSO), oil-red-O stain, radioimmunoprecipitation assay (RIPA) buffer and protease inhibitor cocktail were purchased from Sigma - Aldrich Co. (St. Louis, MO, USA). The cell culture flasks and plates were from BD Biosciences (USA). Fetal bovine serum (FBS), penicillin and streptomycin antibiotics, trypsin - ethylenediaminetetraacetic acid (EDTA), phosphate buffered saline (PBS) and Hank's balanced salt solution (HBSS), bovine serum albumin (BSA), minimum essential medium (MEM) were from Gibco, USA. The triglyceride assay kit, glycerol assay kit and intracellular cholesterol detection assay kit were from Cayman chemical company (MI, USA). Antibodies against FAS, ACC- α , p-ACC- α and β actin were obtained from Santa Cruz Biotechnology (CA, USA). All other chemicals used were of analytical grade.

2.2.2 Cell culture

HepG2 cells (American Type Culture Collection, (ATCC) Rockville, MD USA) were cultured as per supplier's instructions. In brief, the cells were grown in T-25 flask containing

MEM supplemented with 10% heat-inactivated FBS and 1X penicillin streptomycin solution at 37°C and 5% CO₂ in a humidified incubator (Eppendorf, USA). When the cells reached 80% confluence, the cells were trypsinized and reseeded onto a new flask for further experiments.

2.2.3 Fructose and palmitate treatments of HepG2 cells

Fructose stock solution was prepared by dissolving in HBSS and was used to produce different concentrations of fructose treatment in serum free MEM. Palmitate stock solution (10 mM) was prepared by dissolving sodium palmitate in 0.1 N NaOH at 75°C for 5 min. The stock solution was further mixed with fatty acid free BSA to make a final concentration of 1 mM. The 1 mM working solution was then diluted to the desired treatment concentration (100 µM) in 1% MEM. Treatment was applied on day 3 and the experiments were performed after 24 hrs of treatment with fructose and palmitate (Figure 2.1).

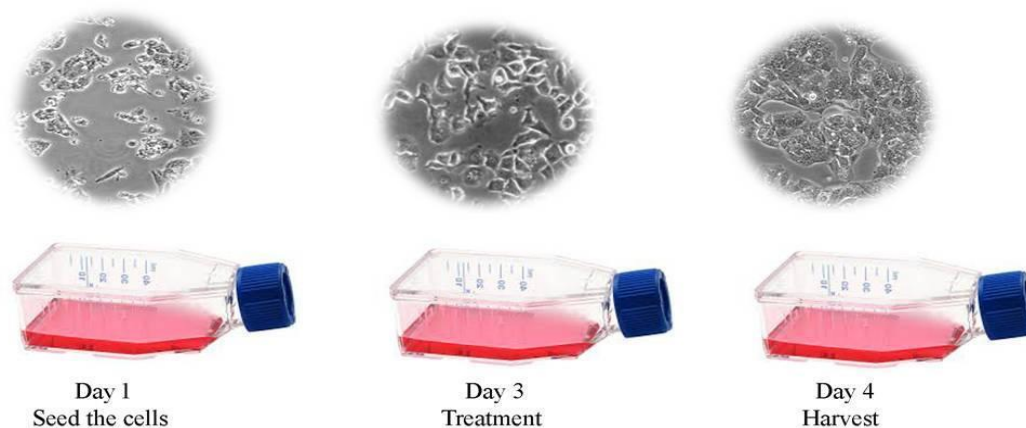


Figure 2.1 Schematic experimental setup of cell culture

The experimental groups consist of C - control ; F 50 - fructose 50 mM; F 100 - fructose 100 mM; P 100 - palmitate 100 µM; F 50 + P 100 - fructose 50 mM + palmitate 100 µM; F 100 + P 100 - fructose 100 mM + palmitate 100 µM; fenofibrate - fenofibrate (25 µM) (positive control).

2.2.4 Cell viability

Cell viability was determined by MTT assay, which relies on the enzymatic reduction of 3-[4,5-dimethylthiazole-2-yl]-2,5-diphenyltetrazolium bromide to MTT formazan catalyzed by the enzyme mitochondrial succinate dehydrogenase. Briefly, the cells were seeded in a 96-well plate at a seeding density of 5×10^3 per well. The cells were then incubated for about 24 hrs. After incubation, 100 µL of MTT solution (5 mg/mL) was added to each well and incubated for another 4 hrs at 37°C in the dark. The solution was removed from each well and 100 µL of

DMSO was added to dissolve the formazan crystals. The culture plate was placed on a shaker for about 20 min. The blue colored tetrazolium crystals were dissolved in DMSO. Absorbance was measured at 570 nm in a spectrophotometer (Biotek Synergy 4, USA).

2.2.5 Oil-red-O staining

Oil-red-O stain was used to detect the intracellular lipid accumulation. Briefly 2×10^5 cells were seeded on a 12-well plate and treated as mentioned earlier. At the end of the treatment period, the media was aspirated from the culture plates and the cells were rinsed with PBS and fixed in 4% paraformaldehyde. Fixation is followed by permeabilization using 0.1% Triton X-100. Stock oil-red-O solution was prepared in isopropyl alcohol and diluted 3:2 in ddH₂O. Diluted oil-red-O solution was added to the fixed cells for 15 min, after which it was aspirated away, washed with ddH₂O. The oil droplets in HepG2 cells were visualized and captured at 40X on phase contrast microscope (Nikon Eclipse TS 100, Japan) using NIS Elements software. For the quantification of lipid droplets, isopropyl alcohol was added to each well and lipid accumulation was measured using a spectrophotometer at 490 nm absorbance (Biotek Synergy 4, USA).

2.2.6 Triglyceride assay

To evaluate the extent of steatosis in cells from various experimental groups, the concentration of triglyceride was measured using triglyceride colorimetric assay kit. This assay explores the enzymatic hydrolysis of triglycerides by lipases to produce glycerol and free fatty acids. The glycerol thus formed is phosphorylated and converted to glycerol-3-phosphate by glycerol kinase. Glycerol-3-phosphate undergoes oxidation to produce dihydroxyacetone phosphate and H₂O₂. The presence of peroxidase catalyzes the redox-coupled reaction of H₂O₂ with 4-aminoantipyrine and N-ethyl-N-(3-sulfopropyl)-m-anisidine, producing a bright purple colour. The assay was performed as per manufacturer's instructions. Briefly, after incubation the cells were collected by centrifugation and resuspended the cell pellet in cold diluted standard diluent. After sonication, the cell suspensions were centrifuged at 10,000 x g for 10 min at 4°C. The resulting supernatant was collected to which diluted enzyme mixture was added and incubated for about 15 minutes. The absorbance was measured at 530 - 550 nm.

2.2.7 Glycerol assay

Lipolysis was assessed by measuring the amount of glycerol released into the culture medium and was determined by using a glycerol assay kit. The glycerol assay measures glycerol

by a series of enzymatic reactions where glycerol is phosphorylated by glycerol kinase. The resultant product glycerol - 3 - phosphate gets oxidized to form dihydroxyacetone phosphate and H₂O₂. Peroxidase catalyzes the redox coupled reaction of H₂O₂ with 4 - aminoantipyrine and N - ethyl - N - (3 - sulfopropyl) - m - anisidine producing a brilliant purple product quinoneimine dye. Briefly, the cells were seeded in a 96-well plate. After respective treatments, cell culture supernatants were collected from each well and placed in glycerol free containers. 100 µl of reconstituted free glycerol assay reagents were added and incubated at room temperature for about 15 min. The absorbance was read at 540 nm.

2.2.8 Intracellular cholesterol accumulation

The intracellular cholesterol accumulation in treated HepG2 cells was visualized by using cell based cholesterol detection assay kit. Briefly, 3×10⁴ cells were seeded in 96-well black plates. After treatment, cholesterol localization was done by the Filipin III solution, a widely used probe for sterol location in biological membranes (Castanho, 1992) followed by fixation with cell-based assay fixative solution. The stain was washed off with HBSS and examined under a spinning disk imaging system (BD PathwayTM Bioimager System, BD Biosciences, USA). Cholesterol accumulation was examined under a fluorescent microscope at an excitation of 340 -380 nm and emission of 385 - 470 nm.

2.2.9 Western blot

After respective treatments cells were harvested and proteins were extracted from HepG2 cells by using an ice cold RIPA buffer containing protease inhibitor cocktail. It was then incubated on ice for about 20 min and cell suspensions were centrifuged at 12,000 rpm for 20 min at 4°C. The supernatant was collected and used for further immunoblot analysis. The protein concentration of the cell lysate was measured by using bicinchoninic acid kit (Pierce, Rockford, IL, USA) as per manufacturer's instruction. Proteins thus extracted were separated by sodium dodecyl sulfate polyacrylamide gel electrophoresis (SDS-PAGE) and were transferred to polyvinylidene difluoride (PVDF) membrane using Trans-Blot® TurboTM Transfer system (Bio-Rad, USA). The membrane was then blocked with 5% skimmed milk in TBST for 1 hr at room temperature then probed with specific primary antibodies against FAS, ACC, p-ACC and β - actin (1:1000 dilutions) at 4°C overnight. After washing with TBST, specific horseradish peroxidase conjugated secondary antibodies (1:2000 dilutions) were added and the membranes were incubated for about 2 hrs. After washing, the immune complex was visualized using

Clarity™ Western ECL Substrate (Bio-Rad,USA).The images were analyzed in the ChemiDoc XRS system (Bio-Rad,USA) using Image Lab software.

2.2.10 Statistical analysis

Statistical analysis was carried out by the SPSS statistical program. The data were represented as mean \pm SD. The data were subjected to one - way analysis of variance (ANOVA) and the differences among the means of the groups were assessed using Duncan's multiple range tests using OriginPro version 8.5 (OriginLab Corporation, Massachusetts, USA). The statistical significance was accepted at $p \leq 0.05$.

2.3 Results

2.3.1 Effect of fructose and palmitate on cell viability

The cell viability of F50, F100 and P100 treated cells did not show significant cytotoxic effects compared to the control group (Figure 2.2). More than 95% of the treated cells were viable. The F50 + P100 and F100 + P100 treated HepG2 cells showed significant cytotoxicity (10.6% and 13.5% respectively, $p \leq 0.05$) compared to the control group (Figure 2.2).

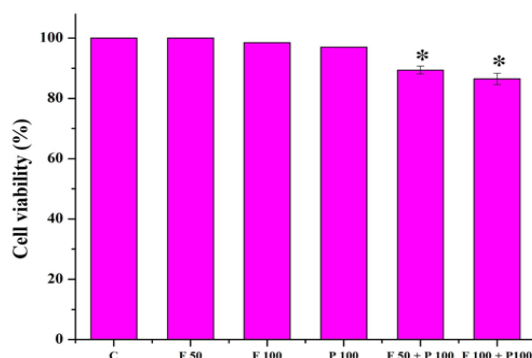


Figure 2.2 Fructose and palmitate affect the cell viability of HepG2 cells: HepG2 cells were treated with different concentrations of fructose and palmitate and the cell viability was detected by MTT assay. C indicates control ; F50 - fructose 50 mM; F100 - fructose 100 mM; P100 - palmitate 100 μ M; F50 + P100 - fructose 50 mM + palmitate 100 μ M; F100 + P100 - fructose 100 mM + palmitate 100 μ M. Values are expressed as mean \pm SD, where $n = 6$. * indicates significantly different from the control group ($p \leq 0.05$).

2.3.2 Effect of fructose and palmitate on lipid accumulation

Lipid accumulation is the characteristic feature of steatosis. The intracellular lipid accumulation in treated cells revealed that very little lipid accumulation was observed in control and F50 treated cells (22.22 %, Figure 2.3). Treatment of HepG2 cells with F100 and P100 causes a significant ($p \leq 0.05$) rise in lipid accumulation to 77.77% and 101.2% respectively

(Figure 2.3). Moreover, significant ($p \leq 0.05$) lipid accumulation can be seen in F50 + P100 and F100 + P100 treated groups, where intracellular lipid content increases in a dose dependent manner (166.89% and 333.33% respectively) (Figure 2.3). The lipid lowering drug fenofibrate (25 μ M) prevented the lipid accumulation in HepG2 cells significantly by 91.02% ($p \leq 0.05$) (Figure 2.3). The results from this study clearly demonstrated that fructose and palmitate induce steatosis in HepG2 cells under *in vitro* conditions.

A

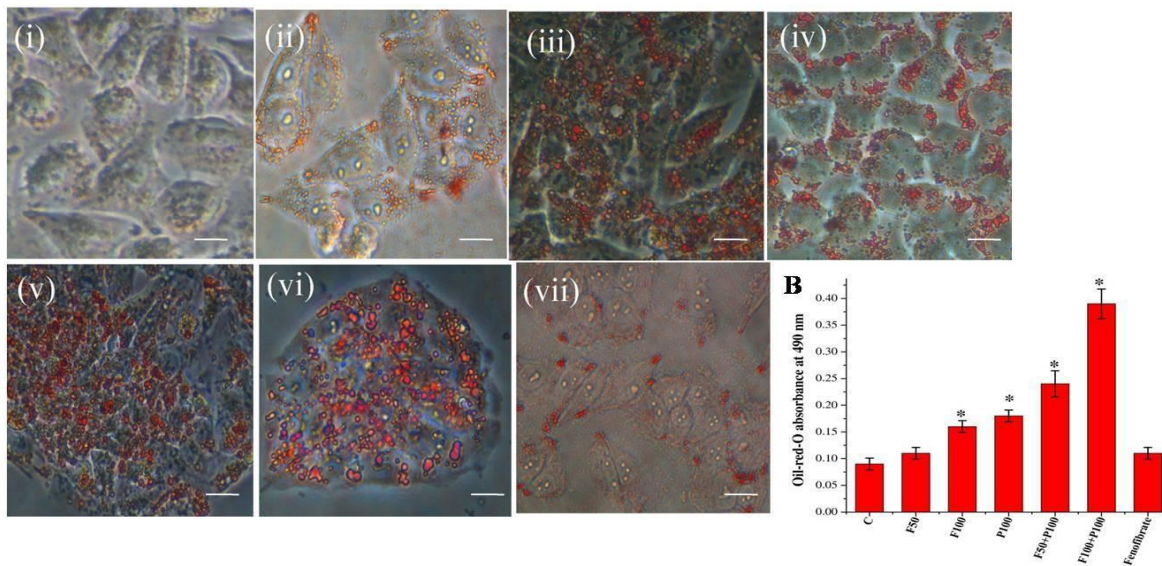


Figure 2.3 Fructose and palmitate induced intracellular lipid accumulation: (A) Representative microscopic images of HepG2 cells from different experimental groups. HepG2 cells were treated with various concentrations of fructose and palmitate for 24 hrs and stained with oil-red-O to visualize the intracellular lipid contents. (i) C - control; (ii) F50 - fructose 50 mM; (iii) F100 - fructose 100 mM; (iv) P100 - palmitate 100 μ M; (v) F50 + P100 - fructose 50 mM + palmitate 100 μ M; (vi) F100 + P100 - fructose 100 mM + palmitate 100 μ M; (vii) fenofibrate (25 μ M). Original magnification 40X. Scale bar corresponds to 50 μ M. (B) Absorbance was read at 490 nm after oil-red-O staining. Data are expressed as mean \pm SD; where n = 6. * indicates significantly different from the control group ($p \leq 0.05$).

2.3.3 Effect of fructose and palmitate on intracellular TG content

To confirm the results obtained from oil-red-O staining, the TG content in fructose palmitate treated HepG2 cells were measured. Both fructose and palmitate are found to have a tendency to increase TG content. Treatment with F50, F100 and P100 showed a significant increase ($p \leq 0.05$) of TG to 34%, 100.66% and 112% respectively (Figure 2.4) in TG compared to the control. Treatment with F50 + P100 and F100 + P100 treatment also significantly

increased ($p \leq 0.05$) the intracellular TG to 159.33% and 230.61% respectively (Figure 2.4). Moreover, fenofibrate significantly ($p \leq 0.05$) reduced the TG content to 72.45% (Figure 2.4).

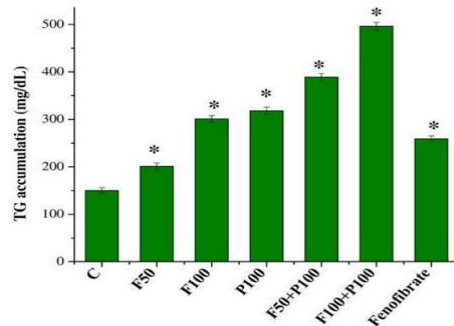


Figure 2.4 Fructose and palmitate induced TG accumulation: HepG2 cells were treated with various concentrations of fructose and palmitate for 24 hrs and measured the intracellular TG content. C indicates control ; F50 - fructose 50 mM; F100 - fructose 100 mM; P100 - palmitate 100 μ M; F50 + P100 - fructose 50 mM + palmitate 100 μ M; F100 + P100 - fructose 100 mM + palmitate 100 μ M. Data are expressed as mean \pm SD; where n = 6. * indicates significantly different from the control group ($p \leq 0.05$).

2.3.4 Effect of fructose and palmitate on lipolysis

We also explored the effect of fructose and palmitate on lipolysis in HepG2 cells. Treatment with F50, F100 and P100 showed a significant ($p \leq 0.05$) reduction of lipolysis to 19.57%, 24.60% and 41.79% respectively (Figure 2.5). Significant ($p \leq 0.05$) reduction in lipolysis was also observed in F50 + P100 and F100 + P100 treated groups (47.61% and 60.31% respectively) (Figure 2.5). Treatment with fenofibrate significantly attenuated lipolysis in HepG2 cells by 80.52%, $p \leq 0.05$ (Figure 2.5). These results revealed the role of fructose and palmitate in reducing β oxidation and increasing lipid accumulation.

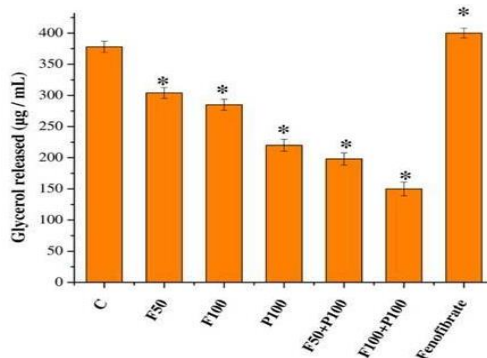


Figure 2.5 Fructose and palmitate mediated lipolysis: HepG2 cells were treated with various concentrations of fructose and palmitate for 24 hrs and lipolysis was assessed by glycerol release into the

medium. C indicates control ; F50 - fructose 50 mM; F100 - fructose 100 mM; P100 - palmitate 100 μ M; F50 + P100 - fructose 50 mM + palmitate 100 μ M; F100 + P100 - fructose 100 mM + palmitate 100 μ M. Data are expressed as mean \pm SD; where n = 6. * indicates significantly different from the control group ($p \leq 0.05$).

2.3.5 Effect of fructose and palmitate on cholesterol accumulation

The effect of fructose and palmitate on cholesterol synthesis in HepG2 cells was determined. From Figure 2.6, it is evident that fructose and palmitate treatment increased the intracellular cholesterol content. There was a significant increase ($p \leq 0.05$) of cholesterol in F50, F100 and P100 treated HepG2 cells by 30%, 40.45% and 45.90% respectively (Figure 2.6). Treatment with F50 + P100 and F100 + P100 increased the cholesterol significantly (93.63% and 154.09% respectively). Fenofibrate significantly reduced ($p \leq 0.05$) the abundance of cholesterol accumulation in HepG2 cells to 81.45% (Figure 2.6).

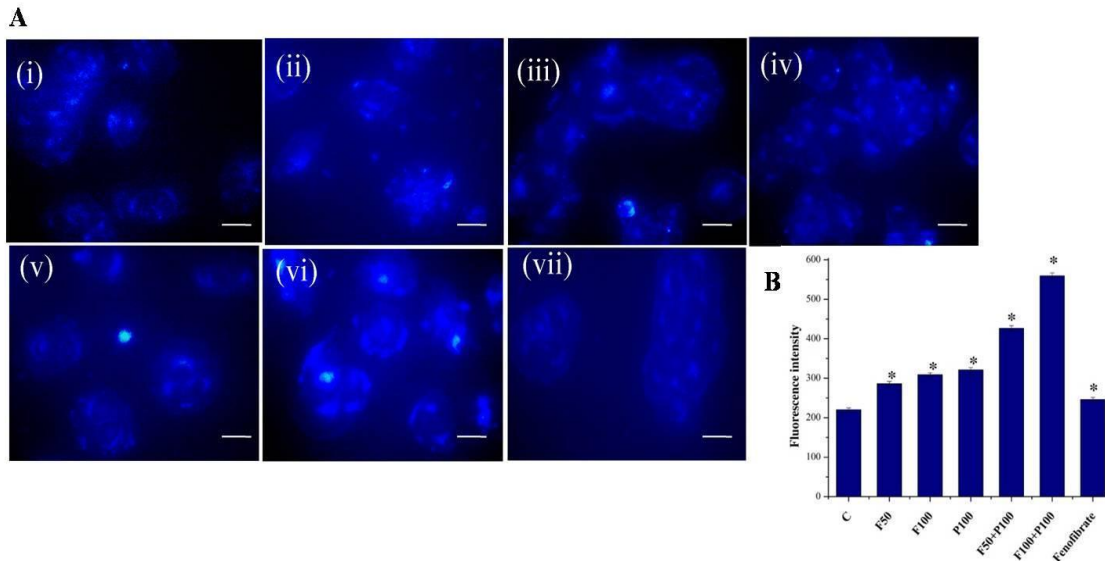


Figure 2.6 Fructose and palmitate induced intracellular cholesterol accumulation: (A) Representative microscopic images of intracellular cholesterol content in various concentrations of fructose and palmitate treated HepG2 cells. (i) C - control; (ii) F50 - fructose 50 mM; (iii) F100 - fructose 100 mM; (iv) P100 - palmitate 100 μ M; (v) F50 + P100 - fructose 50 mM + palmitate 100 μ M; (vi) F100 + P100 - fructose 100 mM + palmitate 100 μ M; (vii) fenofibrate (25 μ M). Original magnification 40X. Scale bar corresponds to 50 μ M. (B) Fluorescence was measured at 470 nm. Values are expressed as mean \pm SD (n=6). * indicates significantly different from the control group ($p \leq 0.05$).

2.3.6 Effect of fructose and palmitate on lipid metabolism

To confirm the lipid accumulation by fructose and palmitate during steatosis at molecular level, protein expression study was conducted for some of the major lipogenic enzymes such as FAS, ACC- α and p-ACC α . FAS and ACC- α are the major enzymes involved in lipid biosynthesis and are the key regulators of fatty acid oxidation. There was a significant increase in the expression of FAS in F50, F100 and P100 treated groups by 52.8%, 79.85% and 117.25% ($p \leq 0.05$) respectively (Figure 2.7). However, treatment with F50 + P100 reduces the expression level to 32.45% (Figure 2.7). F100 + P100 treatment upregulated the expression of FAS significantly to 368.05% ($p \leq 0.05$) and fenofibrate improved the condition to 121.65% (Figure 2.7). Furthermore the expression of phosphorylated form of ACC- α was decreased after fructose palmitate treatment. F50, F100 and P100 treatment significantly reduces the expression of p-ACC- α to 38.78%, 49.29% and 61.78% respectively ($p \leq 0.05$) (Figure 2.7). Significant down regulation of p-ACC also occurred in F50 + P100 and F100 + P100 treated groups by 129.47% and 132.78% respectively ($p \leq 0.05$) (Figure 2.7).

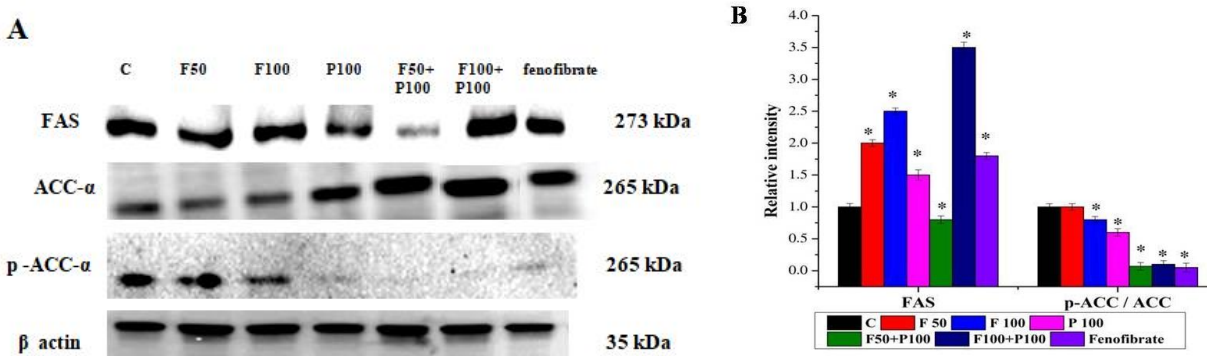


Figure 2.7 Fructose and palmitate induced steatogenesis in HepG2 cells: (A) The protein expression of FAS, ACC- α , and p-ACC- α during different concentrations of fructose and palmitate treated conditions. C indicates control ; F50 - fructose 50 mM; F100 - fructose 100 mM; P100 - palmitate 100 μ M; F50 + P100 - fructose 50 mM + palmitate 100 μ M; F100 + P100 - fructose 100 mM + palmitate 100 μ M. (B) The relative intensity of each band was quantified with β actin. Data are expressed as mean \pm SD; where $n = 3$. * indicates significantly different from the control group ($p \leq 0.05$).

2.4 Discussion

In recent times the development of liver diseases especially NAFLD and NASH is increasing rapidly. Since there is no FDA approved drug for the treatment of these diseases, there has been a growing interest in the development of new drugs for these diseases. In view of this

an *in vitro* cell based model of human hepatic steatosis is essential that provides insights into the pathogenesis of liver disease. Establishment of a proper *in vitro* model and mechanistic knowledge of the genesis of liver disease also aided in the discovery of early biomarkers and design of drugs development for liver diseases in due course.

In the present study, we developed an *in vitro* model of hepatic steatosis using fructose and palmitate. We clearly demonstrated its potential effect on HepG2 cells in terms of lipid accumulation, the classical feature of hepatic steatosis. Fructose was used here since dietary fructose from added sugar in the form of HFCS is the leading factor behind fatty liver disease and other metabolic diseases. Fatty liver disease comprises a spectrum of manifestations ranging from steatosis, steatosis along with inflammation, steatosis with hepatocytes injury, or steatosis with fibrosis (Sharma & Arora, 2020). The rationale for selecting palmitate in this study is that many junk foods and western diets contain trans fat that behave like saturated fatty acid when it gets into the body. Palmitate is a typical saturated fatty acid and is more lipotoxic in nature than unsaturated fatty acids (Ogawa et al., 2018). Moreover it is the most abundant circulating fatty acid in humans. It has been reported that the concentration of palmitate have been increased significantly in patients with NASH (De Almeida et al., 2002) and elevated level of hepatic palmitate was also detected in NASH patients than non - NAFLD patients (Allard et al., 2008).

In this study, we investigated whether fructose and palmitate could play a role in the development of steatosis. Fructose at higher doses together with palmitate confirmed its effect upon HepG2 cells. The treatment with fructose at 100 mM concentration did not affect the cell viability in the present study. However the presence of palmitate along with fructose was found to affect cell viability significantly. HepG2 cells were also found to be more susceptible to fructose and palmitate treatment by having a significant degree of intracellular lipid. A series of lipogenic programs occurs after high doses of fructose treatment leading to hepatic lipid accumulation (Softic et al., 2016). At cellular level, fructose is preferentially converted into fructose-1-phosphate. The phosphotriose produced from fructose-1-phosphate can be converted to glucose, lactate and fatty acids (Tappy & Le, 2010). Even though the lipogenic pathway is numerically minor under physiological conditions, it becomes effective after fructose overload (Herman & Samuel, 2016) *via* increased lipogenic precursors. Moreover, bypassing the committed reaction mediated by phosphofructokinase of glycolysis favors the unregulated entry and metabolism of fructose in hepatocytes. Our result was in line with other research (Yu, et al.,

2018; Li et al., 2019) which also found elevated lipid accumulation during fructose treatment. Experiments revealed that palmitate stimulated intracellular lipid accumulation and was more active at micromolar concentrations. This is also in agreement with literature using similar *in vitro* models used in this chapter (Ricchi et al., 2009, Zhao et al., 2017, Zhao et al., 2021). The lipid accumulation in HepG2 cells *via* palmitate treatment was also time dependent. A previous study reported that maximum lipid accumulation will occur within 24 hrs of palmitate incubation, irrespective of the concentration selected (Gomez et al., 2007). The presence of high fructose also increases TG synthesis and suppressed lipolysis mainly by saturating the glycolytic pathway. This result in an accumulation of glycolysis intermediates that can be later converted to glycerol-3-phosphate, used in TG synthesis. Likewise, the phosphorylation of hormone sensitive lipase and the expression of triacylglycerol lipase was significantly downregulated if fructose was present in the medium, which would potentially lead to the retention of TG (Huang et al., 2011). Present study also demonstrated that fructose and palmitate contribute to TG synthesis and suppressed lipolysis in hepatocytes. Palmitate reduces the release of glycerol from HepG2 cells suggesting the possibility that palmitate can efficiently regulate lipid metabolism in the liver and promote dyslipidemia.

We further investigated the effect of fructose and palmitate on cholesterol accumulation in HepG2 cells. The cholesterol homeostasis is highly essential for the proper cellular and systemic functions. The level of cholesterol in cells reflects the dynamic balance between synthesis, uptake, export and esterification. In the present study, the dietary components fructose and palmitate are directly influencing the cholesterol content in hepatocytes. In point of fact, cholesterol and saturated fat has been correlated with hepatic steatosis (Cheng et al., 2016; Luukkonen et al., 2018). The cellular cholesterol synthesis is regulated by a membrane bound transcription factor called SREBP-2. Its expression is higher in the liver and its activity gets enhanced with increased liver fat content (Caballero et al., 2009). Certain studies reported the effect of high fructose on plasma concentrations of low - density lipoprotein (LDL) cholesterol, oxidized LDL and small dense LDL (Stanhope et al., 2009). The esterification of fatty acids in hepatocytes also leads to the formation of cholesterol in order to generate cholesterol esters. The presence of fructose, glycerol and to a lesser extent glucose stimulated the esterification of fatty acids in liver cells. A large number of various kinds of diet induced animal models have been established to explore the effects of distinct macronutrients on liver metabolism and pathogenesis

of NASH. Most of the studies suggested a synergistic effect of fat and fructose on biological parameters of NASH (DiStefano, 2020). It has been reported that diet induced hypercholesterolemia causes oxidative stress, altered Ψ_m and hepatic steatosis in mice (Dominguez, 2019).

Next we investigated the effect of fructose and palmitate on expression of lipogenic proteins to reveal the underlying mechanism behind lipid content in treated HepG2 cells. The synthesis of fatty acid begins with acetyl CoA and the length of the fatty acid chain is increased by the addition of two carbon units. The rate limiting step in lipogenesis; conversion of acetyl CoA to malonyl CoA is catalyzed by ACC (Munday, 2002). The acetyl CoA, malonyl CoA and NADPH were utilized by FAS and helps in the elongation of fatty acids to form palmitic acid (Jensen & Semenkovich, 2012). For this reason, we examined those key enzymes involved in lipid metabolism in HepG2 cells. Fructose and palmitate stimulated the protein expression of ACC and FAS, primary enzymes of lipogenesis. The combined effect of both results in a drastic increase in the expression of lipogenic enzymes, suggesting that both are stimulating de novo fatty acid synthesis in HepG2 cells. Further we also found that phosphorylated form of ACC- α was significantly decreased in fructose palmitate treated HepG2 cells. It has been reported that the levels of TG, total cholesterol as well as increased expression of genes involved in carbohydrate and lipid metabolism occurred in HepG2 cells treated with a mixture of glucose, fructose and fatty acids (Hirahatake et al., 2011). However fructose alone is insufficient to affect the expression of lipogenic genes (Zhao et al., 2016). *In vivo* studies demonstrated the increased expression of lipogenic genes during fructose feeding, while inhibiting the expression of genes in fatty acid oxidation (DiStefano, 2019). In humans, ten weeks fructose consumption led to increased hepatic DNL implicating the effect of fructose in contributing to NASH development (Stanhope et al., 2009). The PPAR α agonist, fenofibrate have been manifested in several hepatic cell lines, rodents fed with high fat diet and also in humans (van der Veen et al., 2017; Kostapanos et al., 2013; Cornwell et al., 2004) and proved its hypolipidemic effects. In the present study, fenofibrate reduces the lipid and TG accumulation induced by fructose and palmitate. But it is not effective to bring back the lipid control to normal.

From the overall experiments, we found that incubation of HepG2 cells with fructose (100 mM) and palmitate (100 μ M) induce surplus lipogenesis. So this model is found to be an

ideal one for the detailed mechanistic studies on liver disorder to elucidate various molecular mechanisms.

2.5 Summary and conclusion

Based on the preliminary investigations, it is clear that combination of 100 mM fructose and 100 μ M palmitate sufficiently induces steatosis in HepG2 cells after 24 hrs treatment. So this concentration is selected for further mechanistic study of steatosis and the final experimental design based on preliminary experiments include (i) C - control, (ii) HFP - high fructose (100 mM) and palmitate (100 μ M), (iii) HFP + fenofibrate - (high fructose and palmitate) + fenofibrate (25 μ M).

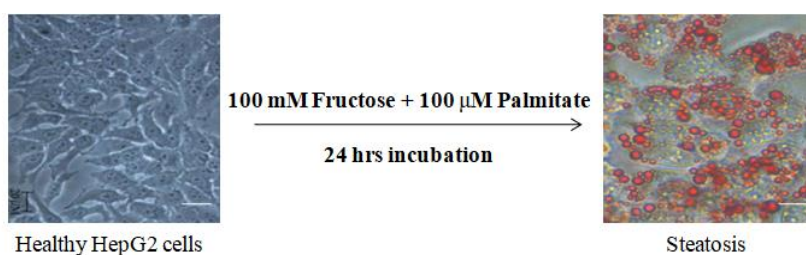


Figure 2.8 Standardized *in vitro* cell based model of steatosis

References

- Aden, D.P., Fogel, A., Plotkin, S., Damjanov, I. and Knowles, B.B., 1979. Controlled synthesis of HBsAg in a differentiated human liver carcinoma-derived cell line. *Nature*, 282(5739), pp.615-616.
- Allard, J.P., Aghdassi, E., Mohammed, S., Raman, M., Avand, G., Arendt, B.M., Jalali, P., Kandasamy, T., Prayitno, N., Sherman, M. and Guindi, M., 2008. Nutritional assessment and hepatic fatty acid composition in non-alcoholic fatty liver disease (NAFLD): a cross-sectional study. *Journal of hepatology*, 48(2), pp.300-307.
- Caballero, F., Fernández, A., De Lacy, A.M., Fernández-Checa, J.C., Caballería, J. and García-Ruiz, C., 2009. Enhanced free cholesterol, SREBP-2 and StAR expression in human NASH. *Journal of hepatology*, 50(4), pp.789-796.
- Castanho, M.A., Coutinho, A. and Prieto, M.J., 1992. Absorption and fluorescence spectra of polyene antibiotics in the presence of cholesterol. *Journal of Biological Chemistry*, 267(1), pp.204-209.

- Chavez-Tapia, N.C., Rosso, N. and Tiribelli, C., 2012. Effect of intracellular lipid accumulation in a new model of non-alcoholic fatty liver disease. *BMC gastroenterology*, 12(1), pp.1-10.
- Cheng, Y., Zhang, K., Chen, Y., Li, Y., Li, Y., Fu, K. and Feng, R., 2016. Associations between dietary nutrient intakes and hepatic lipid contents in NAFLD patients quantified by 1H-MRS and dual-Echo MRI. *Nutrients*, 8(9), p.527.
- Collison, K.S., Saleh, S.M., Bakheet, R.H., Al-Rabiah, R.K., Inglis, A.L., Makhoul, N.J., Maqbool, Z.M., Zaidi, M.Z., Al-Johi, M.A. and Al-Mohanna, F.A., 2009. Diabetes of the liver: the link between nonalcoholic fatty liver disease and HFCS-55. *Obesity*, 17(11), pp.2003-2013.
- Cornwell, P.D., De Souza, A.T. and Ulrich, R.G., 2004. Profiling of hepatic gene expression in rats treated with fibric acid analogs. *Mutation Research/Fundamental and Molecular Mechanisms of Mutagenesis*, 549(1-2), pp.131-145.
- Dave, T., Tilles, A.W. and Vemula, M., 2018. A cell-based assay to investigate hypolipidemic effects of nonalcoholic fatty liver disease therapeutics. *SLAS DISCOVERY: Advancing Life Sciences R&D*, 23(3), pp.274-282.
- De Almeida, I.T., Cortez-Pinto, H., Fidalgo, G., Rodrigues, D. and Camilo, M.E., 2002. Plasma total and free fatty acids composition in human non-alcoholic steatohepatitis. *Clinical nutrition*, 21(3), pp.219-223.
- Dhamija, E., Paul, S.B. and Kedia, S., 2019. Non-alcoholic fatty liver disease associated with hepatocellular carcinoma: An increasing concern. *The Indian journal of medical research*, 149(1), p.9.
- DiStefano, J.K., 2020. Fructose-mediated effects on gene expression and epigenetic mechanisms associated with NAFLD pathogenesis. *Cellular and Molecular Life Sciences*, 77(11), pp.2079-2090.
- Domínguez-Pérez, M., Simoni-Nieves, A., Rosales, P., Nuño-Lámbarri, N., Rosas-Lemus, M., Souza, V., Miranda, R.U., Bucio, L., Uribe Carvajal, S., Marquardt, J.U. and Seo, D., 2019. Cholesterol burden in the liver induces mitochondrial dynamic changes and resistance to apoptosis. *Journal of cellular physiology*, 234(5), pp.7213-7223.

- Donato, M.T., Tolosa, L. and Gómez-Lechón, M.J., 2015. Culture and functional characterization of human hepatoma HepG2 cells. In *Protocols in In Vitro Hepatocyte Research* (pp. 77-93). Humana Press, New York, NY.
- Dongiovanni, P., Valenti, L., Fracanzani, A.L., Gatti, S., Cairo, G. and Fargion, S., 2008. Iron depletion by deferoxamine up-regulates glucose uptake and insulin signaling in hepatoma cells and in rat liver. *The American journal of pathology*, 172(3), pp.738-747.
- Fearn, R.A. and Hirst, B.H., 2006. Predicting oral drug absorption and hepatobiliary clearance: Human intestinal and hepatic in vitro cell models. *Environmental toxicology and pharmacology*, 21(2), pp.168-178.
- Gomez-Lechon, M.J., Donato, M.T., Martínez-Romero, A., Jiménez, N., Castell, J.V. and O'Connor, J.E., 2007. A human hepatocellular in vitro model to investigate steatosis. *Chemico-biological interactions*, 165(2), pp.106-116.
- Grasselli, E., Canesi, L., Portincasa, P., Voci, A., Vergani, L. and Demori, I., 2017. Models of non-alcoholic fatty liver disease and potential translational value: The effects of 3, 5-L-diiodothyronine. *Annals of hepatology*, 16(5), pp.707-719.
- Herman, M.A. and Samuel, V.T., 2016. The sweet path to metabolic demise: fructose and lipid synthesis. *Trends in Endocrinology & Metabolism*, 27(10), pp.719-730.
- Hetherington, A.M., Sawyez, C.G., Zilberman, E., Stoianov, A.M., Robson, D.L. and Borradaile, N.M., 2016. Differential lipotoxic effects of palmitate and oleate in activated human hepatic stellate cells and epithelial hepatoma cells. *Cellular Physiology and Biochemistry*, 39(4), pp.1648-1662.
- Hirahatake, K.M., Meissen, J.K., Fiehn, O. and Adams, S.H., 2011. Comparative effects of fructose and glucose on lipogenic gene expression and intermediary metabolism in HepG2 liver cells. *PLoS One*, 6(11), p.e26583.
- Huang, D., Dhawan, T., Young, S., Yong, W.H., Boros, L.G. and Heaney, A.P., 2011. Fructose impairs glucose-induced hepatic triglyceride synthesis. *Lipids in health and disease*, 10(1), pp.1-10.
- Javitt, N.B., 1990. Hep G2 cells as a resource for metabolic studies: lipoprotein, cholesterol, and bile acids. *The FASEB Journal*, 4(2), pp.161-168.

- Jensen-Urstad, A.P. and Semenkovich, C.F., 2012. Fatty acid synthase and liver triglyceride metabolism: housekeeper or messenger?. *Biochimica et Biophysica Acta (BBA)-Molecular and Cell Biology of Lipids*, 1821(5), pp.747-753.
- Knowles, B.B., Howe, C.C. and Aden, D.P., 1980. Human hepatocellular carcinoma cell lines secrete the major plasma proteins and hepatitis B surface antigen. *Science*, 209(4455), pp.497-499.
- Kostapanos, M.S., Kei, A. and Elisaf, M.S., 2013. Current role of fenofibrate in the prevention and management of non-alcoholic fatty liver disease. *World Journal of Hepatology*, 5(9), p.470.
- Li, Y., Ren, L., Song, G., Zhang, P., Yang, L., Chen, X., Yu, X. and Chen, S., 2019. Silibinin ameliorates fructose-induced lipid accumulation and activates autophagy in HepG2 Cells. *Endocrine, Metabolic & Immune Disorders-Drug Targets (Formerly Current Drug Targets-Immune, Endocrine & Metabolic Disorders)*, 19(5), pp.632-642.
- Luukkonen, P.K., Sadevirta, S., Zhou, Y., Kayser, B., Ali, A., Ahonen, L., Lallukka, S., Pelloux, V., Gaggini, M., Jian, C. and Hakkarainen, A., 2018. Saturated fat is more metabolically harmful for the human liver than unsaturated fat or simple sugars. *Diabetes care*, 41(8), pp.1732-1739.
- Munday, M.R., 2002. Regulation of mammalian acetyl-CoA carboxylase. *Biochemical Society Transactions*, 30(6), pp.1059-1064.
- Ogawa, Y., Imajo, K., Honda, Y., Kessoku, T., Tomeno, W., Kato, S., Fujita, K., Yoneda, M., Saito, S., Saigusa, Y. and Hyogo, H., 2018. Palmitate-induced lipotoxicity is crucial for the pathogenesis of nonalcoholic fatty liver disease in cooperation with gut-derived endotoxin. *Scientific reports*, 8(1), pp.1-14.
- Ricchi, M., Odoardi, M.R., Carulli, L., Anzivino, C., Ballestri, S., Pinetti, A., Fantoni, L.I., Marra, F., Bertolotti, M., Banni, S. and Lonardo, A., 2009. Differential effect of oleic and palmitic acid on lipid accumulation and apoptosis in cultured hepatocytes. *Journal of gastroenterology and hepatology*, 24(5), pp.830-840.
- Sharma, P. and Arora, A., 2020. Clinical presentation of alcoholic liver disease and non-alcoholic fatty liver disease: spectrum and diagnosis. *Translational gastroenterology and hepatology*, 5.

- Softic, S., Cohen, D.E. and Kahn, C.R., 2016. Role of dietary fructose and hepatic de novo lipogenesis in fatty liver disease. *Digestive diseases and sciences*, 61(5), pp.1282-1293.
- Stanhope, K.L., Schwarz, J.M., Keim, N.L., Griffen, S.C., Bremer, A.A., Graham, J.L., Hatcher, B., Cox, C.L., Dyachenko, A., Zhang, W. and McGahan, J.P., 2009. Consuming fructose-sweetened, not glucose-sweetened, beverages increases visceral adiposity and lipids and decreases insulin sensitivity in overweight/obese humans. *The Journal of clinical investigation*, 119(5), pp.1322-1334.
- Tappy, L. and Lê, K.A., 2010. Metabolic effects of fructose and the worldwide increase in obesity. *Physiological reviews*.
- van der Veen, J.N., Lingrell, S., Gao, X., Takawale, A., Kassiri, Z., Vance, D.E. and Jacobs, R.L., 2017. Fenofibrate, but not ezetimibe, prevents fatty liver disease in mice lacking phosphatidylethanolamine N-methyltransferase. *Journal of lipid research*, 58(4), pp.656-667.
- Yu, X., Ren, L.P., Wang, C., Zhu, Y.J., Xing, H.Y., Zhao, J. and Song, G.Y., 2018. Role of X-box binding protein-1 in fructose-induced de novo lipogenesis in HepG2 cells. *Chinese medical journal*, 131(19), p.2310.
- Zhao, N.Q., Li, X.Y., Wang, L., Feng, Z.L., Li, X.F., Wen, Y.F. and Han, J.X., 2017. Palmitate induces fat accumulation by activating C/EBP β -mediated G0S2 expression in HepG2 cells. *World journal of gastroenterology*, 23(43), p.7705.
- Zhao, N., Tan, H., Wang, L., Han, L., Cheng, Y., Feng, Y., Li, T. and Liu, X., 2021. Palmitate induces fat accumulation via repressing FoxO1-mediated ATGL-dependent lipolysis in HepG2 hepatocytes. *PloS one*, 16(1), p.e0243938.
- Zhao, L., Guo, X., Wang, O., Zhang, H., Wang, Y., Zhou, F., Liu, J. and Ji, B., 2016. Fructose and glucose combined with free fatty acids induce metabolic disorders in HepG2 cell: A new model to study the impacts of high-fructose / sucrose and high-fat diets in vitro. *Molecular nutrition & food research*, 60(4), pp.909-921.

CHAPTER 3

EFFECT OF HIGH FRUCTOSE AND PALMITATE ON MITOCHONDRIAL BIOENERGETICS

3.1 Introduction

The biological impact of diet in the pathogenesis of NASH has been thoroughly demonstrated. The majority of people of the modern world are pursuing an unhealthy dietary pattern and a sedentary lifestyle. A shift from the conventional homemade food to a refined and attractive one in a very colorful packet with ready-to-use options is one cause for the high prevalence of lifestyle-related diseases. The consumption of high-calorie foods widely known as junk foods or empty calorie foods is now the attraction of the new generation. It not only affects the absorption and storage of nutrients but also leads to the development of chronic diseases like obesity, diabetes, cardiovascular diseases, fatty liver diseases etc.

NAFLD is a chronic condition responsible for most of the morbidity and mortality related to liver disease. It represents a spectrum of hepatic steatosis, liver fibrosis, liver cirrhosis, and HCC. NASH is the earliest stage of NAFLD and is characterized by excessive hepatic TG concentration exceeding 5.5% (55 mg/g liver) (Szczepaniak et al., 2005). This is also accompanied by lobular inflammation, hepatocyte ballooning, fibrosis (Day, 2002) and over expression of inflammatory cytokines (Tilg & Diehl, 2000; Situnayake et al., 1990). About 30% of the general populations in Western countries are affected by NAFLD and it is perceived as the common cause of liver dysfunction worldwide (Chalasani et al., 2012). Variation in food habits such as replacement of fresh fiber-rich foods by processed foods, foods rich in saturated fats like palmitate and added sugars plays an exaggerated role in the development of NASH. It is proved that fructose causes deleterious effects on appetite regulation (Stanhope et al., 2013). Along with palmitate, fructose is highly lipogenic and readily contributes to IR and hepatic inflammation (Miller & Adeli, 2008). Moreover, fructose metabolism primarily takes place in the liver where it can be stored in the form of TG (Softic et al., 2016). Since fructose induces a greater degree of DNL than glucose, it is justifiable that fructose leads to a more subtle decrease in fatty acid oxidation. The continuous consumption of fructose may exert a metabolic strain on the liver

through the induction of FAS and fructokinase (Chong et al., 2007). In the liver, fructokinase C is the principal isoform of fructokinase. In the absence of a negative feedback mechanism fructokinase C phosphorylate fructose and results in a drop in ATP and intracellular phosphate level. This stimulates a series of reactions including short-term block in protein synthesis, generation of oxidative stress and mitochondrial dysfunction. Moreover fructose stimulates the production of uric acid from amino acid precursors (Van den Berghe, 1986), which do not occur during glucose metabolism. High fructose consumption also imposes metabolic burden in hepatocytes by stimulating the excess production of acetyl - CoA in mitochondria. The acetyl - CoA thus formed will enter the cytoplasm through tricarboxylate transport system, where it is utilized for the synthesis of fatty acids and cholesterol *via* SREBP-1/1c, ACC- α , FAS and SCD-1. Increasing lipogenesis in the liver also favors the production of malonyl - CoA, which inhibits the major transcriptional factor of fatty acid oxidation, PPAR α and thus starts mitochondrial dysfunction.

3.1.1 NASH and hepatic mitochondria

During NASH, there will be an alteration in hepatic mitochondria both at the structural and molecular level (Einer et al., 2018). As the powerhouse of the cell, alteration in mitochondria may aggravate metabolic disturbances and potentially contribute to disease progression. However, the sequence of events and signaling pathways that links mitochondrial dysfunction and NASH progression remains uncertain.

Fructose induces hepatic mitochondrial dysfunction mainly by the lipotoxicity related to the fructose induced disruption of hepatic lipid metabolism (Alwahsh et al., 2014). The various mechanisms by which fructose induced mitochondrial dysfunction includes downregulation of PPAR α that regulates genes involved in β oxidation of fatty acids and reduced expression of PGC-1 α . Mitochondria encompasses numerous enzymes of which aconitase - 2 in the Krebs's cycle and enoyl CoA hydratase involved in fatty acid oxidation are well known to be sensitive to oxidative stress. The presence of fructose reduces the activity of aconitase - 2, resulting in an accumulation of citrate that enters the cytoplasm and activates lipogenesis (Lanaspa et al., 2012). It has been reported that the initial oxidative stress in mitochondria is mediated by NADPH oxidase and later it is carried out by ETC leading to ER stress and SREBP-1c activation. Further lipogenesis is catalyzed by ACC- α and FAS (Le et al., 2012).

The hepatic mitochondria of patients with NASH exhibited markedly reduced activities of ETC and have decreased mtDNA levels (Haque et al., 2002). Cardiolipin, one of the major phospholipids seen in the inner mitochondrial membrane gets severely damaged due to ROS. Since cardiolipin is pretended to raise the respiratory chain activity especially the complex I of ETC, oxidative damage of cardiolipin culminates in an imbalance of OXPHOS activity. This results in the release of reactive lipid peroxidation products that blocks the electron flow in ETC and further enhances more ROS formation and a vicious cycle occurs. Certainly, along with lipid peroxidation, excessive ROS can cause the release of several proinflammatory molecules and upregulate the expression of several cytokines including TGF- β , IL-8 and Fas ligand, which provide a signal for releasing biologically active aldehydes and malondialdehyde. The products of both cytokines and lipid peroxidation may act together to bring about the diverse lesions of NASH.

In healthy cells, mitochondria possess an elongated and interconnected structure. However when the cell becomes apoptotic, due to the release of cytotoxic proteins such as cytochrome C (Cyt c) the mitochondrial network gets disrupted to form disconnected structures. In liver cells, apoptosis can be carried out by several intrinsic and extrinsic pathways. Intrinsic pathway of apoptosis can be initiated by ROS mediated cellular injury and DNA damage, resulting in outer mitochondrial membrane permeabilization and release of proapoptotic factors like Cyt c to the cytosol. Activation of caspase 3 by Cyt c leads to apoptosis. On the other hand, the extrinsic pathway of apoptosis is mediated by the binding of death signals to the extracellular receptors. Here caspase 8 is responsible for apoptosis *via* caspase 3. Thus mitochondria play an inevitable role in hepatocellular apoptosis during fatty liver disease. An increased expression of apoptotic enzymes and proteins was reported in the murine models of fatty liver disease (Feldstein & Gores, 2005). In hepatocytes, the presence of saturated fatty acids can also induce apoptosis by directly activating JNK and mitochondrial pathways (Idrissova et al., 2015). There are certain studies revealing the role of mitochondria in the genesis of NAFLD in animal models. It has been reported that inhibition of mitochondrial fission enhances proton leak under conditions of free fatty acid incubation, implicating bioenergetic change (Galloway et al., 2014). In the mouse model of NAFLD, the decreased stability of OXPHOS subunits contributes to deficiency in ATP synthesis *via* the inhibition of ubiquitin - proteasome and mitophagy activation (Lee et al., 2018). Microvesicular steatosis was established in precision-cut liver slices

in liver tissues of male Wistar rats, cultured in supraphysiological concentrations of glucose, fructose, insulin, and palmitic acid to mimic metabolic syndrome (Prins et al., 2019). Nevertheless, one of the major issues in the present research in liver steatosis is the lack of proper *in vitro* models to extrapolate the role of diet in the induction of obesity and molecular mechanisms. Fast and affordable *in vitro* models are essential during the initial period of research to save the time and expenditure of research. The result of *in vitro* experiments is also a turning point in designing a final *in vivo* experiment with a well focused target. Herein, we conduct an *in vitro* mechanistic study to see how fructose and palmitate (mimics high energy diet) induce biochemical lesions of NASH through involvement of mitochondrial dysfunction in HepG2 cells. Detailed investigations linking various functions of mitochondria such as calcium homeostasis, bioenergetics, redox status are conducted here to elucidate the molecular and cellular mechanism underlying the genesis of steatosis *via* high calorie diet. This is essential for identifying suitable targets for the design and development of drugs for NAFLD.

3.2 Materials and methods

3.2.1. Chemicals and reagents

Fructose, sodium palmitate, 3-(4,5-dimethylthiazol-2-yl)-2,5-diphenyl tetrazolium bromide (MTT), dimethyl sulfoxide (DMSO), oil-red-O stain, radioimmunoprecipitation assay (RIPA) buffer and protease inhibitor cocktail were purchased from Sigma - Aldrich Co. (St. Louis, MO, USA). The cell culture flasks and plates were from BD Biosciences (USA). Fetal bovine serum (FBS), penicillin and streptomycin antibiotics, trypsin - ethylenediaminetetraacetic acid (EDTA), phosphate buffered saline (PBS) and Hank's balanced salt solution (HBSS), bovine serum albumin (BSA), minimum essential medium (MEM) were from Gibco, USA. JC-1 stain was purchased from Sigma-Aldrich Co. (St. Louis, MO, USA). MitoSOX™ red and Fura 2-AM were from Invitrogen (Carlsbad, CA, USA). Antibodies against OPA1, MFN2, DRP1, FIS1 and β -actin were obtained from Santa Cruz biotechnology (CA, USA). Antibodies against PGC-1 α , SIRT1, Nrf2, Cyt c were from Abcam. All other chemicals used were of analytical grade.

3.2.2 Cell culture and treatment

HepG2 cells (American Type Culture Collection, (ATCC) Rockville, MD USA) were cultured as per supplier's instructions. In brief, the cells were grown in T-25 flask containing MEM supplemented with 10% heat-inactivated FBS and 1X penicillin streptomycin solution at

37°C and 5% CO₂ in a humidified incubator (Eppendorf, USA). When the cells reached 80% confluence, the cells were trypsinized and reseeded onto a new flask for further experiments.

3.2.3 Fructose and palmitate treatments of HepG2 cells

Fructose stock solution was prepared by dissolving in HBSS and was used to produce different concentrations of fructose treatment in serum free MEM. Palmitate stock solution (10 mM) was prepared by dissolving sodium palmitate in 0.1 N NaOH at 75°C for 5 min. The stock solution was further mixed with fatty acid free BSA to make a final concentration of 1 mM. The 1 mM working solution was then diluted to the desired treatment concentration (100 µM) in 1% MEM. Treatment was applied on day 3 and the experiments were performed after 24 hrs of treatment with fructose and palmitate. The experimental group consists of (i) C - control cells; (ii) HFP - cells treated with high fructose (100 mM) and palmitate (100 µM); (iii) HFP + fenofibrate - cells treated with high fructose, palmitate and fenofibrate (25 µM) (as positive control).

3.2.4 Mitochondrial superoxide production

The production of mitochondrial superoxide was visualized by using fluorogenic dye, MitoSOX™, which is rapidly and selectively targeted to the mitochondria in live cells. It is immediately oxidized by mitochondrial superoxide and the resulting product is extremely fluorescent upon binding to the nucleic acid. Briefly, 5×10^3 cells were seeded in 96-well black plates, a solution of MitoSOX™ in HBSS was added to the treated cells and incubated at 37°C for 20 min. After incubation, the cells were then washed with HBSS and fluorescent images were captured with a fluorescent microscope (BD Pathway™ Bioimager system, USA) at an excitation / emission range of 514/580 nm.

3.2.5 Mitochondrial membrane potential ($\Delta\Psi_m$)

$\Delta\Psi_m$ was observed by using JC-1 mitochondrial membrane potential assay kit that utilizes a cationic carbocyanine dye called JC-1, a sensitive marker for analysing the mitochondrial membrane potential. In healthy cells, the mitochondrial membrane is in a highly polarized state; JC-1 dye accumulates in the mitochondrial matrix and develops an aggregate of red fluorescence. In early apoptotic cells, the membrane potential is highly depolarized, resulting in the development of the monomeric green fluorescent form of JC-1 in the cytosol. Briefly, the cells after seeding and treatment were incubated with JC-1 stain for about 20 min. The stains were washed off with HBSS and visualized under the spinning disk imaging system (BD

Pathway™ Bioimager system, USA). The fluorescence of JC-1 monomers was measured at a wavelength of 490 nm excitation and 530 nm emissions and for JC-1 aggregates, the excitation/emission wavelength ranges from 525 and 590 nm respectively. Valinomycin (1 µg/mL) was used as a negative control.

3.2.6 Mitochondria isolation

After respective treatments, approximately 3×10^7 cells were homogenized in mitochondrial isolation buffer {10 mM Tris (pH 7.4), 250 mM sucrose, 0.15 mM MgCl₂}. The homogenate was then subjected to centrifugation at 800 x g for 5 min at 4°C. To obtain mitochondria enriched pellets, the supernatant was centrifuged at 10,000 x g for 100 min. The pellets were again centrifuged at 12,000 x g for 10 min, pooled, washed and resuspended in a 50 mM/L phosphate buffer (pH 7.0). It was then frozen and thawed 3 - 5 times to discharge the mitochondrial enzymes for activity measurement.

3.2.7 Mitochondrial respiratory complexes

The activity of complex I (NADH dehydrogenase) was assessed spectrophotometrically using the reaction mixture containing 200 µM menadione and 150 µM NADH prepared in a phosphate buffer (0.1 M, pH 8.0). The variation in absorbance at 340 nm for 8 min was monitored.

The activity of complex II (succinate dehydrogenase) was measured with the help of an artificial electron acceptor, dichlorophenolindophenol and succinate as substrate. The isolated mitochondria were added to a mixture of 10 mM EDTA, 20 mM of succinate, 50 µM DCPIP, and 0.1 M phosphate buffer (pH 7.4). The change in absorbance was recorded immediately for 8 min at 30°C.

The Complex III (Ubiquinol-cytochrome reductase) activity was determined as per the method described previously (Chong et al., 2007). In short, mitochondria were mixed with 100 µM/L EDTA, 3 mmol/L sodium azide, 2 mg BSA, 60 µM/L ferricytochrome c, decylubiquinol (1.3 mM) and phosphate buffer (50 mM, pH 8) in a final volume of 1 mL. Decylubiquinone was added to initiate the reaction. The activity was monitored for 2 min at 550 nm and activity of complex III was expressed as mmoles of ferricytochrome c reduced / min / mg protein.

The activity of complex IV (cytochrome c oxidase) was evaluated as per the previous method (Sudheesh et al., 2009). 50 µg of mitochondrial protein was mixed with 1 mL of ferrocyanochrome c solution in a phosphate buffer (30 mM, pH 7.4). The reaction was initiated by

the addition of an enzyme source and was monitored at 550 nm with an interval of 15 s for 4 min. The oxidation of reduced cytochrome c was monitored at 550 nm and expressed as activity of micromoles of ferrocytochrome c oxidized / min / mg protein.

3.2.8 Oxygen consumption assay

The oxygen consumption rate was determined by Cayman's cell based oxygen consumption rate assay kit, using antimycin A as a standard inhibitor (inhibitor of complex III). The rate of oxygen consumption in live cells was measured by using a phosphorescent oxygen probe called MitoXpress®-Xtra. The molecular oxygen in live cells quenches the fluorescent signal of MitoXpress, and the signal is inversely proportional to the extent of oxygen present in the media. Briefly, 5×10^3 cells were seeded in a 96-well black plate and after respective treatments, MitoXpress solution was added to all wells except the blank wells. The wells were then covered with HS mineral oil and fluorescence was read at an excitation/emission rate of 380/650 nm, respectively for 150 min.

3.2.9 Aconitase activity

Aconitase assay measures the absorbance of NADPH, which is generated in the coupled reactions of aconitase with isocitrate dehydrogenase. The rate of NADPH thus generated is directly proportional to the aconitase activity. Briefly, after treatment the cells were washed and covered with enough cold PBS and incubated the cells for about 10 min at 4 °C. Then the cells were collected and centrifuged at 800 x g for 10 min at 4 °C. The pellet is then resuspended in a cold assay buffer and sonicated. The reactions were initiated by adding 50 µL of diluted substrate solution. The absorbance was measured once every minute at 340 nm for 30 min at 37°C.

3.2.10 Intracellular calcium content

Calcium content was detected by staining the cells with Fura2-AM, a high-affinity intracellular calcium indicator. Briefly, 5×10^3 cells were seeded in 96-well black plates and after treatment, cells were incubated with Fura 2-AM (5 µM) for 1 hr at 37°C. After incubation, the cells were washed with HBSS and visualized (BD Pathway™ Bioimager system, USA) at an excitation and emission wavelengths of 340 and 510 nm respectively.

3.2.11 Caspase - 3 fluorometric assay

Apoptosis was assessed by using caspase - 3 fluorometric protease assay kit (Biovision, USA). Briefly, the treated cells were resuspended in a chilled lysis buffer and incubated on ice for 10 min. It is followed by the addition of 50 µL of reaction buffer to each sample and 5 µL of

1 mM (Asp-Glu-Val-Asp)- 7-amino-4-trifluoromethylcoumarin (DEVD-AFC) substrate. The mixture was then incubated for about 1 hr at 37°C. The samples were read at excitation and emission wavelengths of 400 nm and 505 nm, respectively.

3.2.12 Flow cytometric analysis with annexin V/PI

Quantification of apoptotic cells was done by using the annexin V - FITC apoptosis detection kit (Biovision, USA). After respective treatments, cells were collected by centrifugation. The cells were then resuspended in 500 μ L of binding buffer followed by the addition of 5 μ L of Annexin V-FITC and 5 μ L of propidium iodide and incubated at room temperature for 5 min in the dark. Annexin V-FITC binding was analyzed by flow cytometry (Ex = 488 nm; Em = 530 nm) using FITC signal detector (usually Fluorescence 1) and PI staining by the phycoerythrin emission signal detector (usually Fluorescence 2).

3.2.13 Western blot

After respective treatments cells were harvested and proteins were extracted from HepG2 cells by using an ice cold RIPA buffer containing protease inhibitor cocktail. It was then incubated on ice for about 20 min and cell suspensions were centrifuged at 12,000 rpm for 20 min at 4°C. The supernatant was collected and used for further immunoblot analysis. The protein concentration of the cell lysate was measured by using bicinchoninic acid kit (Pierce, Rockford, IL, USA) as per manufacturer's instruction. Proteins thus extracted were separated by SDS-PAGE and were transferred to the PVDF membrane using the Trans-Blot® Turbo™ Transfer system (Bio-Rad, USA). The membrane was then blocked with 5% skimmed milk in TBST for 1 hr at room temperature then probed with specific primary antibodies against DRP1, FIS1, MFN2, OPA1, PGC-1 α , SIRT1, Nrf2, Cyt c and β - actin (1:1000 dilutions) at 4°C overnight. After washing with TBST, specific horseradish peroxidase conjugated secondary antibodies (1:2000 dilutions) were added and the membranes were incubated for about 2 hrs. After washing, the immune complex was visualized using Clarity™ Western ECL Substrate (Bio-Rad,USA).The images were analyzed in the ChemiDoc XRS system (Bio-Rad,USA) using Image Lab software.

3.2.14 Statistical analysis

Statistical analysis was carried out by the SPSS statistical program. The data were represented as mean \pm SD. The data were subjected to one - way analysis of variance (ANOVA) and the differences among the means of the groups were assessed using Duncan's multiple

range tests using OriginPro version 8.5 (OriginLab Corporation, Massachusetts, USA). The statistical significance was accepted at $p \leq 0.05$.

3.3 Results

3.3.1 Effect of HFP on mitochondrial superoxide

Mitochondria are the fundamental sites for ROS production. An excess amount of mitochondrial superoxide production culminates in cell destruction and death. The mitochondrial superoxide production was significantly higher in HFP treated cells (566%, $p \leq 0.05$) compared with the control group (Figure 3.1). A significant decrease in superoxide production (200%, $p \leq 0.05$) was observed in cells treated with fenofibrate (Figure 3.1).

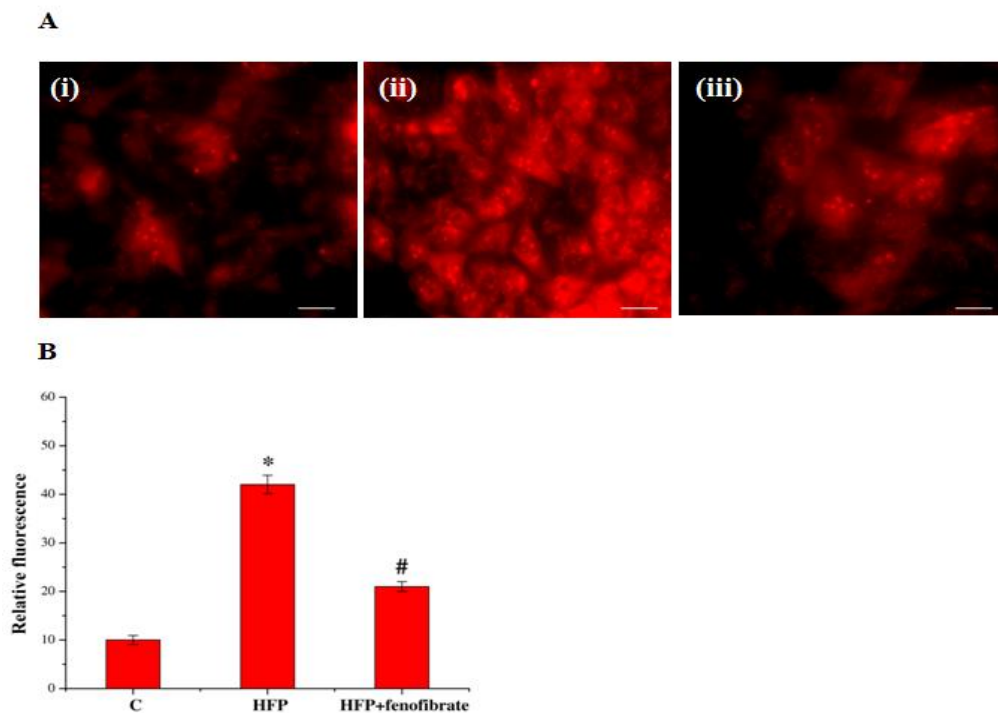


Figure 3.1 HFP induces mitochondrial superoxide generation in HepG2 cells: (A) The fluorescent microscopic images of cells stained with MitoSOX™ Red indicator. (i) C - control cells; (ii) HFP - cells treated with high fructose and palmitate; (iii) HFP + fenofibrate - cells treated with high fructose, palmitate and fenofibrate. Original magnification 40X. Scale bar corresponds to 50 μ M. (B) Fluorescence intensity emitted by MitoSOX™ in control and treated cells. Data are expressed as mean \pm SD; where n = 6. * indicates significantly different from the control group ($p \leq 0.05$). # indicates significantly different from the HFP treated group ($p \leq 0.05$).

3.3.2 Effect of HFP on $\Delta\Psi_m$

The $\Delta\Psi_m$ of control, HFP and HFP + fenofibrate treated cells were depicted in Figure 3.2. In normal mitochondria, JC-1 dye forms red fluorescence as in the control group (Figure 3.2). The presence of HFP in the medium dissipates the $\Delta\Psi_m$, leading to a drift from red to green fluorescence. The green monomers increased significantly ($p \leq 0.05$) by 102.87% (Figure 3.2). On the other hand, fenofibrate treatment prevented the alteration of $\Delta\Psi_m$ significantly by 61.79% ($p \leq 0.05$) compared to HFP (Figure 3.2).

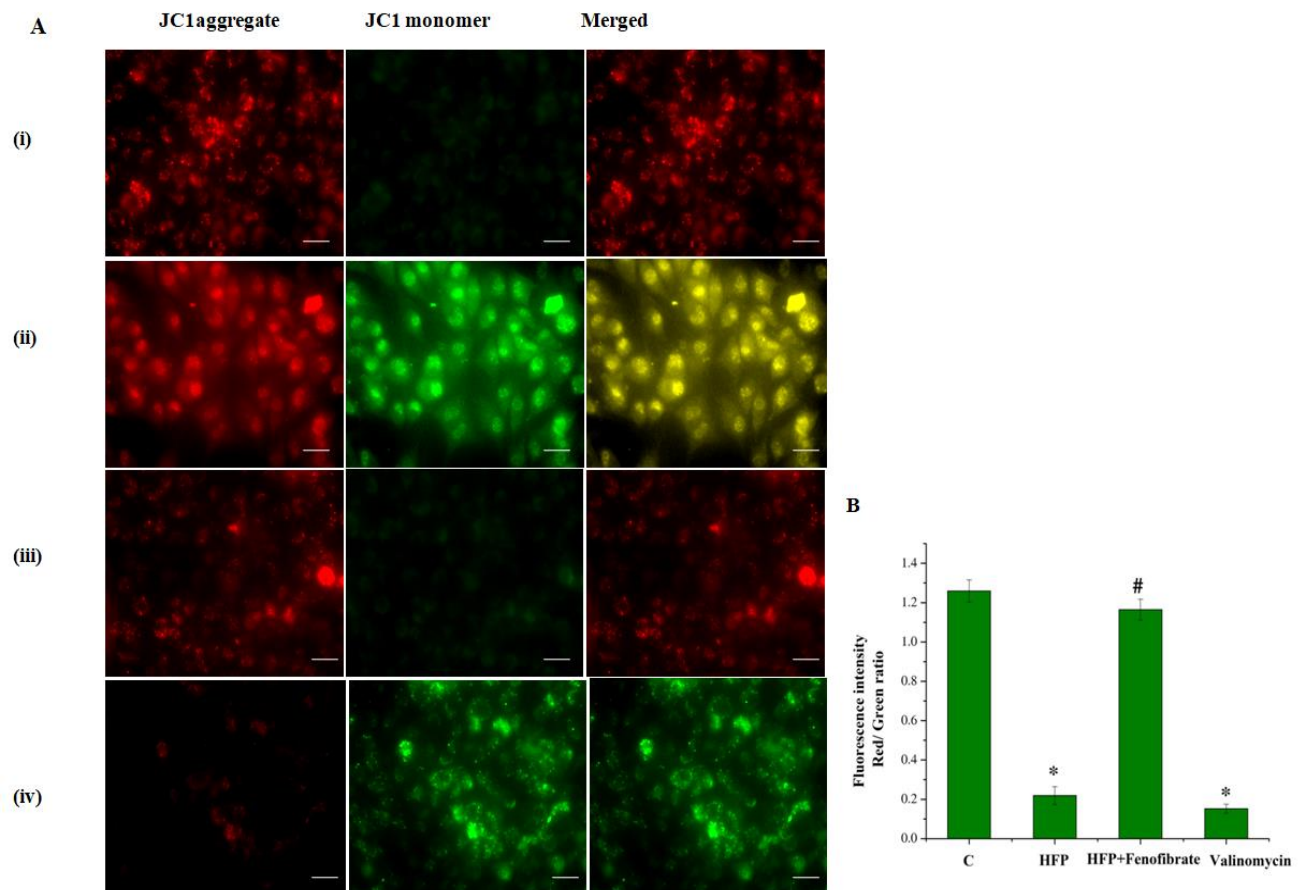


Figure 3.2 HFP causes dissipation of $\Delta\Psi_m$: (A) The fluorescent microscopic images of HepG2 cells. (i) C - control cells; (ii) HFP - cells treated with high fructose and palmitate; (iii) HFP + fenofibrate - cells treated with high fructose, palmitate and fenofibrate; (iv) Valinomycin treated cells. Original magnification 40X. Scale bar corresponds to 50 μM . (B) The graphical representation of JC-1 aggregates to JC-1 monomers (ratio of 590 : 530 nm emission intensity). Data are expressed as mean \pm SD; where $n = 6$. * indicates significantly different from the control group ($p \leq 0.05$). # indicates significantly different from the HFP treated group ($p \leq 0.05$).

3.3.3 Effect of HFP on mitochondrial bioenergetics

HFP adversely affects mitochondrial bioenergetics and aconitase activity during steatosis. The activities of mitochondrial respiratory complexes such as NADH dehydrogenase (complex I), succinate dehydrogenase (complex II), ubiquinol-cytochrome reductase (complex III), cytochrome c oxidase (complex IV) were decreased significantly ($p \leq 0.05$) with HFP treatment (61.79%, 58.07%, 38.72%, 50.63%, $p \leq 0.05$ respectively) compared to control (Figure 3.3).. However, treatment with fenofibrate significantly prevented the sharp decrease ($p \leq 0.05$) of complex activities compared to HFP cells by 36.74% (complex I), 46.71% (complex II), 17.78% (complex III), and 35.28% (complex IV) (Figure 3.3).

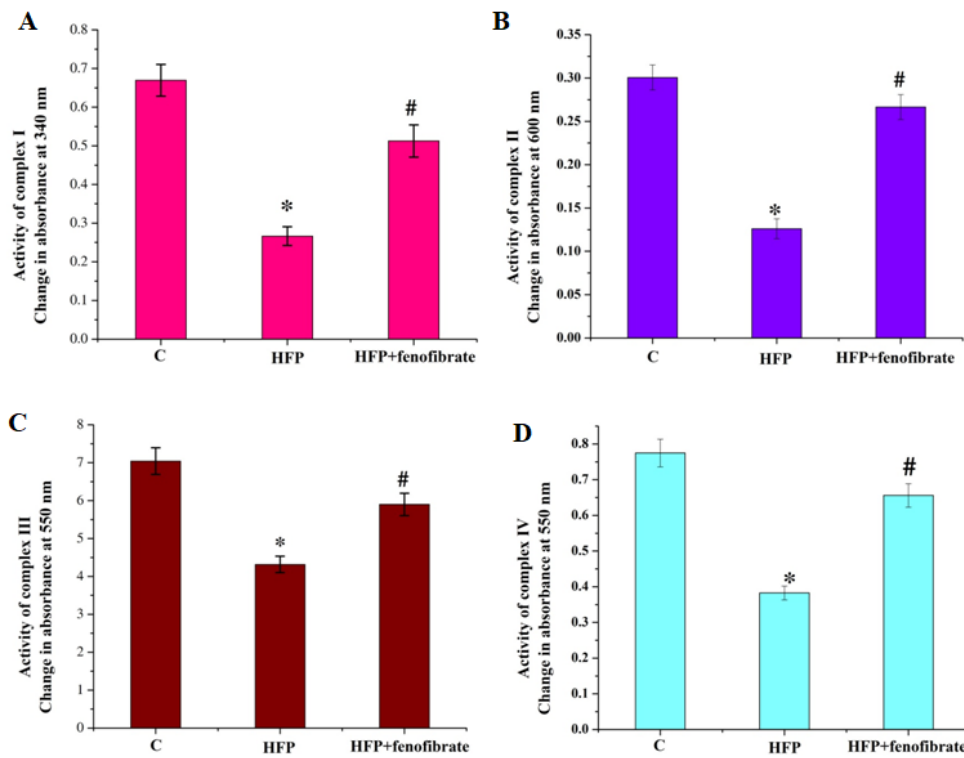


Figure 3.3 HFP adversely affects mitochondrial bioenergetics during steatosis: (A) Activity of mitochondrial respiratory complex I (B) complex II (C) complex III (D) complex IV in HepG2 cells. C - control cells; HFP - cells treated with high fructose and palmitate; HFP + fenofibrate - cells treated with high fructose, palmitate and fenofibrate. Data are expressed as mean \pm SD; where $n = 6$. * indicates significantly different from the control group ($p \leq 0.05$). # indicates significantly different from the HFP treated group ($p \leq 0.05$).

3.3.4 Effect of HFP on oxygen consumption rate and aconitase activity

Oxygen consumption rate in HepG2 cells was interpreted by using a phosphorescent probe, mitoXpress. The fluorescent signal over time is directly proportional to the oxygen consumption rate in cells. The oxygen consumption rate in HFP treated HepG2 cells showed significant reduction (53.4%, $p \leq 0.05$) compared to the control group (Figure 3.4 A) and treatment with fenofibrate significantly improved the condition (28.51%, $p \leq 0.05$) compared to the HFP group (Figure 3.4 A).

The activity of aconitase was reduced significantly ($p \leq 0.05$) during HFP condition (76.76%) compared to control (Figure 3.4 B). Here also, fenofibrate treatment prevented the sharp fall by 40.49% significantly ($p \leq 0.05$) compared to HFP (Figure 3.4 B).

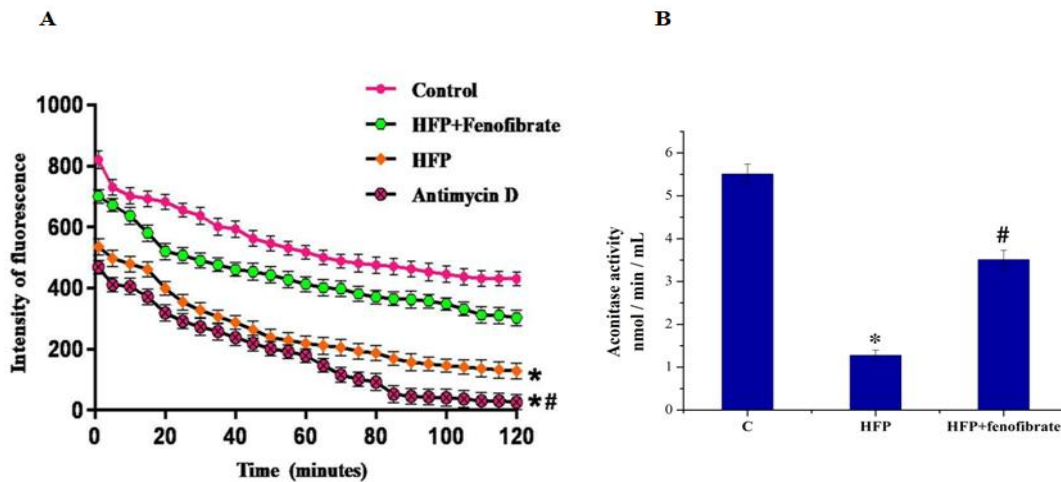


Figure 3.4 HFP adversely affects oxygen consumption and aconitase activity: (A) Alteration in fluorescence indicates the variation in oxygen consumption rate. (B) Activity of mitochondrial aconitase in HepG2 cells during steatosis. C - control cells; HFP - cells treated with high fructose and palmitate; HFP + fenofibrate - cells treated with high fructose, palmitate and fenofibrate. Data are expressed as mean \pm SD; where $n = 6$. * indicates significantly different from the control group ($p \leq 0.05$). # indicates significantly different from the HFP treated group ($p \leq 0.05$).

3.3.5 Effect of HFP on mitochondrial dynamics

During HFP treatment the expression level of mitochondrial fission proteins such as DRP1 and FIS1 was found significantly increased ($p \leq 0.05$) by 27.18% and 277.37% respectively, compared to the control (Figure 3.5). On the other hand, the expression of fusion proteins (MFN2 and OPA1) decreased significantly ($p \leq 0.05$) by 198.18% and 36.67%

respectively compared to control (Figure 3.5). The treatment with fenofibrate significantly downregulated ($p \leq 0.05$) the expression of DRP1 by 16.88%, FIS1 by 219.71% compared to HFP (Figure 3.5). The expression level of MFN2 and OPA1 were also increased significantly ($p \leq 0.05$) by 136.55%, and 30.06% respectively compared to HFP (Figure 3.5).

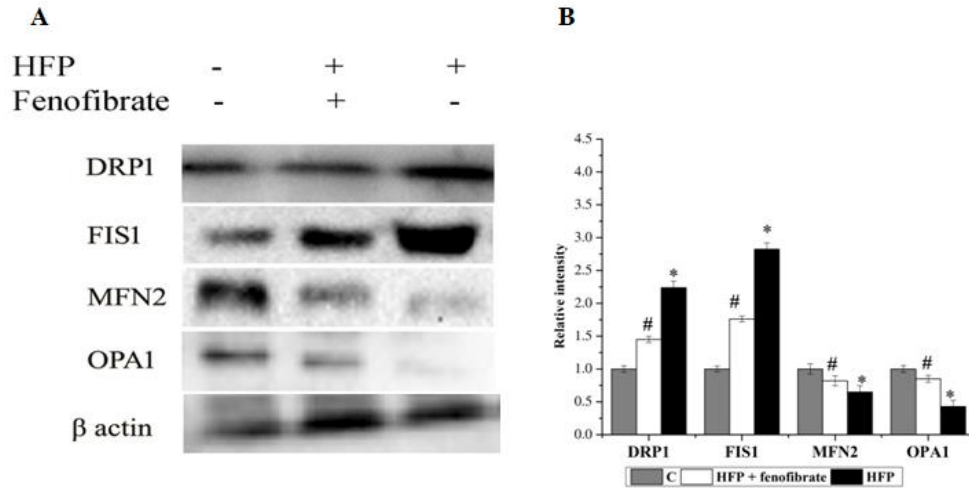


Figure 3.5 HFP induces imbalance in mitochondrial dynamics: (A) The protein expression of DRP1, FIS1, MFN2, and OPA1 during steatosis. C - control cells; HFP + fenofibrate - cells treated with high fructose, palmitate and fenofibrate; HFP - cells treated with high fructose and palmitate. (B) The relative intensity of each band was quantified with β actin. Data are expressed as mean \pm SD; where $n = 3$. * indicates significantly different from the control group ($p \leq 0.05$). # indicates significantly different from the HFP treated group ($p \leq 0.05$).

3.3.6 Effect of HFP on mitochondrial biogenesis

PGC-1 α is the major transcriptional factor that performs a central role in determining the modulation of mitochondrial biogenesis and respiratory function. With HFP incubation expression of PGC-1 α was decreased significantly ($p \leq 0.05$) by 62.59% compared to the control (Figure 3.6). The presence of fenofibrate significantly ($p \leq 0.05$) improves its expression level by 61.36% compared to the HFP group (Figure 3.6). Sirtuins play a major role in hepatic lipid metabolism and ensure protection from the steatosis condition. HFP treatment reduced its expression level significantly ($p \leq 0.05$) by 77.28% compared to the control (Figure 3.6). Co-treatment with fenofibrate enhanced the expression level significantly ($p \leq 0.05$) by 71.3% compared to the HFP (Figure 3.6). The expression of Nrf2 in HFP group is found to be reduced significantly ($p \leq 0.05$) by 72.59% compared to control and the condition is improved

significantly ($p \leq 0.05$) by fenofibrate to 77.65% (Figure 3.6). HFP treatment also caused a significant ($p \leq 0.05$) upregulation in the expression of Cyt c (143.22%) compared to control. Fenofibrate prevented its over expression by 92.59% significantly ($p \leq 0.05$) compared to HFP (Figure 3.6).

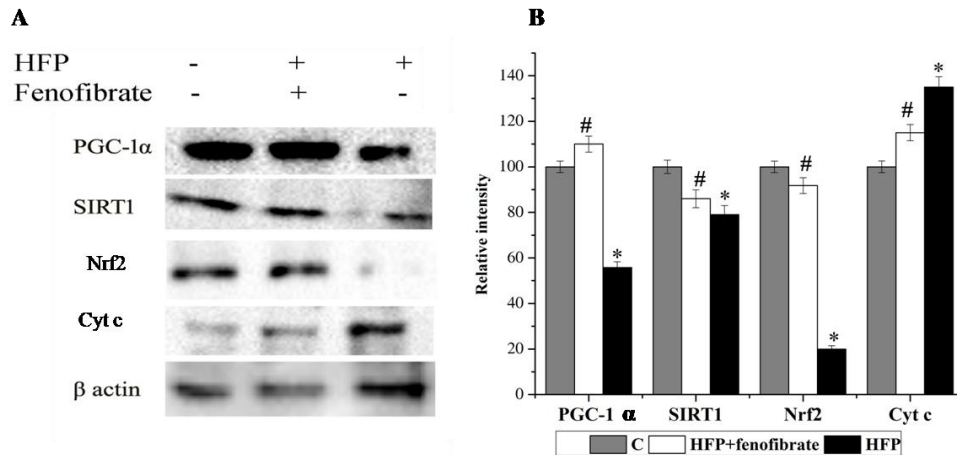


Figure 3.6 HFP reduces mitobiogenesis during steatosis: (A) The protein expression of PGC-1 α , SIRT1, Nrf2, and Cyt c during steatosis. C - control cells; HFP + fenofibrate - cells treated with high fructose, palmitate and fenofibrate; HFP - cells treated with high fructose and palmitate. (B) The relative intensity of each band was quantified with β actin. Data are expressed as mean \pm SD; where $n = 3$. * indicates significantly different from the control group ($p \leq 0.05$). # indicates significantly different from the HFP treated group ($p \leq 0.05$).

3.3.7 Effect of HFP on calcium homeostasis

HFP affects intracellular calcium homeostasis and initiates apoptosis *via* caspase3 activation. The intracellular calcium content in HFP treated cells increased significantly (17%, $p \leq 0.05$), which was obvious from the elevated fluorescence of Fura-2 AM compared to the control group (Figure 3.7). Fenofibrate treatment significantly reduced the calcium overload (35.79%, $p \leq 0.05$) compared to the HFP group (Figure 3.7).

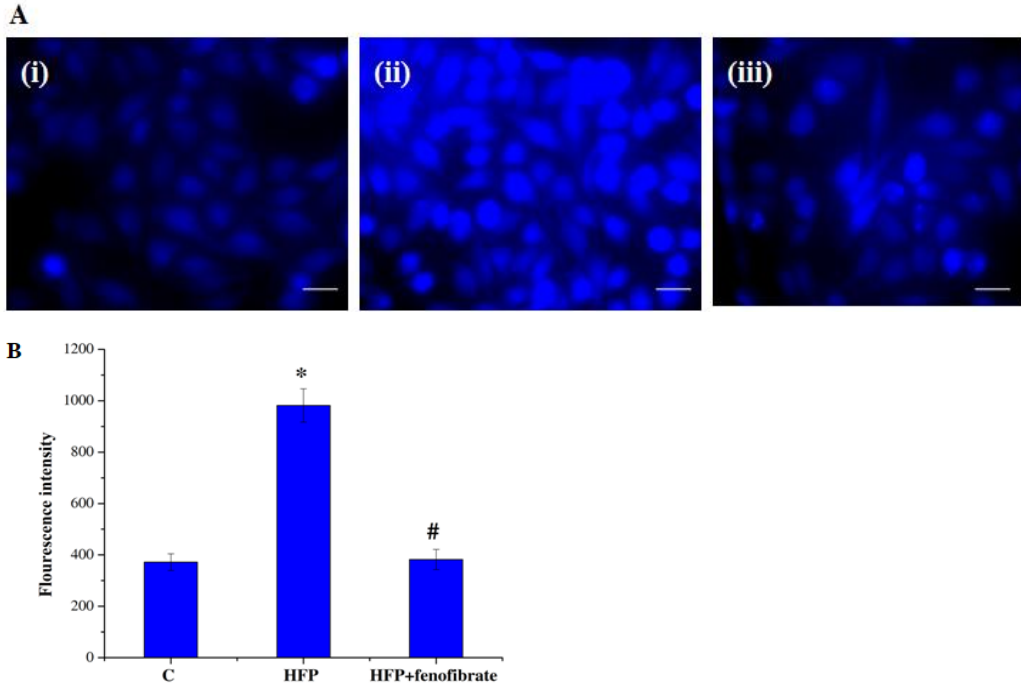


Figure 3.7 HFP affects intracellular calcium homeostasis: (A) The fluorescent microscopic images of HepG2 cells stained with fura-2, AM. C - control cells; (ii) HFP - cells treated with high fructose and palmitate; (iii) HFP + fenofibrate - cells treated with high fructose, palmitate and fenofibrate (B) Fluorescence intensity emitted by fura-2 AM in control and treated cells. Original magnification 40X. Scale bar corresponds to 50 μ M. Data are expressed as mean \pm SD; where n = 6. * indicates significantly different from the control group ($p \leq 0.05$). # indicates significantly different from the HFP treated group ($p \leq 0.05$).

3.3.8 Effect of HFP on apoptosis

There was a slight increase in the number of apoptotic cells following HFP treatment compared with the control group. The results of Annexin V-PI staining revealed that the quadrant of early and late apoptotic cells increased slightly following the exposure to HFP to about 3.1% compared to control. However, treatment with fenofibrate reversed the trend (Figure 3.8 A) compared to HFP. Moreover, the activity of caspase-3 was increased significantly ($p \leq 0.05$) in HFP treated HepG2 cells (42.20%) compared to control, while fenofibrate protected the fall of caspase activity significantly ($p \leq 0.05$) by 30.74% (Figure 3.8 B).

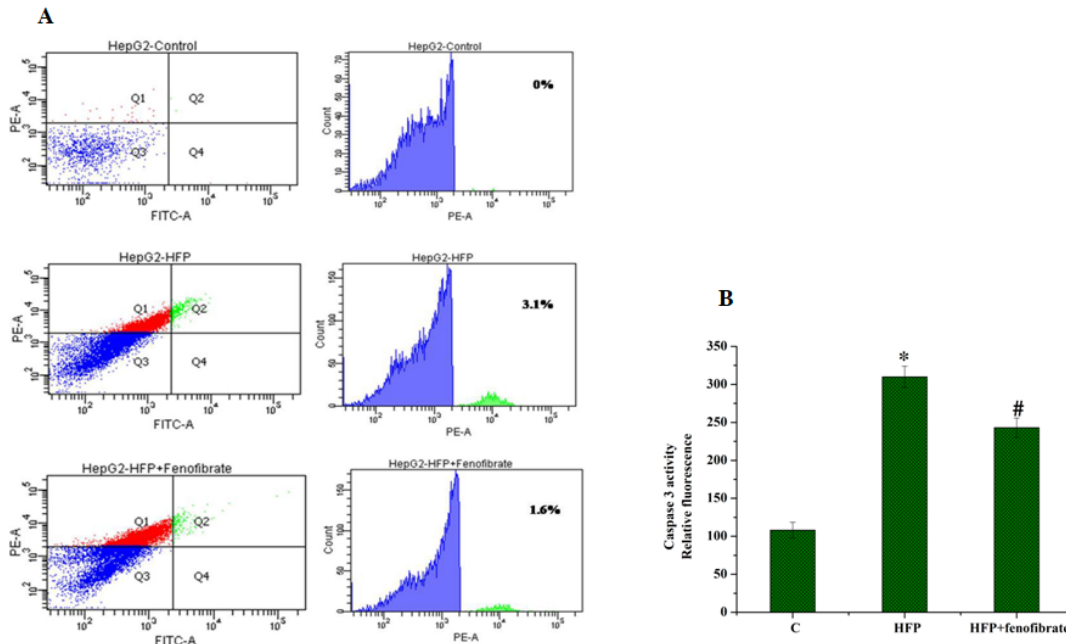


Figure 3.8 HFP initiates apoptosis *via* caspase 3 activation: (A) Detection of apoptosis by annexin V – FITC / PI analysis of HepG2 cells. (B) The relative activity of caspase - 3 / CPP32 in HepG2 cells treated with HFP for 24 hr. C - control cells; (ii) HFP - cells treated with high fructose and palmitate; (iii) HFP + fenofibrate - cells treated with high fructose, palmitate and fenofibrate. Data are expressed as mean \pm SD; where n = 6. * indicates significantly different from the control group ($p \leq 0.05$). # indicates significantly different from the HFP treated group ($p \leq 0.05$).

3.4 Discussion

NAFLD is the most prevalent chronic liver disease in the modern world. The factors that favor the progression of NAFLD include genetic polymorphism, exposure to various xenobiotics, environmental contaminants, and various food items rich in sugars and fats. Since this has a multifactorial origin, identifying real causes is essential for a better understanding of the pathophysiology of genesis. For this, an ideal *in vitro* model is required to start any research on liver steatosis. Keeping this in mind, the present work was planned to develop a suitable model of high energy diet - induced steatosis in the liver utilizing HepG2 cells. The present study tried to reveal the role of alteration in bioenergetics during the genesis of high calorie induced steatosis in HepG2 cells.

Mitochondria are central cytoplasmic organelles that provide excellent platforms for the maintenance of cellular homeostasis (Bagur & Hajnoczky, 2017). The disruption of cellular

homeostasis plays a pivotal role in the progression of chronic liver diseases (Garcia & Fernandez, 2018; Mansouri et al., 2018). High fructose diet promotes the characteristic features of metabolic syndrome and fatty liver (Vasselli et al., 2008), vascular inflammation, and microvascular disease. Moreover, several aspects of fructose metabolism make it principally lipogenic. It enhances the protein levels of all lipogenic enzymes during its conversion into TGs. The fructose also plays a vital role in the depletion of ATP and the inhibition of fatty acid oxidation. This in turn, increases the production of ROS. Thus, disruption of fructose metabolism in the liver may provide a new therapeutic option for steatosis. Palmitic acid is the most abundant saturated fatty acid and in hepatocytes it causes a concentration and time - dependent lipoapoptosis. These toxic fatty acids activate mitochondrial permeabilization, promote the release of Cyt c, and activate caspases 3 and 7. It also affects lipid storage and gene expression in the liver. Thus, chronic palmitic acid - enriched diet may be one of the major causes of NASH, including simple steatosis and hepatic injury.

Herein, we have described the role of fructose and palmitate in mitochondrial integrity, dynamics, and bioenergetics during hepatic steatosis. Our results demonstrate that incubation of HepG2 cells with HFP leads to the surplus accumulation of lipid droplets. During NASH, hepatic lipids are stored in TG form and this indicates the genesis of NASH in this study. Thus hypertriglyceridemia is a major characteristic feature associated with the spectrum of steatosis. The main objective of our study was to evaluate the effect of a high energy diet on the function of mitochondria and its contribution to the development of steatosis. Hepatocytes host a large number of mitochondria (~500 - 4000 mitochondria per hepatocyte) (Degli et al., 2012). The maintenance of healthy mitochondria is an essential prerequisite for the proper functioning of the liver. For that, we studied integrity, dynamics and OXPHOS in detail. We found that HFP downregulates antioxidant ability through the generation of ROS. There are reports to link increased superoxide radical and hepatic steatosis (Sanyal et al., 2001) and also findings from other groups that fructose consumption exerts oxidative stress and damage (Brown et al., 2010; Teodoro et al., 2013) *via* liver glucokinase and reactive oxygen production. The role of mitochondrial superoxide in the initiation of steatosis was also reported (Mitchell et al., 2009). We found that HFP treatment resulted in $\Delta\Psi_m$ dissipation. Alteration in $\Delta\Psi_m$ causes the onset of several pathological changes due to its profound influence in the control of the electrochemical gradient of mitochondria.

We also analyzed the effect of HFP on mitochondrial respiration. The activities of various complexes such as complex I, complex II, complex III and complex IV revealed that HFP inhibits all complexes of the ETC significantly. Generally, deformity in complex I and III are expected to lead to electron leakage (Brown et al., 2010). A reduction in the activity of complex I leads to the aggregation of electrons in the first part of ETC. These electrons are directly translocated to molecular oxygen and favor the progression of radical formation and series of radical-induced impairment to the mitochondrial components (Bagur et al., 2017). Consumption of high calories favors the entry of more substrate into respiratory chain complexes. Subsequently, the number of electrons supplied to the ETC also increases rapidly, resulting in molecular oxygen, superoxide and nitric oxide radical formation. This results in toxic peroxynitrite radical generation (Radi et al., 2002). Lower activity of complexes during HFP is also related to the reduced synthesis of subunits or elevated rate of degradation or the combined effect of both (Garcia et al., 2014). Our result from *in vitro* study is in line with a report of Bagur & Hajnoczky (2017), suggesting that in the mice model of NAFLD, increased degradation of hepatic oxidative phosphorylation leads to mitochondrial impairment. There are reports to link fructose mediated inhibition of aconitase activity and stimulation of lipogenesis due to the accumulation of citrate and activation of citrate lyase. We also found a decrease in aconitase activity with HFP. Since aconitase is a mitochondrial matrix enzyme, this highlights the importance of central organelle in liver disease. The detrimental effect of HFP on oxygen consumption also indicates impaired bioenergetics.

Mitochondria exhibit a dynamic morphology. The dynamicity is mainly by changing their shape *via* fission - fusion processes (Kim & Lemasters, 2011; Twig & Shirihai, 2011) one of the primary quality control mechanisms when the cells experience metabolic or environmental stress. Under pathological conditions, there was an increase in fission proteins (DRP1 and FIS1) and a decrease in fusion proteins (MFN2 and OPA1). The increased activity of DRP1 results in the production of a large number of fragmented mitochondria, which are competent to generate more reactive oxygen species. Similar types of alterations have been reported in the liver of diet - induced obese animals and hepatic steatosis in the murine model of NAFLD (Holmstrom et al., 2012; Lionetti et al., 2014; Yu et al., 2006; Bhatt et al., 2013). Overexpression of FIS1 proteins is mainly due to an excess amount of nutrients. The concept of fusion events in the maintenance of healthy mitochondria is also supported by several studies (Twig et al., 2008; Westermann, 2010).

The activity of fusion proteins like MFN2 and OPA1 is indispensable for normal cellular functioning (Chen et al., 2010). The decreased level of MFN2 and OPA1 may impair mitochondrial quality control mechanisms and diminish mitochondrial networking. Fructose metabolism results in the development of DNL of fatty acids and eventually leads to TG accumulation. In nutshell, mitochondrial fission - fusion proteins regulate hepatic lipid accumulation during NASH. Moreover, the dynamic nature of mitochondria, together with their interdependence with bioenergetics performs a vital role in energy homeostasis.

PGC-1 α is one of the essential transcriptional co - activators responsible for modulating hepatic metabolic pathways. It is also a master regulator of mitochondrial biogenesis, governing mitochondrial function, OXPHOS and oxygen consumption. It promotes the activation of nuclear receptors and performs a significant role in the generation of mitochondria (Ma, 2013). We found that HFP treated cells showed downregulation of PGC-1 α expression. This in turn, causes the suppression of transcription factors and nuclear receptors that control lipid metabolism and mitochondrial biogenesis (Zhang et al., 2009; Wang et al., 2004). The selective downregulation of PGC-1 α will no longer protect the liver and enhances the transition from steatosis to fibrosis. PGC-1 α also regulates the expression of a class of proteins called sirtuins. Sirtuins are a class of highly conserved NAD⁺ dependent histone and protein deacetylases. It has been reported that the expression of SIRT1 protects against alcohol - induced liver disease (Bergeron et al., 2001). As a metabolic modulator, SIRT1 control a series of physiological activities such as regulation of lipogenesis, controlling beta oxidation and hepatic oxidative stress, mediates hepatic inflammation *via* deacetylation of transcriptional modulators and stimulates autophagy (Kemper et al., 2013). Moreover, in the liver SIRT1 is responsible for controlling gluconeogenic activity *via* modulation by PGC-1 α . In the present study, the decreased expression of SIRT1 ceases the functioning of mitochondrial proteins and mito biogenesis, thereby favouring the progression of steatosis.

The interaction of PGC-1 α with transcriptional regulators like Nrf2 alters the expression of genes coding for OXPHOS subunits. For the evidence on the role of PGC-1 α and SIRT1 in liver disorder, we analyzed the protein expression of Nrf2. The Nrf2 is responsible for the maintenance of cellular redox homeostasis, anti-damage and anti-tumor processes (Zeng et al., 2017; Xu et al., 2011). There are reports claiming the crucial role of Nrf2 in the progression of NAFLD to steatohepatitis in mice (Yang et al., 2018). Nrf2 depletion induced ROS production,

liver fibrosis and inflammation, the principal pathological features of NASH has been reported. Various studies have shown that fructose downregulates Nrf2 expression (Yang et al., 2018). But the behavior of Nrf2 expression in HepG2 cells during fructose and palmitate combination is not available in the literature. Herein we report the downregulation of Nrf2 in HepG2 cells with HFP. This reveals the role of Nrf2 in the genesis of steatosis with HFP mimicking a high calorie diet. Recently specific reports have also demonstrated the regulatory role of SIRT1 / Nrf2 in the mitochondrial antioxidant pathway (Huang et al., 2013). It has also been reported that the Nrf2 signaling pathway plays a crucial role in providing hepatoprotection *via* improving the protein expression of antioxidant enzymes (Hu et al., 2017).

During oxidative stress superoxide radical evokes the release of Cyt c from mitochondria, which might be positively correlated with H₂O₂ generation in mitochondria. Both intra and extra mitochondrial H₂O₂ plays a significant role in the release of Cyt c (Ruiz et al., 2015; Trauner et al., 2010). The increased expression of Cyt c can be considered a mechanism of mitochondria entering the apoptotic pathway. Altogether our results suggest that HFP plays an inevitable role in altering mitochondrial biogenesis and thereby stimulates the progression of fatty liver disease. We paid attention to see whether high - calorie induces apoptosis or not. One of its consequences is the genesis of intracellular calcium overload (Kroemer et al., 2000). Calcium acts as the central regulator of hepatic metabolism since it plays a pivotal role in the regulation of mitochondrial oxidative metabolism (Bravo et al., 2011). Impaired intracellular calcium overload occurs in both early and late stages of apoptosis (Oliva et al., 2018), and mediates lethal effects. It has been proposed that increased intracellular calcium concentration favors cell death *via* apoptosis. We also found an increase in caspase - 3 activity, which might be due to increased cytosolic calcium concentration and release of Cyt c from the mitochondria. Activation of caspase - 3 occurs mainly during the final stages of apoptosis *via* the intrinsic mitochondrial pathway. Since caspase - 3 activation promotes the progression of steatohepatitis and fibrosis during glucolipotoxicity, it can be considered as an efficient candidate for the treatment of NASH. It has also been reported that the palmitic acid treatment induces necroptosis, an emerging type of cell death (Gautheron et al., 2014).

3.5 Summary and conclusion

The present *in vitro* study confirmed the involvement of mitochondrial dysfunction and associated complications in the genesis of steatosis with HFP in HepG2 cells. Mitochondrial

integrity, dynamics and OXPHOS were found adversely affected with HFP associated steatosis. Based on this mitochondrial protectants could be explored for therapeutic purposes against liver disease.

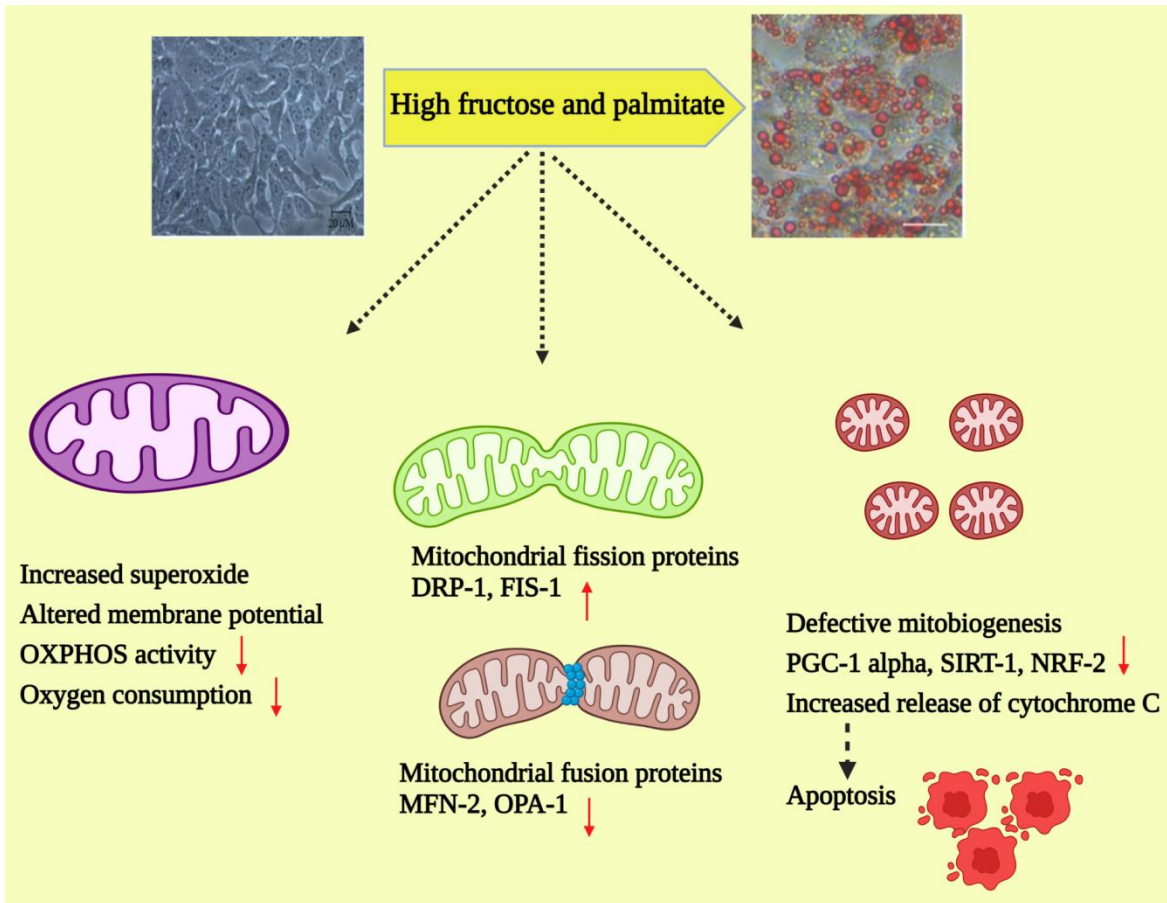


Figure 3.9 Schematic representation of mitochondrial dysfunction during steatosis

References

- Alwahsh, S.M., Xu, M., Seyhan, H.A., Ahmad, S., Mihm, S., Ramadori, G. and Schultze, F.C., 2014. Diet high in fructose leads to an overexpression of lipocalin-2 in rat fatty liver. *World journal of gastroenterology: WJG*, 20(7), p.1807.
- Bagur, R. and Hajnóczky, G., 2017. Intracellular Ca²⁺ sensing: its role in calcium homeostasis and signaling. *Molecular cell*, 66(6), pp.780-788.
- Bergeron, R., Ren, J.M., Cadman, K.S., Moore, I.K., Perret, P., Pypaert, M., Young, L.H., Semenkovich, C.F. and Shulman, G.I., 2001. Chronic activation of AMP kinase

- results in NRF-1 activation and mitochondrial biogenesis. *American Journal of Physiology-Endocrinology And Metabolism*, 281(6), pp.E1340-E1346.
- Bhatt, M.P., Lim, Y.C., Kim, Y.M. and Ha, K.S., 2013. C-peptide activates AMPK α and prevents ROS-mediated mitochondrial fission and endothelial apoptosis in diabetes. *Diabetes*, 62(11), pp.3851-3862.
 - Bravo, R., Vicencio, J.M., Parra, V., Troncoso, R., Munoz, J.P., Bui, M., Quiroga, C., Rodriguez, A.E., Verdejo, H.E., Ferreira, J. and Iglewski, M., 2011. Increased ER–mitochondrial coupling promotes mitochondrial respiration and bioenergetics during early phases of ER stress. *Journal of cell science*, 124(13), pp.2143-2152.
 - Brown, G.C., Murphy, M.P., Jastroch, M., Divakaruni, A.S., Mookerjee, S., Treberg, J.R. and Brand, M.D., 2010. Mitochondrial proton and electron leaks. *Essays in biochemistry*, 47, pp.53-67.
 - Chalasani, N., Younossi, Z., Lavine, J.E., Diehl, A.M., Brunt, E.M., Cusi, K., Charlton, M. and Sanyal, A.J., 2012. The diagnosis and management of non-alcoholic fatty liver disease: Practice Guideline by the American Association for the Study of Liver Diseases, American College of Gastroenterology, and the American Gastroenterological Association. *Hepatology*, 55(6), pp.2005-2023.
 - Chen, H., Vermulst, M., Wang, Y.E., Chomyn, A., Prolla, T.A., McCaffery, J.M. and Chan, D.C., 2010. Mitochondrial fusion is required for mtDNA stability in skeletal muscle and tolerance of mtDNA mutations. *Cell*, 141(2), pp.280-289.
 - Chong, M.F., Fielding, B.A. and Frayn, K.N., 2007. Metabolic interaction of dietary sugars and plasma lipids with a focus on mechanisms and de novo lipogenesis. *Proceedings of the Nutrition Society*, 66(1), pp.52-59.
 - Day, C.P., 2002. Pathogenesis of steatohepatitis. *Best practice & research Clinical gastroenterology*, 16(5), pp.663-678.
 - Degli Esposti, D., Hamelin, J., Bosselut, N., Saffroy, R., Sebah, M., Pommier, A., Martel, C. and Lemoine, A., 2012. Mitochondrial roles and cytoprotection in chronic liver injury. *Biochemistry research international*, 2012.
 - Einer, C., Hohenester, S., Wimmer, R., Wottke, L., Artmann, R., Schulz, S., Gosmann, C., Simmons, A., Leitzinger, C., Eberhagen, C. and Borchard, S., 2018. Mitochondrial adaptation in steatotic mice. *Mitochondrion*, 40, pp.1-12.

- Feldstein, A.E. and Gores, G.J., 2005. Apoptosis in alcoholic and nonalcoholic steatohepatitis. *Front Biosci*, 10(3), pp.3093-9.
- Galloway, C.A., Lee, H., Brookes, P.S. and Yoon, Y., 2014. Decreasing mitochondrial fission alleviates hepatic steatosis in a murine model of nonalcoholic fatty liver disease. *American Journal of Physiology-Gastrointestinal and Liver Physiology*, 307(6), pp.G632-G641.
- García-Ruiz, C. and Fernández-Checa, J.C., 2018. Mitochondrial oxidative stress and antioxidants balance in fatty liver disease. *Hepatology communications*, 2(12), pp.1425-1439.
- García-Ruiz, I., Solís-Muñoz, P., Fernández-Moreira, D., Grau, M., Colina, F., Muñoz-Yagüe, T. and Solís-Herruzo, J.A., 2014. High-fat diet decreases activity of the oxidative phosphorylation complexes and causes nonalcoholic steatohepatitis in mice. *Disease models & mechanisms*, 7(11), pp.1287-1296.
- Gautheron, J., Vucur, M., Reisinger, F., Cardenas, D.V., Roderburg, C., Koppe, C., Kreggenwinkel, K., Schneider, A.T., Bartneck, M., Neumann, U.P. and Canbay, A., 2014. A positive feedback loop between RIP 3 and JNK controls non-alcoholic steatohepatitis. *EMBO molecular medicine*, 6(8), pp.1062-1074.
- Haque, M., Mirshahi, F., Campbell-Sargent, C., Sterling, R.K., Luketic, V.A., Shiffman, M.S.R.T., Stravitz, R.T. and Sanyal, A.J., 2002, October. Nonalcoholic steatohepatitis (NASH) is associated with hepatocyte mitochondrial DNA depletion. In *Hepatology* (Vol. 36, No. 4, pp. 403A-403A).
- Holmström, M.H., Iglesias-Gutierrez, E., Zierath, J.R. and Garcia-Roves, P.M., 2012. Tissue-specific control of mitochondrial respiration in obesity-related insulin resistance and diabetes. *American Journal of Physiology-Endocrinology and Metabolism*, 302(6), pp.E731-E739.
- Hu, Y., Hou, Z., Yi, R., Wang, Z., Sun, P., Li, G., Zhao, X. and Wang, Q., 2017. Tartary buckwheat flavonoids ameliorate high fructose-induced insulin resistance and oxidative stress associated with the insulin signaling and Nrf2/HO-1 pathways in mice. *Food & function*, 8(8), pp.2803-2816.
- Huang, K., Huang, J., Xie, X., Wang, S., Chen, C., Shen, X., Liu, P. and Huang, H., 2013. Sirt1 resists advanced glycation end products-induced expressions of fibronectin

and TGF- β 1 by activating the Nrf2/ARE pathway in glomerular mesangial cells. *Free Radical Biology and Medicine*, 65, pp.528-540.

- Idrissova, L., Malhi, H., Werneburg, N.W., LeBrasseur, N.K., Bronk, S.F., Fingas, C., Tchkonina, T., Pirtskhalava, T., White, T.A., Stout, M.B. and Hirsova, P., 2015. TRAIL receptor deletion in mice suppresses the inflammation of nutrient excess. *Journal of hepatology*, 62(5), pp.1156-1163.
- Kemper, J.K., Choi, S.E. and Kim, D.H., 2013. Sirtuin 1 deacetylase: a key regulator of hepatic lipid metabolism. *Vitamins & hormones*, 91, pp.385-404.
- Kim, I. and Lemasters, J.J., 2011. Mitochondrial degradation by autophagy (mitophagy) in GFP-LC3 transgenic hepatocytes during nutrient deprivation. *American Journal of Physiology-Cell Physiology*.
- Kroemer, G. and Reed, J.C., 2000. Mitochondrial control of cell death. *Nature medicine*, 6(5), pp.513-519.
- Lanaspa, M.A., Sanchez-Lozada, L.G., Choi, Y.J., Cicerchi, C., Kanbay, M., Roncal-Jimenez, C.A., Ishimoto, T., Li, N., Marek, G., Duranay, M. and Schreiner, G., 2012. Uric acid induces hepatic steatosis by generation of mitochondrial oxidative stress: potential role in fructose-dependent and-independent fatty liver. *Journal of Biological Chemistry*, 287(48), pp.40732-40744.
- Le, M.T., Frye, R.F., Rivard, C.J., Cheng, J., McFann, K.K., Segal, M.S., Johnson, R.J. and Johnson, J.A., 2012. Effects of high-fructose corn syrup and sucrose on the pharmacokinetics of fructose and acute metabolic and hemodynamic responses in healthy subjects. *Metabolism*, 61(5), pp.641-651.
- Lee, K., Haddad, A., Osme, A., Kim, C., Borzou, A., Ilchenko, S., Allende, D., Dasarathy, S., McCullough, A.J., Sadygov, R.G. and Kasumov, T., 2018. Hepatic mitochondrial defects in a mouse model of NAFLD are associated with increased degradation of oxidative phosphorylation subunits. *Molecular & Cellular Proteomics*.
- Lionetti, L., Mollica, M.P., Donizzetti, I., Gifuni, G., Sica, R., Pignalosa, A., Cavaliere, G., Gaita, M., De Filippo, C., Zorzano, A. and Putti, R., 2014. High-lard and high-fish-oil diets differ in their effects on function and dynamic behaviour of rat hepatic mitochondria. *PloS one*, 9(3), p.e92753.

- Ma, Q., 2013. Role of nrf2 in oxidative stress and toxicity. *Annual review of pharmacology and toxicology*, 53, pp.401-426.
- Mansouri, A., Gattolliat, C.H. and Asselah, T., 2018. Mitochondrial dysfunction and signaling in chronic liver diseases. *Gastroenterology*, 155(3), pp.629-647.
- Miller, A. and Adeli, K., 2008. Dietary fructose and the metabolic syndrome. *Current opinion in gastroenterology*, 24(2), pp.204-209.
- Mitchell, C., Robin, M.A., Mayeuf, A., Mahrouf-Yorgov, M., Mansouri, A., Hamard, M., Couton, D., Fromenty, B. and Gilgenkrantz, H., 2009. Protection against hepatocyte mitochondrial dysfunction delays fibrosis progression in mice. *The American journal of pathology*, 175(5), pp.1929-1937.
- Oliva-Vilarnau, N., Hankeova, S., Vorrink, S.U., Mkrtchian, S., Andersson, E.R. and Lauschke, V.M., 2018. Calcium signaling in liver injury and regeneration. *Frontiers in medicine*, 5, p.192.
- Prins, G.H., Luangmonkong, T., Oosterhuis, D., Mutsaers, H.A., Dekker, F.J. and Olinga, P., 2019. A pathophysiological model of non-alcoholic fatty liver disease using precision-cut liver slices. *Nutrients*, 11(3), p.507.
- Radi, R., Cassina, A. and Hodara, R., 2002. Nitric oxide and peroxynitrite interactions with mitochondria.
- Ruiz-Ramírez, A., Barrios-Maya, M.A., López-Acosta, O., Molina-Ortiz, D. and El-Hafidi, M., 2015. Cytochrome c release from rat liver mitochondria is compromised by increased saturated cardiolipin species induced by sucrose feeding. *American Journal of Physiology-Endocrinology and Metabolism*, 309(9), pp.E777-E786.
- Sanyal, A.J., Campbell–Sargent, C., Mirshahi, F., Rizzo, W.B., Contos, M.J., Sterling, R.K., Luketic, V.A., Shiffman, M.L. and Clore, J.N., 2001. Nonalcoholic steatohepatitis: association of insulin resistance and mitochondrial abnormalities. *Gastroenterology*, 120(5), pp.1183-1192.
- Schwarz, J.M., Noworolski, S.M., Wen, M.J., Dyachenko, A., Prior, J.L., Weinberg, M.E., Herraiz, L.A., Tai, V.W., Bergeron, N., Bersot, T.P. and Rao, M.N., 2015. Effect of a high-fructose weight-maintaining diet on lipogenesis and liver fat. *The Journal of Clinical Endocrinology & Metabolism*, 100(6), pp.2434-2442.

- Situnayake, R.D., Crump, B.J., Thurnham, D.I., Davies, J.A., Gearty, J. and Davis, M., 1990. Lipid peroxidation and hepatic antioxidants in alcoholic liver disease. *Gut*, 31(11), pp.1311-1317.
- Softic, S., Cohen, D.E. and Kahn, C.R., 2016. Role of dietary fructose and hepatic de novo lipogenesis in fatty liver disease. *Digestive diseases and sciences*, 61(5), pp.1282-1293.
- Stanhope, K.L., Schwarz, J.M. and Havel, P.J., 2013. Adverse metabolic effects of dietary fructose: results from recent epidemiological, clinical, and mechanistic studies. *Current opinion in lipidology*, 24(3), p.198.
- Sudheesh, N.P., Ajith, T.A. and Janardhanan, K.K., 2009. Ganoderma lucidum (Fr.) P. Karst enhances activities of heart mitochondrial enzymes and respiratory chain complexes in the aged rat. *Biogerontology*, 10(5), pp.627-636.
- Szczepaniak, L.S., Nurenberg, P., Leonard, D., Browning, J.D., Reingold, J.S., Grundy, S., Hobbs, H.H. and Dobbins, R.L., 2005. Magnetic resonance spectroscopy to measure hepatic triglyceride content: prevalence of hepatic steatosis in the general population. *American Journal of Physiology-Endocrinology and Metabolism*, 288(2), pp.E462-E468.
- Teodoro, J.S., Duarte, F.V., Gomes, A.P., Varela, A.T., Peixoto, F.M., Rolo, A.P. and Palmeira, C.M., 2013. Berberine reverts hepatic mitochondrial dysfunction in high-fat fed rats: a possible role for SirT3 activation. *Mitochondrion*, 13(6), pp.637-646.
- Tilg, H. and Diehl, A.M., 2000. Cytokines in alcoholic and nonalcoholic steatohepatitis. *New England Journal of Medicine*, 343(20), pp.1467-1476.
- Trauner, M., Arrese, M. and Wagner, M., 2010. Fatty liver and lipotoxicity. *Biochimica et biophysica Acta (BBA)-Molecular and Cell biology of lipids*, 1801(3), pp.299-310.
- Twig, G. and Shirihai, O.S., 2011. The interplay between mitochondrial dynamics and mitophagy. *Antioxidants & redox signaling*, 14(10), pp.1939-1951.
- Twig, G., Elorza, A., Molina, A.J., Mohamed, H., Wikstrom, J.D., Walzer, G., Stiles, L., Haigh, S.E., Katz, S., Las, G. and Alroy, J., 2008. Fission and selective fusion govern mitochondrial segregation and elimination by autophagy. *The EMBO journal*, 27(2), pp.433-446.
- Van den Berghe, G., 1986. Fructose: metabolism and short-term effects on carbohydrate and purine metabolic pathways. *Progress in biochemical pharmacology*, 21, pp.1-32.

- Vasselli, J.R., 2008. Fructose-induced leptin resistance: discovery of an unsuspected form of the phenomenon and its significance. Focus on “Fructose-induced leptin resistance exacerbates weight gain in response to subsequent high-fat feeding,” by Shapiro et al. *American Journal of Physiology-Regulatory, Integrative and Comparative Physiology*, 295(5), pp.R1365-R1369.
- Wang, C.H., Ciliberti, N., Li, S.H., Szmitko, P.E., Weisel, R.D., Fedak, P.W., Al-Omran, M., Cherng, W.J., Li, R.K., Stanford, W.L. and Verma, S., 2004. Rosiglitazone facilitates angiogenic progenitor cell differentiation toward endothelial lineage: a new paradigm in glitazone pleiotropy. *Circulation*, 109(11), pp.1392-1400.
- Westermann, B., 2010, August. Mitochondrial dynamics in model organisms: what yeasts, worms and flies have taught us about fusion and fission of mitochondria. In *Seminars in cell & developmental biology* (Vol. 21, No. 6, pp. 542-549). Academic Press.
- Xu, W., Shao, L., Zhou, C., Wang, H. and Guo, J., 2011. Upregulation of Nrf2 expression in non-alcoholic fatty liver and steatohepatitis. *Hepato-gastroenterology*, 58(112), pp.2077-2080.
- Yang, Y., Wang, J., Zhang, Y., Li, J. and Sun, W., 2018. Black sesame seeds ethanol extract ameliorates hepatic lipid accumulation, oxidative stress, and insulin resistance in fructose-induced nonalcoholic fatty liver disease. *Journal of agricultural and food chemistry*, 66(40), pp.10458-10469.
- Yu, T., Robotham, J.L. and Yoon, Y., 2006. Increased production of reactive oxygen species in hyperglycemic conditions requires dynamic change of mitochondrial morphology. *Proceedings of the National Academy of Sciences*, 103(8), pp.2653-2658.
- Zeng, X.P., Li, X.J., Zhang, Q.Y., Liu, Q.W., Li, L., Xiong, Y., He, C.X., Wang, Y.F. and Ye, Q.F., 2017, March. Tert-Butylhydroquinone protects liver against ischemia/reperfusion injury in rats through Nrf2-activating anti-oxidative activity. In *Transplantation proceedings* (Vol. 49, No. 2, pp. 366-372). Elsevier.
- Zhang, H.F., Hu, X.M., Wang, L.X., Xu, S.Q. and Zeng, F.D., 2009. Protective effects of scutellarin against cerebral ischemia in rats: evidence for inhibition of the apoptosis-inducing factor pathway. *Planta medica*, 75(02), pp.121-126.

CHAPTER 4

UPR^{ER} AND UPR^{mt}: MOLECULAR TARGETS OF FRUCTOSE AND PALMITATE INDUCED STEATOSIS IN HEPG2 CELLS

4.1 Introduction

The global epidemic of metabolic syndrome imposes drastic threats to the public health system due to the prevalence of associated comorbidities. The development of caloric exuberance and sedentary lifestyle leads to an imbalance between energy uptake and its utilization. This negatively affects liver function and its homeostasis. NASH is the most common hepatic disorder affecting 25% of the general population worldwide (Younossi et al., 2016). It encompasses a spectrum of clinical and histopathological features, varying from simple steatosis to cirrhosis, fibrosis and HCC (Vernon et al., 2011).

Liver is the major organ responsible for metabolic, secretory and excretory functions to maintain body homeostasis. About 70% of the total liver cells are represented by hepatocytes, essential for lipogenesis, cholesterol biosynthesis, glucose and drug metabolism. Similar to other secretory cells, hepatocytes are also rich in mitochondria and ER. Recent findings revealed that interconnections between mitochondria and ER are highly crucial for various cellular mechanisms in both physiological and pathological conditions (Molledo et al., 2019). The molecular interaction between mitochondria and ER executes as a signaling hub in various diseases. All these life - threatening diseases have a link with continuous consumption of high calorie food. High energy food stimulates lipogenesis that promotes the conversion of excess carbohydrates into fatty acids that are later esterified to store triacylglycerols. It has been reported that glucose is not the only saccharide that induces DNL, but fructose as well (Softic et al; 2016). Moreover, the metabolism of fructose takes place only in the liver, but glucose metabolism occurs in all cells. Because of this reason, the harmful effects of fructose impose a great threat to the liver over years (Speliotes et al., 2019). One of the major factors behind the pathogenesis of NAFLD includes alteration in hepatic cholesterol homeostasis and liver free

cholesterol accumulation (Perla et al., 2017). Both factors contribute to the activation of UPR systems in mitochondria and ER.

4.1.1 Unfolded protein response in endoplasmic reticulum (UPR^{ER}) and NASH

In eukaryotic cells, ER is one of the largest organelle in the cell important for protein synthesis and its folding. ER contains a large concentration of protein chaperones that assist in the folding of nascent polypeptides and also prevent the aggregation of folding intermediates (Gething & Sambrook, 1992). Certain chaperones are supposed to act as a quality control system to assure that only properly folded proteins are transported to Golgi for further modifications and secretions. The condition that diminishes ER protein homeostasis or changes the ER protein folding capacity can lead to the development of ER stress and induces the activation of UPR. When the UPR system has been compromised, the cells are no longer capable of maintaining ER homeostasis. This leads to the activation of intracellular pathways that promotes programmed cell death. Moreover, ER stress response seems to have a crucial role in several other non - parenchymal liver cells supporting that definite understanding of UPR biology in cell and context dependent aspects is relevant.

The first stage of fatty liver disease is steatosis, characterized by TG accumulation in hepatocytes. Since the majority of lipid synthesis takes place in smooth ER, the role of ER stress responses is highly significant in the genesis of steatosis. In hepatocytes, the IRE1 α - XBP1 arm of UPR^{ER} regulates hepatic lipid metabolism by binding to the promoters of lipogenic genes (SCD-1, ACC2) and also by regulating VLDL secretion (Lee et al., 2008). Recent studies have detected IRE1 α mediated XBP1 splicing in the liver in response to hyperinsulinemia (Ning et al., 2011). PERK and p-eIF2 α also regulate lipogenesis and steatosis. In the liver, increased phosphorylation of eIF2 α is associated with NASH and during fatty liver disorders there is a failure to activate the downstream UPR pathways. It has been reported that in liver cells palmitate and other saturated fatty acids activate UPR system which is characterized by preferred induction of PERK signaling (Cao et al., 2012). Furthermore, cholesterol and saturated fatty acids possess a synergistic effect to stimulate ER stress. Additional studies showed that palmitate also induces the increased abundance of ATF4, CHOP, and transcriptional targets of ATF6 α . It has been reported that deficiency of ATF4 provides protection by down regulating the expression of SCD1 against high carbohydrate diet induced steatosis (Li et al., 2011). In addition, ATF4 knockout high fructose fed mice were also protected from steatosis and hypertriglyceridemia due

to reduced expression of lipogenic genes including PPAR γ (Xiao et al., 2013). Another important factor that links ER stress to NASH is CHOP dependent hepatocyte lipotoxicity where apoptosis occurs mainly due to the expression of proapoptotic Bcl-2 family proteins. In addition, ER stress promotes the activation of transcription factors: JNK, NF- κ B and SREBP which are involved in inflammation and cell death and thus plays a significant role in the progression of NASH.

4.1.2 Unfolded protein response in mitochondria (UPR^{mt}) and NASH

The accumulation of oxidatively damaged misfolded proteins is highly toxic to the cells. As part of a protective mechanism, organelle specific signaling pathways called UPR gets activated in mitochondria called UPR^{mt} in addition to ER and cytoplasm. In contrast to UPR^{ER}, the signaling pathways involved in UPR^{mt} are less subjected for investigation. However, it is well known that UPR^{mt} is active in those cells where there is an increased ROS production and defective mitochondria (Hamanaka & Chandel, 2010). Since most of the mitochondrial proteins are encoded by the nuclear genome and imported to the mitochondria in an unfolded state, they undergo chaperone mediated folding and get assembled into multiprotein units. Hence chaperones play a vital role in mitochondrial homeostasis. Any alteration in mitochondrial proteostasis and dysfunction stimulate a retrograde signal from mitochondria to nucleus that results in the upregulation of chaperones and retain mitochondrial function. The primary axis of UPR^{mt} was mediated by the transcription factor CHOP, resulting in the upregulation of several mitochondrial proteases and chaperones (Horibe & Hoogenraad, 2007). Much of the research on UPR^{mt} has been focused on the chaperone Hsp60, which has been considered as the reporter of UPR^{mt}. Since metabolic liver diseases are tightly related to alteration in mitochondrial function, bringing out UPR^{mt} not only inhibits the progression of NAFLD, but also helps in the amelioration of fibrosis and alcohol induced liver injury in mice (Chung et al., 2017). During NASH, liver mitochondria become distracted both structurally and functionally due to the interruption of electron flow through ETC. Several alterations like oxidation of cardiolipin, lipid peroxidation, MDA formation, deterioration of OXPHOS activity and mtDNA are few of them. In general, UPR^{mt} is associated with several pathologies induced by proteotoxic stress such as in NASH.

4.1.3 Mitochondria associated ER membrane (MAM) and NASH

Compartmentalization is one of the fundamental features of all eukaryotic cells. It will be effective only when the coordination between different organelles runs in an integrative manner.

In eukaryotic cells, one of the excellent organellar crosstalk is the interaction site that exists between ER and mitochondria, referred to as MAM. Several lines of evidence demonstrated that cross talk between UPR^{ER} and UPR^{mt} is acting mainly through MAM. It has been reported that in the case of obesity induced NAFLD, the liver develops the physical interaction between ER and mitochondria which is highly essential in determining cell viability during excess nutrients. MAM acts as structural bridges that chiefly exchange calcium ion, ROS and lipids. Hence manifestation of normal ER - mitochondrial communication is essential for its structural and functional integrity (Wang et al., 2020). Disruption of MAM integrity leads to altered calcium homeostasis along with several factors including mitochondrial dysfunction, oxidative stress, UPR^{ER} and IR that favors the progression of NASH. The exchange of calcium from ER to mitochondria is mediated by GRP75. It forms a complex with voltage-dependent anion channels (VDAC) in the outer mitochondrial membrane to inositol 1,4,5-trisphosphate receptors (IP3R), calcium release channel of ER and thus serve as signaling molecules inclusive of calcium, metabolites and apoptotic signals. MAM is also the centre for synthesis and transportation of several proteins, lipids like glycosphingolipids and phospholipids. Recently the role of MFN1/2 has been shown that it exerts a negative regulatory effect on the distance between ER and mitochondria. The interaction of MFN1/2 increases the distance between the two organelles and obstructs the excess contact between them. Moreover removal of MFN1/2 reduces the absorption of calcium ions in Hela cells (Filadi et al.,2015).

The major factors associated with metabolic diseases including NASH is the availability of excess nutrients and metabolic inflexibility. Since ER and mitochondria possess a central role in lipid synthesis and transportation, their miscommunication will lead to pathological conditions (Sasi et al., 2020). Recent studies also revealed the role of MAM in hepatic insulin signaling, nutrient sensing and also in glucose homeostasis (Theurey et al., 2016). Consequently disruption of MAM could worsen hepatic lipid accumulation and organellar miscommunication appears to be related to hepatic metabolic diseases.

Not much research has been done in this area highlighting the role of UPR^{ER} and UPR^{mt} in diet - induced steatosis in HepG2 cells. This study is essential for explaining various molecular events involved in the genesis of diet - induced steatosis in HepG2 cells. Since UPR pathways have multifaceted effects on disease progression, targeting specific effectors involved in NASH would be preferable. It is also expected to aid in the discovery of early biomarkers for

diagnosis and design of drugs for liver diseases in due course. In the present study, we focus on the contribution of UPR^{ER} and UPR^{mt} in the genesis of fructose and palmitate induced steatosis in HepG2 cells.

4.2 Materials and methods

4.2.1 Chemicals and reagents

Fructose, sodium palmitate, radioimmunoprecipitation assay (RIPA) buffer and protease inhibitor cocktail were purchased from Sigma - Aldrich Co. (St. Louis, MO, USA). The cell culture flasks and plates were from BD Biosciences (USA). Fetal bovine serum (FBS), penicillin and streptomycin antibiotics, trypsin - ethylenediaminetetraacetic acid (EDTA), phosphate buffered saline (PBS) and Hank's balanced salt solution (HBSS), bovine serum albumin (BSA), minimum essential medium (MEM) were from Gibco, USA. Antibodies against ATF6, p-eIF2 α , GRP78, Hsp60, Hsp70, BNIP3, and SREBP-1c were from Santa Cruz Biotechnology. Antibodies against IRE1, p-IRE1, CHOP, C/EBP α , XBP1, PERK, p-PERK, PDI, SIRT3, IP3R2, VDAC1, PACS2 were from Cell Signaling Technology, USA. All other chemicals used were of analytical grade.

4.2.2 Cell culture and treatment

HepG2 cells (American Type Culture Collection, (ATCC) Rockville, MD USA) were cultured as per supplier's instructions. In brief, the cells were grown in T-25 flask containing MEM supplemented with 10% heat-inactivated FBS and 1X penicillin streptomycin solution at 37°C and 5% CO₂ in a humidified incubator (Eppendorf, USA). When the cells reached 80% confluence, the cells were trypsinized and reseeded onto a new flask for further experiments.

4.2.3 Fructose and palmitate treatments of HepG2 cells

Fructose stock solution was prepared by dissolving in HBSS and was used to produce different concentrations of fructose treatment in serum free MEM. Palmitate stock solution (10 mM) was prepared by dissolving sodium palmitate in 0.1 N NaOH at 75°C for 5 min. The stock solution was further mixed with fatty acid free BSA to make a final concentration of 1 mM. The 1 mM working solution was then diluted to the desired treatment concentration (100 μ M) in 1% MEM. Treatment was applied on day 3 and the experiments were performed after 24 hrs of treatment with fructose and palmitate. The experimental group consists of (i) C - control cells; (ii) HFP - cells treated with high fructose (100 mM) and palmitate (100 μ M); (iii) HFP +

fenofibrate - cells treated with high fructose, palmitate and fenofibrate (25 μ M) (as positive control).

4.2.4 Enzyme - linked immunosorbent assay (ELISA)

Indirect ELISA was carried out using specific primary antibody and HRP - conjugated secondary antibody. The concentration of IP3R2, VDAC and PACS2 in the cells were quantified by this method. The cell lysates (10 μ g / mL) were pre - coated onto the 96 well ELISA plate and incubated overnight at 4°C. After three washes with PBST, 100 μ L of antibodies (1:500 dilutions) were added to the wells and further incubated for about 2 hrs. Followed by washing with PBS - tween 20, it was incubated with HRP - conjugated secondary antibody for about 2 hrs. After three PBST washes, TMB substrate was added to each well and the signal was stopped by the addition of a stop solution (0.1N HCl). The absorbance was measured at 450 nm using the plate reader (Tecan Infinite M200PRO, Tecan, Austria).

4.2.5 Immunofluorescence analysis

HepG2 cells were cultured in a 96 well culture plate and treated as described earlier. The cells were washed thrice in ice cold PBS and fixed in paraformaldehyde for 10 min at room temperature. After washing, the cells were permeabilized with Triton - X - 100 for 15 min at room temperature. It was followed by blocking with PBS containing goat serum. The cells were then incubated with primary antibody against p-IRE1 and p-PERK at 4°C and after washing it was again incubated with FITC conjugated secondary antibody for 1 hr. This was followed by washing and staining with DAPI for 5 min. The cells were visualized under Olympus immunofluorescence microscope.

4.2.6 Western blot

After respective treatments cells were harvested and proteins were extracted from HepG2 cells by using an ice cold RIPA buffer containing protease inhibitor cocktail. It was then incubated on ice for about 20 min and cell suspensions were centrifuged at 12,000 rpm for 20 min at 4°C. The supernatant was collected and used for further immunoblot analysis. The protein concentration of the cell lysate was measured by using bicinchoninic acid kit (Pierce, Rockford, IL, USA) as per manufacturer's instruction. Proteins thus extracted were separated by SDS-PAGE and were transferred to the PVDF membrane using the Trans-Blot® Turbo™ Transfer system (Bio-Rad, USA). The membrane was then blocked with 5% skimmed milk in TBST for 1 hr at room temperature then probed with specific primary antibodies against IRE1, XBP1,

Hsp70, SREBP-1c, GRP78, ATF6, PERK, p-eIF2 α , CHOP, PDI, Hsp60, C/EBP α , SIRT3, BNIP3 and β - actin (1:1000 dilutions) at 4°C overnight. After washing with TBST, specific horseradish peroxidase conjugated secondary antibodies (1:2000 dilutions) were added and the membranes were incubated for about 2 hrs. After washing, the immune complex was visualized using Clarity™ Western ECL Substrate (Bio-Rad,USA).The images were analyzed in the ChemiDoc XRS system (Bio-Rad,USA) using Image Lab software.

4.2.7 Statistical analysis

Statistical analysis was carried out by the SPSS statistical program. The data were represented as mean \pm SD. The data were subjected to one - way analysis of variance (ANOVA) and the differences among the means of the groups were assessed using Duncan’s multiple range tests using OriginPro version 8.5 (OriginLab Corporation, Massachusetts, USA). The statistical significance was accepted at $p \leq 0.05$.

4.3 Results

4.3.1 Effect of HFP on lipogenesis *via* IRE1 α / XBP1 arm of UPR^{ER}

To investigate the presumed link between steatosis and ER signaling pathway, we examined the expression levels of various proteins involved in UPR^{ER} activation pathway upon HFP treatment.

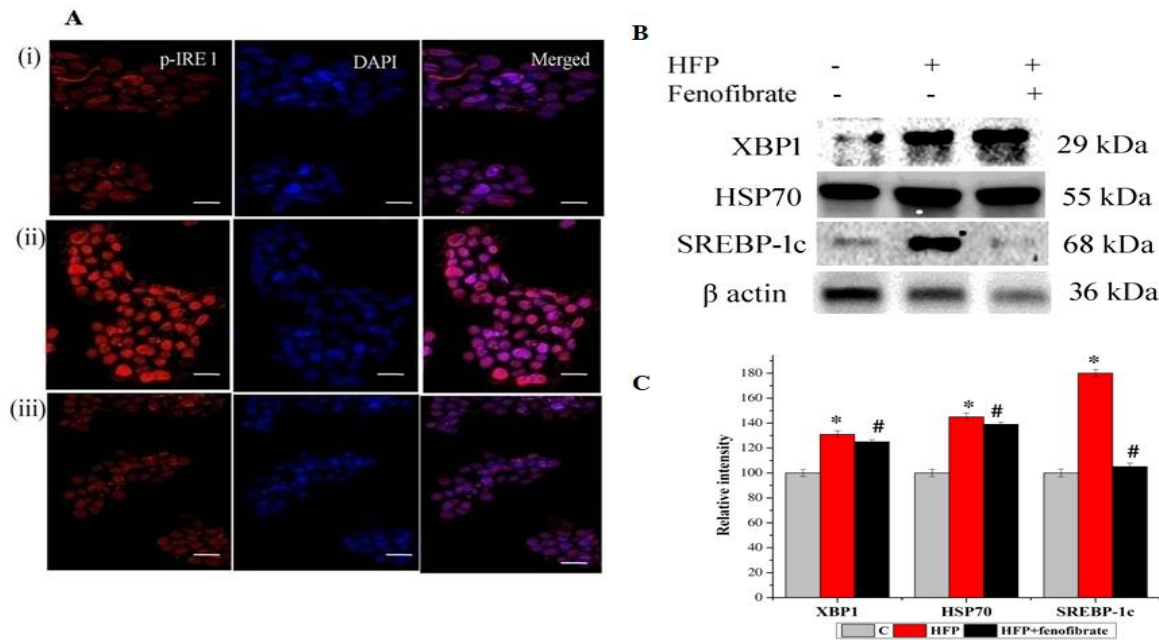


Figure 4.1 HFP stimulates lipogenesis *via* activation of IRE1 / XBP1 arm of UPR^{ER} in HepG2 cells: (A) Immunofluorescence analysis of p-IRE1 during steatosis. (i) C - control cells; (ii) HFP - cells treated

with high fructose and palmitate; (iii) HFP + fenofibrate - cells treated with high fructose, palmitate and fenofibrate. Original magnifications 40X. Scale bar corresponds to 20 μ M. (B) The protein expression of XBP1, Hsp70 and SREBP-1c during steatosis. (C) The relative intensity of each band was quantified with β actin. Data are expressed as mean \pm SD; where n = 3. * indicates significantly different from the control group ($p \leq 0.05$). # indicates significantly different from the HFP treated group ($p \leq 0.05$).

The expression of p-IRE1 α was increased in HFP treated HepG2 cells compared to the control (Figure 4.1A). Moreover, protein expression studies revealed that the expression of XBP1, Hsp70 and SREBP-1c were elevated significantly ($p \leq 0.05$) by 72%, 87.89%, and 72.56% respectively in HepG2 cells induced by HFP (Figure 4.1B), whereas treatment with fenofibrate significantly ($p \leq 0.05$) decreased the protein expression of XBP1 by 68.78%, Hsp70 by 59.12% and SREBP-1c by 23.2% (Figure 4.1B). In addition, the protein level of SREBP-2 showed a significant ($p \leq 0.05$) increase of 43.86 % confirming surplus cholesterol in the HFP treated group and the condition is significantly ($p \leq 0.05$) reversed by fenofibrate to 75.85% (Figure 4.1D).

4.3.2 Effect of HFP on ATF6 pathway of UPR^{ER}

The expression of ER chaperone Grp78 / BiP was upregulated significantly to about 57.6% ($p \leq 0.05$) in HFP treated HepG2 cells compared to the control (Figure 4.2). Treatment with fenofibrate significantly ($p \leq 0.05$) prevented the upregulation by 62.40% (Figure 4.2). The expression level of ATF6 was also significantly ($p \leq 0.05$) higher compared to the control group during HFP induced steatosis condition (79.84%) and the condition is reversed by fenofibrate significantly ($p \leq 0.05$) to 26.90% (Figure 4.2).

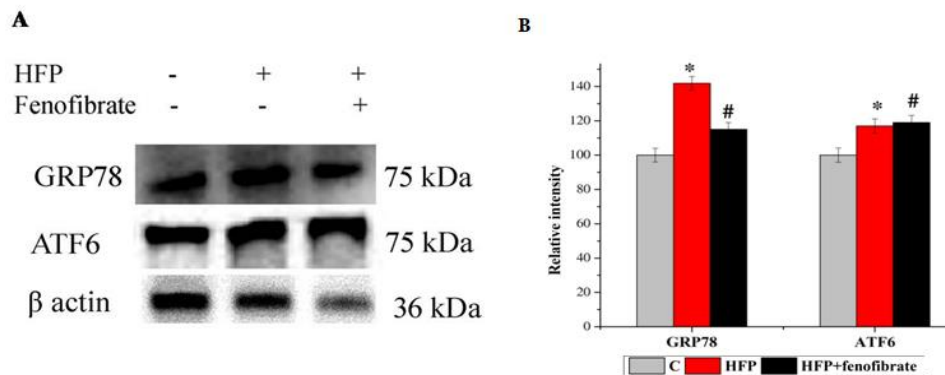


Figure 4.2 HFP induces ER stress in HepG2 cells via upregulation of ATF6 pathway of UPR^{ER}: (A) The protein expression of GRP78 and ATF6 during steatosis. C - control cells; HFP - cells treated with high fructose and palmitate; HFP + fenofibrate - cells treated with high fructose, palmitate and

fenofibrate. (B) The relative intensity of each band was quantified with β actin. Data are expressed as mean \pm SD; where $n = 3$. * indicates significantly different from the control group ($p \leq 0.05$). # indicates significantly different from the HFP treated group ($p \leq 0.05$).

4.3.3 Effect of HFP on PERK pathway of UPR^{ER}

The immunofluorescence staining shows that the expression of p-PERK was higher in HFP treated cells compared to the control (Figure 4.3A). In addition, the level of p-eIF2 α and CHOP was significantly ($p \leq 0.05$) higher (15.6%, 43.3%, respectively) in HFP treated cells compared to the control (Figure 4.3B). Treatment with fenofibrate prevented the upregulation significantly ($p \leq 0.05$) by 20.46% and 49.35% for p-eIF2 α and CHOP respectively (Figure 4.3B).

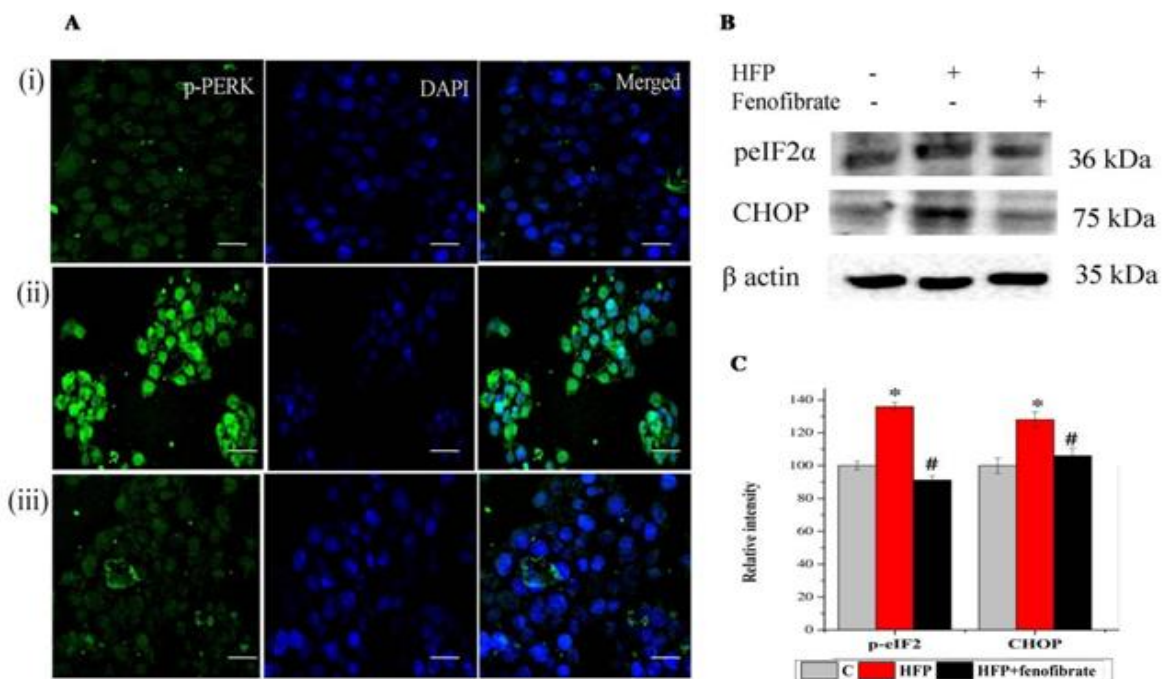


Figure 4.3 HFP stimulates the activation of PERK pathway of ER stress: (A) Immunofluorescence analysis of p-PERK during steatosis. (i) C - control cells; (ii) HFP - cells treated with high fructose and palmitate; (iii) HFP + fenofibrate - cells treated with high fructose, palmitate and fenofibrate. Original magnifications 40X. Scale bar corresponds to 20 μ M. (B) The protein expression of p-eIF2 α and CHOP during steatosis. (C) The relative intensity of each band was quantified with β actin. Data are expressed as mean \pm SD; where $n = 3$. * indicates significantly different from the control group ($p \leq 0.05$). # indicates significantly different from the HFP treated group ($p \leq 0.05$).

4.3.4 Effect of HFP on UPR^{mt} pathway

The combined action of various regulatory components links UPR with the function and modulation of mitochondria. Therefore, we investigated the activation of UPR^{mt} during steatosis. The expression of biomarkers of UPR^{mt} like Hsp60, C/EBP α and BNIP3 was upregulated significantly ($p \leq 0.05$) by 214.12%, 96.41%, 120.91% respectively (Figure 4.4) and expression of SIRT3 was downregulated significantly ($p \leq 0.05$) by 46.43% in HFP treated cells compared to the control (Figure 4.4). The overexpression of UPR^{mt} proteins indicates the accumulation of unfolded or misfolded proteins in the mitochondria. Co-treatment with fenofibrate significantly ($p \leq 0.05$) down regulated the expression of Hsp60 by 52.12%, C/EBP α by 116.32%, BNIP3 by 28.63% and upregulated the expression of SIRT3 by 53.86% (Figure 4.4).

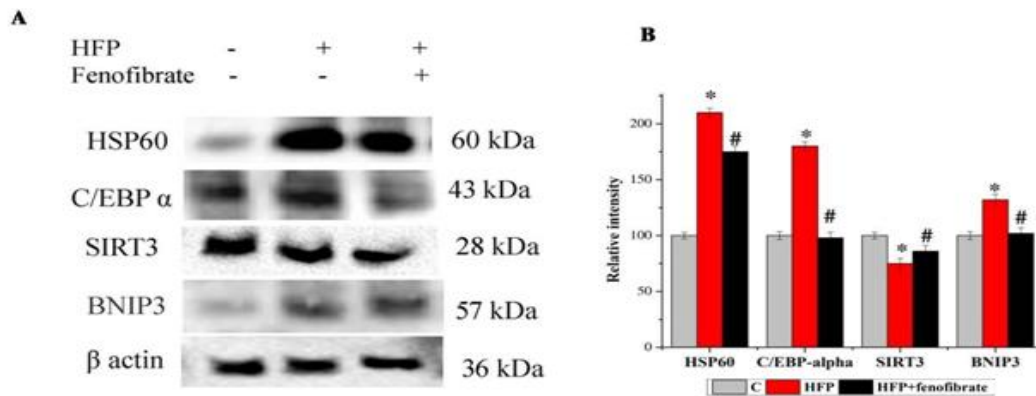


Figure 4.4 Conserved stress response pathway UPR^{mt} was adversely affected during steatosis: (A) The protein expression of Hsp60, C/EBP α , SIRT3, and BNIP3 during steatosis. C - control cells; HFP - cells treated with high fructose and palmitate; HFP + fenofibrate - cells treated with high fructose, palmitate and fenofibrate. (B) The relative intensity of each band was quantified with β actin. Data are expressed as mean \pm SD; where $n = 3$. * indicates significantly different from the control group ($p \leq 0.05$). # indicates significantly different from the HFP treated group ($p \leq 0.05$).

4.3.5 Effect of HFP on mutual interaction between ER and mitochondria

The interaction between ER and mitochondria can be studied by analyzing the protein concentration of various proteins that favor the interaction between these two organelles. The major proteins that maintain ER - mitochondria networks include IP3R2, VDAC1 and PACS2. In the present study, the HFP treated HepG2 cells shows a significant ($p \leq 0.05$) reduction in the level of IP3R2, VDAC1 and PACS2 to about 18.88%, 9.13% and 12.96% respectively (Figure

4.5). Treatment with fenofibrate significantly ($p \leq 0.05$) improved the IP3R2 by 29.07%, VDAC1 by 10.85% and PACS2 by 15.79% (Figure 4.5).

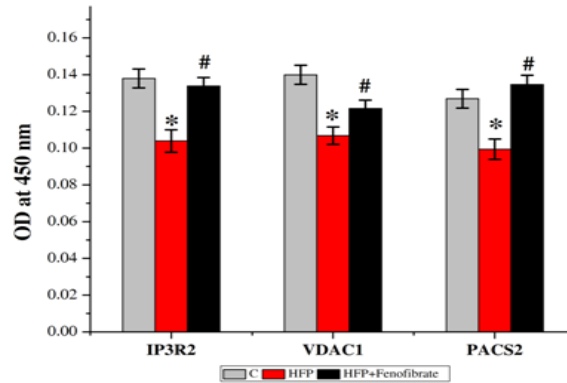


Figure 4.5 HFP induced steatosis impaired the mutual interaction between ER and mitochondria: Detection of MAM proteins IP3R2, VDAC1, and PACS2 by ELISA. C - control cells; HFP - cells treated with high fructose and palmitate; HFP + fenofibrate - cells treated with high fructose, palmitate and fenofibrate. Data are expressed as mean \pm SD; where $n = 6$. * indicates significantly different from the control group ($p \leq 0.05$). # indicates significantly different from the HFP treated group ($p \leq 0.05$).

4.4 Discussion

One of the major factors behind the development of liver diseases is the imbalance between anabolic and catabolic processes. The trade mark in the progression of steatosis is the abnormal rise of TG rich lipid droplets in the liver. Increased lipids along with cholesterol accumulation have been linked to the activation of ER UPR pathways; can be considered as potential targets for liver disease. However, the exact molecular events in the development of this phenotype remain uncertain. In this study, we tried to reveal the significance of UPR^{ER} and UPR^{mt} in the genesis of steatosis in HepG2 cells. Even though the two systems are conceptually similar, control of UPR^{mt} is entirely different and independent of UPR^{ER}. The significance of ER mitochondria communication during steatosis was also considered.

The gradual development of steatotic features in HepG2 cells may activate ER stress *via* oxygen deprivation and build up of acidic waste materials. Induction of UPR^{ER} involves the activation of ER transmembrane stress sensors like IRE1, ATF6 and PERK (Mohan et al., 2019). During normal conditions, all these sensor proteins are maintained in an inactive form with the help of GRP78 / BiP. HFP mediated ER stress results in the dissociation of GRP78 / BiP due to the formation of misfolded proteins above the threshold level. Development of ER stress and

activation of GRP78 is directly or indirectly correlated with up-regulation of SREBPs and severity of pathological condition (Kammoun et al., 2009). This in turn causes the release of IRE1, ATF6 and PERK thereby stimulating all branches for activation. The phosphorylation of IRE1 α modulates the expression of genes involved in ER membrane biogenesis, protein folding, trafficking and degradation. Upregulation of phosphorylated IRE1 stimulates the splicing of XBP1 as reflected by its protein level in HFP treated HepG2 cells. Prolonged IRE1 activation stimulates the JNK pathway and triggers the cue for apoptosis (Wang et al., 2015). We also report here that in *in vitro* condition, the level of Hsp70 was markedly elevated during steatosis. Furthermore, it promotes the activation of SREBP-1c and SREBP2, in turn results in the elevation of major lipogenic proteins such as FAS, SCD1 and ACC α to stimulate lipogenesis. This implies that Hsp70 promotes lipid accumulation in hepatocytes during steatosis *via* increased lipogenesis and not by decreased oxidation of fatty acid. Several studies revealed that overconsumption of fructose stimulates SREBP-1c expression and hepatic lipid accumulation (Zhang et al., 2012). The presence of high carbohydrate either monosaccharide or disaccharide induces palmitic acid to promote dyslipidemia and hyperglycemia. Imbalance in palmitic acid composition activates SREBP localized in the ER membrane *via* AMP kinase and increases hepatocytes cholesterol biosynthesis (Deng et al., 2015). SREBPs are a family of transcription factors that plays a central role in fatty acids, cholesterol and triglyceride biogenesis. In addition to their physiological effects, they are involved in several pathological conditions like NAFLD, NASH, hepatitis and hepatic cancer. Hepatocytes are enriched with both rough and smooth ER and are primarily responsible for lipogenesis, cholesterol biosynthesis, glucose and xenobiotic metabolism (Wang & Kaufman, 2016). Even though the concentration of cholesterol in mitochondria is lesser compared to other organelles, the perception ability towards membrane fluidity is higher by cholesterol enrichment (Montero, 2010). Moreover, it has been reported that saturated fatty acids have a greater detrimental effect on hepatocytes and its function including ER homeostasis than unsaturated fatty acids. Our data thus revealed that increased cholesterol formation activates different arms of UPR^{ER}, a vital regulatory system responsible for restoring ER homeostasis.

GRP78 plays a pivotal role in ER stress regulation and involved in the regulation of array of biological functions along with protein folding, ER calcium binding and activation of transmembrane ER stress sensors. Furthermore ATF6 a basic leucine-zipper transcription factor

gets cleaved during ER stress and its cytosolic domain translocates to the nucleus (Teodoro, 2012). PERK dependent signaling plays a crucial role in the modulation of lipogenic enzymes including ATP citrate lyase (Bobrovnikova et al., 2008). The activation of PERK - eIF2 α - ATF4 complex also enhances the transcription of pro-apoptotic factors. It is well known that prolonged ER stress is accompanied by increased expression of CHOP, the major ER stress related apoptotic protein. The activation of these proteins was detected during HFP induced steatosis. This results in a shift from prosurvival to proapoptotic role of UPR system. The presence of transient UPR provides protection from steatosis however, chronic ER stress provokes hepatic steatosis.

In contrast to the UPR^{ER}, the signaling pathway involved in UPR^{mt} is poorly subjected for investigation. Mitochondria also raise an UPR system like ER which is tightly associated with steatosis and fibrotic liver disease and is activated by multiple forms of mitochondrial dysfunction (Yi, 2019). Our previous study reported the various alterations occurred in mitochondria during high calorie induced steatosis (Sasi et al., 2020). The present study also explored the role of UPR^{mt} during HFP mediated steatosis. There are reports to support the significance of UPR^{mt} in the genesis of diabetes, fatty liver diseases and cancer. In UPR^{mt}, the fundamental element of mitohormetic response exploits a retrograde signaling pathway from mitochondria to the nucleus network to establish the function of molecular chaperones, proteases and antioxidant enzymes in the matrix. Most of the mitochondrial proteins are synthesized in the cytosol and nascent polypeptides are translocated to the matrix. The activation of UPR^{mt} is due to the inactivation of about 171 genes; many of its protein products are in mitochondria. This in turn leads to alteration in membrane potential across the inner mitochondrial membrane. Drop in membrane potential is followed by reduction in import of functional proteins into the organelle. Lack of functional proteins and presence of increased mitochondrial proteotoxic stress results in the activation of UPR^{mt} and upregulate definite sets of genes involved in mitochondrial chaperone systems (Aldridge et al., 2007).

The study of UPR^{mt} revealed the role of CHOP in the initial axis of UPR^{mt}, which is a transcription factor essential for UPR^{ER}. The binding of CHOP to the promoter of target genes provides context specificity to CHOP. Hsp60 is recognized as the major nuclear encoded chaperone of UPR^{mt} by acting as a defense system against proteotoxic cellular damage (Lin et al., 2001). In the present study, nutritional overload induces the expression of Hsp60 suggesting

its possible role in cellular protection and also an indicator of mitochondrial damage. It has been reported that Hsp60 protects tumor cells from Bax-dependent and CypD-dependent cell death by regulating mitochondrial permeability transition (Ghosh et al., 2010). The activities of Hsp60 are regulated by the proteins belonging to the CREB family. The same CREB family proteins act as a downstream effector of UPR^{ER} PERK/ eIF2 α pathway and mitochondrial stress response in mammals (Quiros et al., 2017). The activation of UPR^{mt} leads to the upregulation of CHOP and dimerize with transcription factors belonging to the C/EBP α family. The expression of C/EBP α occurs only in UPR^{mt} but not for the induction of UPR^{ER} where it results in TG formation. In HFP treated HepG2 cells, increased expression of Hsp60 stimulates C/EBP α for inducing apoptosis *via* caspase activation. The mitochondrial resident protein SIRT3 possesses various effects such as metabolic reprogramming, antioxidant defense mechanisms, tumor suppression. Recent report argues that SIRT3 promotes acyl carnitine metabolism during fatty liver (Wang et al., 2018) and downregulates during liver ischaemia - reperfusion injury. The presence of surplus calories reduces the activity of SIRT3 in the liver and stimulates hyperacetylation of several mitochondrial proteins (Hirschey, 2011). Decline in SIRT3 negatively affects the antioxidant system due to its interaction with MnSOD and isocitrate dehydrogenase 2. We found significant down regulation of SIRT3 during HFP which can be correlated with altered membrane potential and superoxide production. This reveals the fact that SIRT3 could be a potential therapeutic target for steatosis and sirtuin enhancers will be highly beneficial to treat hepatic steatosis. The process of mitophagy in hepatocytes is under the modulation of BNIP3 (Zhou et al., 2018). It is a member of the Bcl-2 protein family, which can induce cell death assisting with cell survival. The formation of BNIP3 homo and hetero oligomers regulate the permeability of mitochondrial membrane. High calorie induced BNIP3 over expression results in an alteration in mitochondrial membrane potential. We also observed the dissipation of $\Delta\Psi_m$ with an increase in BNIP3 during steatosis. The role of mitochondrial chaperones has also been predicted in fatty liver disease *via* regulation of mitochondrial protein homeostasis. Our results also reveal the involvement of mitochondrial chaperones in the genesis of biochemical alteration in HepG2 cells similar to fatty liver disease in animals.

Since UPR^{ER} and UPR^{mt} plays an indispensable role in the progression of steatosis, the inter organellar communication site that exists between ER and mitochondria is also relevant. The junction between ER and mitochondria referred to as MAM helps in the exchange of

molecules and ions from one to the next for maintaining cellular health. In the present study, we also analyzed the concentration of proteins involved in the interaction between ER and mitochondria since dysfunction in ER - mitochondria architecture is linked to several pathological conditions. It has been found that metabolic disturbances like high calorie can disrupt ER - mitochondria contact sites. The concentration of MAM proteins like VDAC, PACS2 and IP3R2 were decreased drastically under a high calorie environment. Reduced levels of MAM proteins indicate that the release of several molecules and ions from ER to mitochondria gets diminished. So that the vital activities like ATP production, mitobiogenesis, organelle dynamicity gets impaired. This result is in line with another study which states the potential role of palmitate in suppressing the functional interaction between ER and mitochondria (Shinjo et al., 2017). It is suggested that during the early stages of ER stress, the interaction of MAM proteins increases, however prolonged organelle stress reduces the interaction. However, there is a considerable disparity regarding the mutual interaction between ER and mitochondria.

4.5 Summary and conclusion

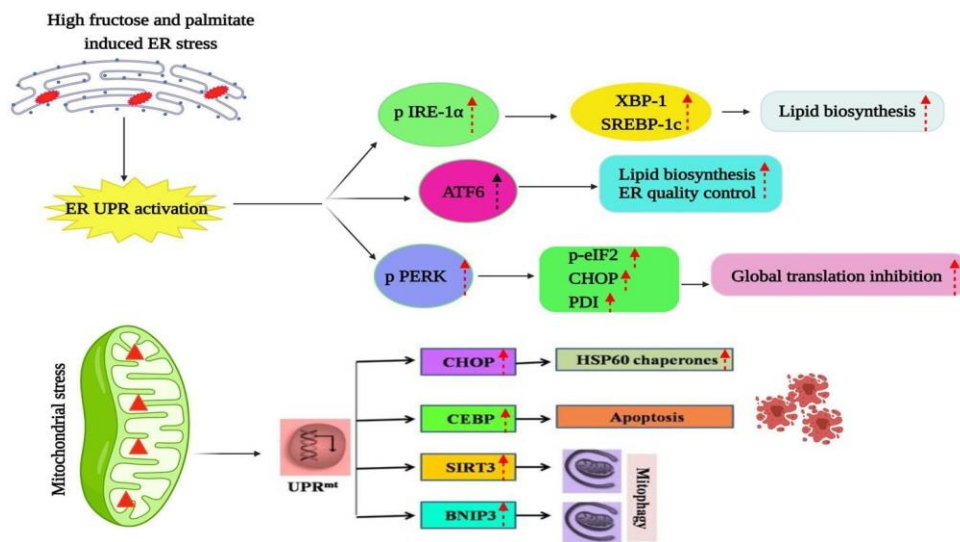


Figure 4.6 Schematic representation of altered UPR system during high calorie induced steatosis

From the overall results, it is clear that both UPR^{ER} and UPR^{mt} were altered during HFP treatment. This shows the importance of UPR^{ER} and UPR^{mt} as targets in the development of therapies for NAFLD in the future. Moreover, we found that UPR^{ER} and UPR^{mt} play a significant

role in ER - mitochondria contact surface and greatly decrease under nutrient rich conditions. Specific changes in UPR^{ER} and UPR^{mt} proteins characterize hepatic steatosis with reduction in organelle interactions.

References

- Aldridge, J.E., Horibe, T. and Hoogenraad, N.J., 2007. Discovery of genes activated by the mitochondrial unfolded protein response (mtUPR) and cognate promoter elements. *PloS one*, 2(9), p.e874.
- Bobrovnikova-Marjon, E., Hatzivassiliou, G., Grigoriadou, C., Romero, M., Cavener, D.R., Thompson, C.B. and Diehl, J.A., 2008. PERK-dependent regulation of lipogenesis during mouse mammary gland development and adipocyte differentiation. *Proceedings of the National Academy of Sciences*, 105(42), pp.16314-16319.
- Cao, J., Dai, D.L., Yao, L., Yu, H.H., Ning, B., Zhang, Q., Chen, J., Cheng, W.H., Shen, W. and Yang, Z.X., 2012. Saturated fatty acid induction of endoplasmic reticulum stress and apoptosis in human liver cells via the PERK/ATF4/CHOP signaling pathway. *Molecular and cellular biochemistry*, 364(1), pp.115-129.
- Chung, H.K., Kim, J.T., Kim, H.W., Kwon, M., Kim, S.Y., Shong, M., Kim, K.S. and Yi, H.S., 2017. GDF15 deficiency exacerbates chronic alcohol-and carbon tetrachloride-induced liver injury. *Scientific reports*, 7(1), pp.1-13.
- Deng, X., Dong, Q., Bridges, D., Raghov, R., Park, E.A. and Elam, M.B., 2015. Docosahexaenoic acid inhibits proteolytic processing of sterol regulatory element-binding protein-1c (SREBP-1c) via activation of AMP-activated kinase. *Biochimica et Biophysica Acta (BBA)-Molecular and Cell Biology of Lipids*, 1851(12), pp.1521-1529.
- Filadi, R., Greotti, E., Turacchio, G., Luini, A., Pozzan, T. and Pizzo, P., 2015. Mitofusin 2 ablation increases endoplasmic reticulum-mitochondria coupling. *Proceedings of the National Academy of Sciences*, 112(17), pp.E2174-E2181.
- Gething, M.J. and Sambrook, J., 1992. Protein folding in the cell. *Nature*, 355(6355), pp.33-45.

- Ghosh, J.C., Siegelin, M.D., Dohi, T. and Altieri, D.C., 2010. Heat shock protein 60 regulation of the mitochondrial permeability transition pore in tumor cells. *Cancer research*, 70(22), pp.8988-8993.
- Hamanaka, R.B. and Chandel, N.S., 2010. Mitochondrial reactive oxygen species regulate cellular signaling and dictate biological outcomes. *Trends in biochemical sciences*, 35(9), pp.505-513.
- Hirschey, M.D., Shimazu, T., Huang, J.Y., Schwer, B. and Verdin, E., 2011, January. SIRT3 regulates mitochondrial protein acetylation and intermediary metabolism. In *Cold Spring Harbor symposia on quantitative biology* (Vol. 76, pp. 267-277). Cold Spring Harbor Laboratory Press.
- Horibe, T. and Hoogenraad, N.J., 2007. The chop gene contains an element for the positive regulation of the mitochondrial unfolded protein response. *PloS one*, 2(9), p.e835.
- Kammoun, H.L., Chabanon, H., Hainault, I., Luquet, S., Magnan, C., Koike, T., Ferré, P. and Foufelle, F., 2009. GRP78 expression inhibits insulin and ER stress–induced SREBP-1c activation and reduces hepatic steatosis in mice. *The Journal of clinical investigation*, 119(5), pp.1201-1215.
- Lee, A.H., Scapa, E.F., Cohen, D.E. and Glimcher, L.H., 2008. Regulation of hepatic lipogenesis by the transcription factor XBP1. *Science*, 320(5882), pp.1492-1496.
- Li, H., Meng, Q., Xiao, F., Chen, S., Du, Y., Yu, J., Wang, C. and Guo, F., 2011. ATF4 deficiency protects mice from high-carbohydrate-diet-induced liver steatosis. *Biochemical Journal*, 438(2), pp.283-289.
- Lin, K.M., Lin, B., Lian, I.Y., Mestril, R., Scheffler, I.E. and Dillmann, W.H., 2001. Combined and individual mitochondrial HSP60 and HSP10 expression in cardiac myocytes protects mitochondrial function and prevents apoptotic cell deaths induced by simulated ischemia-reoxygenation. *Circulation*, 103(13), pp.1787-1792.
- Mohan, S., Brown, L. and Ayyappan, P., 2019. Endoplasmic reticulum stress: a master regulator of metabolic syndrome. *European journal of pharmacology*, 860, p.172553.
- Moltedo, O., Remondelli, P. and Amodio, G., 2019. The mitochondria–endoplasmic reticulum contacts and their critical role in aging and age-associated diseases. *Frontiers in cell and developmental biology*, 7, p.172.

- Montero, J., Mari, M., Colell, A., Morales, A., Basañez, G., Garcia-Ruiz, C. and Fernández-Checa, J.C., 2010. Cholesterol and peroxidized cardiolipin in mitochondrial membrane properties, permeabilization and cell death. *Biochimica et Biophysica Acta (BBA)-Bioenergetics*, 1797(6-7), pp.1217-1224.
- Ning, J., Hong, T., Ward, A., Pi, J., Liu, Z., Liu, H.Y. and Cao, W., 2011. Constitutive role for IRE1 α -XBP1 signaling pathway in the insulin-mediated hepatic lipogenic program. *Endocrinology*, 152(6), pp.2247-2255.
- Perla, F.M., Prelati, M., Lavorato, M., Visicchio, D. and Anania, C., 2017. The role of lipid and lipoprotein metabolism in non-alcoholic fatty liver disease. *Children*, 4(6), p.46.
- Quirós, P.M., Prado, M.A., Zamboni, N., D'Amico, D., Williams, R.W., Finley, D., Gygi, S.P. and Auwerx, J., 2017. Multi-omics analysis identifies ATF4 as a key regulator of the mitochondrial stress response in mammals. *Journal of Cell Biology*, 216(7), pp.2027-2045.
- Sasi, U.S., Ganapathy, S., Palayyan, S.R. and Gopal, R.K., 2020. Mitochondria associated membranes (MAMs): emerging drug targets for diabetes. *Current medicinal chemistry*, 27(20), pp.3362-3385.
- Shinjo, S., Jiang, S., Nameta, M., Suzuki, T., Kanai, M., Nomura, Y. and Goda, N., 2017. Disruption of the mitochondria-associated ER membrane (MAM) plays a central role in palmitic acid-induced insulin resistance. *Experimental cell research*, 359(1), pp.86-93.
- Softic, S., Cohen, D.E. and Kahn, C.R., 2016. Role of dietary fructose and hepatic de novo lipogenesis in fatty liver disease. *Digestive diseases and sciences*, 61(5), pp.1282-1293.
- Speliotes, E.K., Balakrishnan, M., Friedman, L.S. and Corey, K.E., 2019. treatment of Dyslipidemia in Common liver Diseases.
- Teodoro, T., Odisho, T., Sidorova, E. and Volchuk, A., 2012. Pancreatic β -cells depend on basal expression of active ATF6 α -p50 for cell survival even under nonstress conditions. *American Journal of Physiology-Cell Physiology*, 302(7), pp.C992-C1003.
- Theurey, P., Tubbs, E., Vial, G., Jacquemetton, J., Bendridi, N., Chauvin, M.A., Alam, M.R., Le Romancer, M., Vidal, H. and Rieusset, J., 2016. Mitochondria-associated endoplasmic reticulum membranes allow adaptation of mitochondrial metabolism to glucose availability in the liver. *Journal of molecular cell biology*, 8(2), pp.129-143.

- Vernon, G., Baranova, A. and Younossi, Z.M., 2011. Systematic review: the epidemiology and natural history of non-alcoholic fatty liver disease and non-alcoholic steatohepatitis in adults. *Alimentary pharmacology & therapeutics*, 34(3), pp.274-285.
- Wang, Y., Yamada, E., Zong, H. and Pessin, J.E., 2015. Fyn activation of mTORC1 stimulates the IRE1 α -JNK pathway, leading to cell death. *Journal of Biological Chemistry*, 290(41), pp.24772-24783.
- Wang, M. and Kaufman, R.J., 2016. Protein misfolding in the endoplasmic reticulum as a conduit to human disease. *Nature*, 529(7586), pp.326-335.
- Wang, G.E., Li, Y.F., Zhai, Y.J., Gong, L., Tian, J.Y., Hong, M., Yao, N., Wu, Y.P., Kurihara, H. and He, R.R., 2018. Theacrine protects against nonalcoholic fatty liver disease by regulating acylcarnitine metabolism. *Metabolism*, 85, pp.227-239.
- Wang, J., He, W., Tsai, P.J., Chen, P.H., Ye, M., Guo, J. and Su, Z., 2020. Mutual interaction between endoplasmic reticulum and mitochondria in nonalcoholic fatty liver disease. *Lipids in health and disease*, 19, pp.1-19.
- Xiao, G., Zhang, T., Yu, S., Lee, S., Calabuig-Navarro, V., Yamauchi, J., Ringquist, S. and Dong, H.H., 2013. ATF4 protein deficiency protects against high fructose-induced hypertriglyceridemia in mice. *Journal of biological chemistry*, 288(35), pp.25350-25361.
- Yi, H.S., 2019. Implications of mitochondrial unfolded protein response and mitokines: a perspective on fatty liver diseases. *Endocrinology and Metabolism*, 34(1), p.39.
- Younossi, Z.M., Koenig, A.B., Abdelatif, D., Fazel, Y., Henry, L. and Wymer, M., 2016. Global epidemiology of nonalcoholic fatty liver disease—meta-analytic assessment of prevalence, incidence, and outcomes. *Hepatology*, 64(1), pp.73-84.
- Zhang, C., Chen, X., Zhu, R.M., Zhang, Y., Yu, T., Wang, H., Zhao, H., Zhao, M., Ji, Y.L., Chen, Y.H. and Meng, X.H., 2012. Endoplasmic reticulum stress is involved in hepatic SREBP-1c activation and lipid accumulation in fructose-fed mice. *Toxicology letters*, 212(3), pp.229-240.
- Zhou, H., Du, W., Li, Y.E., Shi, C., Hu, N., Ma, S., Wang, W. and Ren, J., 2018. Effects of melatonin on fatty liver disease: The role of NR 4A1/DNA-PK α /p53 pathway, mitochondrial fission, and mitophagy. *Journal of Pineal Research*, 64(1), p.e12450.

CHAPTER 5

ROLE OF IRON AND VITAMIN K ON FRUCTOSE AND PALMITATE INDUCED STEATOSIS IN HEPG2 CELLS

5.1 Introduction

Iron is an indispensable element required for performing diverse biological functions for the human body. The human body possesses an average of 2 - 4 g of iron, of which 80% is bound with hemoglobin. The iron homeostasis is successfully maintained in the biological system due to the consistent harmony between its uptake, storage, transportation and utilization. It provides an excellent platform for several metabolic processes comprising oxygen transportation, in particular hemoglobin and myoglobin, synthesis of DNA molecules, formation of heme enzymes, other iron - containing enzymes involved in ETC and several oxidation - reduction reactions (Abbaspour et al., 2014). The deficiency of iron decreases the production of hemoglobin and leads to anemia. On the other hand, iron overload results in the deposition of excess iron in tissues and can cause cell damage (Fung & Nemeth, 2013).

Although an essential nutrient in various cellular processes and erythropoiesis, the reactivity of iron is potentially cytotoxic in nature, due to the production of highly reactive and toxic free radicals (Eid et al., 2017)). In order to prevent the adverse effects of iron, the cells must stringently regulate the uptake and storage of iron. Dysregulation in iron metabolism results in the development of a spectrum of diseases ranging from anemia to iron overload. For instance, in patients with hereditary hemochromatosis, iron overload is caused due to the mutation of the Hfe gene. Higher iron levels are also observed in those with ALD, NAFLD and hepatitis C viral infection. Due to this, iron absorption in the duodenum gets increased producing excessive iron accumulation in the liver. This leads to tissue damage and fibrosis. Liver fibrosis is a pathological condition in ALD, NAFLD, and NASH. NAFLD is now becoming the most frequent liver disease and hepatic iron overload is commonly observed in NAFLD patients and is correlated with organ dysfunction secondary to ROS generation. Iron combined with ROS and thus enhances the level of hydroxyl radicals which are solely responsible for phospholipid

peroxidation, oxidation of amino acid side chain and protein fragmentation. Increased iron storage may also elevate the possibilities of ballooning of hepatocytes, inflammation and liver fibrosis (Aly & Kleiner, 2011). Chronic liver disease adversely affects liver function including the production of hepcidin, a key protein involved in iron metabolism. Moreover, defects in iron metabolism and increased facilitation of iron storage have been described in hepatocytes exposed to FFA and also in patients with NAFLD and copper deficiency (Aigner et al., 2008).

It has been documented that during NASH, there will be abnormal iron indices (ferritin / transferrin saturation) and virtuous hepatic iron concentration (Bacon et al., 1994). Since iron plays a crucial role in lipid peroxidation and fibrogenesis, it is expected to play a central role in the development and progression of NASH. In contrast, some groups of researchers reported that iron accumulation is not seen in patients with NASH and there is no association between hepatic iron and aggressive histological or clinical outcome (Younossi et al., 1999). Some authors concluded that hyperferritinemia in NASH is a non - specific effect of necroinflammation and elevated ferritin level is due to its release from damaged hepatocytes (Chitturi, 2002). However it is plausible that elevated ferritin during NASH may be due to some oxidative stress like free fatty acid, cytokines, lipid peroxidation and induction of cytochrome P450 enzymes.

In cultured hepatocytes, addition of iron salts has been shown to cause an increase in lipid peroxidation. Certain *in vivo* models of oxidative injury also manifested the potential role of iron. In some animal models, it has been cleared that dietary modifications have a significant role in altering iron homeostasis. In rabbits fed with a high fat diet revealed an increase in hepatic iron, hepatic stellate cell activation as well as an upregulation in the mRNA expression of TGF β 1, and proinflammatory cytokines (Otogawa et al., 2007).

The objective of the present study was to characterize biochemically the cell response to iron during high fructose and palmitate induced steatosis conditions in HepG2 cells. For this alteration in iron indices, oxidative stress, inflammation and apoptosis during high calorie induced steatosis were also examined in this *in vitro* model system.

5.2 Materials and methods

5.2.1 Chemicals and reagents

Fructose, sodium palmitate, radioimmunoprecipitation assay (RIPA) buffer and protease inhibitor cocktail, hydrochloric acid, potassium ferrocyanide, ferrous sulphate (FeSO₄.7H₂O), Dichloro-dihydro-fluorescein diacetate (DCFH-DA), 4'6 - diamidini-2-phenylindole (DAPI),

and vitamin K₁ were purchased from Sigma - Aldrich Co. (St. Louis, MO, USA). The cell culture flasks and plates were from BD Biosciences (USA). Fetal bovine serum (FBS), penicillin and streptomycin antibiotics, trypsin - ethylenediaminetetraacetic acid (EDTA), phosphate buffered saline (PBS) and Hank's balanced salt solution (HBSS), bovine serum albumin (BSA), minimum essential medium (MEM) were from Gibco, USA. Antibodies against heme oxygenase (HO-1), NF- κ B, Bax, Bad, Cyt c, TNF- α , IL-1 β , IL-6, MCP-1, IL-10, FAS, SCD-1, JNK, p-JNK, ERK1/2, p-ERK1/2, phospho p38 and GAPDH were from Santa Cruz Biotechnology. Antibodies against Nrf2, ferritin, transferrin were from Abcam All other chemicals used were of analytical grade.

5.2.2 Cell culture and treatment

HepG2 cells (American Type Culture Collection, (ATCC) Rockville, MD USA) were cultured as per supplier's instructions. In brief, the cells were grown in T-25 flask containing MEM supplemented with 10% heat-inactivated FBS and 1X penicillin streptomycin solution at 37°C and 5% CO₂ in a humidified incubator (Eppendorf, USA). When the cells reached 80% confluence, the cells were trypsinized and reseeded onto a new flask for further experiments.

5.2.3 Induction of steatosis and treatment

Fructose stock solution was prepared by dissolving in HBSS and was used to produce different concentrations of fructose treatment in serum free MEM. Palmitate stock solution (10 mM) was prepared by dissolving sodium palmitate in 0.1 N NaOH at 75°C for 5 min. The stock solution was further mixed with fatty acid free BSA to make a final concentration of 1 mM. The 1 mM working solution was then diluted to the desired treatment concentration (100 μ M) in 1% MEM. To evaluate the role of iron during steatosis, the cells were co-supplemented with iron in the form of FeSO₄.7H₂O. Treatment was applied on day 3 and the experiments were performed after 24 hrs of treatment.

The experimental group consists of (i) C - control cells; (ii) HFP - cells treated with high fructose (100 mM) and palmitate (100 μ M); (iii) HFP + Fe 5 - cells treated with high fructose, palmitate and iron (5 μ M); (iv) HFP + Fe 250 - cells treated with high fructose, palmitate and iron (250 μ M).

5.2.4 Cell viability assay

Cell viability was determined by MTT assay, which relies on the enzymatic reduction of 3-[4,5-dimethylthiazole-2-yl]-2,5-diphenyltetrazolium bromide to MTT formazan catalyzed by

the enzyme mitochondrial succinate dehydrogenase. Briefly, the cells were seeded in a 96-well plate at a seeding density of 5×10^3 per well. The cells were then incubated for about 24 hrs. After incubation, 100 μ L of MTT solution (5 mg/mL) was added to each well and incubated for another 4 hrs at 37°C in the dark. The solution was removed from each well and 100 μ L of DMSO was added to dissolve the formazan crystals. The culture plate was placed on a shaker for about 20 min. The blue colored tetrazolium crystals were dissolved in DMSO. Absorbance was measured at 570 nm in a spectrophotometer (Biotek Synergy 4, USA).

5.2.5 Prussian blue staining

This method was used to detect the cellular iron deposition in various experimental groups. In this method, if any ferric ion (+3) is present, it combines with ferrocyanide and results in the formation of a bright blue pigment called Prussian blue. Briefly, the cells were seeded in a 96-well plate and after respective treatments, cells were fixed in formalin. Then equal parts of 20% aqueous solution of hydrochloric acid and 10% of aqueous solution of potassium ferrocyanide were prepared immediately before use and added around 100 μ L to each well. It was rinsed with PBS thrice and cellular ferric ions can be seen as bright blue pigments (Nikon Eclipse TS 100, Japan)

5.2.6 Oil-red-O staining

Oil-red-O stain was used to detect the intracellular lipid accumulation. Briefly 2×10^5 cells were seeded on a 12-well plate and treated as mentioned earlier. At the end of the treatment period, the media was aspirated from the culture plates and the cells were rinsed with PBS and fixed in 4% paraformaldehyde. Fixation is followed by permeabilization using 0.1% Triton X-100. Stock oil-red-O solution was prepared in isopropyl alcohol and diluted 3:2 in ddH₂O. Diluted oil-red-O solution was added to the fixed cells for 15 min, after which it was aspirated away, washed with ddH₂O. The oil droplets in HepG2 cells were visualized and captured at 40X on a phase contrast microscope (Nikon Eclipse TS 100, Japan) using NIS Elements software. For the quantification of lipid droplets, isopropyl alcohol was added to each well and lipid accumulation was measured using a spectrophotometer at 490 nm absorbance (Biotek Synergy 4, USA).

5.2.7 Lipid peroxidation

Thiobarbituric acid assay (TBA) was performed to determine the levels of lipid peroxides and aldehydes in the control and treated group. Briefly, treated HepG2 cells were resuspended in

1 mL PBS and lysed in SDS solution. To the cell lysate, 50 μ L of 2,6-di-tert-butyl-4-methylphenol butylated hydroxytoluene (BHT) was added to assure that no lipid peroxidation occurred during the assay. To this 1.5 mL of 0.5 M HCl, 1.5 mL of 20 mM TBA and 250 μ L distilled water were added. The reaction mixture was then mixed well and heated for 30 min in a boiling water bath, then placed on an ice bath for 10 min to stop the reaction. After incubation it was then centrifuged for 10 min at 1600 x g at 4°C and incubated at room temperature for 30 min. From this 150 μ L of samples were transferred to the plate and the absorbance of the colored product was measured at 530 nm.

5.2.8 Preparation of cell lysate for antioxidant enzyme activities

The treated cells were homogenized with a 20 mM Tris/ HCl buffer (pH 7.5) containing 0.2% Triton X-100 and 0.5mM PMSF, sonicated for about 30 sec on ice. Total cell lysates were centrifuged at 3000 rpm at 4°C for 15 minutes and aliquots of the supernatant were utilized for subsequent enzymatic activities.

5.2.8.1 Activity of superoxide dismutase

The activity of superoxide dismutase was assessed by dissolving the harvested cells in 1.2 mL of sodium pyrophosphate buffer, 0.1 mL of phenazine methosulphate (PMS), 0.3 mL of nitroblue tetrazolium (NBT), 0.2 mL of cell extract and water in a total volume of 2.8 mL. The reaction was initiated by the addition of 0.2 mL of NADH. The mixture was then incubated at 30°C for 90 sec. It is followed by the addition of 1.0 mL of glacial acetic acid. The mixture was shaken well with 4.0 mL of n - butanol and allowed to stand for 10 min and centrifuged. The intensity of chromogen in the butanol layer was read at 560 nm.

5.2.8.2 Determination of catalase activity

The activity of catalase was assessed by monitoring the dissipation of H₂O₂. Briefly, 100 μ L of cell lysate was mixed with 1.9 mL of 50 mM phosphate buffer (pH 7.0). The reaction was initiated after the addition of 1 mL of freshly prepared 30 mM H₂O₂ and absorbance was read at 240 nm. The enzyme activity was expressed as the amount of enzyme that favoured the conversion of 1 μ M H₂O₂ per minute per mg protein.

5.2.8.3 Activity of glutathione

The estimation of glutathione has been done by using Cayman's glutathione assay kit. Briefly, the cell pellets were collected and sonicated in 1 - 2 mL cold buffer and centrifuged at 10,000 x g for 15 min at 4°C. The supernatant is then collected and mixed with 150 μ L of assay

cocktail and incubated for about 25 min in the dark. The samples were then read at 405 - 414 nm by end point method.

5.2.9 Acridine orange / ethidium bromide staining (AO / EtBr)

For the detection of apoptotic and necrotic cells, 3×10^4 cells were seeded in a 96 - well black plate. After respective treatment, the cells in all experimental groups were stained with AO (excitation: 502 nm; emission: 525 nm) and EtBr (excitation: 510 nm; emission: 595 nm). The working stain (10 mg/mL of AO and 1 mg/mL EtBr in PBS) was added to the cells and examined under the fluorescent microscope.

5.2.10 Detection of ROS

HepG2 cells were seeded in a 96 - well clear black plate at a density of 5×10^3 cells per well. Intracellular ROS production in treated cells was assessed by staining the cells with cell permeable fluorescent probe DCFH-DA. After washing with PBS, fluorescence intensity was measured using a spectrophotometer at an excitation emission wavelength of 488 nm and 525 nm respectively. Observations were made under the spinning disk imaging system (BD Pathway™ Bioimager system, USA).

5.2.11 Detection of secretory cytokines by ELISA

The cell lysates (10 μ g / mL) were pre - coated onto the 96 well ELISA plate and incubated overnight at 4°C. The sample was aspirated and washed with 0.05% PBST. It was followed by primary antibody (1:500 dilutions) incubation against at 4°C for 2 hrs. Followed by washing with PBS - tween 20, it was incubated with HRP - conjugated secondary antibody for about 2 hrs. After three PBST washes, TMB substrate was added to each well and the signal was stopped by the addition of a stop solution (0.1N HCl). The absorbance was measured at 450 nm using the plate reader (Tecan Infinite M200PRO, Tecan, Austria).

5.2.12 Immunofluorescence Analysis

HepG2 cells were cultured in a 96 well culture plate and treated as described earlier. The cells were washed thrice in ice cold PBS and fixed in paraformaldehyde for 10 min at room temperature. After washing, the cells were permeabilized with Triton - X - 100 for 15 min at room temperature. It was followed by blocking with PBS containing goat serum. The cells were then incubated with primary antibody against transferrin, NF- κ B, phospho p38 at 4°C and after washing it was again incubated with FITC conjugated secondary antibody for 1 hr. This was

followed by washing and staining with DAPI for 5 min. The cells were visualized Olympus fluorescence microscope.

5.2.13 Western blot

After respective treatments cells were harvested and proteins were extracted from HepG2 cells by using an ice cold RIPA buffer containing protease inhibitor cocktail. It was then incubated on ice for about 20 min and cell suspensions were centrifuged at 12,000 rpm for 20 min at 4°C. The supernatant was collected and used for further immunoblot analysis. The protein concentration of the cell lysate was measured by using bicinchoninic acid kit (Pierce, Rockford, IL, USA) as per manufacturer's instruction. Proteins thus extracted were separated by SDS-PAGE and were transferred to the PVDF membrane using the Trans-Blot® Turbo™ Transfer system (Bio-Rad, USA). The membrane was then blocked with 5% skimmed milk in TBST for 1 hr at room temperature then probed with specific primary antibodies against ferritin, HO-1, Bad, Bax, Cyt c, FAS, SCD-1, Nrf2, JNK, p-JNK, ERK1/2, p-ERK1/2 and GAPDH (1:1000 dilutions) at 4°C overnight. After washing with TBST, specific horseradish peroxidase conjugated secondary antibodies (1:2000 dilutions) were added and the membranes were incubated for about 2 hrs. After washing, the immune complex was visualized using Clarity™ Western ECL Substrate (Bio-Rad,USA).The images were analyzed in the ChemiDoc XRS system (Bio-Rad,USA) using Image Lab software.

5.2.14 Statistical Analysis

Statistical analysis was carried out by the SPSS statistical program. The data were represented as mean ± SD. The data were subjected to one - way analysis of variance (ANOVA) and the differences among the means of the groups were assessed using Duncan's multiple range tests using OriginPro version 8.5 (OriginLab Corporation, Massachusetts, USA). The statistical significance was accepted at $p \leq 0.05$.

5.3 Results

5.3.1 Effect of iron on cell viability

The cell viability assay revealed more than 80% of the iron (5 µM, 25 µM, 50 µM, 75 µM, 100 µM, 200 µM, 250 µM) treated cells shows viability (Figure 5.1A).

5.3.2 Effect of iron on HFP induced cell death

HepG2 cells were treated with HFP and incubated with different concentrations of iron for 24 hrs and checked the cell viability. The results showed that incubation of HepG2 cells with

HFP caused 15% cell death. Treatment with iron of 5 μM , 25 μM , 50 μM and 75 μM significantly ($p \leq 0.05$) improves the cell viability compared to HFP group (5.3%, 10.1% and 12.6% respectively) (Figure 5.1B). However when the cells were treated with 200 μM and 250 μM iron along with HFP, the cell viability was significantly ($p \leq 0.05$) reduced to 24.81% and 31.15 % respectively (Figure 5.1B).

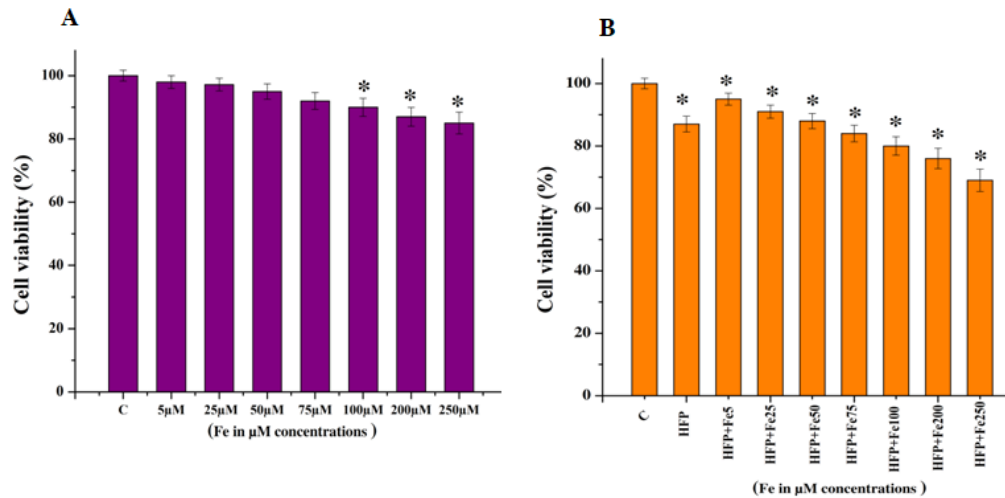


Figure 5.1 Role of iron on cell viability: (A) HepG2 cells were treated with different concentrations of iron (5 μM , 25 μM , 50 μM , 75 μM , 100 μM , 200 μM , 250 μM) and viability was assessed by MTT assay. B) Cytotoxicity in HepG2 cells following treatment with HFP and amelioration with iron. (i) C - control cells; (ii) HFP - cells treated with high fructose and palmitate; (iii) HFP + Fe 5 - cells treated with high fructose, palmitate and 5 μM iron; (iv) HFP + Fe 25 - cells treated with high fructose, palmitate and 25 μM iron; (v) HFP + Fe 50 - cells treated with high fructose, palmitate and 50 μM iron; (vi) HFP + Fe 75 - cells treated with high fructose, palmitate and 75 μM iron; (vii) HFP + Fe 100 - cells treated with high fructose, palmitate and 100 μM iron; (viii) HFP + Fe 200 - cells treated with high fructose, palmitate and 200 μM iron; (ix) HFP + Fe 250 - cells treated with high fructose, palmitate and 250 μM iron. Data are expressed as mean \pm SD; where $n = 6$. * indicates significantly different from the control group ($p \leq 0.05$).

5.3.3 Iron uptake in HepG2 cells

In order to detect the presence of iron in cell samples, Prussian blue staining has been done. It usually detects iron in Fe^{3+} or ferric state. From the Figure 5.2 it is clearly visible that, as the concentration of iron increases, cellular deposition of Fe^{3+} is also found to be increased. The Fe^{3+} concentration in the control and HFP treated group is 12.45% and 16.11% respectively. The

treatment with 5 μM , 25 μM , 50 μM , 75 μM and 100 μM concentrations of iron in HFP induced steatosis cells shows an elevation of Fe^{3+} to 28.83%, 44.92%, 65.87%, 72.15%, and 122.42% respectively ($p \leq 0.05$, Figure 5.2). Maximum ferric ion is detected in cells treated with 200 μM and 250 μM iron (227.22% and 319.76% respectively at $p \leq 0.05$) (Figure 5.2).

A

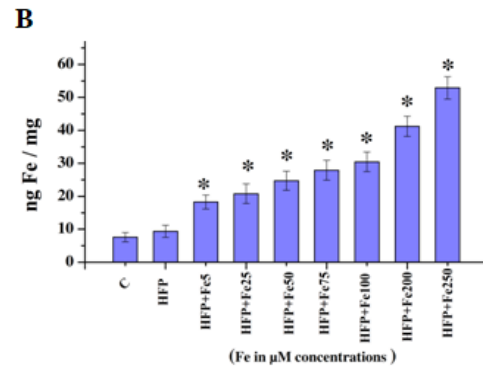
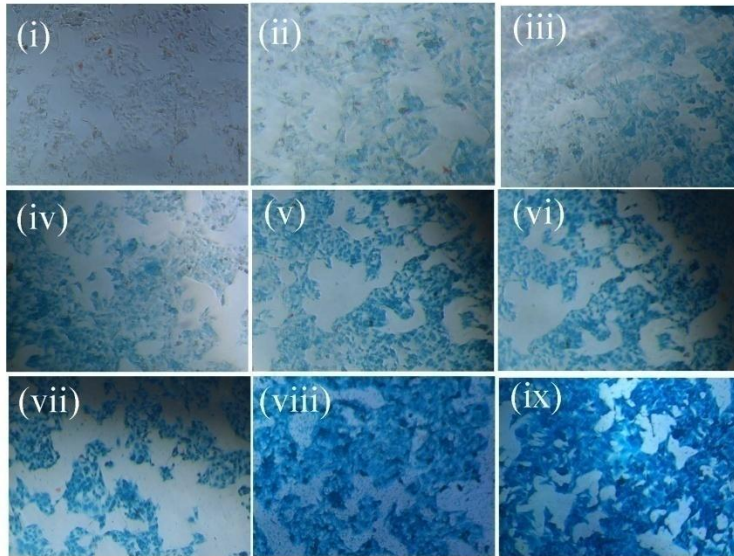


Figure 5.2 Prussian blue staining of treated HepG2 cells: (A) The iron uptake in HepG2 cells were determined by Prussian blue staining. (i) C - control cells; (ii) HFP - cells treated with high fructose and palmitate; (iii) HFP + Fe 5 - cells treated with high fructose, palmitate and 5 μM iron; (iv) HFP + Fe 25 - cells treated with high fructose, palmitate and 25 μM iron; (v) HFP + Fe 50 - cells treated with high fructose, palmitate and 50 μM iron; (vi) HFP + Fe 75 - cells treated with high fructose, palmitate and 75 μM iron; (vii) HFP + Fe 100 - cells treated with high fructose, palmitate and 100 μM iron; (viii) HFP + Fe 200 - cells treated with high fructose, palmitate and 200 μM iron; (ix) HFP + Fe 250 - cells treated with high fructose, palmitate and 250 μM iron. Original magnification 40X. Scale bar corresponds to 50 μM . (B) Quantification of iron in various groups. Data are expressed as mean \pm SD; where $n = 6$. * indicates significantly different from the control group ($p \leq 0.05$).

5.3.4 Effect of iron on HFP induced lipid accumulation

To analyze the role of iron on hepatic lipid accumulation, steatosis was induced by HFP in HepG2 cells. The lipid accumulation was significantly ($p \leq 0.05$) higher in the HFP treated group compared to the control (380%) (Figure 5.3). Treatment with iron significantly ($p \leq 0.05$) reduces the lipid accumulation by 340%, 260% and 182% respectively at 5 μM , 25 μM and 50

μM of iron (Figure 5.3). Similarly treatment with 75 μM and 100 μM concentrations of iron also significantly ($p \leq 0.05$) reduces the lipid accumulation compared to HFP (146% and 75% respectively) (Figure 5.3). On the other hand, treatment with 200 μM and 250 μM iron aggravates the lipid accumulation significantly ($p \leq 0.05$) compared to the HFP treated group (71.25% and 280% respectively) (Figure 5.3).

For detailed investigation, the iron concentration of 5 μM which resulted in lowered lipid accumulation (indicated as HFP + Fe 5 μM) and 250 μM concentration resulted in highest lipid accumulation (indicated as HFP + Fe 250 μM) was chosen based on the results.

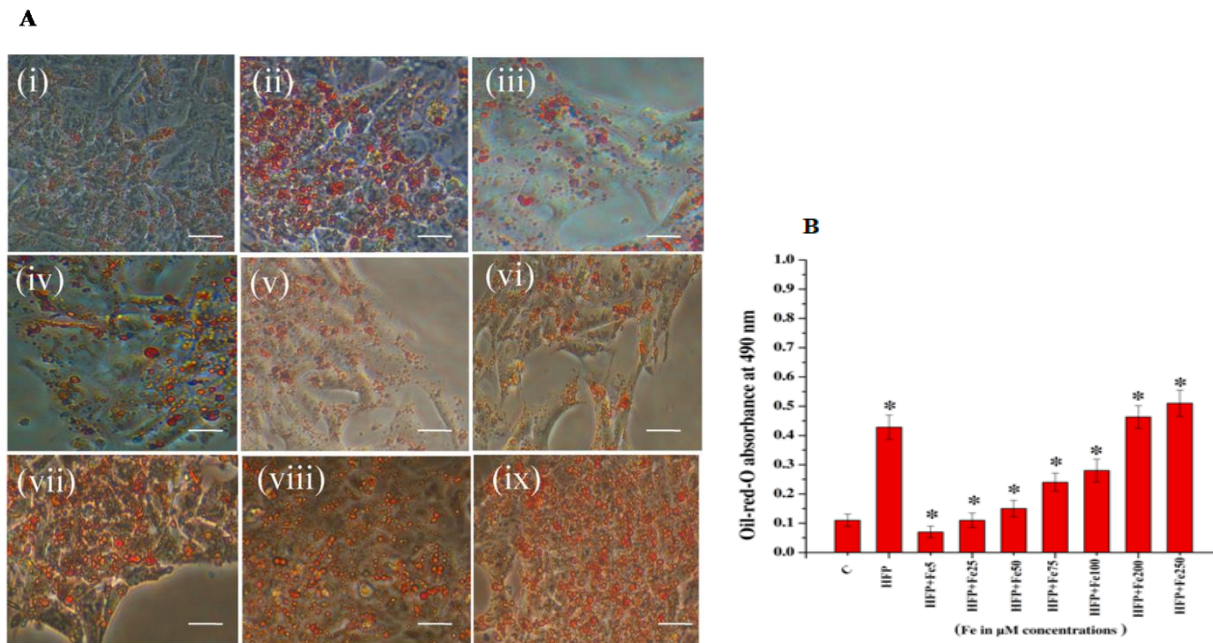
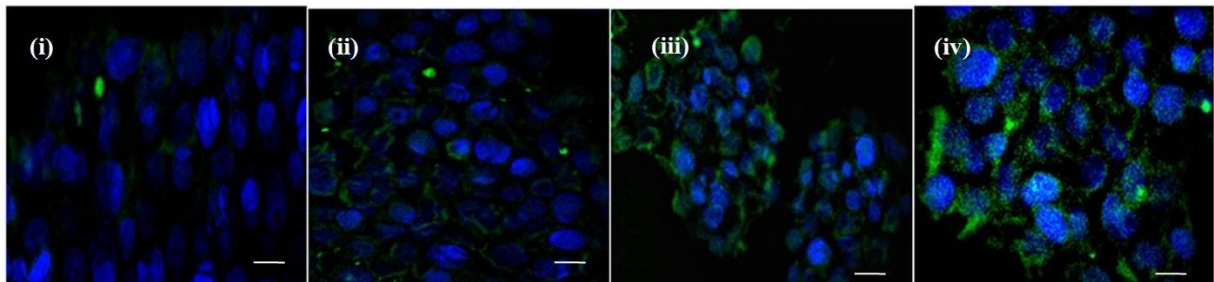


Figure 5.3 Effect of iron on lipid accumulation during HFP induced steatosis: The cultured HepG2 cells were treated with various concentrations of iron along with HFP for 24 hrs. (A) Microscopic images of HepG2 cells with Oil-red-O-staining from different experimental groups. (i) C - control cells; (ii) HFP - cells treated with high fructose and palmitate; (iii) HFP + Fe 5 - cells treated with high fructose, palmitate and 5 μM iron; (iv) HFP + Fe 25 - cells treated with high fructose, palmitate and 25 μM iron; (v) HFP + Fe 50 - cells treated with high fructose, palmitate and 50 μM iron; (vi) HFP + Fe 75 - cells treated with high fructose, palmitate and 75 μM iron; (vii) HFP + Fe 100 - cells treated with high fructose, palmitate and 100 μM iron; (viii) HFP + Fe 200 - cells treated with high fructose, palmitate and 200 μM iron; (ix) HFP + Fe 250 - cells treated with high fructose, palmitate and 250 μM iron. Original magnification 40X. Scale bar corresponds to 50 μM . (B) Absorbance was read at 490 nm after oil-red-O staining. Data are expressed as mean \pm SD; where $n = 6$. * indicates significantly different from the control group ($p \leq 0.05$).

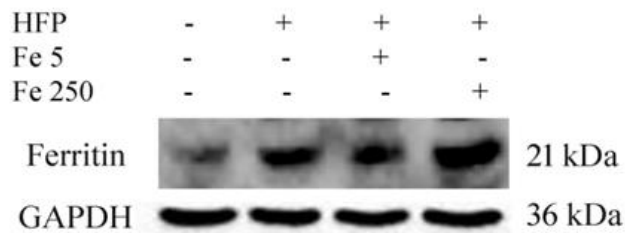
5.3.5 Expression of transferrin receptor and ferritin during steatosis

To confirm the presence of iron receptors in treated cells, expression studies of transferrin and ferritin were conducted. Immunofluorescence staining of HepG2 cells treated with HFP showed a slight increase in the expression of transferrin receptors compared to the control group (Figure 5.4A). Treatment with HFP + Fe 5 μ M and HFP + Fe 250 μ M showed evident expression of transferrin receptor compared to the HFP treated cells (Figure 5.4A). Moreover, protein expression study indicated that HFP treated cells shows a significant ($p \leq 0.05$) increase in the expression of ferritin (105.89%) compared to the control group (Figure 5.4B). Treatment with HFP + Fe 5 μ M resulted in downregulation of ferritin level to 54.45% and HFP + Fe 250 μ M resulted in an upregulation of ferritin to 160.24% significantly ($p \leq 0.05$) compared to HFP treated cells (Figure 5.4B).

A



B



C

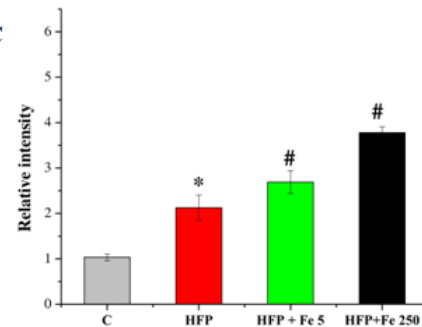


Figure 5.4 Detection of iron proteins during HFP induced steatosis: (A) Immunofluorescence detection of transferrin receptors after treating the cells with HFP and iron. (i) C - control cells; (ii) HFP - cells treated with high fructose and palmitate; (iii) HFP + Fe 5 - cells treated with high fructose, palmitate and 5 μ M iron; (iv) HFP + Fe 250 - cells treated with high fructose, palmitate and 250 μ M iron. TFR (Green fluorescence) and nucleus (blue fluorescence). Original magnification 40X. Scale bar corresponds to 20 μ M. (B) The protein expression of ferritin during steatosis. (C) The relative intensity of each band was quantified with GAPDH. Data are expressed as mean \pm SD; where $n = 3$. * indicates significantly

different from the control group ($p \leq 0.05$). # indicates significantly different from the HFP treated group ($p \leq 0.05$).

5.3.6 Effect of iron on HFP induced oxidative stress

Next we examined the role of iron on oxidative stress during steatosis. The treatment of HepG2 cells with HFP led to a significant ($p \leq 0.05$) increase in lipid peroxidation (228.76%) compared to the control (Figure 5.5A). The lipid peroxidation were found to be reduced significantly ($p \leq 0.05$) to 156.78% after treatment with HFP + Fe 5, thereby favoring the reestablishment of the physiological oxidation state (Figure 5.5A). By contrast, HFP + Fe 250 treatment increases lipid peroxidation significantly ($p \leq 0.05$) to 136.66% compared to HFP, indicating that higher concentration of iron induces oxidative stress *via* Fenton reaction (Figure 5.5A).

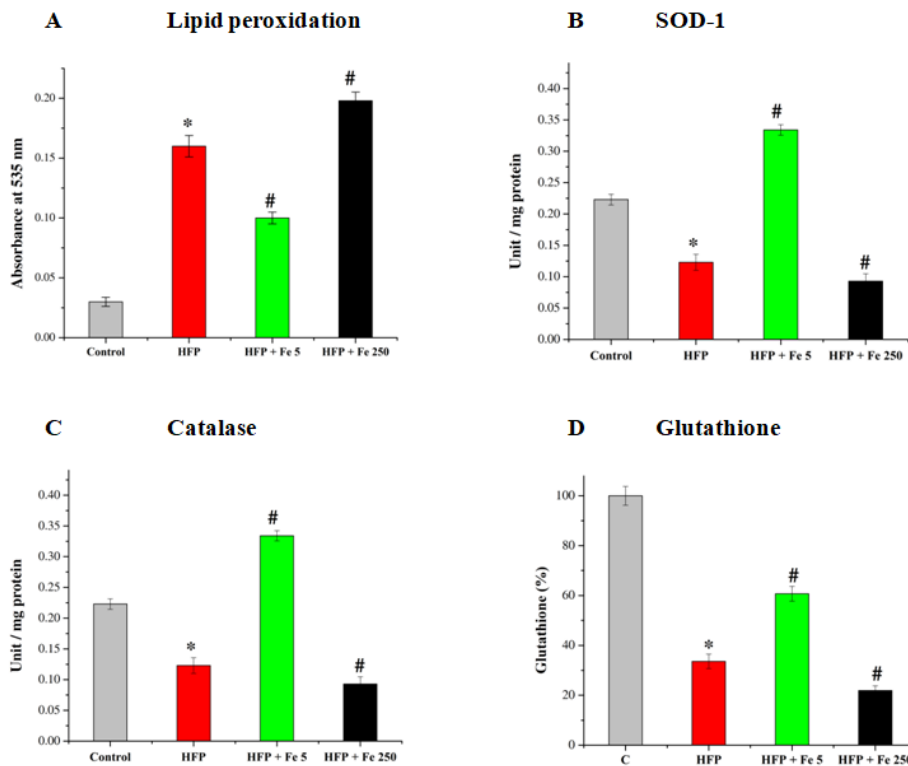


Figure 5.5 Effect of iron on oxidative stress during HFP induced steatosis: (A) Detection of cellular lipid peroxidation in HepG2 cells treated with HFP and iron (B) Detection of SOD-1 (C) Detection of catalase (D). Detection of glutathione. C - control cells; HFP - cells treated with high fructose and palmitate; HFP + Fe 5 - cells treated with high fructose, palmitate and 5 μ M iron; HFP + Fe 250 - cells treated with high fructose, palmitate and 250 μ M iron. Data are expressed as mean \pm SD; where n = 6. *

indicates significantly different from the control group. # indicates significantly different from the HFP treated group ($p \leq 0.05$).

To investigate the extent of oxidative stress, we also measured SOD-1, catalase and glutathione. The results showed that the level of SOD-1, catalase and glutathione in HFP treated HepG2 cells decreased significantly ($p \leq 0.05$) by 44.84%, 45.45% and 66.4% respectively compared to the control group (Figure 5.5B, C, D). Treatment with HFP + Fe 5 increases the level of SOD-1 by 94.61%, catalase by 66.79% and glutathione by 27.12% significantly ($p \leq 0.05$) compared to HFP. On the other hand, HFP + Fe 250 treatment results in significant ($p \leq 0.05$) reduction of SOD-1 by 13.45%, catalase by 27.55% and glutathione by 11.7% (Figure 5.5B, C, D). The above data indicates that during steatosis low concentration of iron ameliorates oxidative stress and excess of iron exacerbates oxidative stress.

5.3.7 Effect of iron on HO-1 during steatosis

HO-1 is an important antioxidant enzyme that provides protection against oxidative stress. We found that HFP treatment causes a slight reduction on the expression of HO-1 (5%) (Figure 5.6). However HFP + Fe 5 treatment results in a significant ($p \leq 0.05$) upregulation of 26% and HFP + Fe 250 treatment leads to a significant ($p \leq 0.05$) downregulation of 15.89% (Figure 5.6).

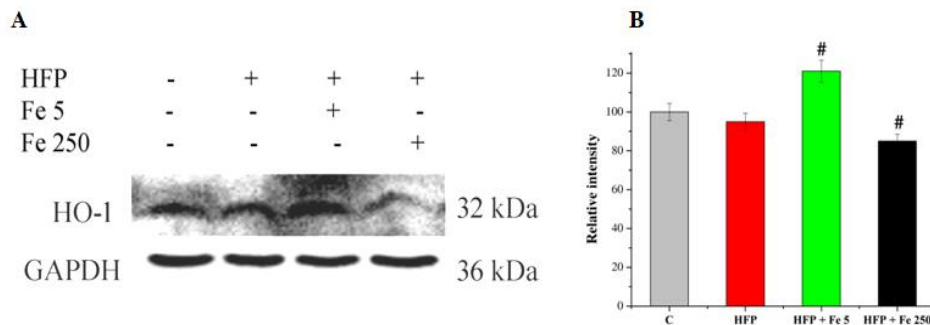


Figure 5.6 Effect of iron on the expression of HO-1 during steatosis: (A) The protein expression of HO-1 during steatosis. (i) C - control cells; (ii) HFP - cells treated with high fructose and palmitate; (iii) HFP + Fe 5 - cells treated with high fructose, palmitate and 5 μ M iron; (iv) HFP + Fe 250 - cells treated with high fructose, palmitate and 250 μ M iron. (B) The relative intensity of each band was quantified with GAPDH. Data are expressed as mean \pm SD; where $n = 3$. # indicates significantly different from the HFP treated group ($p \leq 0.05$).

5.3.8 Effect of iron on HFP mediated inflammation through NF- κ B translocation

Since inflammation plays a central role in the development of simple steatosis to NASH, we analyzed the inflammatory signaling through NF- κ B and quantified the levels of proinflammatory cytokines to assess the effects of iron during steatosis. As in Figure 5.7, it is clear that in the control group NF- κ B was mainly located in the cytoplasm as in normal physiological condition. The translocation to the nucleus is clearly visible when the HepG2 cells were treated with HFP (Figure 5.7). However, treatment with HFP + Fe 5 inhibited the nuclear translocation and HFP + Fe 250 activated the nuclear translocation of NF- κ B (Figure 5.7). This result suggests that iron can ameliorate and exacerbate HFP induced liver inflammation at different concentrations.

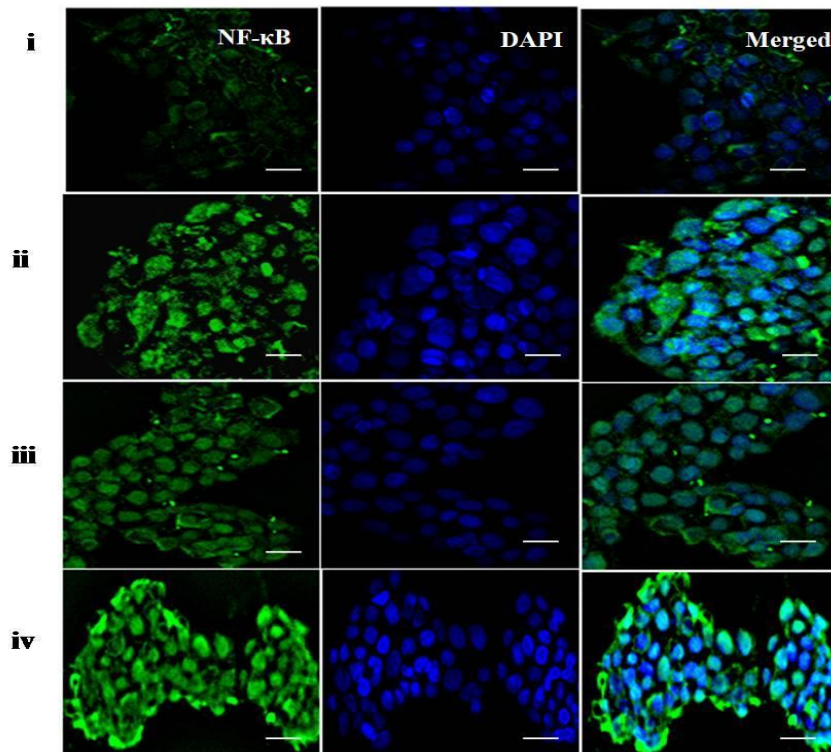


Figure 5.7 Effect of iron on NF- κ B translocation during HFP induced steatosis: Immunofluorescence staining showing NF- κ B distribution in HFP induced steatosis in HepG2 cells. The cells were stained by DAPI (blue) and anti- NF- κ B antibody (green). (i) C - control cells; (ii) HFP - cells treated with high fructose and palmitate; (iii) HFP + Fe 5 - cells treated with high fructose, palmitate and 5 μ M iron; (iv) HFP + Fe 250 - cells treated with high fructose, palmitate and 250 μ M iron. Original magnification 40X. Scale bar corresponds to 20 μ M.

5.3.9 Effect of iron on HFP induced cytokine secretion

It is well known that NAFLD induces inflammation and promotes the release of certain cytokines. In the present study, during HFP treatment the levels of proinflammatory cytokines such as TNF- α , IL-1 β , IL-6 and MCP-1 were increased (Figure 5.8 A, B, C, D) whereas a decreased level of IL-10 was observed (Figure 5.8 E). Treatment with HFP + Fe 5 significantly ($p \leq 0.05$) suppressed the secretion of TNF- α (44%), IL-1 β (53%), IL-6 (17%) and MCP-1 (71%) in HepG2 cells along with significant increase in the level of IL-10 (35%) (Figure 5.8A, B, C, D, E). However, HFP + Fe 250 treatment significantly ($p \leq 0.05$) increased the level of TNF- α by 27% (Figure 5.8A) and no significant alteration was observed in the level of IL-1 β , IL-6 and MCP-1. But the level of IL-10 decreased significantly ($p \leq 0.05$) to about 29% (Figure 5.8 B, C, D, E).

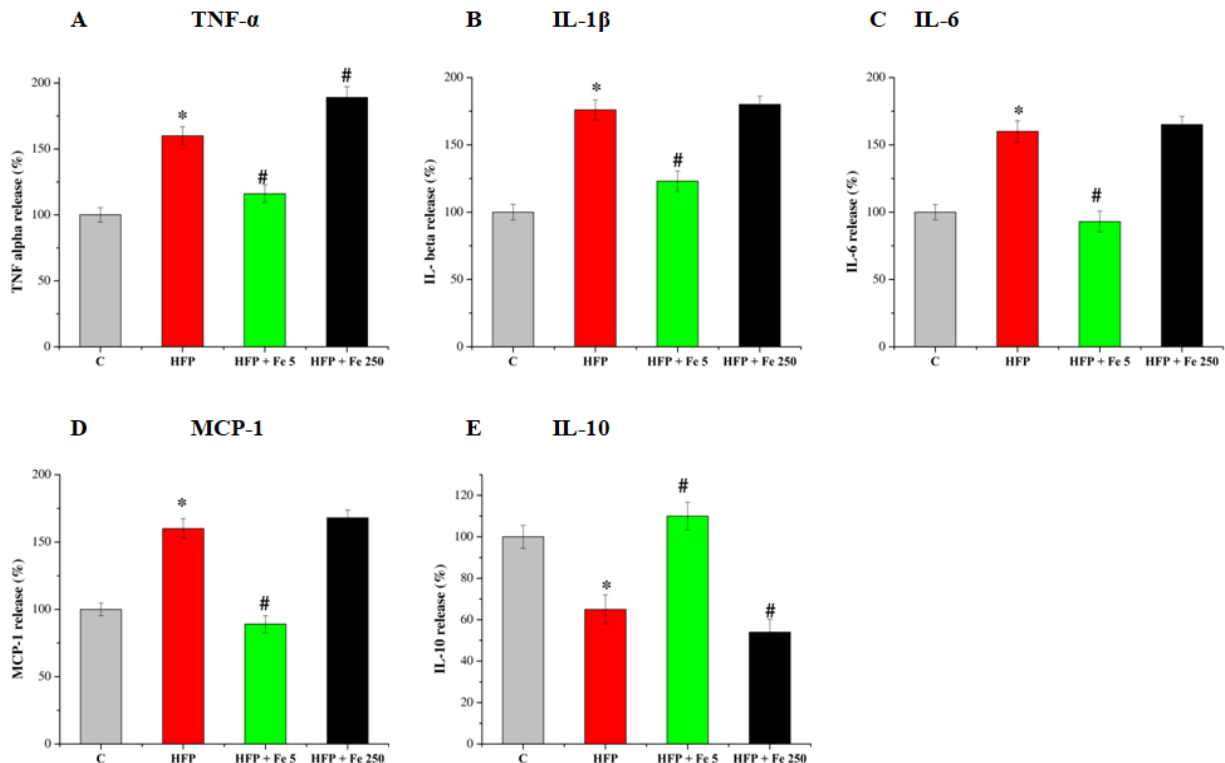


Figure 5.8 Effect of iron on proinflammatory cytokines during HFP induced steatosis: (A) Secretion of TNF- α ; (B) Secretion of IL-1 β ; (C) Secretion of IL-6; (D) Secretion of MCP-1; (E) Secretion of IL-10. C - control cells; HFP - cells treated with high fructose and palmitate; HFP + Fe 5 - cells treated with high fructose, palmitate and 5 μ M iron; HFP + Fe 250 - cells treated with high fructose, palmitate and 250 μ M iron. Data are expressed as mean \pm SD; where n = 6. * indicates significantly different from the control group. # indicates significantly different from the HFP treated group ($p \leq 0.05$).

5.3.10 Effect of iron on HFP induced apoptotic and necrotic effects

The HepG2 cells treated with HFP and iron were also subjected to AO / EtBr fluorescence staining. AO usually enters the nucleus and stains live cells as green color. Due to the loss of membrane integrity EtBr penetrates the nucleus of dead cells and stains as red color. In this experiment, the cells that appeared as green fluorescence are viable (as in the control group) and early apoptotic cells appeared as green orange / yellow color (as in HFP treated and HFP + Fe 5 treated group). The late apoptotic cells and necrotic cells appeared as orange to red color (as in HFP + Fe 250) (Figure 5.9).

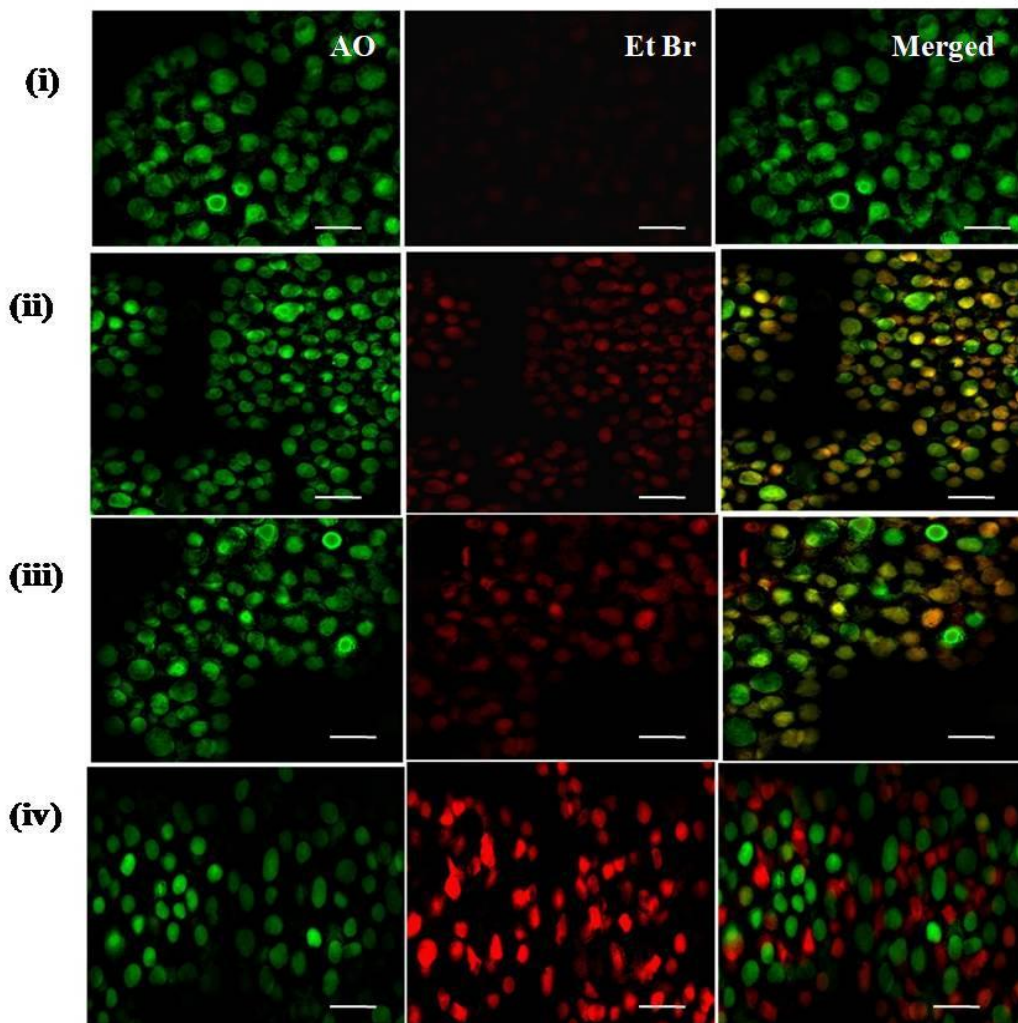


Figure 5.9 Effect of iron on apoptotic and necrotic cells during HFP induced steatosis: (A) Representative photomicrographs of HepG2 cells stained with acridine orange (AO, green) and ethidium bromide (EtBr, red) fluorescent dyes, viable cells (green), early apoptotic (yellow), late apoptotic (orange) and necrotic cells (red). (i) C - control cells; (ii) HFP - cells treated with high fructose and palmitate; (iii)

HFP + Fe 5 - cells treated with high fructose, palmitate and 5 μ M iron; (iv) HFP + Fe 250 - cells treated with high fructose, palmitate and 250 μ M iron. Original magnification 40X. Scale bar corresponds to 20 μ M.

5.3.11 Effect of iron on intrinsic pathway of apoptosis

To investigate the role of iron in the intrinsic pathway of apoptosis during high calorie induced steatosis, the protein expression studies were conducted. The expression of Bad, Bax and Cyt c during HFP condition were reduced significantly ($p \leq 0.05$) by 89%, 64% and 32% respectively compared to the control (Figure 5.10A). Treatment with HFP + Fe 5 resulted in significant ($p \leq 0.05$) down regulation of Bad to 103%, Bax to 30%, and Cyt c to 55% compared to HFP (Figure 5.10). However, treatment with HFP + Fe 250 significantly ($p \leq 0.05$) upregulated the expression of Bad and Cyt c to 33% and 55% respectively (Figure 5.10A). There is no significant alteration can be observed in the expression of Bax compared to HFP (Figure 5.10A).

The activity of caspase-3 was also increased significantly ($p \leq 0.05$) in HFP and HFP + Fe 250 treated groups compared to the control (73.23% and 79.82% respectively) while HFP + Fe 5 treatment prevented the rise by 42.38% (Figure 5.10 C).

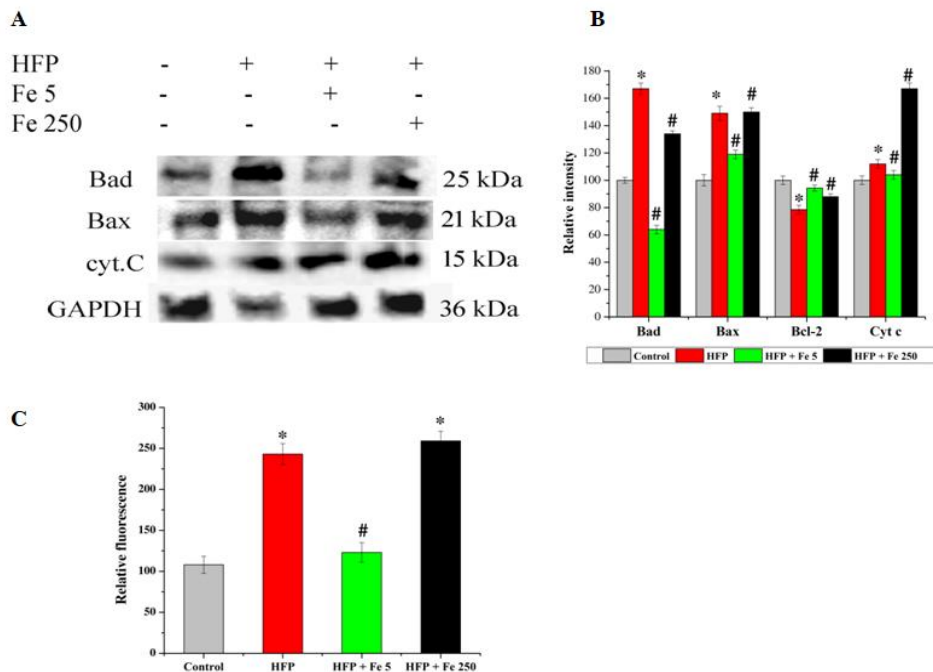


Figure 5.10 Effect of iron on apoptosis during HFP induced steatosis: (A) The protein expression of Bad, Bax, Bcl-2 and Cyt c during steatosis. C - control cells; HFP - cells treated with high fructose and palmitate; HFP + Fe 5 - cells treated with high fructose, palmitate and 5 μ M iron; HFP + Fe 250 - cells

treated with high fructose, palmitate and 250 μ M iron. (B) The relative intensity of each band was quantified with GAPDH. (C) Activity of caspase 3. Data are expressed as mean \pm SD; where n = 3. * indicates significantly different from the control group ($p \leq 0.05$). # indicates significantly different from the HFP treated group ($p \leq 0.05$).

5.4 Discussion

Iron is an essential element for a large number of physiological processes. Hepatic iron overload plays a crucial role in the progression of steatosis to NASH. The present study mainly focused on the role of iron at lower and higher concentrations during steatosis and cellular responses involved in hepatocytes.

Lipids are the major sources of cellular energy. However excess lipids have detrimental effects on cellular functions. Iron plays a central role in promoting both fatty acid import and lipid droplet formation. Certain studies reported that iron deficiency can either increase or decrease hepatic lipogenesis in normal liver (Ahmed et al., 2012). Iron in its ferrous form may indirectly affect lipid metabolism through its ability to induce oxidative stress and inflammation. However, lesser investigations are available about the role of iron in steatosis. In the present study we found that during steatosis the presence of lower concentration of iron reduces the lipid accumulation and provides a protective effect against steatosis. However higher concentration of iron indirectly affects lipid metabolism due to its ability to generate free radicals. This in turn results in the progression of liver disease from steatosis to NASH. There are certain reports that reveal the effect of iron in decreasing hepatic lipid synthesis by decreasing the activity of either FAS or enzymes involved in redox potential for lipogenesis (Stangl & Kirchgessner, 1998).

The major iron receptors like transferrin and ferritin expression were increased in a concentration dependent manner. The iron carrier transferrin receptor is central for iron trafficking and it delivers iron to the cells (Hentze et., 2010). In hepatocytes transferrin is essential for iron loading but dispensable for basal iron uptake (Fillebeen et al., 2019). The expression of transferrin receptor might be increased in regenerating hepatocytes after liver injury (Lee et al., 2003). Intracellular iron is utilized for performing diverse biological functions and if not used it is stored within ferritin. It is a multi-subunit iron storage protein and hepatocytes serve as the major site of synthesis. Oxidative stress, hypoxia and cytokines play a key role in ferritin expression (Anderson & Shah, 2013). Ferritin is critical for iron homeostasis which makes iron available for cellular processes. At the same time it also protects the cellular

components from iron toxicity by sequestering potentially toxic labile iron (Eid et al., 2017). Thus ferritin can be considered as an endogenous antioxidant and major marker protein of iron. Ferritin level becomes low when there is iron deficiency and becomes high during iron overload or inflammation. It has been reported that serum ferritin level may be elevated with level of hepatic iron in patients with NAFLD (Ryan et al., 2018). This may point to the pathological role of iron metabolism in NAFLD patients.

It is widely accepted that iron overload may play a fundamental role in the progression of NAFLD *via* stimulating the “second hit”. Since iron participates in Fenton reaction for the generation of ROS, which in turn damages lipids *via* peroxidation, a phenomenon observed in NASH. The oxidative process that results in lipid peroxidation modifies the fatty acid composition of cellular membranes thereby leading to organelle damage. This in turn is associated with depletion of cellular antioxidant systems (Valko et al., 2007). The major endogenous antioxidants that maintain the redox status of the cell includes SOD, catalase and glutathione. There are three specific SODs, each of which is present in a definite compartment of human cells and performs specific functions. SOD1 (Cu/Zn-SOD) is seen in the cytosol whereas SOD2 (Mn-SOD) is in the mitochondria. On the other hand, SOD3 is exclusively extracellular (Crichton et al., 2002). Catalase is mainly found in the peroxisomes and glutathione is ubiquitous in nature. All these antioxidant enzymes play a pivotal role under conditions of oxidative stress.

The present study indicates that dosage of iron appears to be an important factor that may influence the severity of NASH since low iron improves the antioxidant system and excess of iron reduces the efficiency of the antioxidant system. HO-1 is a crucial component of the defense mechanism. It provides cellular protection by breakdown toxic heme into metabolites and thereby conserves cellular integrity. It has been reported that alteration in hepatic HO-1 extremely affects hepatic steatosis (Raffaele et al., 2019). We found that treatment with low iron during steatosis results in the induction of HO-1. This indicates that hepatic induction of HO-1 reduces hepatic steatosis and also plays a central role in decreasing inflammatory factors such as interleukins and TNF- α . In addition, activated HO-1 decreases MCP-1, and potentiates the level of anti-inflammatory cytokine IL-10 (Deshmane et al., 2009). Alteration in all these factors as mentioned are observed in low iron treated conditions. It has also been reported that HO-1 also alters the levels of several genes involved in hepatic fatty acid metabolism (Hinds et al., 2014). We found that presence of excess iron is a major mechanism that leads to the blockage of HO-1,

resulting in enhanced lipid accumulation through ROS generation. Moreover, steatosis, oxidative stress and cytokines work in a feed forward manner and develops more oxidative stress and inflammation. This provides a hostile environment for the development of “third hit” (Diehl, 2005).

Iron possesses a highly sophisticated role in stimulating hepatic inflammation (Bloomer & Brown, 2019). A well known mechanism of iron mediated inflammation is the effect of iron on NF- κ B signaling. NF- κ B is a redox sensitive transcription factor that stimulates the transcription of proinflammatory cytokines such as TNF- α , IL-6, IL-1 β and MCP-1. In normal cells, NF- κ B is bound to I κ B which sequesters the protein complex in cytosol. The development of oxidative stress removes the inhibitory effect of I κ B on NF- κ B, resulting in the translocation of NF- κ B to the nucleus. The role of iron in activating NF- κ B has been evident in certain *in vitro* and *in vivo* models. Moreover it also stimulates the expression of TNF- α mRNA, and other proinflammatory cytokines. All these point out the role of iron in modulating inflammation in various forms of liver injury. However it is noteworthy that presence of iron is usually not accompanied by conspicuous inflammatory response and is chiefly dosage dependent. At certain concentrations iron also provides a protective effect during steatosis.

Apoptosis is one of the major pathways having substantial attention and is the basic mechanism that contributes to hepatocellular death during NAFLD (Peng et al., 2020). Intrinsic pathway of apoptosis is mainly activated by several stresses that occur in various intracellular organelles like mitochondria, ER etc. The development of mitochondrial dysfunction and ER stress were explained in detail in previous chapters. The mitochondrial dysfunction results in the release of several proapoptotic proteins to the cytosol including Cyt c results in the formation of apoptosome complex (Wanderoy et al., 2021). In our study also, the level of apoptosis proteins increased significantly. This promotes the release of Cyt c from mitochondria to cytosol where it activates execution caspases like caspase 3. Different concentrations of iron exhibit differential activity during steatosis. During steatosis, iron protects the cell from apoptosis at lower concentration however; it aggravates the expression of apoptosis proteins at higher concentration. This demonstrates that the excess iron becomes problematic during disease conditions.

ROLE OF VITAMIN K ON FRUCTOSE AND PALMITATE INDUCED STEATOSIS

5.5 Introduction

Globally, the prevalence of NAFLD is approximately 25% (Araujo et al., 2018). A histopathological spectrum from simple steatosis to NASH has potentially progressive stages leading to cirrhosis, HCC and liver transplantation. Steatosis usually occurs due to the accumulation of TG in the liver along with impaired lipid metabolism. Yet hereditary factors have been associated to the pathogenesis of liver diseases; sedentary lifestyle, dietary habits, alcohol consumption and administration of certain classes of drugs enhances the acceleration of disease development (Hooper et al., 2011). Moreover, consumption of a high fructose diet, high saturated fats and deep fried foods increases the predisposition of steatosis. Even though the liver disease is emerging as a global concern, no drug treatment has been accredited for steatosis. Only nutritional guidelines are marked to reduce its progression. Lifestyle modifications involving exercise and dietary adjustment with reduced caloric content are the primary treatment strategy. Emerging clinical manifestations are strongly recommending the use of dietary agents such as nutraceuticals or functional foods in disease management (Sorrentino et al., 2015). However, several studies revealed the fact that reduction in energy alone is insufficient for the prevention of NAFLD. Both the micronutrient and macronutrient play a pivotal role in the manifestation of this disease. Recently researchers have highlighted the significance of dietary vitamin composition and liver. Vitamins are essential micronutrients required for normal growth and development. Currently 13 known vitamins are recognized: four lipid soluble vitamins (A,D,E,K) and nine water soluble vitamins (B complex and C). Among these, vitamin K is a fat soluble vitamin that exists in two forms: phytonadione or phylloquinone (VK₁) and menaquinone (VK₂). The chemical structure of VK₁ and VK₂ differ from each other in length and saturation of side chains, differ in half life period, bioavailability and rate of absorption (Schurgers & Vermeer, 2002). VK₁ is mainly present in our diet from both animal and vegetable sources including green leafy vegetables, fruits, nuts and oils. VK₂ is predominantly synthesized by the bacterial flora and is found in hepatic tissues. It also acts as a co-factor in gamma carboxylation of multiple glutamate residues. Since this vitamin is mainly involved in the blood coagulation process, bone metabolism, and blood calcium regulation, its role in lipid metabolism and hepatoprotection is not much subjected for investigation. Even though vitamin K is an essential cofactor for the liver to synthesize various clotting factors (Shearer, 2009), its efficacy has been

controversial in the treatment of liver diseases. So the present study focuses on the role of VK₁ in the development of steatosis.

5.6 Cell culture and treatment

HepG2 cells (American Type Culture Collection, (ATCC) Rockville, MD USA) were cultured as per supplier's instructions. In brief, the cells were grown in T-25 flask containing MEM supplemented with 10% heat-inactivated FBS and 1X penicillin streptomycin solution at 37°C and 5% CO₂ in a humidified incubator (Eppendorf, USA). When the cells reached 80% confluence, the cells were trypsinized and reseeded onto a new flask for further experiments.

5.7 Induction of steatosis and treatment

Fructose stock solution was prepared by dissolving in HBSS and was used to produce different concentrations of fructose treatment in serum free MEM. Palmitate stock solution (10 mM) was prepared by dissolving sodium palmitate in 0.1 N NaOH at 75°C for 5 min. The stock solution was further mixed with fatty acid free BSA to make a final concentration of 1 mM. The 1 mM working solution was then diluted to the desired treatment concentration (100 µM) in 1% MEM. To evaluate the role of VK₁, the cells were co-supplemented with VK₁. The stock solution of VK₁ was prepared by dissolving it in ethanol to a concentration of 10 mM. The resulting solution was then dissolved in MEM to make a final concentration of 1mM. Treatment was applied on day 3 and the experiments were performed after 24 hrs of treatment.

The experimental group consists of (i) C - control cells; (ii) HFP - cells treated with high fructose (100 mM) and palmitate (100 µM); (iii) VK10 - cells treated with high fructose, palmitate and VK₁ (10 µM); (iv) VK20 - cells treated with high fructose, palmitate and VK₁ (20 µM).

5.8 Results

5.8.1 Effect of VK₁ on cell viability

Various concentrations of VK₁ (1 µM, 5 µM, 10 µM, 20 µM and 50 µM) did not show cytotoxicity in HepG2 cells on 24 hrs treatment (Figure 5.11A).

5.8.2 Effect of VK₁ on HFP induced cell death

We also evaluated the effect of VK₁ (10 µM and 20 µM) in HFP treated HepG2 cells. No significant cytotoxicity was observed here also (Figure 5.11B). The results showed that incubation of HepG2 cells with HFP caused 15.82% cytotoxicity. Treatment with VK 10 and VK 20 significantly ($p \leq 0.05$) improved the cell viability compared to HFP group (5.3%, 10.1% and

12.6% respectively) (Figure 5.11B). However when the cells were treated with 200 μM and 250 μM iron along with HFP, the cell viability was significantly ($p \leq 0.05$) reduced to 24.81% and 31.15 % respectively (Figure 5.1B).

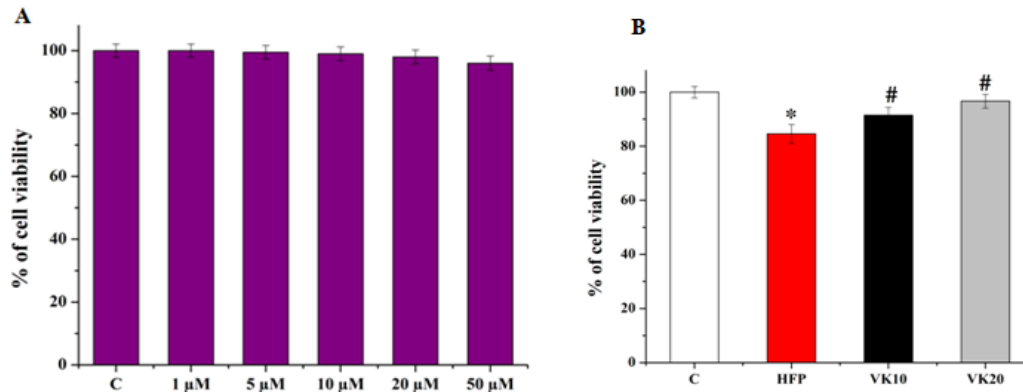


Figure 5.11 Effect of VK₁ on cell viability: (A) HepG2 cells were treated with different concentrations of VK₁ (1 μM , 5 μM , 10 μM , 20 μM and 50 μM) and viability was assessed by MTT assay. B) Cytotoxicity in HepG2 cells following treatment with HFP and VK₁. (i) C - control cells; (ii) HFP - cells treated with high fructose and palmitate; (iii) VK₁₀ - cells treated with high fructose, palmitate and 10 μM VK₁; (iv) VK₂₀ - cells treated with high fructose, palmitate and 20 μM VK₁. Data are expressed as mean \pm SD; where n = 6. * indicates significantly different from the control group ($p \leq 0.05$). # indicates significant difference from the HFP treated group ($p \leq 0.05$).

5.8.3 Effect of VK₁ on lipid accumulation

Treatment of HepG2 cells with HFP causes a significant ($p \leq 0.05$) rise in lipid accumulation (68.59%) compared to the control (Figure 5.12A). Treatment with VK₁₀ and VK₂₀ showed significant reduction in lipid accumulation. Treatment with VK₁₀ and VK₂₀ resulted in a significant ($p \leq 0.05$) decrease in intracellular fat accumulation by 32% and 43% respectively compared to the HFP group (Figure 5.12A). Moreover the expression of lipogenic proteins such as FAS and SCD-1 increased significantly ($p \leq 0.05$) during HFP to about 220.43% and 258.88% respectively compared to the control group (Figure 5.12C). The treatment with VK₁₀ significantly ($p \leq 0.05$) reduced the expression of FAS to 61.85% and VK₂₀ by 67.38% compared to HFP (Figure 5.12.C). Similarly, the protein expression of SCD-1 was reduced to 35.09% by VK₁₀ and 56.64% by VK₂₀, compared to HFP ($p \leq 0.05$) (Figure 5.12.C).

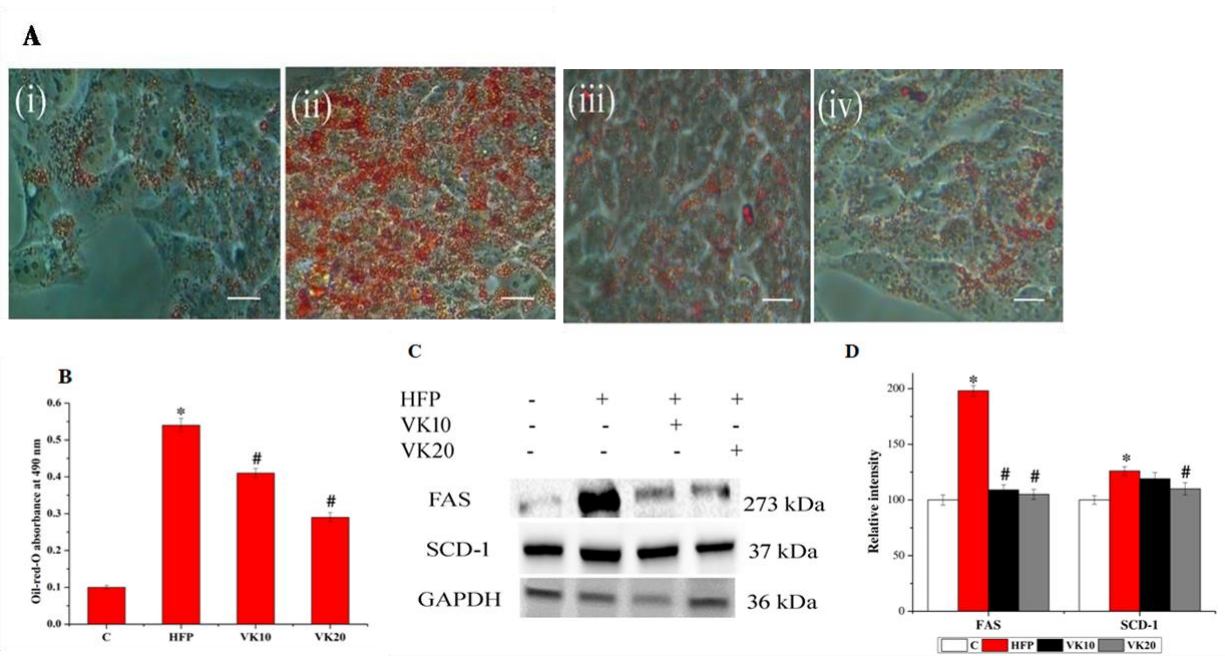


Figure 5.12 Effect of VK₁ on intracellular lipid accumulation during HFP induced steatosis: (A) Microscopic images of HepG2 cells with Oil-red-O-staining from different experimental groups under phase contrast microscope. (i) C - control cells; (ii) HFP - cells treated with high fructose and palmitate; (iii) VK10 - cells treated with high fructose, palmitate and 10 μ M VK₁; (iv) VK20 - cells treated with high fructose, palmitate and 20 μ M VK₁. Original magnification 40X. Scale bar corresponds to 50 μ M. (B) Absorbance was read at 490 nm after oil-red-O staining. (C) The protein expression of FAS and SCD-1 during VK₁ treatment. (D) The relative intensity of each band was quantified with GAPDH. Data are expressed as mean \pm SD; where n = 3. * indicates significantly different from the control group ($p \leq 0.05$). # indicates significant difference from the HFP treated group ($p \leq 0.05$).

5.8.4 Effect of VK₁ on intracellular ROS generation and Nrf2 expression

The radical scavenging activity of VK₁ at different concentrations against ROS was determined. The results showed that in HFP treated cells there was a significant ($p \leq 0.05$) increase in ROS to about 433% compared to the control group (Figure 5.13A). Treatment with VK10 and VK20 significantly ($p \leq 0.05$) reduced ROS generation to 280.66% and 395.16% respectively compared to the HFP group (Figure 5.13A). In addition, the protein expression of Nrf2, master regulator of oxidative stress significantly ($p \leq 0.05$) increased to 325.94% during

steatosis (Figure 5.13.C). Co-treatment with VK₁ (10 and 20 μM) significantly ($p \leq 0.05$) increased the protein level to 105.16% and 154.07% respectively (Figure 5.13.C).

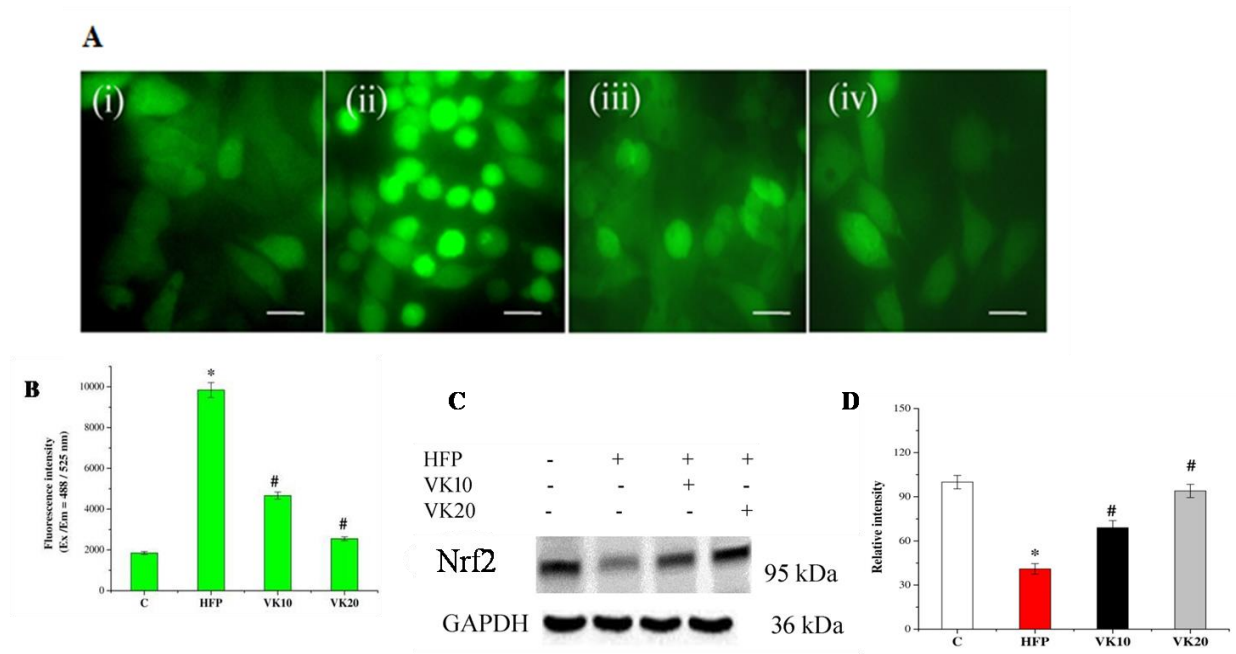


Figure 5.13 Effect of VK₁ on oxidative stress during HFP induced steatosis: (A) Analysis of intracellular ROS generation after treatment with VK₁ in HFP treated HepG2 cells were determined using fluorescent probe DCFH-DA. (i) C - control cells; (ii) HFP - cells treated with high fructose and palmitate; (iii) VK10 - cells treated with high fructose, palmitate and 10 μM VK₁; (iv) VK20 - cells treated with high fructose, palmitate and 20 μM VK₁. Original magnification 40X. Scale bar corresponds to 50 μM. (B) Determination of relative fluorescent intensity. (C) Protein expression of Nrf2 after VK₁ treatment in HFP treated cells: (D) The relative intensity of each band was quantified with GAPDH. Data are expressed as mean ± SD; where n = 3. * indicates significantly different from the control group ($p \leq 0.05$). # indicates significant difference from the HFP treated group ($p \leq 0.05$).

5.8.5 Effect of VK₁ on antioxidant enzyme activity

Our results showed that VK₁ treatment potentiates the activity of antioxidant enzymes altered by HFP. HFP caused a significant ($p \leq 0.05$) decline in the activity of SOD and catalase (66.92% and 45.45% respectively) and the inhibitory effect is reversed by VK₁ (Figure 5.14A, B). VK10 and VK20 causes a significant ($p \leq 0.05$) rise in the activity of SOD by 97.17% and 184.80% respectively and catalase by 69.36% and 173.48% respectively (Figure 5.14A, B). HFP significantly ($p \leq 0.05$) reduces the total glutathione content by 40.80% and the condition is

significantly ($p \leq 0.05$) improved to 17.07% and 36.83% by VK10 and VK20 (Figure 5.14C). This clearly demonstrates that VK₁ exerts a direct effect in reducing cellular damages resulting from HFP induced steatosis.

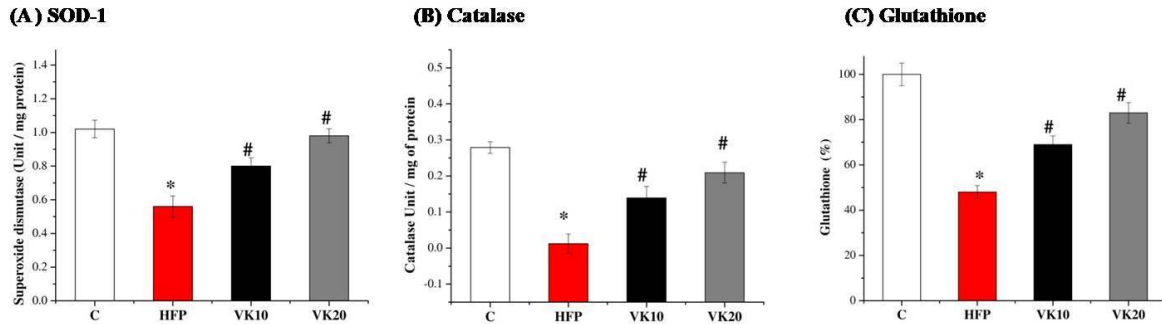


Figure 5.14 Effect of VK₁ on endogenous antioxidant status during HFP induced steatosis: (A) Activity of SOD-1 (B) Activity of catalase (C) Total glutathione. C - control cells; HFP - cells treated with high fructose and palmitate; VK10 - cells treated with high fructose, palmitate and 10 μ M VK₁; VK20 - cells treated with high fructose, palmitate and 20 μ M VK₁. Data are expressed as mean \pm SD; where n = 6. * indicates significantly different from the control group ($p \leq 0.05$). # indicates significant difference from the HFP treated group ($p \leq 0.05$).

5.8.6 Effect of VK₁ on NF- κ B translocation during cellular steatosis

Here we investigated the potential effect of VK₁ on NF- κ B translocation during HFP induced steatosis. The detection of NF- κ B by immunofluorescence reveals that HFP plays a crucial role in hepatic steatosis *via* increased nuclear translocation of NF- κ B (Figure 5.15) in HepG2 cells. The translocation was found to be reduced in VK₁ (10 and 20 μ M) treated groups (Figure 5.15).

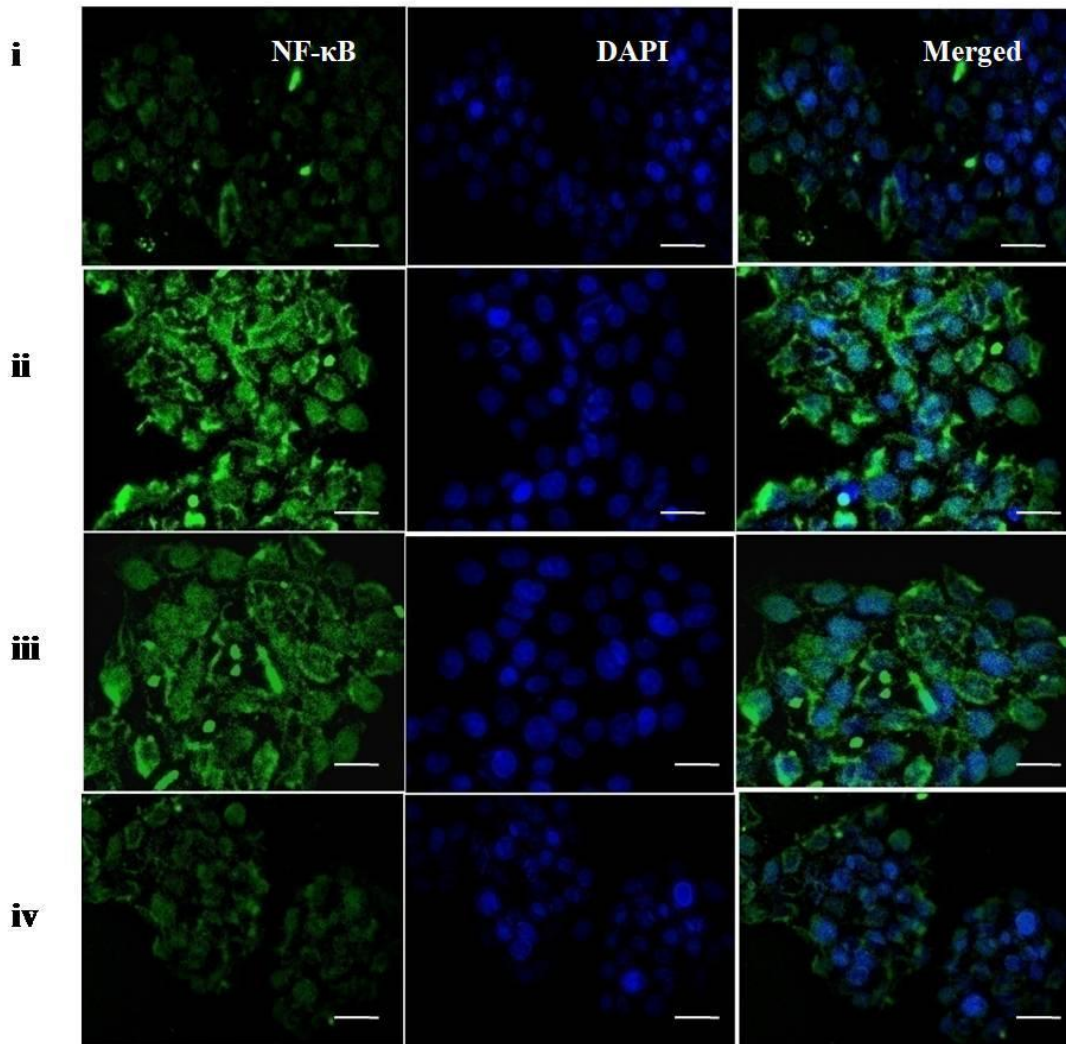


Figure 5.15 Effect of VK₁ on NF-κB translocation during HFP induced steatosis: Immunofluorescence staining showing NF-κB distribution in HFP induced steatosis in HepG2 cells. The cells were stained by DAPI (blue) and anti- NF-κB antibody (green). (i) C - control cells; (ii) HFP - cells treated with high fructose and palmitate; (iii) VK10 - cells treated with high fructose, palmitate and 10 μM VK₁; (iv) VK20 - cells treated with high fructose, palmitate and 20 μM VK₁. Original magnification 40X. Scale bar corresponds to 20 μM.

5.8.7 Effect of VK₁ on proinflammatory cytokine formation *via* oxidative stress during steatosis

Formation of proinflammatory markers is one of the characteristic features of hepatic steatosis. The results showed that HFP treatment leads to a significant ($p \leq 0.05$) increase in the production of TNF- α , IL-1 β , IL-6 and MCP-1 (Figure 5.16). However, treatment with VK10 and VK20

significantly ($p \leq 0.05$) reduced the formation of pro-inflammatory cytokines. VK10 and VK20 reduces TNF- α by 14.45% and 36.20, IL-1 β by 31.33% and 52.32%, IL-6 by 22.95% and 50.83%, MCP-1 by 23.49% and 52.18% respectively (Figure 5.16). Similarly, there was a significant ($p \leq 0.05$) decrease in the level of IL-10, an anti-inflammatory marker in HFP treated HepG2 cells to 32.86% (Figure 5.16E). Treatment with VK10 significantly ($p \leq 0.05$) increased the level of IL-10 by 23.91% and VK20 by 30.76% at $p \leq 0.05$ (Figure 5.16).

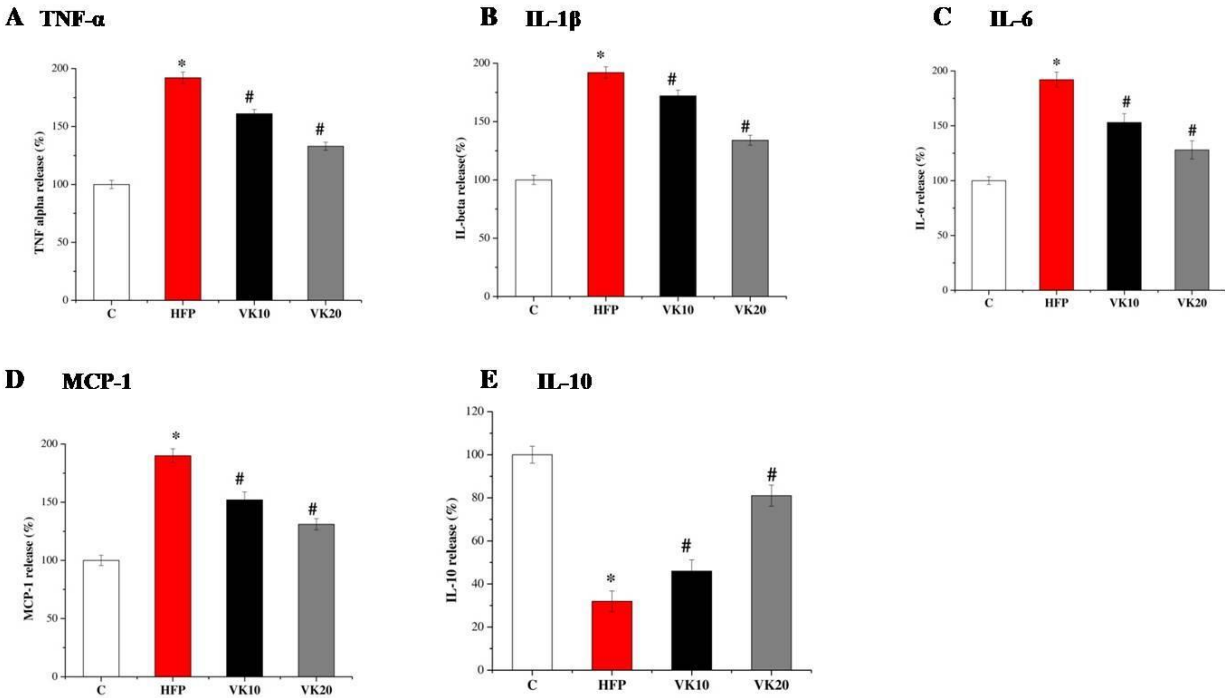


Figure 5.16 Effect of VK₁ on proinflammatory cytokines during HFP induced steatosis: (A) Secretion of TNF- α ; (B) Secretion of IL-1 β ; (C) Secretion of IL-6; (D) Secretion of MCP-1; (E) Secretion of IL-10. C - control cells; HFP - cells treated with high fructose and palmitate; VK10 - cells treated with high fructose, palmitate and 10 μ M VK₁; VK20 - cells treated with high fructose, palmitate and 20 μ M VK₁. Data are expressed as mean \pm SD; where n = 6. * indicates significantly different from the control group ($p \leq 0.05$). # indicates significant difference from the HFP treated group ($p \leq 0.05$).

5.8.8 Effect of VK₁ on MAPKs pathway in HepG2 cells during steatosis

Generally, increase in lipogenesis is directly correlated with MAPKs activation. In order to investigate the effect of HFP and possible role of VK₁ during cellular steatosis, we examined the protein expression of MAP kinases such as JNK, p-JNK, ERK1/2 and p-ERK1/2. HFP treatment significantly ($p \leq 0.05$) increased the expression of p-JNK to 104.54% and p-ERK1/2 to 179.112

% compared to the control group (Figure 5.17A). VK10 significantly ($p \leq 0.05$) downregulated the expression of p-JNK and p-ERK1/2 to 278.49 % and 131.36% respectively (Figure 5.17A). Similarly treatment with VK20 also significantly ($p \leq 0.05$) reduced the expression of p-JNK to 598.60% and p-ERK1/2 to 159.76% at (Figure 5.17A). Similarly, Figure 5.17C shows the expression of phospho p38 during steatosis. The increased expression of phospho p38 is reduced by VK10 and VK20.

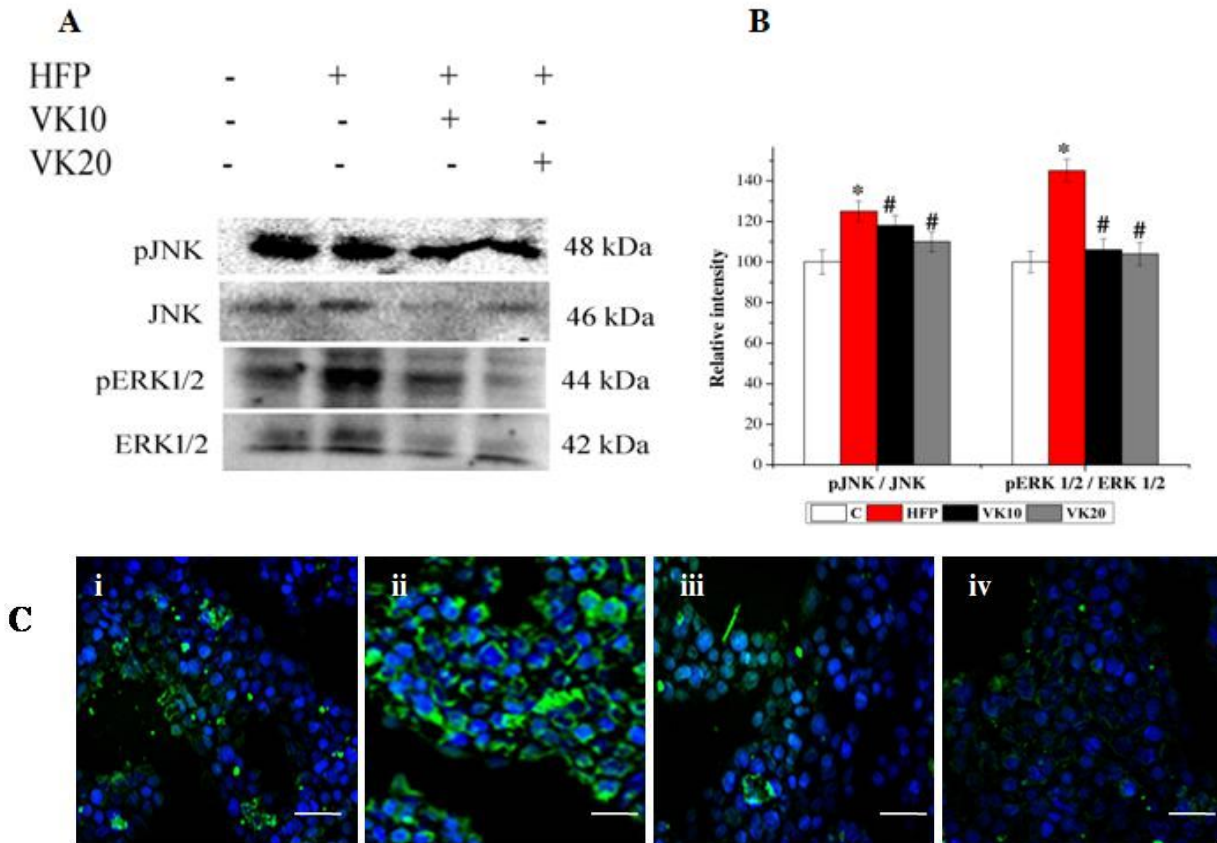


Figure 5.17 Effect of VK₁ on signaling factors involved in MAPKs pathway during HFP induced steatosis: HepG2 cells were co-treated with HFP and VK₁ for 24 hrs. (A) Western blot showing the protein expression of p-JNK, JNK, p-ERK1/2, ERK1/2. (i) C - control cells; (ii) HFP - cells treated with high fructose and palmitate; (iii) VK10 - cells treated with high fructose, palmitate and 10 μ M VK₁; (iv) VK20 - cells treated with high fructose, palmitate and 20 μ M VK₁. (B) The relative intensity of each band was quantified. Data are expressed as mean \pm SD; where $n = 3$. (C) Immunofluorescence staining showing expression of p-p38. Original magnification 40X. Scale bar corresponds to 20 μ M. * indicates significantly different from the control group ($p \leq 0.05$). # indicates significant difference from the HFP treated group ($p \leq 0.05$).

5.9 Discussion

Liver is the major organ responsible for the regulation of entire body metabolism of energy supplements (Bae et al., 2017). Non-alcoholic fatty liver otherwise hepatic steatosis is indicated by excess lipid and triglyceride accumulation in hepatocytes. A healthy liver always maintains a constant physiological balance between anabolism and catabolism of lipid by regulating the delivery of dietary fat to liver, uptake of free fatty acids from adipose tissue, and synthesis and secretion of lipoproteins (Almeda et al., 2014). Several researches revealed that the progression of NAFLD is favored by lipid deposition, oxidative stress, and inflammatory responses. Remarkably, all these factors cross talk with each other, inflammation plays a pivotal role in the progression of NAFLD (Tian et al., 2017). Nonetheless, disruption in normal homeostatic pathways and aberrant lipid metabolism in the liver culminates in hepatic steatosis. Lipotoxicity is the major risk factor for the development of NASH, T2DM, and obesity (Cnop et al., 2012). Currently there is no FDA approved class of drugs for NAFLD, attention has mainly oriented on the control of liver diseases using micronutrient antioxidants and dietary components such as vitamins, polyphenols, resveratrol, carotenoid and curcumin. (Ipsen et al., 2014; Li, 2016; Bae et al., 2017). The effect and possible mechanism of action of almost all the vitamins has been reported. The inhibitory action of vitamins C and E in the propagation of radical reactions during oxidative stress relevant situations are established (Ipsen et al., 2014). However, the possible aspect of vitamin K in NAFLD, especially under *in vitro* condition is very limited. For the general population, it is easily available especially through dietary resources such as green leafy vegetables (VK₁), meats, curd, egg, fermented soybeans and cheese (VK₂) (Dahlberg & Schott, 2018). The storage of vitamin K in adipocytes has also been reported (Shea et al., 2010) and there exists a positive correlation between adult obesity and vitamin K. Nonetheless, studies are inadequate whether these micronutrients have a possible role in lipid metabolism and inflammatory responses during NAFLD.

Vitamin K is a fat soluble vitamin, essential for the proper functioning of coagulation. VK₁ and VK₂ differ in source, absorption rates, tissue distribution, bioavailability and target activity. (Bolton et al., 2000). Vitamin K has health benefits to an extent beyond blood homeostasis and shown vital role in bone health, insulin sensitivity, reduces vascular calcification, cardiovascular diseases, dementia, cognitive impairment, chronic kidney diseases, rheumatoid arthritis, cancer and frailty (Simes et al., 2019). Since most of the health conditions

are in close relation with inflammation, the role of vitamin K is being highlighted. Dietary fatty acid plays a crucial role in NAFLD development and mode of lipotoxicity varies with different types of dietary fatty acids. Palmitic acid is the most abundant saturated fatty acid able to generate lipotoxicity in hepatocytes, β cells, muscular cells and so on (Barlow et al., 2016). Moreover, excessive fructose consumption favors NAFLD by acting as both a substrate and inducer of de novo lipogenesis. The multifaceted form of fructose metabolism results in the outset of cellular stress and hepatic inflammation. In addition to this, it may impose direct and indirect effects at the peripheral level. Therefore, the present study aims to explore the role of VK₁ in the amelioration of lipid deposition, oxidative stress and inflammation for NAFLD, since it is a dietary supplement, easily available and possesses various modes of action in the biological system.

To analyze the hepatoprotective activity of VK₁, an *in vitro* steatosis model was developed using high fructose and palmitate in HepG2 cell line. To inspect the anti-steatosis effect of VK₁ we have executed research from several aspects. Based on our results, VK₁ possesses a significant activity against steatosis in terms of decreased lipid droplet accumulation and reduction in the expression of lipogenic proteins such as FAS and SCD-1 in HepG2 cell line. Under physiological conditions, the lipogenic pathway is tentatively minor and gets active after a high calorie diet. The consumption of high fructose results in the saturation of the glycolysis pathway thereby leading to the aggregation of glycolytic intermediates. These intermediates can be transformed to glycerol-3-phosphate, used in TG synthesis (Jegatheesan & De Bandt, 2017). It is established that dyslipidemia has a crucial role in the pathogenesis of microvascular complications (Warraich & Rana, 2017). The protective role of VK₁ against TG has been reported in diabetic mice along with the regulation of lipid oxidation, peroxisome proliferator-activated receptor alpha (PPAR- α), carnitine palmitoyltransferase 1A (CPT1A) (Dhingia et al., 2018).

Oxidative stress is due to the imbalance between free radicals and antioxidant defense systems of the body and is a key component during the progression of chronic diseases. The advancement of oxidative stress can be abolished by improving the antioxidant potential of the body. Vitamin A, C and E are well known antioxidants. However in many cases some of the ignored antioxidants like vitamin K, D, niacin, riboflavin and pyridoxine also act as coenzymes and attack free radicals. In the present study, VK₁ shows significant radical scavenging activity.

As expected, HFP treatment exerts oxidative stress in HepG2 cells and VK₁ significantly affects the functioning of several important antioxidant enzymes and decrease in ROS production through reduced expression of Nrf2. It has been reported that in oligodendrocytes VK₁ has the potential to block the activation of 12-lipoxygenase in arachidonic acid induced oxidative injury (Li et al., 2009). We also observed that over production of ROS causes a significant depletion in the level of antioxidant enzymes such as SOD-1, catalase and glutathione during HFP mediated steatosis, making the liver more susceptible for oxidative injury. Weakened antioxidant systems also enhance the rate of lipid peroxidation which in turn leads to hepatocytes necrosis and death and promote the synthesis of collagen ie; fibrosis. Impairment in the antioxidant system is the proposed justification for antioxidant supplementation in the management of NAFLD. Steatosis induced oxidative stress obscures the antioxidant system. Hence VK₁ as an antioxidant minimizes oxidative stress when supplied exogenously.

Pro and anti-inflammatory cytokines possess sophisticated roles in the pathophysiology of NAFLD. Recent studies explained various prospects including inflammation due to oxidative stress correlated with lipid peroxidation, activation of cytokines and endogenous toxins of fructose metabolites (Nomura & Yamanouchi, 2012). In hepatocytes, fat accumulation during the early stage of NAFLD is mediated by TNF- α . It also promotes the disease progression to a more advanced stage. IL-1 β also stimulates fat accumulation and then inflammation followed by fibrosis (Mirea et al., 2020). IL-6 is pleiotropic cytokine mainly employed in immune response and also suggested as a mediator of NAFLD. Even though IL-6 plays a defensive role in liver fibrosis by protecting against oxidative stress and mitochondrial dysfunction (El-Assal et al., 2004), a positive correlation was also established between the hepatic expression of IL-6 and NAFLD (Wieckowska et al., 2008). The primary function of MCP-1 is to attract monocytes, macrophages and polymorphonuclear leukocytes to the site of inflammation. Our result shows an increase in proinflammatory cytokines during steatosis. If vitamin plays any role in alleviating steatosis, inflammatory cytokines have to be reduced eventually. In this aspect, our results confirmed a decline in the level of inflammatory cytokines TNF- α , IL-1 β , IL-6 and MCP-1 after VK₁ treatment. This suggested the possible role of VK₁ in hepatoprotective function against steatosis through its anti-inflammatory activity. In addition, the formation of anti-inflammatory cytokine IL-10 was reduced during steatosis and VK₁ reverses the condition. The MAPKs is the central signaling pathway that regulates hepatic metabolism. It transduces extracellular and

intracellular signals to various messenger molecules within the cell by phosphorylating target proteins. Under pathological conditions, regulation of glucose and lipid metabolism remains dysfunctional. Various stress factors promote the activation of hepatic MAPKs, reflecting impaired lipid metabolism. The present study reported that VK₁ suppresses pathways involved in inflammation and cytokine production including MAPKs and NF- κ B. VK₁ exhibits diverse effects on phosphorylation states of various proteins. The involvement of VK₁ in PKA, PKC, NF- κ B, STAT and MAPK pathways are reported by modulating the protein kinases and phosphatases. Since increased accumulation of macrophages is an indication of NAFLD, the present study provides a connecting link between VK₁ and inflammation response, which is a key event in NAFLD. Generally NF- κ B the transcription factor remains inactive in the cytoplasm by binding with inhibitory protein I κ B. During steatosis, I κ B becomes phosphorylated and degrades results in the translocation of NF- κ B to the nucleus where it activates the genes responsible for inflammation. However VK₁ imposes a significant inhibitory action on NF- κ B translocation.

5.10 Summary and conclusion

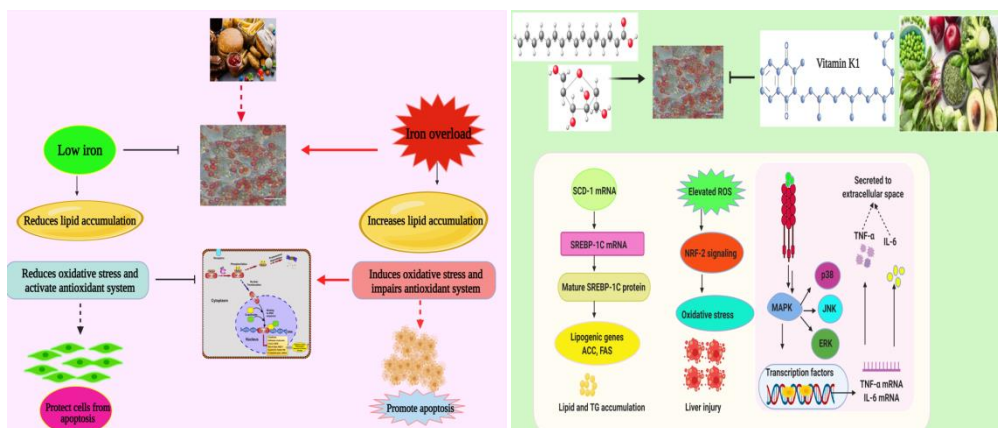


Figure 5.18 Schematic representations on the role of iron and vitamin K during steatosis

In this study, we demonstrated the possible role of VK₁ in HFP induced steatosis in HepG2 cells. Our data revealed that VK₁ has a potential effect against steatosis in addition to its role in ameliorating coagulopathy associated with liver disease. It also improves antioxidant status and reduces lipogenesis mediated proinflammatory cytokine secretion. It also inhibited MAPK signaling pathway and NF- κ B translocation. Since VK₁ possesses broad functional action

it is inevitable to manifest the prestige of VK₁ as a dietary supplement for anti-steatosis through an *in vivo* study.

References

- Abbaspour, N., Hurrell, R. and Kelishadi, R., 2014. Review on iron and its importance for human health. *Journal of research in medical sciences: the official journal of Isfahan University of Medical Sciences*, 19(2), p.164.
- Ahmed, U., Latham, P.S. and Oates, P.S., 2012. Interactions between hepatic iron and lipid metabolism with possible relevance to steatohepatitis. *World journal of gastroenterology: WJG*, 18(34), p.4651.
- Aigner, E., Theurl, I., Haufe, H., Seifert, M., Hohla, F., Scharinger, L., Stickel, F., Murlane, F., Weiss, G. and Datz, C., 2008. Copper availability contributes to iron perturbations in human nonalcoholic fatty liver disease. *Gastroenterology*, 135(2), pp.680-688.
- Almeda-Valdes, P., Aguilar-Olivos, N., Uribe, M. and Méndez-Sánchez, N., 2014. Common features of the metabolic syndrome and nonalcoholic fatty liver disease. *Reviews on recent clinical trials*, 9(3), pp.148-158.
- Aly, F.Z. and Kleiner, D., 2011. Update on fatty liver disease and steatohepatitis. *Advances in anatomic pathology*, 18(4), p.294.
- Anderson, E.R. and Shah, Y.M., 2013. Iron homeostasis in the liver. *Comprehensive Physiology*, 3(1), pp.315-330.
- Araujo, A.R., Rosso, N., Bedogni, G., Tiribelli, C. and Bellentani, S., 2018. Global epidemiology of non-alcoholic fatty liver disease/non-alcoholic steatohepatitis: What we need in the future. *Liver International*, 38, pp.47-51.
- Bacon, B.R., Farahvash, M.J., Janney, C.G. and Neuschwander-Tetri, B.A., 1994. Nonalcoholic steatohepatitis: an expanded clinical entity. *Gastroenterology*, 107(4), pp.1103-1109.
- Bae, M., Park, Y.K. and Lee, J.Y., 2018. Food components with antifibrotic activity and implications in prevention of liver disease. *The Journal of nutritional biochemistry*, 55, pp.1-11.

- Barlow, J., Jensen, V.H., Jastroch, M. and Affourtit, C., 2016. Palmitate-induced impairment of glucose-stimulated insulin secretion precedes mitochondrial dysfunction in mouse pancreatic islets. *Biochemical Journal*, 473(4), pp.487-496.
- Bloomer, S.A. and Brown, K.E., 2019. Iron-induced liver injury: a critical reappraisal. *International journal of molecular sciences*, 20(9), p.2132.
- Bolton-Smith, C., Price, R.J., Fenton, S.T., Harrington, D.J. and Shearer, M.J., 2000. Compilation of a provisional UK database for the phyloquinone (vitamin K1) content of foods. *British Journal of Nutrition*, 83(4), pp.389-399.
- Chitturi, S., Weltman, M., Farrell, G.C., McDonald, D., Liddle, C., Samarasinghe, D., Lin, R., Abeygunasekera, S. and George, J., 2002. HFE mutations, hepatic iron, and fibrosis: ethnic-specific association of NASH with C282Y but not with fibrotic severity. *Hepatology*, 36(1), pp.142-149.
- Cnop, M., Foufelle, F. and Velloso, L.A., 2012. Endoplasmic reticulum stress, obesity and diabetes. *Trends in molecular medicine*, 18(1), pp.59-68.
- Crichton, R.R., Wilmet, S., Legssyer, R. and Ward, R.J., 2002. Molecular and cellular mechanisms of iron homeostasis and toxicity in mammalian cells. *Journal of inorganic biochemistry*, 91(1), pp.9-18.
- Dahlberg, S. and Schott, U., 2018. Vitamin K and its role in diabetic vascular complications and low-grade inflammation. *Journal of Diabetes and Treatment*, 10(1), pp.2574-7568.
- Deshmane, S.L., Kremlev, S., Amini, S. and Sawaya, B.E., 2009. Monocyte chemoattractant protein-1 (MCP-1): an overview. *Journal of interferon & cytokine research*, 29(6), pp.313-326.
- Diehl, A.M., 2005. Lessons from animal models of NASH. *Hepatology Research*, 33(2), pp.138-144.
- Dihingia, A., Ozah, D., Ghosh, S., Sarkar, A., Baruah, P.K., Kalita, J., Sil, P.C. and Manna, P., 2018. Vitamin K1 inversely correlates with glycemia and insulin resistance in patients with type 2 diabetes (T2D) and positively regulates SIRT1/AMPK pathway of glucose metabolism in liver of T2D mice and hepatocytes cultured in high glucose. *The Journal of nutritional biochemistry*, 52, pp.103-114.

- Eid, R., Arab, N.T. and Greenwood, M.T., 2017. Iron mediated toxicity and programmed cell death: A review and a re-examination of existing paradigms. *Biochimica et Biophysica Acta (BBA)-Molecular Cell Research*, 1864(2), pp.399-430.
- El-Assal, O., Hong, F., Kim, W.H., Radaeva, S. and Gao, B., 2004. IL-6-deficient mice are susceptible to ethanol-induced hepatic steatosis: IL-6 protects against ethanol-induced oxidative stress and mitochondrial permeability transition in the liver. *Cell Mol Immunol*, 1(3), pp.205-211.
- Fillebeen, C., Charlebois, E., Wagner, J., Katsarou, A., Mui, J., Vali, H., Garcia-Santos, D., Ponka, P., Presley, J. and Pantopoulos, K., 2019. Transferrin receptor 1 controls systemic iron homeostasis by fine-tuning hepcidin expression to hepatocellular iron load. *Blood, The Journal of the American Society of Hematology*, 133(4), pp.344-355.
- Fung, E. and Nemeth, E., 2013. Manipulation of the hepcidin pathway for therapeutic purposes. *Haematologica*, 98(11), p.1667.
- Hentze, M.W., Muckenthaler, M.U., Galy, B. and Camaschella, C., 2010. Two to tango: regulation of Mammalian iron metabolism. *Cell*, 142(1), pp.24-38.
- Hinds Jr, T.D., Sodhi, K., Meadows, C., Fedorova, L., Puri, N., Kim, D.H., Peterson, S.J., Shapiro, J., Abraham, N.G. and Kappas, A., 2014. Increased HO-1 levels ameliorate fatty liver development through a reduction of heme and recruitment of FGF21. *Obesity*, 22(3), pp.705-712.
- Hooper, A.J., Adams, L.A. and Burnett, J.R., 2011. Genetic determinants of hepatic steatosis in man. *Journal of lipid research*, 52(4), pp.593-617.
- Ipsen, D.H., Tveden-Nyborg, P. and Lykkesfeldt, J., 2014. Does vitamin C deficiency promote fatty liver disease development?. *Nutrients*, 6(12), pp.5473-5499.
- Jegatheesan, P. and De Bandt, J.P., 2017. Fructose and NAFLD: the multifaceted aspects of fructose metabolism. *Nutrients*, 9(3), p.230.
- Lee, A.W., Oates, P.S. and Trinder, D., 2003. Effects of cell proliferation on the uptake of transferrin-bound iron by human hepatoma cells. *Hepatology*, 38(4), pp.967-977.
- Li, J., Cordero, P., Nguyen, V.I. and Oben, J.A., 2016. The role of vitamins in the pathogenesis of non-alcoholic fatty liver disease. *Integrative Medicine Insights*, 11, pp.IMI-S31451.

- Li, J., Wang, H. and Rosenberg, P.A., 2009. Vitamin K prevents oxidative cell death by inhibiting activation of 12-lipoxygenase in developing oligodendrocytes. *Journal of neuroscience research*, 87(9), pp.1997-2005.
- Mirea, A.M., Stienstra, R., Kanneganti, T.D., Tack, C.J., Chavakis, T., Toonen, E.J. and Joosten, L.A., 2020. Mice deficient in the IL-1 β activation genes Prtn3, elane, and Casp1 are protected against the development of obesity-induced NAFLD. *Inflammation*, 43(3), pp.1054-1064.
- Nomura, K. and Yamanouchi, T., 2012. The role of fructose-enriched diets in mechanisms of nonalcoholic fatty liver disease. *The Journal of nutritional biochemistry*, 23(3), pp.203-208.
- Otagawa, K., Kinoshita, K., Fujii, H., Sakabe, M., Shiga, R., Nakatani, K., Ikeda, K., Nakajima, Y., Ikura, Y., Ueda, M. and Arakawa, T., 2007. Erythrophagocytosis by liver macrophages (Kupffer cells) promotes oxidative stress, inflammation, and fibrosis in a rabbit model of steatohepatitis: implications for the pathogenesis of human nonalcoholic steatohepatitis. *The American journal of pathology*, 170(3), pp.967-980.
- Peng, C., Stewart, A.G., Woodman, O.L., Ritchie, R.H. and Qin, C.X., 2020. Non-alcoholic steatohepatitis: A review of its mechanism, models and medical treatments. *Frontiers in Pharmacology*, 11, p.1864.
- Raffaele, M., Carota, G., Sferrazzo, G., Licari, M., Barbagallo, I., Sorrenti, V., Signorelli, S.S. and Vanella, L., 2019. Inhibition of heme oxygenase antioxidant activity exacerbates hepatic steatosis and fibrosis in vitro. *Antioxidants*, 8(8), p.277.
- Ryan, J.D., Armitage, A.E., Cobbold, J.F., Banerjee, R., Borsani, O., Dongiovanni, P., Neubauer, S., Morovat, R., Wang, L.M., Pasricha, S.R. and Fargion, S., 2018. Hepatic iron is the major determinant of serum ferritin in NAFLD patients. *Liver International*, 38(1), pp.164-173.
- Schurgers, L.J. and Vermeer, C., 2002. Differential lipoprotein transport pathways of K-vitamins in healthy subjects. *Biochimica et Biophysica Acta (BBA)-General Subjects*, 1570(1), pp.27-32.
- Shea, M.K., Booth, S.L., Gundberg, C.M., Peterson, J.W., Waddell, C., Dawson-Hughes, B. and Saltzman, E., 2010. Adulthood obesity is positively associated with adipose tissue

concentrations of vitamin K and inversely associated with circulating indicators of vitamin K status in men and women. *The Journal of nutrition*, 140(5), pp.1029-1034.

- Shearer, M.J., 2009. Vitamin K in parenteral nutrition. *Gastroenterology*, 137(5), pp.S105-S118.
- Simes, D.C., Viegas, C.S., Araújo, N. and Marreiros, C., 2019. Vitamin K as a powerful micronutrient in aging and age-related diseases: pros and cons from clinical studies. *International journal of molecular sciences*, 20(17), p.4150.
- Sorrentino, G., Crispino, P., Coppola, D. and De Stefano, G., 2015. Efficacy of lifestyle changes in subjects with non-alcoholic liver steatosis and metabolic syndrome may be improved with an antioxidant nutraceutical: a controlled clinical study. *Drugs in R&D*, 15(1), pp.21-25.
- Stangl, G.I. and Kirchgessner, M., 1998. Different degrees of moderate iron deficiency modulate lipid metabolism of rats. *Lipids*, 33(9), pp.889-895.
- Tian, W., Chen, L., Zhang, L., Wang, B., Li, X.B., Fan, K.R., Ai, C.H., Xia, X., Li, S.D. and Li, Y., 2017. Effects of ginsenoside Rg1 on glucose metabolism and liver injury in streptozotocin-induced type 2 diabetic rats. *Genet Mol Res*, 16(1), p.gmr16019463.
- Valko, M., Leibfritz, D., Moncol, J., Cronin, M.T., Mazur, M. and Telser, J., 2007. Free radicals and antioxidants in normal physiological functions and human disease. *The international journal of biochemistry & cell biology*, 39(1), pp.44-84.
- Wanderoy, S., Hees, J.T., Klesse, R., Edlich, F. and Harbauer, A.B., 2021. Kill one or kill the many: interplay between mitophagy and apoptosis. *Biological chemistry*, 402(1), pp.73-88.
- Warraich, H.J. and Rana, J.S., 2017. Dyslipidemia in diabetes mellitus and cardiovascular disease. *Cardiovascular endocrinology*, 6(1), p.27.
- Wieckowska, A., Papouchado, B.G., Li, Z., Lopez, R., Zein, N.N. and Feldstein, A.E., 2008. Increased hepatic and circulating interleukin-6 levels in human nonalcoholic steatohepatitis. *Official journal of the American College of Gastroenterology| ACG*, 103(6), pp.1372-1379.
- Younossi, Z.M., Gramlich, T., Bacon, B.R., Matteoni, C.A., Boparai, N., O'Neill, R. and McCullough, A.J., 1999. Hepatic iron and nonalcoholic fatty liver disease. *Hepatology*, 30(4), pp.847-850.

Chapter 6

SUMMARY AND CONCLUSION

In the present study, HepG2 cell lines have been used to investigate various aspects of NASH pathophysiology, especially the effects of fructose and palmitate treatments on lipid accumulation, mitochondrial dysfunction, ER stress and the mechanism of UPR. The potential role of minerals like iron and vitamin K were also subjected for study. But further work is required to confirm the effects of iron treatment in the steatosis model. This study developed a robust *in vitro* model of NASH by incubating HepG2 cells with fructose and palmitate. This is found to be an ideal *in vitro* model for research on high energy induced NASH.

It is well established that metabolic diseases including NAFLD are associated with excess energy intake and least energy expenditure. Our study revealed that surplus lipid accumulation plays a central role in the progression of NASH. The fructose and palmitate increases the lipid accumulation and intracellular TG content along with intracellular cholesterol accumulation in treated HepG2 cells. Moreover fructose and palmitate also alter the expression of proteins involved in lipid metabolism such as ACC α , p-ACC α and FAS. In the studies presented here, co-treatment with fructose and palmitate induces mitochondrial dysfunction. It adversely affects the vital functions of mitochondria by generating superoxide production. Moreover alteration in mitochondrial transmembrane potential, impairment in the activity of ETC and oxygen consumption was also observed. Fructose - palmitate induced steatosis also mediates an imbalance in mitochondrial dynamics and mitobiogenesis. Altered mitochondrial dynamics were confirmed mainly by the increased protein expression of fission proteins like DRP1 and FIS1 and decreased expression of fusion proteins like MFN2 and OPA1. The marker proteins of mitobiogenesis such as PGC-1 α , SIRT1 and Nrf2 were also downregulated. The increased expression of Cyt c in the fructose palmitate treated group is a key indication for apoptosis. The elevation of intracellular calcium level is also higher during steatosis followed by increased caspase 3 activity in turn promotes apoptosis.

Alteration of lipid homeostasis in hepatocytes leads to transitory development of toxic lipids that result in ER stress along with inflammation and hepatocellular damage. ER stress

activates the UPR pathway which is considered as an adaptive pathway to maintain protein folding homeostasis. Recent studies have unveiled the contribution of the UPR in the regulation of hepatic steatosis and in the cellular response to lipotoxic stress. Interestingly, we found that UPR sensors can be directly activated during high caloric conditions. Both ER and mitochondria develop the UPR response system. The cross talk between the UPR^{ER} and UPR^{mt} revealed the possible therapeutic potential of targeting the UPR in NASH.

By considering the significance of minerals and nutrients in steatosis, the potential role of iron and vitamin K₁ were also subjected for investigation. Iron is an essential mineral, which is required for vital functions throughout the body. An excess of iron is also a crucial factor for cellular injury from oxidative stress. In the present work, we evaluated the association of iron with risk of NAFLD. We found that high concentration of iron was strongly associated with increased risk of NASH while low iron was associated with decreased risk of NASH. During NASH, in hepatocytes the presence of low iron leads to a reduction in lipid accumulation along with reduced oxidative stress, inflammation and apoptosis. Reverse occurred as in the case of high concentration of iron. The unusual effects of iron on hepatocytes may be explained by the differences in effects on iron stored within the cells. Nonetheless, several limitations of our study require consideration when interpreting findings. First, dual function of iron at lower and higher concentrations during NASH must be confirmed by *in vivo* studies. Our study can only provide etiological clues in exploring the association between iron and NASH.

Diet contains macronutrients which provide energy for body functions, and micronutrients that perform regulatory functions. Vitamins are essential micronutrients in our diet which are well known to affect the immune system, including both innate and adaptive response. The immune system is particularly involved in the development and progression of NAFLD. We attempted to highlight the relation between dietary vitamins like vitamin K₁ and steatosis in HepG2 cells. Vitamin K₁ has the ability to reduce lipid accumulation and change the expression of lipogenic proteins thereby decelerating the pathogenesis of NASH. It also has the capacity to reduce oxidative stress developed during high calorie and prevent NASH by modulating antioxidant enzyme systems. Vitamin K₁ suppresses the expression of pro-inflammatory cytokines such as TNF- α , interleukins (IL-1 β , IL-6, MCP-1) and thus lowers inflammatory response during NASH. It also plays a central role in the MAPK signaling pathway and lowers the levels of MAPK proteins such as pJNK, pERK1/2. However, further *in*

vivo studies are required to evaluate the safety and efficacy of vitamin K as a therapeutic agent in NASH. The deficiency of several micronutrients, especially minerals and vitamins is commonly associated with NASH and has been correlated with disease severity. Several pieces of experimental data have shown that deficiency of different vitamins may cause metabolic dysregulation. More clinical trials are warranted to directly evaluate the efficacy of supplementation of these minerals and vitamins on disease progression, as some of them may also have adverse outcomes like excess iron. It is also crucial to study the interactions of these minerals and vitamins and how their intake affects lipid metabolism. However, unveiling the specific contributions of micronutrients remains challenging because human diets are complex and fail to replicate experimental dietary models.

ABSTRACT

Name of the Student: Swapna Sasi U S

Registration No. : 10BB16A39016

Faculty of Study: Biological Sciences

Year of Submission: 2021

AcSIR academic centre/CSIR Lab: NIIST

Name of the Supervisor(s): Dr. K G Raghu

Title of the thesis: *In vitro* based mechanistic study on the role of fructose and palmitate in the genesis of steatosis in HepG2 cell line

Non - alcoholic steatohepatitis (NASH) is one of the most common chronic liver diseases. Many research groups are actively working on various aspects of hepatic physiology for definite clues on the genesis of NASH. The aim of this study was to validate the potential role of high fructose and palmitate, similar to our modern high energy dietary pattern and validate whether it could contribute hepatic steatosis and elucidate the molecular mechanism behind the progression of NASH. The present study developed an *in vitro* model in HepG2 cell line to mimic high energy diet induced steatosis in liver. For this, HepG2 cells were treated with fructose (100 mM) and palmitate (100 μ M) for 24 hrs and subjected for biochemical analysis.

Our findings suggested that the presence of high fructose and palmitate efficiently developed steatosis under *in vitro* conditions. Detailed investigation on vital parameters of mitochondria revealed that high calorie induces mitochondrial superoxide generation along with alteration in membrane potential and bioenergetics. Moreover the mitochondrial dynamics was also impaired due to the increased expression of fission proteins (DRP1 and FIS1) and decreased expression of fusion proteins (MFN2 and OPA1) and mitobiogenesis marker proteins (PGC-1 α , SITR1 and Nrf2). The activation of UPR signaling pathways in both mitochondria and ER drives the pathogenesis of liver disease *via* its involvement in steatosis, inflammation, and apoptosis. The expressions of UPR^{ER} marker proteins were increased along with expression of biomarkers of UPR^{mt} with considerable decrease in SIRT3 expression. The communication between ER and mitochondria was also found to be adversely affected. All these results indicate that UPR^{mt} and UPR^{ER} play a crucial role in the initiation and progression of steatosis thereby revealing their role in designing new therapeutic strategies for hepatic steatosis. Since liver plays a central role in micronutrient metabolism, impairment in micronutrient metabolism may involve in the pathogenesis of liver disease. The investigation on the role of iron during steatosis revealed that excessive micronutrient contributes to dysregulation in lipid homeostasis and antioxidant pathways. Moreover excess iron was also leads to the development of inflammation by elevating the secretion of proinflammatory cytokines. It also stimulates intrinsic pathway of apoptosis by upregulating the expressions of Bad, Bax and cyt C. On the contrary, lower concentration of iron ameliorates steatosis, which implies that intake of both macro and micronutrients is beneficial only at required quantities. We also found a beneficial effect of vitamin K₁ in the amelioration of steatosis in HepG2 cells by improving the expression of lipogenic proteins, antioxidant system, and also alleviate the secretion of proinflammatory cytokines mainly *via* MAKs pathway.

Publications

From thesis

1. **U S Swapna Sasi.**, Sindhu, G. and Raghu, K.G., 2020. Fructose-palmitate based high calorie induce steatosis in HepG2 cells via mitochondrial dysfunction: An in vitro approach. *Toxicology in Vitro*, 68, p.104952.

Other than thesis

2. **U S Swapna Sasi.**, Ganapathy, S., Palayyan, S.R. and Gopal, R.K., 2020. Mitochondria associated membranes (MAMs): emerging drug targets for diabetes. *Current medicinal chemistry*, 27(20), pp.3362-3385.
3. Salin Raj, P., **U S Swapna Sasi.** and Raghu, K.G., 2019. High glucose induced calcium overload via impairment of SERCA/PLN pathway and mitochondrial dysfunction leads to oxidative stress in H9c2 cells and amelioration with ferulic acid. *Fundamental & clinical pharmacology*, 33(4), pp.412-425.

Scientific Conferences

Poster presentations:

1. **Swapna Sasi U S & Raghu K G.** Emerging targets for future drug discovery and development for diabetes: A literature review at International Conference on Diabetes and Phytotherapy (ICDP), on 18 - 20 August 2017 at Dept. of Biochemistry & Biotechnology, Annamalai University, Tamilnadu (**Best poster presentation award**).
2. **Swapna Sasi U S & Raghu K G.** Emerging targets for future drug discovery and development for diabetes: A literature review at International Conference on Advances in Degenerative Diseases and Molecular Interventions (ADDMI), on 23-24th November 2017 at Hycinth, Trivandrum.
3. **Swapna Sasi U S & Raghu K G.** Emerging targets for future drug discovery and development for diabetes: A literature review at International Seminar on Phytochemistry (ISP), on 26 - 27 March 2018 at Jawaharlal Nehru Tropical Botanical Garden and Research Institute, Palode, Trivandrum.
4. **Swapna Sasi U S & Raghu K G.** High fructose and palmitate induced lipid accumulation with mitochondrial dysfunction revealing the possible significance of bioenergetics in the genesis of liver diseases at International Congress on Obesity and Metabolic Syndromes (ICOMES & AOCO 2019), on 29th – 31st August 2019 at Conrad Hotel, Seoul, South Korea, (**Received CSIR - travel grant award**).
5. **Swapna Sasi U S & Raghu K G.** High fructose and palmitate induced lipid accumulation with mitochondrial dysfunction revealing the possible significance of bioenergetics in the genesis of liver diseases at International Conference of Indian Academy of Biomedical Sciences (IABSCON) on 27th-29th February 2020 at D.Y.Patil Medical College at Kolhapur, Maharashtra.

Oral paper presentation:

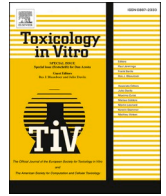
1. **Swapna Sasi U S & Raghu K G.** High calorie induce hepatopathology *via* mitochondrial dysfunction: An *in vitro* approach at International Conference on Deliberation on Translation of Basic Scientific Insights into Affordable Health care Products (IABSCON), on 25th-27th February 2019 at CSIR - National Institute for Interdisciplinary Science & Technology, Trivandrum.



Contents lists available at [ScienceDirect](#)

Toxicology in Vitro

journal homepage: www.elsevier.com/locate/toxinvit



Corrigendum

Corrigendum to 'Fructose-palmitate based high calorie induce steatosis in HepG2 cells via mitochondrial dysfunction: An *in vitro* approach' [Toxicology in Vitro 68 (2020) 104952]

U.S. Swapna Sasi ^{a,b}, G. Sindhu ^a, K.G. Raghu ^{a,b,*}

^a Biochemistry and Molecular Mechanism Laboratory, Agro-Processing and Technology Division, CSIR- National Institute for Interdisciplinary Science and Technology (NIIST), Thiruvananthapuram, Kerala 695019, India

^b Academy of Scientific and Innovative Research (AcSIR), Ghaziabad, Uttar Pradesh 201002, India

The authors regret < ^bAcademy of Scientific and Innovative Research (AcSIR), Ghaziabad, Uttar Pradesh, 201,002, India >.

The authors would like to apologise for any inconvenience caused.

DOI of original article: <<https://doi.org/10.1016/j.tiv.2020.104952>>.



DOI of original article: <https://doi.org/10.1016/j.tiv.2020.104952>.

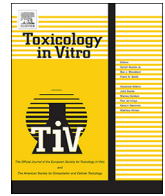
* Corresponding author at: Biochemistry and Molecular Mechanism Laboratory, Agro-Processing and Technology Division, CSIR - National Institute for Interdisciplinary Science and Technology (NIIST), Industrial Estate P.O., Pappanamcode, Thiruvananthapuram, Kerala 695019, India.

E-mail address: raghukgopal@niist.res.in (K.G. Raghu).

<https://doi.org/10.1016/j.tiv.2021.105177>

Available online 22 April 2021

0887-2333/© 2020 Elsevier Ltd. All rights reserved.



Fructose-palmitate based high calorie induce steatosis in HepG2 cells via mitochondrial dysfunction: An *in vitro* approach

U S Swapna Sasi^{a,b}, G Sindhu^b, K.G. Raghu^{a,b,*}

^a Academy of Scientific & Innovative Research (AcSIR), CSIR-HRDC, Ghaziabad, Uttar Pradesh 201002, India

^b Biochemistry and Molecular Mechanism Laboratory, Agro-processing and Technology Division, CSIR-National Institute for Interdisciplinary Science and Technology (NIIST), Thiruvananthapuram, Kerala, 695019, India

ARTICLE INFO

Keywords:

Fructose
Mitochondria
Non-alcoholic fatty liver disease
Palmitate
Steatosis

ABSTRACT

A proper *in vitro* model for conducting research on high energy food induced steatosis via defective energy metabolism in the liver is not visible in the literature. The present study developed an *in vitro* model in HepG2 cell line to mimic high energy diet induced steatosis in liver via mitochondrial dysfunction. For this, HepG2 cells were treated with fructose (100 mM) and palmitate (100 μ M) for about 24 h and subjected for biochemical analysis relevant to lipogenesis and mitochondrial biology. Our findings showed that fructose-palmitate treatment caused significant lipid accumulation and rise in lipogenic proteins. Further studies showed alteration in mitochondrial integrity, dynamics and oxidative phosphorylation. Mitochondrial integrity was affected by the dissipation of trans-membrane potential, surplus mitochondrial superoxide with calcium overload. Similarly, mitochondrial dynamics were altered with up regulation of mitochondrial fission proteins: DRP1 and FIS1, cytochrome *c* release, caspase-3 activity and apoptosis. Various components of the electron transport chain: complex I, II, III and IV were altered with significant depletion in oxygen consumption. Overall our findings illustrate the dominant role of mitochondria in the genesis of high fructose-palmitate induced steatosis in HepG2 cells. Since continuous high energy food consumption is the main inducer of steatosis, this model is found to be an ideal one for preliminary and basic research in the area of liver disease via mitochondrial dysfunction.

1. Introduction

The biological impact of diet in the pathogenesis of NAFLD has been thoroughly demonstrated. The majority of people of the modern world are pursuing an unhealthy dietary pattern and a sedentary lifestyle. A shift from the conventional homemade food to a refined and attractive one in a very colorful packet with ready to use options is one of the causes for the high prevalence of lifestyle-related diseases. The consumption of high-calorie foods, widely known as junk foods or empty calorie foods, is now the attraction of the new generation. It not only affects the absorption and storage of nutrients but also leads to the development of chronic diseases like obesity, diabetes, cardiovascular diseases, fatty liver diseases *etc.*

NAFLD is a chronic condition responsible for most of the morbidity

and mortality related to liver disease. It represents a spectrum of hepatic steatosis, liver fibrosis, liver cirrhosis, and hepatocellular carcinoma. NASH is the earliest stage of NAFLD and is characterized by excessive hepatic triglyceride concentration exceeding 5.5% (55 mg/g liver) (Szczeplaniak *et al.*, 2005). This is also accompanied by lobular inflammation, hepatocyte ballooning, fibrosis (Day, 2002) and over expression of inflammatory cytokines (Tilg and Diehl, 2000; Situnayake *et al.*, 1990). About 30% of the general populations in Western countries are affected by NAFLD and it is perceived as the common cause of liver dysfunction worldwide (Chalasanani *et al.*, 2012). Variation in food habits such as replacement of fresh fiber-rich foods by processed foods, foods rich in saturated fats like palmitate and added sugars principally in the form of HFCS plays an exaggerated role in the development of NAFLD. It is proved that fructose causes deleterious effects on appetite

Abbreviations: ACC, acetyl-CoA carboxylase; DCPIP, dichlorophenolindophenol; MEM, minimum essential medium; DMSO, dimethyl sulfoxide; EDTA, ethylenediaminetetraacetate; ETC, electron transport chain; FAS, fatty acid synthase; FBS, fetal bovine serum; H₂O₂, hydrogen peroxide; HBSS, Hank's balanced saline solution; HepG2, Hepatocellular carcinoma cells; HFCS, high fructose corn syrup; HFP, high fructose and palmitate; JC-1, 5,5',6,6'-tetrachloro-1,1',3,3'-tetraethylbenzimidazole carbocyanine iodide; MTT, dimethylthiazol-2-yl]-2,5 diphenyl tetrazolium bromide; NAFLD, non-alcoholic fatty liver disease; NASH, non-alcoholic steatohepatitis; NRF2, nuclear factor erythroid-2-related factor; OXPHOS, oxidative phosphorylation; pACC, phosphorylated ACC; PBS, phosphate buffer saline; PGC-1 α , peroxisome proliferator – activated receptor gamma coactivator 1 α ; TG, triglyceride

* Corresponding author at: Academy of Scientific & Innovative Research (AcSIR), CSIR-HRDC, Ghaziabad, Uttar Pradesh 201002, India.

E-mail addresses: swapnaussasi@gmail.com (U.S. Swapna Sasi), sindhu.ganapathy@gmail.com (G. Sindhu), raghukgopal@niist.res.in (K.G. Raghu).

<https://doi.org/10.1016/j.tiv.2020.104952>

Received 29 April 2020; Received in revised form 10 July 2020; Accepted 23 July 2020

Available online 27 July 2020

0887-2333/ © 2020 Elsevier Ltd. All rights reserved.

regulation (Stanhope et al., 2013). Along with palmitate, fructose is highly lipogenic and readily contributes to insulin resistance and hepatic inflammation (Miller and Adeli, 2008). Moreover, fructose metabolism primarily takes place in the liver where it can be stored in the form of triglycerides (Softic et al., 2016). The continuous consumption of fructose may cause metabolic strain on the liver through the induction of fatty acid synthase and fructokinase (Chong et al., 2007).

There are certain studies revealing the role of mitochondria in the genesis of NAFLD in animal models. It has been reported that inhibition of mitochondrial fission enhances proton leak under conditions of free fatty acid incubation, implicating bioenergetic change (Galloway et al., 2014). In the mouse model of NAFLD, the decreased stability of OXPHOS subunits contributes to deficiency in ATP synthesis via the inhibition of ubiquitin-proteasome and mitophagy activation (Lee et al., 2018). Microvesicular steatosis was established in precision-cut liver slices in liver tissues of male Wistar rats, cultured in supraphysiological concentrations of glucose, fructose, insulin, and palmitic acid to mimic metabolic syndrome (Prins et al., 2019).

Nevertheless, one of the major issues in the present research in liver steatosis is the lack of proper *in vitro* models to extrapolate the role of diet in the induction of obesity and molecular mechanisms. Fast and affordable *in vitro* models are essential during the initial period of research to save the time and expenditure of research. The result of *in vitro* experiments is also a turning point in designing a final *in vivo* experiment with a well focused target. Herein, we conduct an *in vitro* mechanistic study to see how fructose and palmitate (mimics high energy diet) induce biochemical lesions of NAFLD through involvement of mitochondrial dysfunction in HepG2 cells. Detailed investigations linking various functions of mitochondria such as calcium homeostasis, bioenergetics, redox status are conducted here to elucidate the molecular and cellular mechanism underlying the genesis of steatosis via high calorie diet. This is essential for identifying suitable targets for the design and development of drugs for NAFLD.

2. Materials and methods

2.1. Materials

The cell culture flasks and plates were from BD Biosciences (USA). FBS, penicillin-streptomycin antibiotics, trypsin - EDTA, HBSS and PBS were from Gibco, USA. MTT, JC-1, fructose, sodium palmitate, DMSO and oil-red-O stain were purchased from Sigma-Aldrich Co. (St. Louis, MO, USA). The triglyceride assay kit was purchased from Cayman chemical company (MI, USA). MitoSOX™ red and Fura 2-AM were from Invitrogen (Carlsbad, CA, USA). Antibodies against ACC, pACC, FAS, OPA1, MFN2, DRP1, FIS1 and β -actin were obtained from Santa Cruz biotechnology (CA, USA). Anti PGC1 α , anti SIRT1, anti NRF2, anti-cytochrome *c* was from Abcam. All other chemicals were of analytical grade.

2.2. Cell culture

HepG2 cells from American Type Culture Collection were cultured and maintained in growth medium MEM supplemented with 10% heat-inactivated FBS and 1% penicillin/streptomycin solution. The cells were cultured in a humidified atmosphere with 5% CO₂ and 37 °C. Cultures were used at 80% confluency. For sub culturing, the cells were washed with pre-warmed PBS and detached by treating with 0.25% trypsin. The experimental groups consist of (a) control group (assuming HepG2 cells without treatment), (b) positive control group (cells treated with HFP + 25 μ M fenofibrate), (c) high fructose and palmitate treated group (indicated as HFP). All the experiments were performed after 24 h of treatment.

2.3. Preparation of fructose and BSA-palmitate complex

Fructose stock solution was prepared by dissolving in HBSS. Working concentration of 100 mM was prepared by diluting the stock concentration in 1% MEM. Palmitate stock solution (10 mM) was prepared by dissolving sodium palmitate in 0.1 N NaOH at 75 °C for 5 min. The stock solution was then mixed with fatty acid free BSA (10% in MEM) to make a final concentration of 1 mM. The solution was then diluted in 1% culture media to give a final concentration of 100 μ M.

2.4. Cell viability assay

To determine the cell viability, MTT assay was performed after treating the cells with fructose and palmitate. This assay relies on the enzymatic reduction of 3-[4,5-dimethylthiazole-2-yl]-2,5-diphenyltetrazolium bromide to MTT formazan catalyzed by the enzyme mitochondrial succinate dehydrogenase.

For this, HepG2 cells were seeded in 96-well plates at a density of 5×10^3 per well. The cells were then treated with different combinations of HFP for about 24 h. After incubation, 100 μ L of MTT solution (5 mg/mL) was added to each well and incubated for another 4 h at 37 °C. The solution was dislodged from each well, and 100 μ L of DMSO was added. The culture plates were placed on a shaker for about 20 min. The blue-colored tetrazolium crystals were dissolved in DMSO. Then the absorbance was measured at 570 nm in a spectrophotometer (Biotek Synergy 4, USA).

2.5. Oil-red-O staining

The lipophilic dye oil-red-O is used for the detection of intracellular lipid droplets accumulation. After respective treatments, the cells were washed twice with PBS and fixed in 4% paraformaldehyde. After fixation, the cells were washed with PBS and permeabilized using 0.1% Triton X 100, followed by oil-red-O staining for 20 min at room temperature. The cells were then visualized under a light microscope.

2.6. Triglyceride colorimetric assay

To evaluate the extent of steatosis in cells from various groups, the concentration of triglyceride was measured using triglyceride colorimetric assay kit. This assay explores the enzymatic hydrolysis of triglycerides by lipases to produce glycerol and free fatty acids. The glycerol thus formed is phosphorylated and converted to glycerol-3-phosphate by glycerol kinase. Glycerol-3-phosphate undergoes oxidation to produce dihydroxyacetone phosphate and H₂O₂. The presence of peroxidase catalyzes the redox-coupled reaction of H₂O₂ with 4-aminoantipyrine and N-ethyl-N-(3-sulfopropyl)-m-anisidine, producing a bright purple colour. The absorbance was measured at 530–550 nm.

2.7. Detection of mitochondrial superoxide production

The production of mitochondrial superoxide was visualized by using fluorogenic dye, MitoSOX™, which is rapidly and selectively targeted to the mitochondria in live cells. It is immediately oxidized by mitochondrial superoxide and the resulting product is extremely fluorescent upon binding to the nucleic acid. Briefly, 5×10^3 cells were seeded in 96-well black plates, a solution of MitoSOX™ in HBSS was added to the treated cells and incubated at 37 °C for 20 min. After incubation, the cells were then washed with HBSS and fluorescent images were captured with a fluorescent microscope (BD Pathway™ Bioimager system, USA) at excitation/emission range of 514/580 nm.

2.8. Analysis of change in mitochondrial membrane potential ($\Delta\Psi_m$)

$\Delta\Psi_m$ was observed by using JC-1 mitochondrial membrane potential assay kit that utilizes a cationic carbocyanine dye called JC-1, a

sensitive marker for determining the mitochondrial membrane potential. In healthy cells, the mitochondrial membrane is in a highly polarized state; JC-1 dye accumulates in the mitochondrial matrix and develops an aggregate of red fluorescence. In early apoptotic cells, the membrane potential is highly depolarized, resulting in the development of the monomeric green fluorescent form of JC-1 in the cytosol. Briefly, the cells after seeding and treatment were incubated with JC-1 stain for about 20 min. The stains were washed off with HBSS and visualized under the spinning disk imaging system (BD Pathway™ Bioimager system, USA). The fluorescence of JC-1 monomers was measured at a wavelength of 490 nm excitation and 530 nm emissions and for JC-1 aggregates, the excitation/emission wavelength ranges from 525 and 590 nm respectively. Valinomycin (1 µg/mL) was used as a negative control.

2.9. Mitochondria isolation

After respective treatments, approximately 3×10^7 cells were homogenized in mitochondrial isolation buffer (10 mM Tris (pH 7.4), 250 mM sucrose, 0.15 mM MgCl₂). The homogenate was then subjected to centrifugation at $800 \times g$ for 5 min at 4 °C. To obtain mitochondria enriched pellet, the supernatant was centrifuged at $10,000 \times g$ for 100 min. The pellets were again centrifuged at $12,000 \times g$ for 10 min, pooled, washed and resuspended in a 50 mM/L phosphate buffer (pH 7.0). It was then frozen and thawed 3–5 times to discharge the mitochondrial enzymes for activity measurement.

2.10. Determination of the activity of mitochondrial respiratory complexes

The effect of HFP on complex I (NADH dehydrogenase) was assessed by spectrophotometrically using the reaction mixture containing 200 µM menadione and 150 µM NADH prepared in phosphate buffer (0.1 M, pH 8.0). The variation in absorbance at 340 nm for 8 min was monitored.

The activity of complex II (succinate dehydrogenase) was measured with the help of an artificial electron acceptor, dichlorophenolindophenol and succinate as substrate. The mitochondria were added to a mixture of 10 mM EDTA, 20 mM of succinate, 50 µM DCPIP, and 0.1 M phosphate buffer (pH 7.4). The change in absorbance was recorded immediately for 8 min at 30 °C.

Complex III (Ubiquinol-cytochrome reductase) activity was determined as per the method described previously (Chong et al., 2007). In short, mitochondria were mixed with 100 µM/L EDTA, 3 mmol/L sodium azide, 2 mg BSA, 60 µM/L ferricytochrome *c*, decylubiquinol (1.3 mM) and phosphate buffer (50 mM, pH 8) in a final volume of 1 mL. Decylubiquinol was added to initiate the reaction. The activity was monitored for 2 min at 550 nm and activity of complex III was expressed as mmoles of ferricytochrome *c* reduced/min/mg protein.

The activity of complex IV (cytochrome *c* oxidase) was evaluated as per the previous method (Sudheesh et al., 2009). 50 µg of mitochondrial protein was mixed with 1 mL of ferrocyanide solution in phosphate buffer (30 mM, pH 7.4). The reaction was initiated by the addition of an enzyme source and was monitored at 550 nm with an interval of 15 s for 4 min. The oxidation of reduced cytochrome *c* was monitored at 550 nm and expressed as activity of micromoles of ferrocyanide oxidized/min/mg protein.

2.11. Oxygen consumption assay

The oxygen consumption rate was determined by Cayman's cell-based oxygen consumption rate assay kit, using Antimycin A as a standard inhibitor (inhibitor of complex III). The rate of oxygen consumption in live cells was measured by using a phosphorescent oxygen probe called MitoXpress®-Xtra. The molecular oxygen in live cells quenches the fluorescent signal of MitoXpress, and the signal is

inversely proportional to the extent of oxygen present in the media. Briefly, 5×10^3 cells were seeded in 96-well black plate and after respective treatments, MitoXpress solution was added to all wells except the blank wells. The wells were then covered with HS mineral oil and fluorescence was read at an excitation/emission rate of 380/650 nm, respectively for 150 min.

2.12. Aconitase activity

Aconitase assay measures the absorbance of NADPH, which is generated in the coupled reactions of aconitase with isocitrate dehydrogenase. The rate of NADPH thus generated is directly proportional to the aconitase activity. Briefly, after treatment the cells were washed and covered with enough cold PBS and incubated the cells for about 10 min at 4 °C. Then the cells were collected and centrifuged at $800 \times g$ for 10 min at 4 °C. The pellet is then resuspended in cold assay buffer and sonicated at $20 \times$ at 1 s bursts. The reactions were initiated by adding 50 µL of diluted substrate solution. The absorbance was measured once every minute at 340 nm for 30 min at 37 °C.

2.13. Intracellular calcium content

Calcium content was detected by staining the cells with Fura2-AM, a high-affinity intracellular calcium indicator. Briefly, 5×10^3 cells were seeded in 96-well black plates and after treatment, cells were incubated with Fura 2-AM (5 µM) for 1 h at 37 °C. After incubation, the cells were washed with HBSS and visualized (BD Pathway™ Bioimager system, USA) at excitation and emission wavelengths of 340 and 510 nm respectively.

2.14. Caspase-3 fluorometric assay

Apoptosis was assessed by using caspase-3 fluorometric protease assay kit (Biovision, USA). Briefly, the treated cells were resuspended in a chilled lysis buffer and incubated on ice for 10 min. It is followed by the addition of 50 µL of reaction buffer to each sample and 5 µL of 1 mM (Asp-Glu-Val-Asp)-7-amino-4-trifluoromethylcoumarin (DEVD-AFC) substrate. The mixture was then incubated for about 1 h at 37 °C. The samples were read at excitation and emission wavelengths of 400 nm and 505 nm, respectively.

2.15. Flow cytometric analysis with annexin V/PI

Quantification of apoptotic cells was done by using the annexin V-FITC apoptosis detection kit (Biovision, USA). After respective treatments, cells were collected by centrifugation. The cells were then resuspended in 500 µL of binding buffer, followed by the addition of 5 µL of Annexin V-FITC and 5 µL of propidium iodide and incubated at room temperature for 5 min in the dark. Annexin V-FITC binding was analyzed by flow cytometry (Ex = 488 nm; Em = 530 nm) using FITC signal detector (usually Fluorescence 1) and PI staining by the phycoerythrin emission signal detector (usually Fluorescence 2).

2.16. Western blot analysis

After respective treatments, proteins were extracted from cell lysates using an ice-cold radio immunoprecipitation assay buffer containing a protease inhibitor cocktail. The cell suspension was centrifuged at 12,000 rpm for 20 min at 4 °C. Protein content in the supernatant was estimated by bicinchoninic acid protein assay kit as per manufacturer's instructions. Proteins thus extracted were separated by sodium dodecyl sulfate polyacrylamide gel electrophoresis and transferred to polyvinylidene difluoride membranes. The membrane was blocked with 5% skimmed milk in TBST for 1 h at room temperature. The membranes were probed with antibodies followed by incubation with HRP conjugated secondary antibodies. After washing,

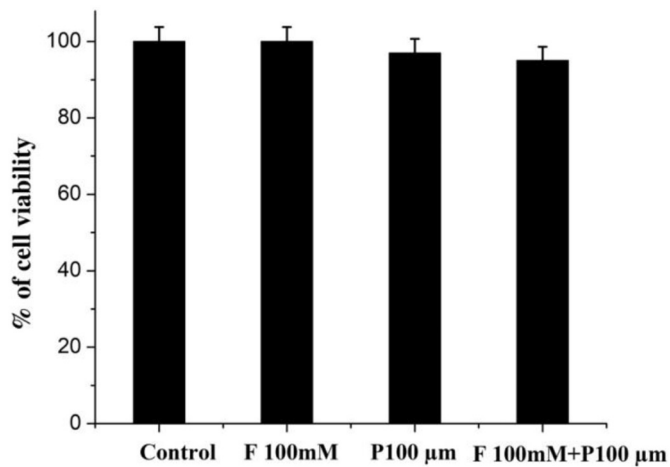


Fig. 1. Cell viability assay. HepG2 cells were exposed to fructose (F 100 mM) and palmitate (P 100 μM) for 24 h. Then the cells were subjected to MTT assay. Data are expressed as mean \pm SD, where $n = 6$.

the membrane was developed using Clarity™ Western ECL Substrate (BIO-RAD, USA). The immunoblot images were analyzed in the ChemiDoc XRS system using Image Lab software.

2.17. Statistical analysis

Data are expressed as mean \pm SD. Data were analyzed using *t*-tests with Bonferroni-Dunn *post hoc* correction when multiple comparisons were performed on data followed by Duncan's multiple range tests using SPSS for Windows standard version 7.5.1 (SPSS, Inc.). Significance was defined as $p \leq .05$.

3. Results

3.1. HFP does not affect cell viability of HepG2 cells

The effect of fructose and palmitate on HepG2 cells was analyzed after 24 h of incubation and cell viability was checked by MTT assay. There is no significant cell death occurring in treated groups. (Fig. 1).

3.2. HFP induces steatogenesis effect in HepG2 cells

Exposure of HepG2 cells to HFP caused a significant increase (576.66%, $p \leq .05$) in the accumulation of intracellular lipid droplets compared to the control group (Fig. 2A, B). The increased lipid accumulation was distinctly visible in cells stained with oil-red-O stain. Incubation of the fenofibrate along with the HFP group significantly reduced the steatosis (276.66%, $p \leq .05$) compared to HFP.

We further measured the TG content in the steatotic hepatocytes to confirm the results obtained from oil-red-O staining. The exposure to HFP resulted in a significant increase in TG accumulation (173.69%, $p \leq .05$) in HepG2 cells compared to the control group. Treatment with fenofibrate prevented TG accumulation by 153.69% ($p \leq .05$), (Fig. 2C) compared to HFP.

ACC- α and FAS are pivotal enzymes involved in the biogenesis of fatty acids and key modulators of fatty acid oxidation. The expression of ACC- α and FAS was increased significantly (240.93% and 568.05%, $p \leq .05$) respectively, (Fig. 2D) after 24 h of incubation with HFP. The expression levels of these proteins were significantly reduced by 177.97% and 426.35% respectively with fenofibrate treatment ($p \leq .05$) compared to HFP. However, the expression level of the phosphorylated form of ACC- α was significantly reduced in HFP groups (27.33%, $p \leq .05$) compared to control but increased in fenofibrate treated cells (56.42%, $p \leq .05$) (Fig. 2D) compared to HFP.

3.3. Impact on mitochondrial function

3.3.1. HFP causes mitochondrial superoxide production and dissipation of $\Delta\Psi_m$

Mitochondria are the fundamental sites for ROS production. An excess amount of mitochondrial superoxide production culminates in cell destruction and death. The mitochondrial superoxide production was higher in HFP treated cells (566%, $p \leq .05$) compared with the control group. A significant decrease in superoxide production (200%, $p \leq .05$) was observed in cells treated with fenofibrate (Fig. 3A, B).

The $\Delta\Psi_m$ of control, HFP + fenofibrate and HFP treated cells were depicted in Fig. 3. The JC-1 dye with normal membrane potential forms red fluorescence in the control group (81.31%, $p \leq .05$). The presence of HFP in the medium dissipates the membrane potential, leading to drift from red to green fluorescence. On the other hand, fenofibrate treatment prevented the alteration significantly in the membrane potential by 61.79% ($p \leq .05$), (Fig. 3C,D) compared to HFP.

3.3.2. HFP adversely affects mitochondrial bioenergetics and aconitase activity during steatosis

The activities of mitochondrial respiratory complexes such as NADH dehydrogenase (complex I), succinate dehydrogenase (complex II), ubiquinol-cytochrome reductase (complex III), cytochrome *c* oxidase (complex IV) were decreased drastically with HFP treatment (61.79%, 58.07%, 38.72%, 50.63%, $p \leq .05$) respectively, compared to control. However, treatment with fenofibrate prevented the sharp decrease of complex activities compared to HFP cells by 36.74% (complex I), 46.71% (complex II), 17.78% (complex III), and 35.28% (complex IV) (Fig. 4A, B, C, D). Oxygen consumption rate in HepG2 cells was interpreted by using a phosphorescent probe, mitoXpress. The fluorescent signal over time is directly proportional to the oxygen consumption rate in cells. The oxygen consumption rate in HFP treated HepG2 cells showed significant reduction (53.4%; $p \leq .05$) compared to the control group (Fig. 4E.), and treatment with fenofibrate improved the condition (28.51%, $p \leq .05$) compared to the HFP group. The activity of aconitase was reduced drastically during HFP condition (76.76%, $p \leq .05$) compared to control. Here also, fenofibrate treatment prevented the sharp fall by 40.49% (Fig. 4F) compared to HFP.

3.3.3. HFP induces imbalance in mitochondrial dynamics and reduces biogenesis

With HFP treatment the expression level of mitochondrial fission proteins such as DRP 1 and FIS 1 was found significantly increased by 27.18% and 277.37% ($p \leq .05$) respectively, whereas the expression of fusion proteins (MFN2 and OPA1) were decreased by 198.18% and 36.67% ($p \leq .05$) respectively (Fig. 5A, B) compared to control. On the other hand, treatment with fenofibrate remarkably reversed the expression of proteins compared to the HFP group (16.88%, 219.71%, 136.55%, and 30.06%, $p \leq .05$ accordingly).

PGC-1 α is the major transcriptional factor that performs a central role in determining the modulation of mitochondrial biogenesis and respiratory function. With HFP incubation expression of PGC-1 α was decreased by 62.59% ($p \leq .05$) compared to the control group. The presence of fenofibrate improves its expression level by 61.36% ($p \leq .05$) compared to HFP group (Fig. 5C). Sirtuins play a significant role in hepatic lipid metabolism and ensure protection from the steatotic condition. HFP treatment reduced its expression level by 77.28% compared to the control group. Co-treatment with fenofibrate enhanced the expression level by 71.3% compared to the HFP group ($p \leq .05$; Fig. 5C). The expression of NRF-2 is found to be reduced by 72.59% with HFP compared to control and improved by 77.65% by fenofibrate. HFP treatment also caused an increase in the expression of cytochrome *c* (143.22%, $p \leq .05$) compared to control. Fenofibrate significantly prevented its over expression by 92.59% (Fig. 5C) compared to HFP.

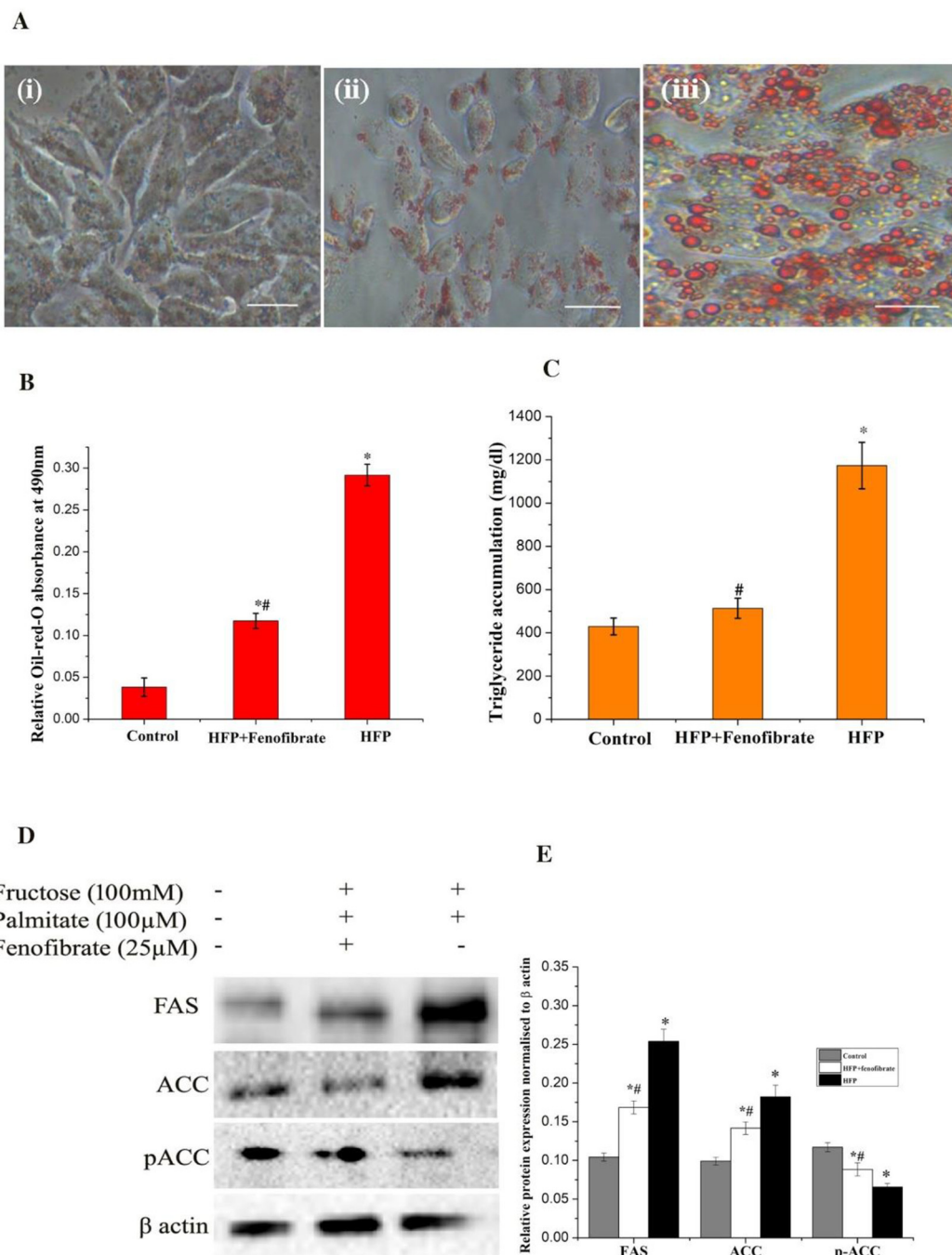


Fig. 2. HFP induces steatogenesis effect in HepG2 cells: (A) Microscopic images of HepG2 cells with Oil-red-O-staining from different experimental groups under phase contrast microscope (Magnification 40×). (i) Control cells; (ii) Cells treated with HFP + Fenofibrate; (iii) Cells treated with HFP. (B) Absorbance was read at 490 nm after oil-red-O staining. Data are expressed as mean ± SD; where $n = 6$. (C) Measurement of intracellular TG content in HepG2 cells. Absorbance was spectrophotometrically measured at 530 nm. Data are expressed as mean ± SD; where $n = 6$. (D) The protein expression of ACC- α , FAS and phosphorylated ACC- α during HFP condition. (E) The relative intensity of each band was quantified with β actin. Data are expressed as mean ± SD; where $n = 3$. * $p \leq .05$ significantly different from the control group. # $p \leq .05$ significantly different from the HFP treated group. Scale bar 50 μ m. (For interpretation of the references to colour in this figure legend, the reader is referred to the web version of this article.)

3.3.4. HFP affects intracellular calcium homeostasis and initiates apoptosis via caspase3 activation

The intracellular calcium content in HFP treated cells was increased (17%, $p \leq .05$), which was obvious from the elevated fluorescence of Fura-2 AM compared to the control group (Fig. 6A,B). Fenofibrate treatment significantly reduced the calcium overload (5.79%, $p \leq .05$) compared to the HFP group. The activity of caspase-3 was increased significantly in HFP treated HepG2 cells (42.20%; $p \leq .05$), compared to control, while fenofibrate protected the fall of caspase activity by

30.74%, $p \leq .05$), (Fig. 6C) in HFP treated cells. Moreover, there was a slight increase in the number of apoptotic cells following HFP treatment compared with the control group. The results of Annexin V-PI staining revealed that the quadrant of early and late apoptotic cells increased slightly following the exposure to HFP to about 3.1% compared to control. However, treatment with fenofibrate reversed the trend (Fig. 6D) compared to HFP.

A

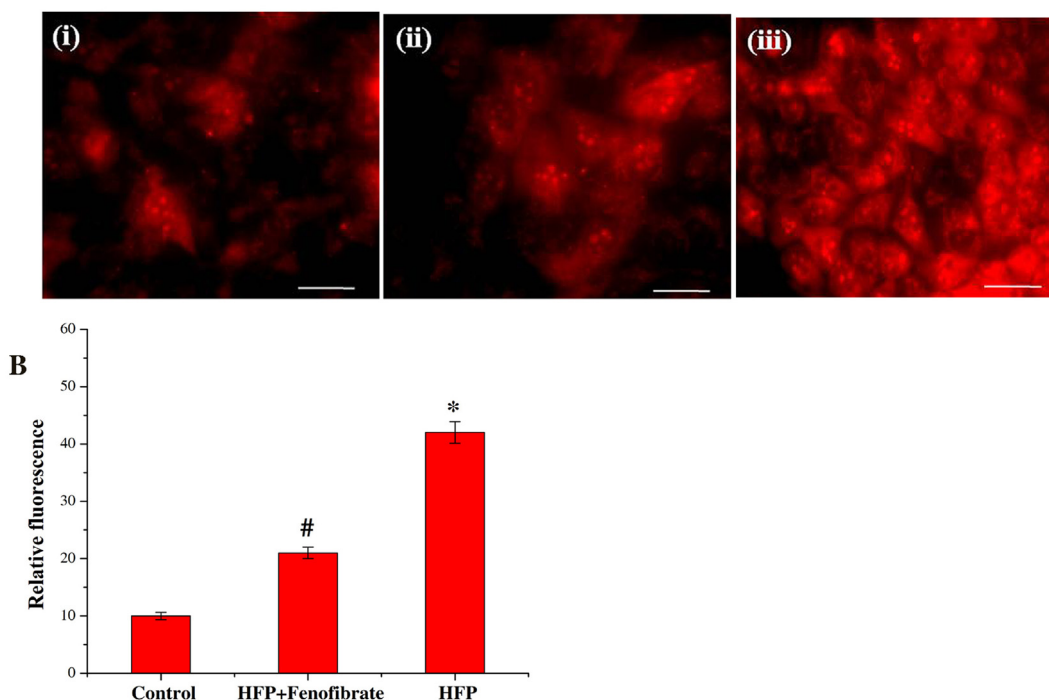


Fig. 3. HFP causes mitochondrial superoxide production and dissipation of $\Delta\Psi_m$: The fluorescent microscopic images of cells stained with MitoSOX™ Red indicator. (i) Control cells; (ii) Cells treated with HFP + fenofibrate; (iii) Cells treated with HFP. (B) Fluorescence intensity emitted by MitoSOX™ in control and treated cells. Data are expressed as mean \pm SD; where $n = 6$. (C) The representative images show JC-1 aggregates, JC-1 monomers and merged images. The HepG2 cells with normal membrane potential are indicated by red JC-1 intensity regions and cells with diminished membrane potential are indicated by green JC-1 intensity regions. (i) Control cells: JC-1 aggregates are more in control cells revealing intact mitochondria; (ii) Cells treated with HFP + fenofibrate: The elevation of JC-1 aggregates and reduction in JC-1 monomers in fenofibrate treated cells reveals its potential role to protect mitochondrial membrane from depolarization. (iii) Cells treated with HFP: The abundance of JC-1 monomers in HFP treated cells shows significant variation from the normal membrane potential. (iv) Valinomycin treated cells (negative control). (D) The graphical representation of JC-1 aggregates to JC-1 monomers (ratio of 590:530 nm emission intensity). Data are expressed as mean \pm SD; where $n = 6$. * $p \leq .05$ significantly different from the control group. # $p \leq .05$ significantly different from the HFP treated group. Scale bar 50 μ M. (For interpretation of the references to colour in this figure legend, the reader is referred to the web version of this article.)

4. Discussion

NAFLD is the most prevalent chronic liver disease in the modern world. The factors that favor the progression of NAFLD include genetic polymorphism, exposure to various xenobiotics, environmental contaminants, and various food items rich in sugars and fats. Since this has a multifactorial origin, identifying real causes is essential for a better understanding of the pathophysiology of genesis. For this, an ideal *in vitro* model is required to start any research on liver steatosis. Keeping this in mind, the present work was planned to develop a suitable model of high energy diet-induced steatosis in the liver utilizing HepG2 cells. The present study tried to reveal the role of alteration in bioenergetics during the genesis of high calorie induced steatosis in HepG2 cells. Mitochondria are central cytoplasmic organelles that provide excellent platforms for the maintenance of cellular homeostasis (Bagur and Hajnóczy, 2017). The disruption of cellular homeostasis plays a pivotal role in the progression of chronic liver diseases (García-Ruiz and Fernández-Checa, 2018; Mansouri et al., 2018). High fructose diet promotes the characteristic features of metabolic syndrome and fatty liver (Vasselli, 2008), vascular inflammation, and microvascular disease. Moreover, several aspects of fructose metabolism make it principally lipogenic. It enhances the protein levels of all lipogenic enzymes during its conversion into triglycerides. The direct activation of SREBP1c by fructose enhances the rate of *de novo* lipogenesis. The fructose also plays a vital role in the depletion of ATP and the inhibition of fatty acid oxidation. This in turn, increases the production of reactive oxygen species. Thus, disruption of fructose metabolism in the liver

may provide a new therapeutic option for steatosis. Palmitic acid is the most abundant saturated fatty acid, and in hepatocytes, it causes a concentration- and time-dependent lipoapoptosis. These toxic fatty acids activate mitochondrial permeabilization, promote the release of cytochrome c, and activate caspases 3 and 7. It also affects lipid storage and gene expression in the liver. Thus, chronic palmitic acid-enriched diet may be one of the major causes of NAFLD, including simple steatosis and hepatic injury.

Herein, we have described the role of fructose and palmitate in mitochondrial integrity, dynamics, and bioenergetics during hepatic steatosis. Our results demonstrate that incubation of HepG2 cells with HFP leads to the surplus accumulation of lipid droplets in HepG2 cells. During NASH, hepatic lipids are stored in TG form and this indicates the genesis of NAFLD in this study. Thus hypertriglyceridemia is a major characteristic feature associated with the spectrum of steatosis. We investigated the alterations of proteins involved in lipid biosynthesis at the molecular level. FAS, a multi-enzyme catalyzes the final step in fatty acid biosynthesis and synthesizes long-chain fatty acids by utilizing Acetyl-CoA. ACC- α is the key enzyme that modulates saturated fatty acid synthesis, highly inactive in its phosphorylated form. Under normal physiological conditions, the lipogenesis pathway is relatively low. It becomes active after an intense load of fructose and palmitate. Palmitate acts as a strong steatogenic agent together with fructose (Softic et al., 2016; Schwarz et al., 2015). In hepatocytes, uncontrolled entry and metabolism of fructose promotes significant amounts of carbohydrate to enter the glycolytic pathway and causes the production of excess acetyl-CoA. The consumption of HFP favors the accumulation

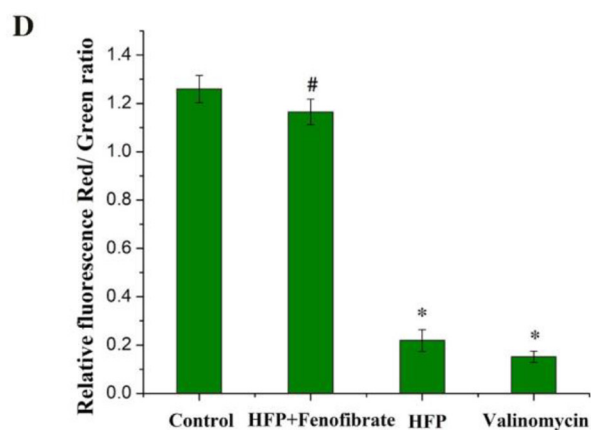
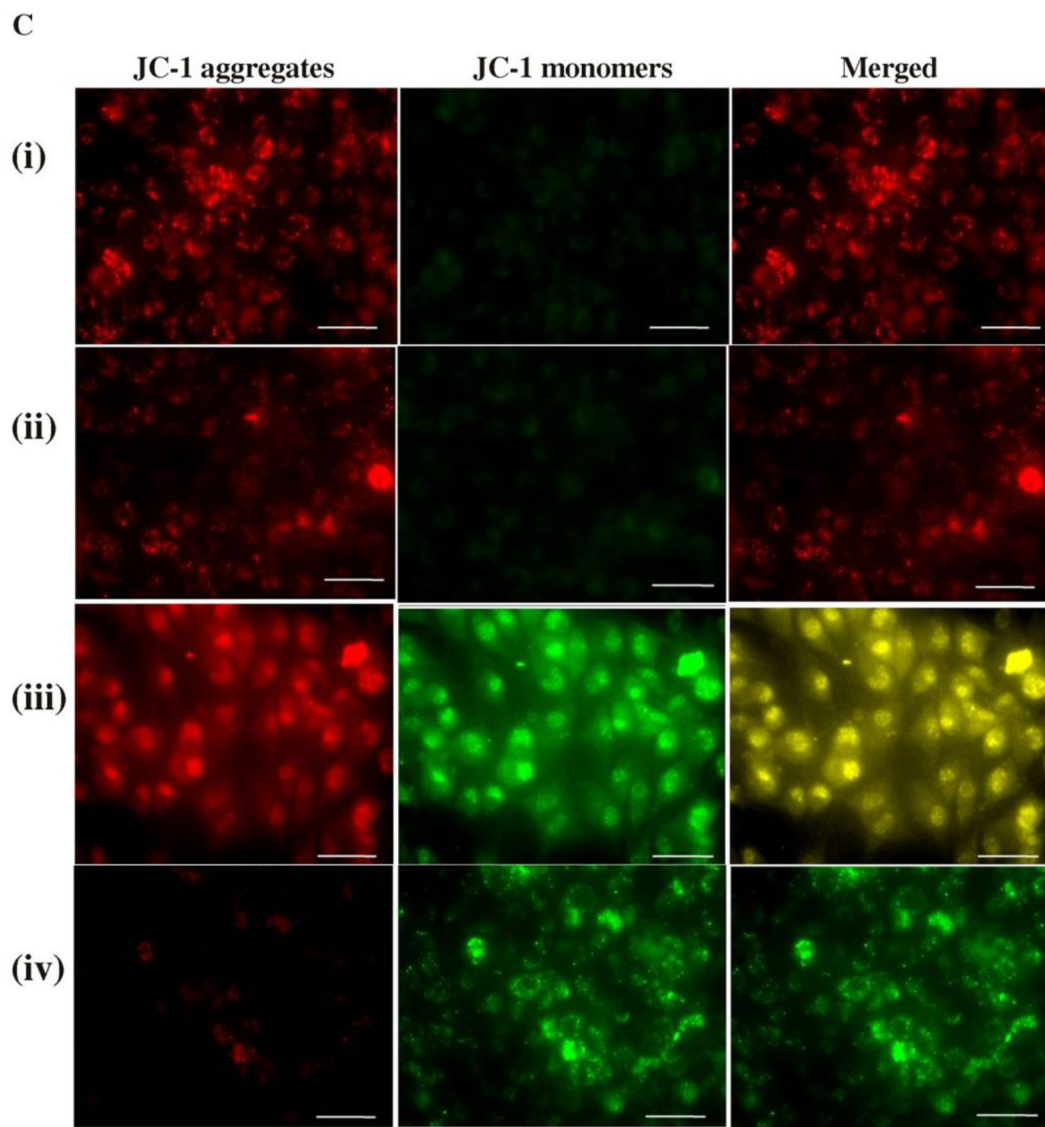


Fig. 3. (continued)

of glycolytic intermediates. These intermediaries are converted to glycerol-3-phosphate for triglyceride synthesis. In short, we found that HFP induces steatotic conditions with overexpression of FAS, ACC and downregulation of phosphorylated ACC- α .

The main objective of our study was to evaluate the effect of a high energy diet on the function of mitochondria and its contribution to the

development of steatosis. Hepatocytes host a large number of mitochondria (~500–4000 mitochondria per hepatocyte) (Degli Esposti et al., 2012). The maintenance of healthy mitochondria is an essential prerequisite for the proper functioning of the liver. For that, we studied integrity, dynamics and OXPHOS in detail. We found that HFP down-regulates antioxidant ability through the generation of reactive oxygen

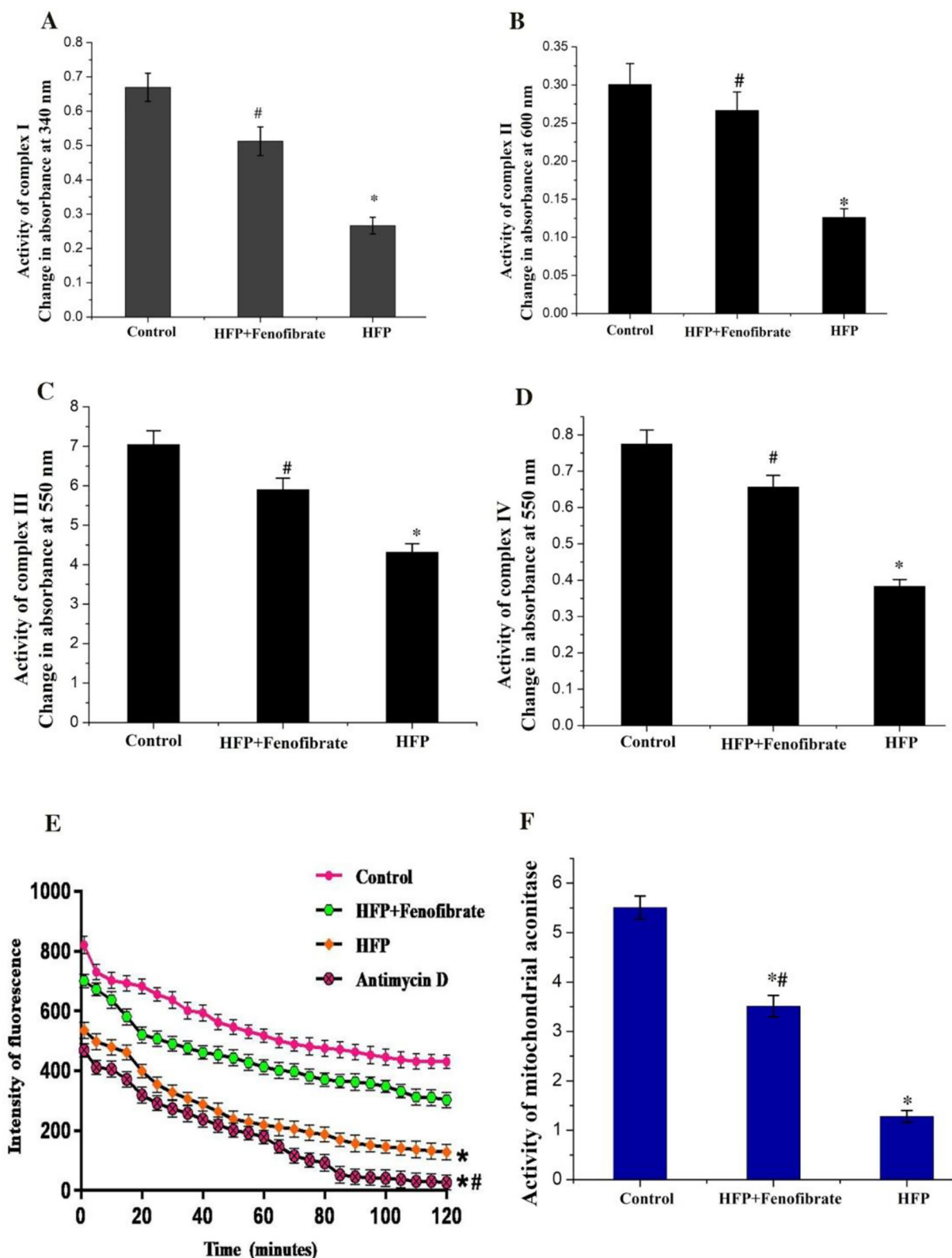


Fig. 4. HFP adversely affects mitochondrial bioenergetics and aconitase activity during steatosis: (A) Activity of mitochondrial respiratory complex 1 (B) complex 2 (C) complex 3 (D) complex 4 in HepG2 cells. Data are expressed as mean \pm SD; where $n = 6$. (E) Alteration in fluorescence indicates the variation in oxygen consumption rate. Data are expressed as mean \pm SD; where $n = 6$. (F) Activity of aconitase in HepG2 cells. Data are expressed as mean \pm SD; where $n = 6$. * $p \leq .05$ significantly different from the control group. # $p \leq .05$ significantly different from the HFP treated group.

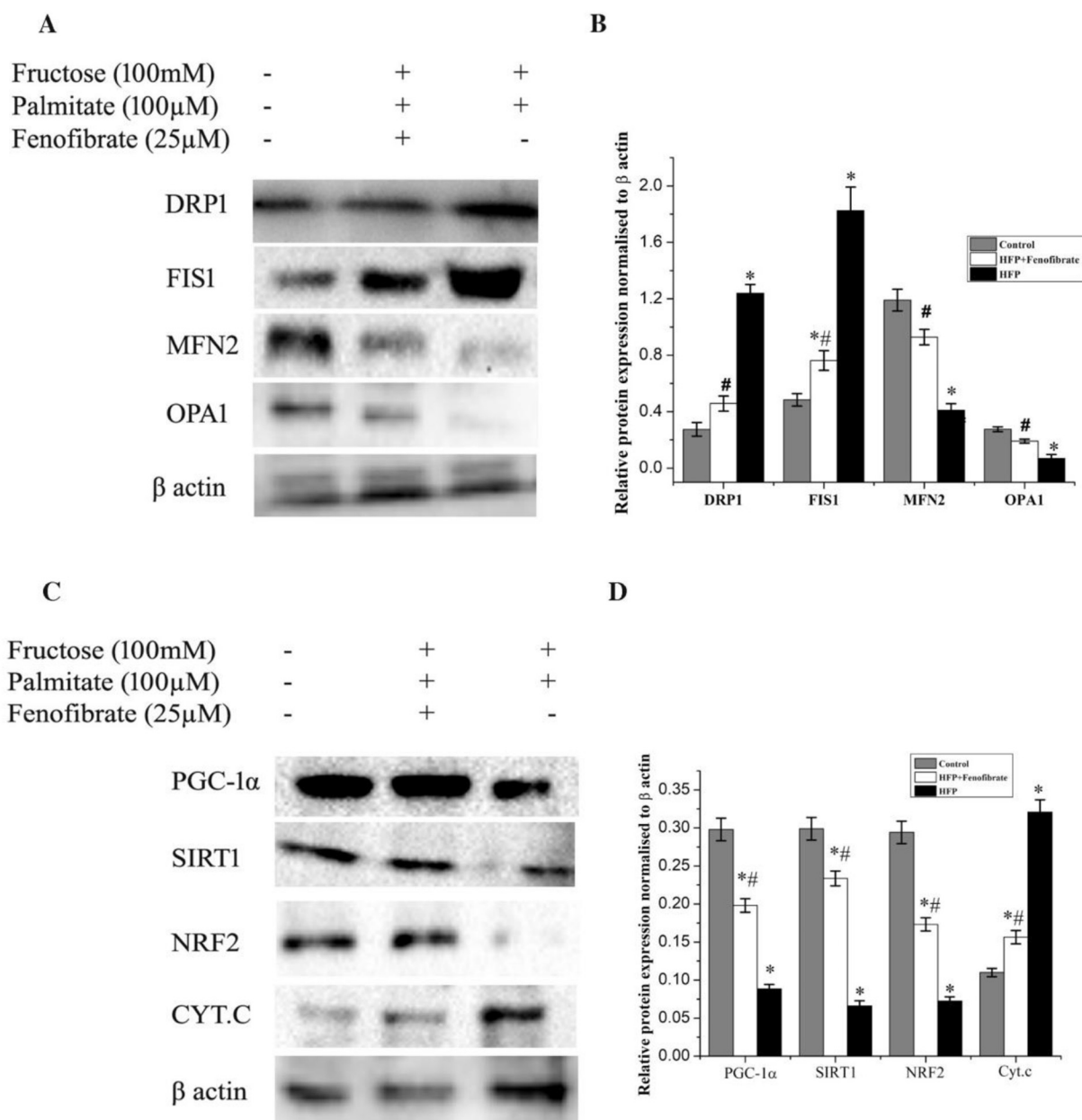


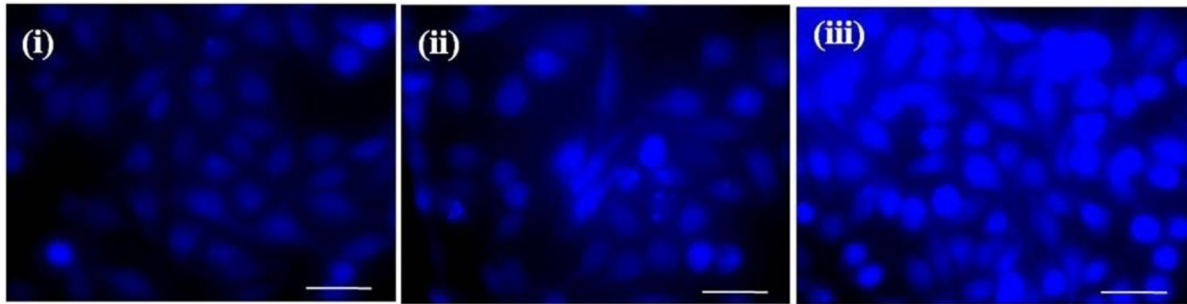
Fig. 5. HFP induces imbalance in mitochondrial dynamics and reduces biogenesis: (A) The protein expression of DRP1, FIS1, MFN2, and OPA1 during HFP condition. (B) The relative intensity of each band was quantified with β actin. Data are expressed as mean \pm SD; where $n = 3$. (C) The protein expression of PGC1 α , SIRT1, NRF2, and cytochrome c during HFP condition. (D) The relative intensity of each band was quantified with β actin. Data are expressed as mean \pm SD; where $n = 3$. * $p \leq .05$ significantly different from the control group. # $p \leq .05$ significantly different from the HFP treated group.

species. There are reports to link increased superoxide radical and hepatic steatosis (Sanyal et al., 2001) and also findings from other groups that fructose consumption exerts oxidative stress and damage (Brown et al., 2010; Teodoro et al., 2013) via liver glucokinase and reactive oxygen production. The role of mitochondrial superoxide in the initiation of steatosis is also reported (Mitchell et al., 2009). We found that HFP treatment resulted in $\Delta\Psi_m$ dissipation.

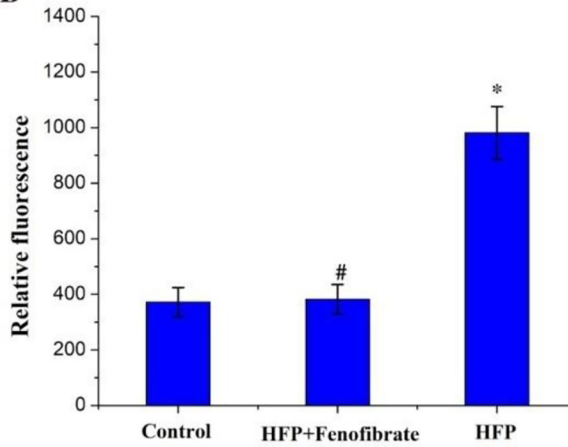
Alteration in $\Delta\Psi_m$ causes the onset of several pathological changes due to its profound influence in the control of the electrochemical gradient of mitochondria. We also analyzed the effect of HFP on mitochondrial respiration. The activities of various complexes such as complex I, complex II, complex III and complex IV revealed that HFP inhibits all complexes of the ETC significantly. Generally, deformity in complex I and III are expected to lead to electron leakage (Brown et al., 2010). A reduction in the activity of complex I leads to the aggregation

of electrons in the first part of ETC. These electrons are directly translocated to molecular oxygen and favor the progression of radical formation and series of radical-induced impairment to the mitochondrial components (Bagur and Hajnóczky, 2017). Consumption of high calorie favors the entry of more substrate into respiratory chain complexes. Subsequently, the number of electrons supplied to the ETC also increases rapidly, resulting in molecular oxygen and superoxide and nitric oxide radical formation. This results in toxic peroxynitrite radical generation (Radi et al., 2002). Lower activity of complexes during HFP is also related to the reduced synthesis of subunits or elevated rate of degradation or the combined effect of both (García-Ruiz et al., 2014). Our result from *in vitro* study is in line with a report of Bagur (Bagur and Hajnóczky, 2017), suggesting that in the mice model of NAFLD, increased degradation of hepatic oxidative phosphorylation leads to mitochondrial impairment. There are reports to link fructose mediated

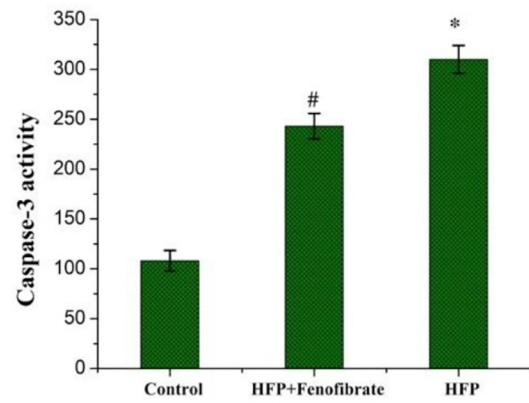
A



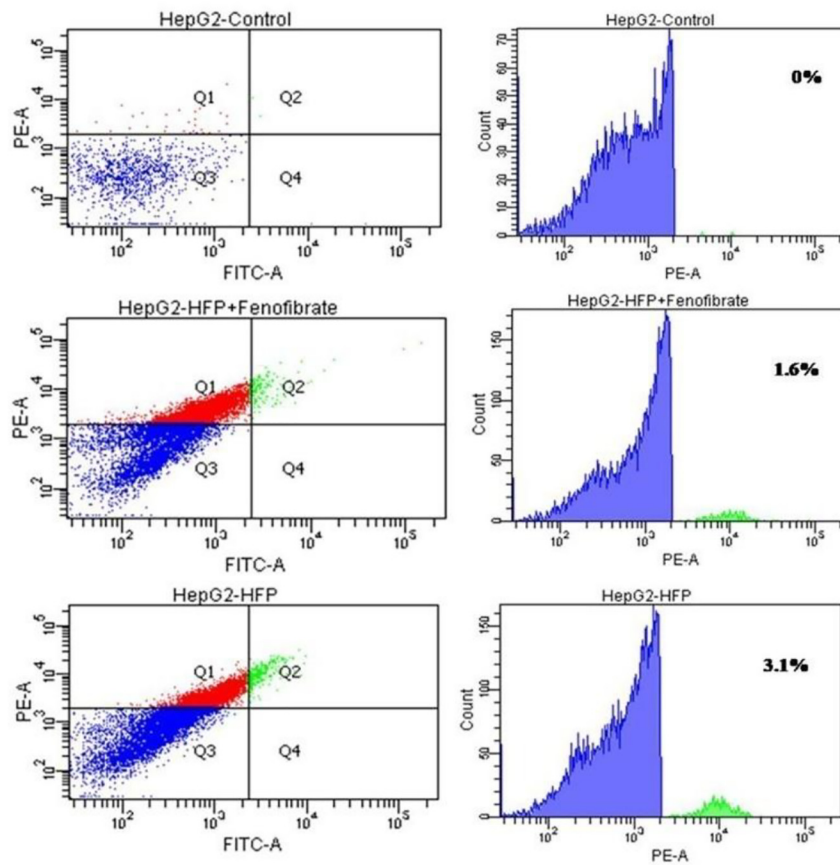
B



C



D



(caption on next page)

Fig. 6. HFP affects intracellular calcium homeostasis and initiates apoptosis *via* caspase 3 activation: (A) The fluorescent microscopic images of HepG2 cells stained with fura-2,AM. (i) Control cells; (ii) Cells treated with HFP + fenofibrate; (iii) Cells treated with HFP. (B) Fluorescence intensity emitted by fura-2 AM in control and treated cells. Data are expressed as mean \pm SD; where $n = 6$. (C) The relative expression of caspase-3 activity in HepG2 cells treated with HFP for 24 h. Data are expressed as mean \pm SD; where $n = 6$. (D) Detection of apoptosis by annexin V-FITC/PI analysis of HepG2 cells: Flow cytometric graph showing different quadrants where early apoptotic or primary necrotic cells (Annexin $-$ /PI $+$) represented in the upper left quadrant (Q1) for each panel. Late apoptotic cells or secondary necrotic cells (Annexin $+$ /PI $+$) are represented in the upper right quadrant (Q2). Viable cells (Annexin $-$ /PI $-$) are shown in the lower left quadrant (Q3) and early apoptotic cells (Annexin $+$ /PI $-$) are shown in the lower right quadrant (Q4). Data are expressed as mean \pm SD; where $n = 6$. * $p \leq .05$ significantly different from the control group. # $p \leq .05$ significantly different from the HFP treated group.

inhibition of aconitase activity and stimulation of lipogenesis due to the accumulation of citrate and activation of citrate lyase (Bagur and Hajnóczky, 2017). We also found a decrease in aconitase activity with HFP. Since aconitase is a mitochondrial matrix enzyme, this highlights the importance of central organelle in liver disease. The detrimental effect of HFP on oxygen consumption also indicates impaired bioenergetics.

Mitochondria exhibit a dynamic morphology. The dynamicity is mainly by changing their shape *via* fission-fusion processes (Kim and Lemasters, 2011; Twig and Shirihai, 2011) one of the primary quality control mechanisms when the cells experience metabolic or environmental stress. Under pathological conditions, there was an increase in fission proteins (DRP1 and FIS1) and a decrease in fusion proteins (MFN2 and OPA 1). The increased activity of DRP1 results in the production of a large number of fragmented mitochondria, which are competent to generate more reactive oxygen species. Similar types of alterations have been reported in the liver of diet-induced obese animals and hepatic steatosis in the murine model of NAFLD (Holmström et al., 2012; Lionetti et al., 2014; Yu et al., 2006; Bhatt et al., 2013). Overexpression of FIS1 proteins is mainly due to an excess amount of nutrients. The concept of fusion events in the maintenance of healthy mitochondria is also supported by several studies (Twig et al., 2008; Westermann, 2010). The activity of fusion proteins like MFN2 and OPA1 is indispensable for normal cellular functioning (Chen et al., 2010). The decreased level of MFN2 and OPA1 may impair mitochondrial quality control mechanisms and diminish mitochondrial networking. Fructose metabolism results in the development of de-novo lipogenesis of fatty acids and eventually leads to triglyceride accumulation. In a nutshell, mitochondrial fission - fusion proteins regulate hepatic lipid accumulation during NAFLD. Moreover, the dynamic nature of mitochondria, together with their interdependence with bioenergetics performs a vital role in energy homeostasis.

PGC-1 α is one of the essential transcriptional co-activators responsible for modulating hepatic metabolic pathways. It is also a master regulator of mitochondrial biogenesis, governing mitochondrial function, oxidative phosphorylation and oxygen consumption. It promotes the activation of nuclear receptors and performs a significant role in the generation of mitochondria (Ma, 2013). We found that HFP treated cells showed downregulation of PGC-1 α expression. This in turn, causes the suppression of transcription factors and nuclear receptors that control lipid metabolism and mitochondrial biogenesis (Zhang et al., 2009; Wang et al., 2004). The selective downregulation of PGC-1 α will no longer protect the liver and enhances the transition from steatosis to fibrosis. PGC-1 α also regulates the expression of a class of proteins called Sirtuins. Sirtuins are a class of highly conserved NAD $^+$ dependent histone and protein deacetylases. It has been reported that the expression of SIRT1 protects against alcohol-induced liver disease (Bergeron et al., 2001). As a metabolic modulator, SIRT1 control a series of physiological activities such as regulation of lipogenesis, controlling beta oxidation and hepatic oxidative stress, mediates hepatic inflammation *via* deacetylation of transcriptional modulators and stimulates autophagy (Kemper et al., 2013). Moreover, in the liver SIRT1 is responsible for controlling gluconeogenic activity *via* modulation by PGC-1 α . In the present study, the decreased expression of SIRT1 ceases the functioning of mitochondrial proteins and mitobiogenesis, thereby favouring the progression of steatosis.

The interaction of PGC-1 α with transcriptional regulators like NRF2 alters the expression of genes coding for OXPHOS subunits. For the evidence of the role of PGC-1 α and SIRT1 in liver disorder, we analyzed the protein expression of NRF2. The NRF2 is responsible for the maintenance of cellular redox homeostasis, anti-damage and anti-tumor processes (Zeng et al., 2017; Xu et al., 2011). There are reports claiming the crucial role of NRF2 in the progression of NAFLD to steatohepatitis in mice (Yang et al., 2018). NRF2 depletion induced ROS production, liver fibrosis and inflammation, the principal pathological features of NASH has been reported. Various studies have shown that fructose downregulates NRF2 expression (Yang et al., 2018). But the behavior of NRF2 expression in HepG2 cells during fructose and palmitate combination is not available in the literature. Herein we report the downregulation of NRF2 in HepG2 cells with HFP. This reveals the role of NRF2 in the genesis of steatosis with HFP mimicking high calorie diet. Recently specific reports have also demonstrated the regulatory role of SIRT1/NRF2 in the mitochondrial antioxidant pathway (Huang et al., 2013). It has also been reported that NRF2 signaling pathway plays a crucial role in providing hepatoprotection *via* improving the protein expression of antioxidant enzymes (Hu et al., 2017). During oxidative stress superoxide radical evokes the release of cytochrome c from mitochondria, which might be positively correlated with H $_2$ O $_2$ generation in mitochondria. Both intra and extra mitochondrial H $_2$ O $_2$ plays a significant role in the release of cytochrome c (Ruiz-Ramírez et al., 2015; Trauner et al., 2010). The increased expression of cytochrome c can be considered a mechanism of mitochondria entering the apoptotic pathway. Altogether our results suggest that HFP plays an inevitable role in altering mitochondrial biogenesis and thereby stimulates the progression of fatty liver disease.

We paid attention to see whether high-calorie induces apoptosis or not. One of its consequences is the genesis of intracellular calcium overload (Kroemer and Reed, 2000). Calcium acts as the central regulator of hepatic metabolism since it plays a pivotal role in the regulation of mitochondrial oxidative metabolism (Bravo et al., 2011). Impaired intracellular calcium overload occurred both early and late stages of apoptosis (Oliva-Vilarnau et al., 2018), and mediates lethal effects. It has been proposed that increased intracellular calcium concentration favors cell death *via* apoptosis. We also found an increase in caspase-3 activity, which might be due to increased cytosolic calcium concentration and release of cytochrome c from the mitochondria. Activation of caspase-3 occurs mainly during the final stages of apoptosis *via* the intrinsic mitochondrial pathway. Since caspase-3 activation promotes the progression of steatohepatitis and fibrosis during gluco-lipototoxicity, it can be considered as an efficient candidate for the treatment of NAFLD. It has also been reported that the palmitic acid treatment induces necroptosis, an emerging type of cell death (Gautheron et al., 2014).

5. Conclusion

The present study confirmed the development of steatosis with high fructose and palmitate in the HepG2 cells *via* mitochondrial dysfunction and associated complications. This is an ideal model to plan research on liver steatosis for academic purposes and drug discovery. Mitochondrial dysfunction and associated complications are reported to play a crucial role in liver disease. This reveals the importance of mitochondria in the

genesis of high energy diet induced liver disease. This model is fast and cost-effective and easy to perform in any labs and will have broad applications in the research field.

Author contributions

Swapna Sasi U S and Sindhu G provide substantial contributions to the conception or design of the work; or the acquisition, analysis, or interpretation of data for the work; and drafting the work or revising it critically for relevant intellectual content. Dr. Raghu K G permits the final approval of the version to be published; and agreement to be accountable for all aspects of the work in ensuring that questions related to the accuracy or integrity of any part of the work are appropriately investigated and resolved.

Declaration of competing interest

The authors declare no conflict of interest, financial or otherwise.

Acknowledgements

Swapna Sasi U S thanks University Grants Commission (Ref.No: 21/06/2015(i) EU-V), Govt. of India for financial assistance to conduct research. Sindhu G thanks Department of Health Research (DHR), Govt. of India, New Delhi, for Fellowship. We are also thankful to the Director, CSIR-IIIST, for providing necessary facilities.

References

- Bagur, R., Hajnóczy, G., 2017 Jun 15. Intracellular Ca²⁺ sensing: its role in calcium homeostasis and signaling. *Mol. Cell* 66 (6), 780–788.
- Bergeron, R., Ren, J.M., Cadman, K.S., Moore, I.K., Perret, P., Pypaert, M., Young, L.H., Semenkovich, C.F., Shulman, G.I., 2001 Dec 1. Chronic activation of AMP kinase results in NRF-1 activation and mitochondrial biogenesis. *Am. J. Physiol. Endocrinol. Metab.* 281 (6), E1340–E1346.
- Bhatt, M.P., Lim, Y.C., Kim, Y.M., Ha, K.S., 2013 Nov 1. C-peptide activates AMPK α and prevents ROS-mediated mitochondrial fission and endothelial apoptosis in diabetes. *Diabetes* 62 (11), 3851–3862.
- Bravo, R., Vicencio, J.M., Parra, V., Troncoso, R., Munoz, J.P., Bui, M., Quiroga, C., Rodriguez, A.E., Verdejo, H.E., Ferreira, J., Iglewski, M., 2011 Jul 1. Increased ER-mitochondrial coupling promotes mitochondrial respiration and bioenergetics during early phases of ER stress. *J. Cell Sci.* 124 (13), 2143–2152.
- Brown, G.C., Murphy, M.P., Jastroch, M., Divakaruni, A.S., Mookerjee, S., Treberg, J.R., Brand, M.D., 2010 Jun 14. Mitochondrial proton and electron leaks. *Essays Biochem.* 47, 53–67.
- Chalasanani, N., Younossi, Z., Lavine, J.E., Diehl, A.M., Brunt, E.M., Cusi, K., Charlton, M., Sanyal, A.J., 2012. The diagnosis and management of non-alcoholic fatty liver disease: practice guideline by the American Association for the Study of Liver Diseases, American College of Gastroenterology, and the American Gastroenterological Association. *Hepatology* 55 (6), 2005–2023.
- Chen, H., Vermulst, M., Wang, Y.E., Chomyn, A., Prolla, T.A., McCaffery, J.M., Chan, D.C., 2010 Apr 16. Mitochondrial fusion is required for mtDNA stability in skeletal muscle and tolerance of mtDNA mutations. *Cell* 141 (2), 280–289.
- Chong, M.F., Fielding, B.A., Frayn, K.N., 2007 Feb. Metabolic interaction of dietary sugars and plasma lipids with a focus on mechanisms and de novo lipogenesis. *Proc. Nutr. Soc.* 66 (1), 52–59.
- Day, C.P., 2002 Oct 1. Pathogenesis of steatohepatitis. *Best Pract. Res. Clin. Gastroenterol.* 16 (5), 663–678.
- Degli Esposti, D., Hamelin, J., Bosselut, N., Saffroy, R., Sebah, M., Pommier, A., Martel, C., Lemoine, A., 2012 Jun 15. Mitochondrial roles and cytoprotection in chronic liver injury. *Biochem. Res. Int.* 2012.
- Galloway, C.A., Lee, H., Brookes, P.S., Yoon, Y., 2014 Sep 15. Decreasing mitochondrial fission alleviates hepatic steatosis in a murine model of nonalcoholic fatty liver disease. *Am. J. Physiol. Gastrointest. Liver Physiol.* 307 (6), G632–G641.
- García-Ruiz, C., Fernández-Checa, J.C., 2018 Dec. Mitochondrial oxidative stress and antioxidants balance in fatty liver disease. *Hepatology* 67 (3), 1425–1439.
- García-Ruiz, I., Solís-Muñoz, P., Fernández-Moreira, D., Grau, M., Colina, F., Muñoz-Yagüe, T., Solís-Herruzo, J.A., 2014 Nov 1. High-fat diet decreases activity of the oxidative phosphorylation complexes and causes nonalcoholic steatohepatitis in mice. *Dis. Model. Mech.* 7 (11), 1287–1296.
- Gautheron, J., Vucur, M., Reisinger, F., Cardenas, D.V., Roderburg, C., Koppe, C., Kreggenwinkel, K., Schneider, A.T., Bartneck, M., Neumann, U.P., Canbay, A., 2014 Aug 1. A positive feedback loop between RIP3 and JNK controls non-alcoholic steatohepatitis. *EMBO Mol. Med.* 6 (8), 1062–1074.
- Holmström, M.H., Iglesias-Gutierrez, E., Zierath, J.R., Garcia-Roves, P.M., 2012 Mar 15. Tissue-specific control of mitochondrial respiration in obesity-related insulin resistance and diabetes. *Am. J. Physiol. Endocrinol. Metab.* 302 (6), E731–E739.
- Hu, Y., Hou, Z., Yi, R., Wang, Z., Sun, P., Li, G., Zhao, X., Wang, Q., 2017. Tartary buckwheat flavonoids ameliorate high fructose-induced insulin resistance and oxidative stress associated with the insulin signaling and Nrf2/HO-1 pathways in mice. *Food Funct.* 8 (8), 2803–2816.
- Huang, K., Huang, J., Xie, X., Wang, S., Chen, C., Shen, X., Liu, P., Huang, H., 2013. Sirt1 resists advanced glycation end products-induced expressions of fibronectin and TGF- β 1 by activating the Nrf2/ARE pathway in glomerular mesangial cells. *Free Radic. Biol. Med.* 65, 528–540.
- Kemper, J.K., Choi, S.E., Kim, D.H., 2013. Sirtuin 1 deacetylase: a key regulator of hepatic lipid metabolism. In: *Vitamins & Hormones*. Vol. 91. pp. 385–404.
- Kim, I., Lemasters, J.J., 2011 Feb. Mitochondrial degradation by autophagy (mitophagy) in GFP-LC3 transgenic hepatocytes during nutrient deprivation. *Am. J. Phys. Cell Phys.* 300 (2), C308–C317.
- Kroemer, G., Reed, J.C., 2000 May. Mitochondrial control of cell death. *Nat. Med.* 6 (5), 513–519.
- Lee, K., Haddad, A., Osme, A., Kim, C., Borzou, A., Ilchenko, S., Allende, D., Dasarathy, S., McCullough, A.J., Sadygov, R.G., Kasumov, T., 2018 Jan. Hepatic mitochondrial defects in a mouse model of NAFLD are associated with increased degradation of oxidative phosphorylation subunits. *Mol. Cell. Proteomics* 1.
- Lionetti, L., Mollica, M.P., Donizzetti, I., Gifuni, G., Sica, R., Pignalosa, A., Cavaliere, G., Gaita, M., De Filippo, C., Zorzano, A., Putti, R., 2014. High-lard and high-fish-oil diets differ in their effects on function and dynamic behaviour of rat hepatic mitochondria. *PLoS One* 9 (3).
- Ma, Q., 2013 Jan 6. Role of nrf2 in oxidative stress and toxicity. *Annu. Rev. Pharmacol. Toxicol.* 53, 401–426.
- Mansouri, A., Gattolliat, C.H., Asselah, T., 2018 Sep 1. Mitochondrial dysfunction and signaling in chronic liver diseases. *Gastroenterology* 155 (3), 629–647.
- Miller, A., Adeli, K., 2008 Mar 1. Dietary fructose and the metabolic syndrome. *Curr. Opin. Gastroenterol.* 24 (2), 204–209.
- Mitchell, C., Robin, M.A., Mayeuf, A., Mahrouf-Yorgov, M., Mansouri, A., Hamard, M., Couton, D., Fromenty, B., Gilgenkrantz, H., 2009 Nov 1. Protection against hepatocyte mitochondrial dysfunction delays fibrosis progression in mice. *Am. J. Pathol.* 175 (5), 1929–1937.
- Oliva-Vilarnau, N., Hankeova, S., Vorrink, S.U., Mkrtrchian, S., Andersson, E.R., Lauschke, V.M., 2018 Jul 4. Calcium signaling in liver injury and regeneration. *Front. Med.* 5, 192.
- Prins, G.H., Luangmonkong, T., Oosterhuis, D., Mutsaers, H.A., Dekker, F.J., Olinga, P., 2019 Mar. A pathophysiological model of non-alcoholic fatty liver disease using precision-cut liver slices. *Nutrients* 11 (3), 507.
- Radi, R., Cassina, A., Hodara, R., 2002 Apr 12. Nitric oxide and peroxynitrite interactions with mitochondria. *Biol. Chem.* 383 (3–4), 401–409.
- Ruiz-Ramírez, A., Barrios-Maya, M.A., López-Acosta, O., Molina-Ortiz, D., El-Hafidi, M., 2015 Nov 1. Cytochrome c release from rat liver mitochondria is compromised by increased saturated cardioliipin species induced by sucrose feeding. *Am. J. Physiol. Endocrinol. Metab.* 309 (9), E777–E786.
- Sanyal, A.J., Campbell-Sargent, C., Mirshahi, F., Rizzo, W.B., Contos, M.J., Sterling, R.K., Luketic, V.A., Shiffman, M.L., Clore, J.N., 2001 Apr 1. Nonalcoholic steatohepatitis: association of insulin resistance and mitochondrial abnormalities. *Gastroenterology* 120 (5), 1183–1192.
- Schwarz, J.M., Noworolski, S.M., Wen, M.J., Dyachenko, A., Prior, J.L., Weinberg, M.E., Herraz, L.A., Tai, V.W., Bergeron, N., Bersot, T.P., Rao, M.N., 2015 Jun 1. Effect of a high-fructose weight-maintaining diet on lipogenesis and liver fat. *J. Clin. Endocrinol. Metab.* 100 (6), 2434–2442.
- Situnayake, R.D., Crump, B.J., Thurnham, D.I., Davies, J.A., Gearty, J., Davis, M., 1990 Nov 1. Lipid peroxidation and hepatic antioxidants in alcoholic liver disease. *Gut* 31 (11), 1311–1317.
- Softic, S., Cohen, D.E., Kahn, C.R., 2016 May 1. Role of dietary fructose and hepatic de novo lipogenesis in fatty liver disease. *Dig. Dis. Sci.* 61 (5), 1282–1293.
- Stanhope, K.L., Schwarz, J.M., Havel, P.J., 2013 Jun. Adverse metabolic effects of dietary fructose: results from recent epidemiological, clinical, and mechanistic studies. *Curr. Opin. Lipidol.* 24 (3), 198.
- Sudheesh, N.P., Ajith, T.A., Janardhanan, K.K., 2009 Oct 1. *Ganoderma lucidum* (Fr.) P. Karst enhances activities of heart mitochondrial enzymes and respiratory chain complexes in the aged rat. *Biogerontology* 10 (5), 627–636.
- Szczepaniak, L.S., Nurenberg, P., Leonard, D., Browning, J.D., Reingold, J.S., Grundy, S., Hobbs, H.H., Dobbins, R.L., 2005 Feb. Magnetic resonance spectroscopy to measure hepatic triglyceride content: prevalence of hepatic steatosis in the general population. *Am. J. Physiol. Endocrinol. Metab.* 288 (2), E462–E468.
- Teodoro, J.S., Duarte, F.V., Gomes, A.P., Varela, A.T., Peixoto, F.M., Rolo, A.P., Palmeira, C.M., 2013 Nov 1. Berberine reverts hepatic mitochondrial dysfunction in high-fat fed rats: a possible role for Sirt3 activation. *Mitochondrion* 13 (6), 637–646.
- Tilg, H., Diehl, A.M., 2000 Nov 16. Cytokines in alcoholic and nonalcoholic steatohepatitis. *N. Engl. J. Med.* 343 (20), 1467–1476.
- Trauner, M., Arrese, M., Wagner, M., 2010 Mar 1. Fatty liver and lipotoxicity. *Biochim. Biophys. Acta Mol. Cell Biol. Lipids* 1801 (3), 299–310.
- Twig, G., Shirihai, O.S., 2011 May 15. The interplay between mitochondrial dynamics and mitophagy. *Antioxid. Redox Signal.* 14 (10), 1939–1951.
- Twig, G., Elorza, A., Molina, A.J., Mohamed, H., Wikstrom, J.D., Walzer, G., Stiles, L., Haigh, S.E., Katz, S., Las, G., Alroy, J., 2008 Jan 23. Fission and selective fusion govern mitochondrial segregation and elimination by autophagy. *EMBO J.* 27 (2), 433–446.
- Vasselli, J.R., 2008 Nov. Fructose-induced leptin resistance: discovery of an unsuspected form of the phenomenon and its significance. Focus on “Fructose-induced leptin resistance exacerbates weight gain in response to subsequent high-fat feeding.” by Shapiro et al. *Am. J. Phys. Regul. Integr. Comp. Phys.* 295 (5), R1365–R1369.

- Wang, C.H., Ciliberti, N., Li, S.H., Szmitko, P.E., Weisel, R.D., Fedak, P.W., Al-Omran, M., Cherng, W.J., Li, R.K., Stanford, W.L., Verma, S., 2004 Mar 23. Rosiglitazone facilitates angiogenic progenitor cell differentiation toward endothelial lineage: a new paradigm in glitazone pleiotropy. *Circulation* 109 (11), 1392–1400.
- Westermann, B., 2010 Aug 1. Mitochondrial dynamics in model organisms: what yeasts, worms and flies have taught us about fusion and fission of mitochondria. In: *Seminars in Cell & Developmental Biology*. Academic Press, pp. 542–549 Vol. 21, No. 6.
- Xu, W., Shao, L., Zhou, C., Wang, H., Guo, J., 2011. Upregulation of Nrf2 expression in non-alcoholic fatty liver and steatohepatitis. *Hepatogastroenterology* 58 (112), 2077–2080.
- Yang, Y., Wang, J., Zhang, Y., Li, J., Sun, W., 2018. Black sesame seeds ethanol extract ameliorates hepatic lipid accumulation, oxidative stress, and insulin resistance in fructose-induced nonalcoholic fatty liver disease. *J. Agric. Food Chem.* 66 (40), 10458–10469.
- Yu, T., Robotham, J.L., Yoon, Y., 2006 Feb 21. Increased production of reactive oxygen species in hyperglycemic conditions requires dynamic change of mitochondrial morphology. *Proc. Natl. Acad. Sci.* 103 (8), 2653–2658.
- Zeng, X.P., Li, X.J., Zhang, Q.Y., Liu, Q.W., Li, L., Xiong, Y., He, C.X., Wang, Y.F., Ye, Q.F., 2017 Mar 1. Tert-Butylhydroquinone protects liver against ischemia/reperfusion injury in rats through Nrf2-activating anti-oxidative activity. In: *Transplantation Proceedings*. Vol. 49. pp. 366–372 No. 2.
- Zhang, H.F., Hu, X.M., Wang, L.X., Xu, S.Q., Zeng, F.D., 2009 Feb. Protective effects of scutellarin against cerebral ischemia in rats: evidence for inhibition of the apoptosis-inducing factor pathway. *Planta Med.* 75 (02), 121–126.